“Survival of the Fittest”

--- *Charles Darwin*

University of Alberta

The Importance of Choline
--- Adaptation to Choline Deprivation

by

©

Zhaoyu Li

A thesis submitted to the Faculty of Graduate Studies and Research in
partial fulfillment of the requirements for
the degree of ***Doctor of Philosophy***

Department of *Biochemistry*

Edmonton, Alberta
Spring 2006

Library and
Archives Canada

Published Heritage
Branch

395 Wellington Street
Ottawa ON K1A 0N4
Canada

Bibliothèque et
Archives Canada

Direction du
Patrimoine de l'édition

395, rue Wellington
Ottawa ON K1A 0N4
Canada

Your file Votre référence
ISBN: 0-494-14010-0
Our file Notre référence
ISBN: 0-494-14010-0

NOTICE:
The author has granted a non-exclusive license allowing Library and Archives Canada to reproduce, publish, archive, preserve, conserve, communicate to the public by telecommunication or on the Internet, loan, distribute and sell theses worldwide, for commercial or non-commercial purposes, in microform, paper, electronic and/or any other formats.

The author retains copyright ownership and moral rights in this thesis. Neither the thesis nor substantial extracts from it may be printed or otherwise reproduced without the author's permission.

AVIS:
L'auteur a accordé une licence non exclusive permettant à la Bibliothèque et Archives Canada de reproduire, publier, archiver, sauvegarder, conserver, transmettre au public par télécommunication ou par l'Internet, prêter, distribuer et vendre des thèses partout dans le monde, à des fins commerciales ou autres, sur support microforme, papier, électronique et/ou autres formats.

L'auteur conserve la propriété du droit d'auteur et des droits moraux qui protège cette thèse. Ni la thèse ni des extraits substantiels de celle-ci ne doivent être imprimés ou autrement reproduits sans son autorisation.

In compliance with the Canadian Privacy Act some supporting forms may have been removed from this thesis.

While these forms may be included in the document page count, their removal does not represent any loss of content from the thesis.

Conformément à la loi canadienne sur la protection de la vie privée, quelques formulaires secondaires ont été enlevés de cette thèse.

Bien que ces formulaires aient inclus dans la pagination, il n'y aura aucun contenu manquant.

Canada

University of Alberta

Library Release Form

Name of Author: *Zhaoyu Li*

Title of Thesis: *The Importance of Choline --- Adaptation to Choline Deprivation*

Degree: *Doctor of Philosophy*

Year this Degree Granted: *2006*

Permission is hereby granted to the University of Alberta Library to reproduce single copies of this thesis and to lend or sell such copies for private, scholarly or scientific research purposes only.

The author reserves all other publication and other rights in association with the copyright in the thesis, and except as herein before provided, neither the thesis nor any substantial portion thereof may be printed or otherwise reproduced in any material form whatsoever without the author's prior written permission.

Signature

Dec. 20, 2005

Abstract

Choline is an important nutrient in animals. Animals can acquire choline from both diet and via *de novo* biosynthesis by converting phosphatidylethanolamine (PE) into phosphatidylcholine (PC) catalyzed by PE *N*-methyltransferase (PEMT). Choline can be depleted via biliary PC excretion and choline oxidation.

"Complete choline deprivation" is achieved by feeding *Pemt*$^{-/-}$ mice a choline-deficient (CD) diet. CD-*Pemt*$^{-/-}$ mice died of acute liver failure and severe steatohepatitis within 4~5 days. Rapid lethality from complete choline deprivation suggests that choline is an essential nutrient. By constructing a mouse model that lacks both PEMT and multiple drug resistant protein 2 (MDR2, ABCB4), a unique PC-specific flippase that mediates PC secretion into bile, we successfully rescued CD-*Pemt*$^{-/-}$ mice. CD-*Abcb4*$^{-/-}$/*Pemt*$^{-/-}$ mice are resistant to liver failure and steatohepatitis and survive for at least 3 months without any input of choline. Comparison of these two mouse models revealed the mechanism of adaptation to choline deprivation in CD-*Abcb4*$^{-/-}$/*Pemt*$^{-/-}$ mice and thereby the mechanism of lethality of complete choline deprivation in CD-*Pemt*$^{-/-}$ mice. Acute lethality in CD-*Pemt*$^{-/-}$ mice is due to rapid depletion of hepatic PC through bile secretion. CD-*Abcb4*$^{-/-}$/*Pemt*$^{-/-}$ mice are resistant to liver failure by preserving membrane integrity through maintaining a normal ratio of PC to PE. The ratio of PC to PE is identified as a key regulator of membrane integrity and plays a critical role in the

progression of steatosis into steatohepatitis. Moreover, choline recycling and choline redistribution are triggered in CD-*Abcb4*$^{-/-}$/*Pemt*$^{-/-}$ mice as adaptations to choline deprivation. Although failed to adapt to choline deprivation, CD-*Pemt*$^{-/-}$ mice also showed an adaptive response to mobilize PC from extrahepatic tissues to liver in a gender-dependent manner.

The goal of this thesis is to demonstrate the importance of choline by illustrating how mice adapt to choline deprivation. The results lead to the finding of a "choline balance theory", that is, there is a balance between gain and loss of choline that determines the survival of choline-containing organisms. Life of these organisms is critically dependent on the maintenance of total choline level. The ratio of PC to PE, choline recycling, choline redistribution and storage, as well as choline acquisition and depletion pathways might be adjusted in adaptations to choline imbalance.

Table of Contents

Chapter 1 - Introduction of Choline 1

Chapter 2 - Choline is an Essential Nutrient --- Adaptation to Choline Deprivation I: Choline Recycling 42

Chapter 3 - The Ratio of PC to PE is a Key Regulator of Membrane Integrity --- Adaptation to Choline Deprivation II: Maintenance of Membrane Integrity via Maintenance of PC/PE Ratio 88

Chapter 4 - Choline Channeling from Peripheral Tissues to Brain and Liver --- Adaptation to Choline Deprivation III: Choline Redistribution 170

Chapter 5 - Mobilization of Extrahepatic Choline via Enhacing HDL-PC Efflux --- Adaptation to Choline Deprivation IV: Choline Storage 205

Chapter 6 - Choline Balance Theory --- Summary 238

Appendix I - Why is Serine Sufficient for Phosphatidylethanolamine Biosynthesis during Cell Culture? 263

Appendix II - Does PEMT protect against Liver Cancer? 284

Appendix III - Where is Anti-PEMT1 Antibody? 293

Chapter 1 – Introduction of Choline 1

1.1 History of choline 2

1.2 Choline homeostasis 2

1.2.1 Choline intake 4

1.2.2 Enzymes in choline metabolism 5

1.2.2.1 Enzymes in PC biosynthesis 5

1.2.2.1.1 The CDP-choline pathway 5

1.2.2.1.1.1 Choline kinase 6

1.2.2.1.1.2 CTP:phosphorylcholine cytidylyltransferase 6

1.2.2.1.1.3 CDP-choline:1,2-diacylglycerol cholinephosphotransferase 7

1.2.2.1.2 The PEMT pathway 7

1.2.2.2 Enzymes in PC catabolism 8

1.2.2.2.1 Phospholipase A_2 and A_1 9

1.2.2.2.2 Phospholipase C 9

1.2.2.2.3 Phospholipase D and phosphatidylserine synthase 1 10

1.2.2.3 Enzyme(s) in choline catabolism 10

1.2.3 Multiple drug resistant protein 2 10

1.3 Functions of choline 11

1.3.1 Functions of PC: membrane integrity, lipoprotein metabolism, bile formation, signaling 12
    1.3.1.1 PC and membrane integrity (phospholipids and membrane integrity) 12
    1.3.1.2 PC and lipoprotein metabolism 13
    1.3.1.3 PC and bile formation 14
    1.3.1.4 PC and cell signaling 14
1.3.2 Acetylcholine: neurotransmitter 15
1.3.3 CDP-choline: memory capability 15
1.3.4 Betaine: osmotic regulation and methyl donor for methionine biosynthesis 16
1.4 Choline metabolism and liver 16
1.5 Choline deficiency 17
1.5.1 Physiological situations of choline deficiency 17
1.5.2 Artificial manipulations of choline deprivation 18
1.5.3 Choline deficiency and liver disorders 18
1.5.4 Choline deficiency and other disorders 19
1.6 Thesis objective 21
Figures and Legends 23
References 26

Chapter 2 - Choline is an Essential Nutrient --- Adaptation to Choline Deprivation I: Choline Recycling. 42

2.1 Introduction 43

2.2 Materials and Methods 44

- 2.2.1 Animals 44
- 2.2.2 Genotyping 45
- 2.2.3 Sample collections 45
- 2.2.4 Preparation of primary hepatocytes 46
- 2.2.5 Enzyme assays 46
- 2.2.6 Analyses of lipids and choline metabolites 48
- 2.2.7 Tracing PC metabolism 48
- 2.2.8 Western blotting for c-Jun 49
- 2.2.9 *In vivo* injection of c-Jun antisense DNA 49

2.3 Results 50

- 2.3.1 Biliary secretion of PC is lethal in CD-*Pemt*$^{-/-}$ mice 50
- 2.3.2 Enhanced PC metabolism in CD-*Pemt*$^{-/-}$/*Abcb4*$^{-/-}$ mice, but not in CD-*Pemt*$^{-/-}$ mice 51
- 2.3.3 Choline metabolites are channeled towards PC biosynthesis 52
- 2.3.4 Adaptation to complete choline deprivation --- choline recycling 53
- 2.3.5 A new choline homeostasis --- life and death 54
- 2.3.6 Exploring regulatory mechanisms of adaptatin to choline deprivation 54

2.4 Discussion 56

Figures and Legends 59

References 83

Chapter 3 - The Ratio of PC to PE is a Key Regulator of Membrane Integrity --- Adaptation to Choline Deprivation II: Maintenance of Membrane Integrity via Maintenance of PC/PE Ratio 88

3.1 Introduction 89

3.2 Materials and Methods 90

3.2.1 Animals 90

3.2.2 Genotyping 90

3.2.3 Sample collections 90

3.2.4 Preparation of primary hepatocytes 90

3.2.5 Lipid Analyses 91

3.2.6 Enzyme assays 91

3.2.7 Preparation of hepatic plasma membranes and assessment of purity 92

3.2.8 Assay of plasma membrane fluidity and potential 93

3.2.9 Detection of PE on the cell surface of hepatocytes 93

3.2.10 Measurement of PE synthesis and degradation 94

3.2.11 Assays of VLDL-PC secretion and HDL-PC uptake rate 94

3.2.12 Permeability assays of large unilamellar vesicles (LUVs) 95

3.2.13 RNA interference (RNAi) of ET in cultured hepatocytes 96

3.2.14 Inhibition of PE catabolism by arachidonyl trifluoromethyl ketone (ATK) 96

3.2.15 *In vivo* injection of ETi 97

3.2.16 Histological and pathological Analysis 97

3.3 Results 98

3.3.1 Liver failure is associated with a decreased ratio of PC to PE 98

3.3.1.1 Hepatic PC/PE ratios correlate with liver damage 98

3.3.1.2 Plasma membrane PC/PE ratios correlate with hepatocyte damage 99

3.3.1.3 Hepatic PC/PE ratios correlate with membrane fluidity 100

3.3.1.4 Increased PE exposure on the cell surface in CD-*Pemt*$^{-/-}$ hepatocytes 100

3.3.1.5 Hypothetical mechanism for liver failure in CD-*Pemt*$^{-/-}$ mice 100

3.3.2 The mechanism of the maintenance of PC/PE ratio in CD-*Pemt*$^{-/-}$/*Abcb4*$^{-/-}$ mice 101

3.3.2.1 Increased PE catabolism causes the decrease in hepatic PE level in CD-*Pemt*$^{-/-}$/*Abcb4*$^{-/-}$ mice 101

3.3.2.2 Different fates for PC removal lead to altered PE metabolism and adaptation to choline deprivation 102

3.3.3 The ratio of PC to PE is a key regulator of membrane integrity 103

3.3.3.1 PC/PE ratios influence membrane integrity of large unilamellar vesicles (LUVs) 103

3.3.3.2 Knockdown of PE biosynthesis in CD-*Pemt*$^{-/-}$ hepatocytes increases PC/PE ratio and attenuates cell damage 104

3.3.3.3 Inhibition of PE degradation in CD-*Abcb4*$^{-/-}$/*Pemt*$^{-/-}$ hepatocytes causes decreased PC/PE ratios and induces cell damage 105

3.3.4 Is PC/PE ratio a critical regulator in developing steatosis into steatohepatitis? 105

3.3.4.1 CD-*Pemt*$^{-/-}$ mice developed steatohepatitis but CD-*Pemt*$^{-/-}$/*Abcb4*$^{-/-}$ mice developed steatosis 106

3.3.4.2 Hepatic PC/PE ratios correlate with the degree of steatohepatitis 106

3.3.4.3 Increased PC/PE ratios reverse steatohepatitis 107

3.3.4.4 Increased PC/PE ratios reverse steatohepatitis, but not steatosis 107

3.4 Discussion 108

Table(s) 112

Figures and Legends 113

References 164

Chapter 4 - Choline Channeling from Peripheral Tissues to Brain and Liver --- Adaptation to Choline Deprivation III: Choline Redistribution 170

4.1 Introduction 171

4.2 Materials and Methods 172

4.2.1 Animals 172

4.2.2 Plasma S100β protein assay 172

4.2.3 Assays for total choline-containing metabolites 172

4.2.4 Lipid analysis 173

4.2.5 Choline oxidase assay 173

4.2.6 Western Blotting for choline high-affinity transporter (CHT) 173

4.2.7 *In vivo* injection of [^{3}H]choline 173

4.3 Results 174

4.3.1 No brain damage occurred during choline deprivation 174

4.3.2 Brain did not face choline deficiency 174

4.3.3 Choline distribution and redistribution during choline deprivation 175

4.3.4 Liver was more active in choline uptake than brain 180

4.4 Discussion 181

Table(s) 185

Figures and Legends 186

References 202

Chapter 5 - Mobilization of Extrahepatic Choline via Enhacing HDL-PC Efflux
--- Adaptation to Choline Deprivation IV: Choline Storage 205

5.1 Introduction 206

5.2 Materials and Methods 206

5.2.1 Animals 206

5.2.2 Liver damage assays 207

5.2.3 Lipid analysis 207

5.2.4 Profiles of choline-containing lipids in plasma lipoproteins 207

5.2.5 Treatment of mice with glybenclamide 208

5.2.6 Preβ HDL particles and ApoAI secretion from primary cultured hepatocytes 208

5.3 Results 209

5.3.1 Gender-dependent response to choline deprivation in *Pemt*$^{-/-}$ mice 209

5.3.2 Gender-dependent difference in PC/PE ratios and PC levels in the liver 210

5.3.3 Gender-dependent PC homeostasis in the liver 211

5.3.4 Glybenclamide blocked HDL-PC efflux and induced liver damage in female *Pemt*$^{-/-}$ mice 212

5.3.5 Exploring the mechanisms of differential regulation of HDL-PC efflux 212

5.4 Discussion 213

Table(s) 218

Figures and Legends 219

References 235

Chapter 6 - Choline Balance Theory --- Summary 238

6.1 Choline balance and imbalance 239

6.2 Classical adaptations to choline imbalance 240

6.2.1 Dietary choline intake 240

6.2.2 The PEMT pathway 240

6.2.3 Biliary PC excretion 241

6.2.4 Choline oxidation 241

6.3 New findings of adaptation to choline deprivation 242

6.3.1 Choline recycling 242

6.3.2 Maintenance of membrane integrity via maintenance of PC/PE ratio 243

6.3.3 Choline redistribution 244

6.3.4 Choline storage 245

6.4 Choline is an essential nutrient 245

6.5 Choline balance theory 246

6.6 Future studies 248

6.6.1 Adaptation to choline excess 249

6.6.2 Choline replacement 250

6.6.3 Generality of newly found adaptations to choline deprivation 251

6.6.4 Regulation of adaptation to choline deprivation 252

Table(s) 253

Figures and Legends 254

References 259

Appendix I - Why is Serine Sufficient for Phosphatidylethanolamine Biosynthesis during Cell Culture? 263

Appendix II - Does PEMT protect against Liver Cancer? 284

Appendix III - Where is Anti-PEMT1 Antibody? 293

List of Tables

Table 3.1 Factors potentially influencing membrane integrity 112

Table 4.1 Body weight and liver weight of *Abcb4*$^{-/-}$/*Pemt*$^{-/-}$ mice 185

Table 5.1 CT and PEMT activities 219

Table 6.1 Choline Balance Theory 254

List of Figures

Fig. 1.1 Structure of choline 23

Fig. 1.2 Choline homeostasis 24

Fig. 2.1 Choline homeostasis in liver 59

Fig. 2.2 Genotyping of *Pemt*$^{-/-}$ and *Abcb4*$^{-/-}$/*Pemt*$^{-/-}$ mice 60

Fig. 2.3 Liver damage was assessed by measurement of plasma alanine/aspartate aminotransferase (ALT/AST) activity 62

Fig. 2.4 Hepatic total choline-containing metabolites (PC, sphingomyelin, lysoPC, glycerophosphocholine, phosphocholine and choline) 64

Fig. 2.5 The amount of biliary PC 67

Fig. 2.6 Hepatic PC catabolism is enhanced by the CD diet in *Abcb4*$^{-/-}$/*Pemt*$^{-/-}$ mice but not in *Pemt*$^{-/-}$ mice 68

Fig. 2.7 Choline oxidase activity was curtailed in livers of both *Pemt*$^{-/-}$ mice and *Abcb4*$^{-/-}$/*Pemt*$^{-/-}$ mice 72

Fig. 2.8 Choline kinase activity in liver homogenates 73

Fig. 2.9 CTP:phosphocholine cytidylyltransferase (CT) activity assays. 74

Fig. 2.10 PC biosynthesis and degradation in intact hepatocytes of *Abcb4*$^{-/-}$/*Pemt*$^{-/-}$ mice 76

Fig. 2.11 Incorporation of [^{3}H]glycerophosphocholine ([^{3}H]GPC) into [^{3}H]phosphatidylcholine in primary cultured hepatocytes of *Abcb4*$^{-/-}$/*Pemt*$^{-/-}$ mice during choline deprivation 77

Fig. 2.12 Relative amounts of water-soluble choline metabolites as a percentage of the mass of total choline-containing metabolites (%) 78

Fig. 2.13 Expression of c-Jun was increased in *Abcb4*$^{-/-}$/*Pemt*$^{-/-}$ mice during choline deprivation, but not in *Pemt*$^{-/-}$ mice 80

Fig. 2.14 c-Jun antisense blocked the adaptive response to choline deprivation in *Abcb4*$^{-/-}$/*Pemt*$^{-/-}$ mice 81

Fig. 2.15 Choline recycling pathways 82

Fig. 3.1 Phosphatidylcholine (PC) homeostasis in the liver 113

Fig. 3.2 Hepatic phospholipid compositions 114

Fig. 3.3 CD-*Abcb4*$^{-/-}$/*Pemt*$^{-/-}$ mice are resistant to liver failure, but not CD-*Pemt*$^{-/-}$ mice 117

Fig. 3.4 Hepatic PC/PE ratios correlate with liver damage 118

Fig. 3.5 The PC/PE ratio is maintained without liver damage in CD-*Pemt*$^{+/+}$ mice 119

Fig. 3.6 Plasma membrane PC/PE ratios correlate with hepatocyte damage 121

Fig. 3.7 Hepatic PC/PE ratios correlate with membrane fluidity 124

Fig. 3.8 PE on the cell surface 125

Fig. 3.9 Hypothetical mechanism for liver failure in CD-*Pemt*$^{-/-}$ mice 127

Fig. 3.10 Increased PE catabolism causes the decrease in hepatic PE level in CD-*Pemt*$^{-/-}$/*Abcb4*$^{-/-}$ mice 128

Fig. 3.11 VLDL-PC secretion and HDL-PC uptake by hepatocytes 129

Fig. 3.12 PLA$_2$ activity is enhanced in CD-*Abcb4*$^{-/-}$/*Pemt*$^{-/-}$ mice, but not in CD-*Pemt*$^{-/-}$ mice 131

Fig. 3.13 Proposed scheme for the maintenance of PC/PE ratios in CD-*Abcb4*$^{-/-}$/*Pemt*$^{-/-}$ mice 133

Fig. 3.14 PC/PE ratios influence membrane integrity of large unilamellar vesicles (LUVs) 134

Fig. 3.15 Choline deprivation does not affect hepatic ET activity 135

Fig. 3.16 Knockdown of PE biosynthesis in CD-*Pemt*$^{-/-}$ hepatocytes by ETi 136

Fig. 3.17 ETi decreases PE levels in hepatocytes 138

Fig. 3.18 ETi increases PC/PE ratio and attenuates cell damage 139

Fig. 3.19 ETi attenuates the incorporation of [^{3}H]ethanolamine into [^{3}H]PE 141

Fig. 3.20 PE exposure on the cell surface after ETi 143

Fig. 3.21 Attenuation of PE catabolism induces cell damage in CD-*Abcb4*$^{-/-}$/*Pemt*$^{-/-}$ murine hepatocytes 144

Fig. 3.22 Liver weight (LW) and body weight (BW) 146

Fig. 3.23 Liver photos 148

Fig. 3.24 Liver histology by hemotoxylin and eosin staining 150

Fig. 3.25 Plasma levels of glucose and insulin 152

Fig. 3.26 Liver histology by hemotoxylin and eosin staining 154

Fig. 3.27 Choline re-feeding reverses both hepatitis and steatosis in CD- *Pemt*$^{-/-}$ mice 156

Fig. 3.28 Increased PC/PE ratio reversed hepatitis, but not steatosis 159

Fig. 3.29 Plasma membrane potentials of hepatocytes 163

Fig. 4.1 Levels of total choline–containing metabolites and phosphatidylcholine (PC) in the brain are not affected by the choline-deficient (CD) diet 186

Fig. 4.2 Choline oxidation in the brain is still active during choline deprivation 188

Fig. 4.3 Expression of choline high-affinity transporter (CHT) in the brain and liver 189

Fig. 4.4 Plasma free choline levels did not decrease significantly on a CD diet whereas plasma PC was decreased markedly 190

Fig. 4.5 Potential choline redistributions among tissues in *Pemt*$^{-/-}$ and *Abcb4*$^{-/-}$/*Pemt*$^{-/-}$ mice during choline deprivation 192

Fig. 4.6 Sum of total radioactivity in all tissues assayed 193

Fig. 4.7 Total radioactivity in the whole tissues of *Pemt*$^{-/-}$ mice 195

Fig. 4.8 Total radioactivity in the whole tissues of *Abcb4*$^{-/-}$/*Pemt*$^{-/-}$ mice 196

Fig. 4.9 Distributions of [^{3}H]choline labeling in PC and free choline in the plasma 197

Fig. 4.10 Specific activities of choline metabolites in brain and liver 199

Fig. 5.1 Liver damage assays 220

Fig. 5.2 Hepatic phospholipid compositions 222

Fig. 5.3 The amount of biliary PC 224

Fig. 5.4 The amount of plasma PC 225

Fig. 5.5 Profiles of choline-containing lipids in plasma lipoproteins 226

Fig. 5.6 Profiles of choline-containing lipids in plasma lipoproteins 227

Fig. 5.7 Profiles of choline-containing lipids in plasma lipoproteins after glybenclamide treatment 228

Fig. 5.8 Hepatic phospholipid compositions after glybenclamide treatment 229

Fig. 5.9 Liver damage assays after glybenclamide treatment 231

Fig. 5.10 HDL and ApoAI secretion from primary cultured hepatocytes 232

Fig. 5.11 The amount of PC associated with ApoAI 234

Fig. 6.1 Scheme of choline balance theory 255

Fig. 6.2 Choline deprivation attenuated liver damage in *Abcb4*$^{-/-}$ mice 256

Fig. 6.3 Choline was not replicable by methionine or propanolamaine 257

Abbreviations

ABCB4	ATP-binding cassette B4
AdoMet	*S*-adenosylmethionine
ALT	Alanine aminotransferase
AP-1	activator protein-1
AP-2	activator protein-2
ApoAI	apolipoprotein AI
ApoB	apolipoprotein B
AST	aspartate aminotransferase
ATK	arachidonoyl trifluoromethyl ketone
BEL	bromoenol lactone
CD	choline-deficient
CEBP	CCAAT/enhancer binding protein
CHT	choline high-affinity transporter
CK	choline kinase
CPT	CDP-choline: 1,2-diacylglycerol cholinephosphotransferase
CRE	cAMP response element
CS	choline-supplemented
CT	CTP:phosphorylcholine cytidylyltransferase
ELISA	enzyme-linked immunosorbent assay
ER	endoplasmic reticulum
ET	CTP:phosphoethanolamine cytidylyltransferase

ETi	RNA interference targeted to ET
FITC	fluorescein isothiocyanate
FPLC	fast-phase liquid chromatography
GFP	green fluorescent protein
GPC	glycerophosphocholine
GR	glucocorticoid receptor
HDL	high density lipoprotein
HPLC	high performance liquid chromatography
HRP	horseradish peroxidase
LDL	low density lipoprotein
LUV	large unilamellar vesicle
lysoPC	lysophosphatidylcholine
MAM	mitochondria-associated membrane
MCD	methionine- and choline- deficient
MDR2	multiple drug resistant protein 2, murine ABCB4
MDR3	multiple drug resistant protein 3, human ABCB4
Met	methionine
NASH	non-alcoholic steatohepatitis
NF-κB	nuclear factor kappa B
PAGE	polyacrylamide gel electrophoresis
PC	phosphatidylcholine
PE	phosphatidylethanolamine
PEMT	phosphatidylethanolamine *N*-methyltransferase

PFIC3	progressive familial intrahepatic cholestasis type 3
PI-PLC	phosphatidylinositol-PLC
PLA_2/A_1	phospholipase A_2 and A_1
PLC	phospholipase C
PLD	phospholipase D
PKC	protein kinase C
PS	phosphatidylserine
PSS1	phosphatidylserine synthase 1
PVDF	polyvinylidene fluoride
RNAi	RNA interference
SM	sphingomyelin
TMB	3, 3', 5, 5'-tetramethylbenzidine
TG	triacylglycerol
VLDL	very low density lipoprotein

Chapter 1

Introduction to Choline

1.1 History of choline

Choline means bile alkline, which is from the original finding of this compound in ox bile (the Greek word is chole) in 1862 (1). Choline is alkaline and hydrophilic. Choline is composed of 3 methyl groups and one ethanol bound to nitrogen (Fig. 1.1). At the beginning of 20th century, people started to realize the importance of choline. In 1932, Charles Best (who was one of the founders of insulin) first reported that choline was an important nutrient for mammals (2). After intense research on choline in the middle of the 20th century (3), choline has become a nutritional topic today (4-8). However, some basic mechanisms of choline metabolism *in vivo* are still unclear. For instance, choline deprivation is not lethal in rodents and humans so it has never been clear that choline is essential for mammalian life despite claims that choline is an essential nutrient (4,8). In 1998, a recommendation for daily intake for humans was made by the 'Food and Nutrition Board' in the U.S. The recommended intake of choline for adults is ~500 mg/day (equal to ~1250 mg choline bitartrate a day). In 2001, U.S. Food and Drug Administration (FDA) released "Nutrient Content Claims Notification for Choline Containing Foods". At this time, choline was officially approved as a nutraceutical (nutrition + pharmaceutical) drug. In addition, several choline derivatives, such as citicoline (CDP-choline) (9,10) and betaine (11), were used in clinical therapy.

1.2 Choline homeostasis

In animals, there are two choline acquisition pathways, including dietary choline intake and the endogenous biosynthesis of choline through the methylations of phosphatidylethanolamine (PE) into phosphatidylcholine (PC) catalyzed by PE *N*-methyltransferase (PEMT) (12), which is the only endogenous pathway of choline biosynthesis (Fig. 1.2). Either exogenous or endogenous choline flows to phosphatidylcholine (PC), which is the major choline metabolite accounting for about 95% of total choline-containing metabolites (5,13). PEMT is found in a significant amount only in the livers of animals and accounts for about 30% of hepatic PC biosynthesis (14-17). The other 70% of hepatic PC is made via the CDP-choline pathway. Intestinal absorption of dietary choline is in the form of lysophosphatidylcholine (lysoPC) and free choline, and the latter is mediated by choline transporters (18). Once choline enters the cell, choline is incorporated into PC via the CDP-choline pathway, in which the rate-limiting step is the conversion of phosphocholine into CDP-choline catalyzed by CTP:phosphocholine cytidylyltransferase (CT) (19). In addition, in the CDP-choline pathway, free choline is phosphorylated to phosphocholine by choline kinase (CK) and CDP-choline is converted into PC with diacylglycerol by CDP-choline: 1,2-diacylglycerol cholinephosphotransferase (CPT) (19). PC is degraded to lysoPC and fatty acid by phospholipases A_2 or A_1 (PLA_2/A_1), into phosphocholine by phospholipase C (PLC) and into free choline by phospholipase D (PLD) and phosphatidylserine synthase 1 (PSS1) (12,20). LysoPC can be reacylated into PC. LysoPC is further degraded into glycerophosphocholine (GPC) and free choline by lysophospholipase and glycerophosphocholinediesterase. The conversion from free choline to acetylcholine is catalyzed by acetylcholine synthase, which is reversible by another enzyme acetylcholine esterase. PC provides phosphocholine for sphingomyelin synthesis (12). In addition, a trace amount of choline is incorporated into ether-linked lipids including plasmanylcholine, choline plasmalogen, platelet-activating factor (PAF) and PAF analogs (21). Choline can be depleted from two ways: catabolism and excretion. The only catabolic pathway of choline is the oxidation of choline to betaine, which is catalyzed by choline oxidase and betaine aldehyde dehydrogenase (12). In the liver betaine is an important donor of methyl group for methionine biosynthesis (12). In addition, choline can be depleted from biliary secretion of PC which is a quantitatively important fate of hepatic PC. The liver of a 20 g mouse contains ~20 mg of PC and secretes ~23 mg of PC into bile each day (22). Transporting PC from hepatocytes into bile is only mediated by a PC-specific flippase, multiple drug resistant protein 2 (MDR2 in mice, MDR3 in humans, generally called ABCB4, ATP-binding cassette B4 encoded by *Abcb4* gene), in hepatocyte canalicular membranes (23). Although over 95% of biliary PC is reabsorbed by intestine (24,25), only ~40% of biliary PC is re-delivered to liver (25). Thus, liver loses ~60% of PC from each enterohepatic circulation of biliary PC. However, there is ~ 5% of biliary PC lost from the whole body in each enterohepatic circulation. Therefore, two depletion pathways of choline in animals are excretion biliary PC and choline oxidation (Fig. 1.2).

1.2.1 Choline intake

Choline intake is dependent on the mechanism of choline transport. Two mechanisms of choline transport are involved in choline intake: lysoPC intake and choline transporter-mediated choline intake. It is still unclear which of these is the major pathway of choline transport/intake. LysoPC can freely pass through cell membranes due to its hydrophobicity. As choline is a charged cation, a carrier-mediated transport is required for choline to cross cell membranes. There are two categories of choline transporters: 1) a high affinity, Na+-dependent transporter and 2) a low affinity, Na+-independent transporter. A choline high-affinity transporter (CHT) in the central nervous system was intensely studied recently (26,27). CHT is ubiquitously distributed in all tissues containing cholinergic neurons in mammals (28). The uptake of choline mediated by CHT is believed to be the rate-limiting step in neuronal acetylcholine synthesis (26,27). Choline transporters found in the intestine have a low-affinity for choline(29), however, whether or not there is a CHT in the intestine is still unclear.

1.2.2 Enzymes in choline metabolism

1.2.2.1 Enzymes in PC biosynthesis

1.2.2.1.1 The CDP-choline pathway

1.2.2.1.1.1 Choline kinase (CK)

Once choline enters into cells, the majority of choline is phosphorylated by CK in the cytosol. Alternatively, choline in some tissues can be delivered into mitochondria and oxidized into betaine. CK is ubiquitously localized in all cell types with two isoforms, CKα and CKβ encoded by two genes (30-32). CK can also phosphorylate ethanolamine. The product of CK, phosphocholine and phosphoethanolamine might be involved in cell signaling (33). Recently CK became a potential therapeutic target of cancer (34,35), since CK plays a critical role in cell growth and cell stress/defense (31). Two putative binding sites of AP-1 (activator protein-1) and CRE (cAMP response element) were found in the promoter region of both CK isoforms (31). AP-1 is a critical transcriptional factor in determining life and death (36). Two members of AP-1 superfamily, c-Jun/c-Jun homodimers and c-Jun/c-fos heterodimers have been intensely studied (36). Recent studies from D. Vance's laboratory suggest that c-Jun is involved in the transcriptional regulation of CK (37).

1.2.2.1.1.2 CTP:phosphorylcholine cytidylyltransferase (CT)

Phosphocholine is the largest pool of water-soluble choline-containing metabolites, since CT is the rate-limiting step of PC biosynthesis through the CDP-choline pathway (12). Four isoforms of CTα, CTβ1 (in human only), CTβ2 and CTβ3 have been found in mammals (12,38,39). CTα is the major isoform in all nucleated cells (12,38,39). CTα$^{-/-}$ mice are embryonic lethal (40), but mice with liver-specific deletion of CTα survive normally (41). CT is activated when translocated to membranes and this activation coincides with dephosphorylation of CT (12). CT is feedback regulated by PC levels (12,42). Lipids, such as oleate, phophatidylglycerol and phosphatidylinositol, are potential activators of CT (43-46). Interestingly, CT overexpression enhanced PC biosynthesis but only caused a minor increase in PC levels since it was coupled with activation of PLA_2 (47). Transcriptional regulation of CT has been intensely investigated recently, and Sp-1, Sp-3, TEF4 and Ets-1 (48) have been found to be involved in transcriptional regulation of CT, especially during cell division. Interestingly, the promoter region of CTα also contains a potential binding site of AP-1, a stress-response element, which suggests that CT may also be up-regulated under stress conditions such as choline deprivation.

1.2.2.1.1.3 CDP-choline: 1,2-diacylglycerol cholinephosphotransferase

The final step of the CDP-choline pathway is catalyzed by CPT, which converts diacylglycerol not only into PC with CDP-choline but also into PE with CDP-ethanolamine (49-51). Thus, CPT is also a CDP-ethanolamine: 1,2-diacylglycerol cholinephosphotransferase (EPT).

1.2.2.1.2 The PEMT pathway

A "milestone" in the research of the PEMT pathway is the successful purification of the transmembrane protein PEMT from rat livers in 1987 (52,53). After that, a series of studies were triggered. PEMT catalyzes all three methylation reactions in converting PE to PC (52). In 1993, the rat *Pemt* gene was cloned and subcellular localizations of PEMT were found to be in endoplasmic reticulum (ER) as PEMT1 and in mitochondria-associated membrane (MAM) as PEMT2 (54). Mouse *Pemt* gene was cloned and characterized in 1996 (55), which led to the establishment of the first gene-knockout mouse model in the phospholipid metabolism, *Pemt*$^{-/-}$ mice in 1997 (56). Subsequently, the human *Pemt* gene was cloned in 2001 (57). The topological structure of this transmembrane protein PEMT was investigated (58-60). PEMT contains four transmembrane regions and both the N and C termini of this enzyme are localized on the cytosolic side of the ER (59).

The development of *Pemt*$^{-/-}$ mice illustrated the evolutionary significance of PEMT as a compensatory pathway for PC biosynthesis when the CDP-choline pathway is impaired (61). *Pemt*$^{-/-}$ mice also provided a chance to fully understand the physiological functions of the PEMT pathway beyond the enzyme itself. Based on the model of *Pemt*$^{-/-}$ mice, the PEMT pathway was suggested to account for the major production of homocysteine *in vivo* (62) and promote VLDL assembly and secretion (63) in a gender-dependent manner (64).

1.2.2.2 Enzymes in PC catabolism

1.2.2.2.1 Phospholipase A_1 and A_2

The cleavage of fatty acyl chains from PC is catalyzed by PLA_2 and PLA_1 in mammals (20). These enzymes not only hydrolyze PC but also share a common substrate, all phospholipids. Unlike in bacteria, the activity of PLA_1 in mammals is only found in hepatic lipases (65).

PLA_2 is believed to be quantitatively the most important enzyme for PC catabolism (20). PLA_2 has been actively studied for over a century. The PLA_2 superfamily is composed of at least 11 groups (I ~ XI), among which cytosolic PLA_2 is believed to be the major one involved in phospholipid catabolism, including calcium-dependent PLA_2 ($cPLA_2$) and –independent PLA_2 ($iPLA_2$). The promoter region of cytosolic PLA_2 contains several potential binding sites for transcriptional factors, AP-1, AP-2 (Activator Protein 2), NF-κB (Nuclear factor kappa B), CEBP (CCAAT/enhancer binding protein) and GR (Glucocorticoid receptor), however, none of them has been reported (66).

1.2.2.2.2 Phospholipase C

There are only two categories of PLC, PC-PLC and phosphatidylinositol-PLC (PI-PLC) (65). These two PLCs are mainly involved in cell signaling, since the products from PC-PLC and PI-PLC hydrolysis, diacylglycerol and/or inositol-1,4,5-triphosphate (IP_3) are both second messengers (67).

1.2.2.2.3 Phospholipase D and phosphatidylserine synthase 1

PLD, found in cytosol as well as in membranes, hydrolyzes all headgroups of phospholipids (65,68). Mammalian PLDs are associated with membrane and also cytosolic (69). PLD is intimately involved in signal transduction since the product of PLD hydrolysis, phosphatidic acid (PA) and its dephosphorylated product, diacylglycerol are both signals in cell signaling (70). PSS1 is a special PLD by exchanging a choline headgroup of PC with serine to generate PS (71,72).

1.2.2.3 Enzyme(s) in choline catabolism

The only choline catabolism *in vivo* is choline oxidation, which is catalyzed by choline oxidase and betaine aldehyde dehydrogenase in mitochondria of liver and kidney (12,73-76). Recently a precursor of choline oxidase was purified and cloned from rat liver (77). However, regulation of mammalian choline oxidases is rarely reported (78,79).

1.2.3 ABCB4 (Multiple drug resistant protein 2)

ABCB4 was found to be a PC-specific transporter from an unexpected result when *Abcb4*$^{-/-}$ mice were constructed (23,80). Later on ABCB4 was found to be a flippase and the mechanism of ABCB4-mediated PC transport was elucidated (81,82). MDR2 is a murine member of the ABC transporter family, ABCB4, called MDR3 in human, in the canalicular membrane of hepatocytes. Humans with deficiency or abnormal mutations of MDR3 develop progressive familiar intrahepatic cholestasis type 3 (PFIC3) (83). *Abcb4*$^{-/-}$ mice develop not only into PFIC3-like cholestasis (23,83), but also cholecystolithiasis and hepatolithiasis spontaneously (84). Expression of ABCB4 is regulated by multiple factors, such as bile salts (82) and peroxisome proliferator-activated receptor α (PPARα) (85).

1.3 Functions of choline

Choline itself does not show any significant physiological role, but its metabolites play key roles in maintaining normal life, such as PC, acetylcholine, CDP-choline and betaine. PC is the major phospholipid in animal cells (12). PC has several functions including membrane barrier, lipoprotein metabolism, bile formation and precursors for signaling (12). It is well known that acetylcholine is a neurotransmitter (7,12). Recently, it was reported that CDP-choline was highly correlated with memory capability (10). The only catabolic metabolite of choline, betaine, acts in osmotic regulation and as a methyl donor for methionine biosynthesis (12,73,76).

1.3.1 Functions of PC: membrane integrity, lipoprotein metabolism, bile formation, signaling

1.3.1.1 PC and membrane integrity (phospholipids and membrane integrity)

A fundamental function of phospholipids is to form membrane bilayers which provide membrane-based boundaries both inside and outside the cell. Phospholipids are asymmetrically distributed in the plasma membrane bilayer (86). PC and PE are two major phospholipids in animals. The majority of PC is localized in the outer leaflet of the plasma membrane bilayer while PE is enriched in the inner leaflet. When the headgroups of phospholipids laterally segregate in the monolayer of the plasma membrane, the hexagonal phase-preferring lipid, PE, may form conical structures that are not as tight as the cylindrical structures formed by PC (86). The final process of cell damage is loss of membrane integrity (87,88). Membrane integrity is influenced by many factors including physical structures of membrane lipids, membrane fluidity, membrane permeability, integral membrane proteins and cell skeletal proteins (86,89-92). All these factors can also be influenced by membrane lipid compositions (86,89-92). For instance, membrane fluidity is regulated by the fatty acyl composition of membrane phospholipid, cholesterol content and phospholipid headgroup (86,90). Sphingomyelin converted from PC is another important phospholipid in the plasma membrane, which also affects membrane fluidity (86). A decrease in hepatic PC/PE ratio coincides with an increase in membrane fluidity in both liver nodules and regenerating livers (93). The PC/PE ratio can also affect membrane permeability during liposome fusion (94). The plasma membrane lipid bilayer is traversed by integral membrane proteins and attached by a two-dimensional scaffold of interconnecting membrane skeletal proteins. Interactions between the membrane lipid bilayer and cell skeletal proteins likely contribute to membrane integrity (91). It has been shown that membrane PE has a higher affinity for membrane skeletal proteins than PC (91,95-97), thus an elevated PC/PE ratio may negatively affect the binding of membrane skeletal proteins to the membrane bilayer. Therefore, membrane phospholipid composition may determine membrane integrity, in which the PC/PE ratio may play a key role.

PC biosynthesis is also critical for cell division. During the cell cycle, not only DNA and protein synthesis but also phospholipid synthesis is enhanced to form the new cell membrane. In this process, CT and the CDP-choline pathway for PC biosynthesis is finely regulated to ensure sufficient PC for membrane formation (12).

1.3.1.2 PC and lipoprotein metabolism

Almost all phospholipids in lipoprotein particles are PC (98). Hepatic PC loading to apolipoprotein B (ApoB) is essential for very low density lipoprotein

(VLDL) assembly and secretion, which is responsible for delivering hepatic fat to extrahepatic tissues (98). Lack of hepatic PC causes decreased VLDL secretion and thereby fat accumulation in the liver (61,98). Hepatic PC efflux to apolipoprotein AI (ApoAI) forms preβ high density lipoprotein (HDL), which is capable of receiving PC and cholesterol from peripheral tissues to form mature HDL particles and transporting these lipids to liver for disposal, so called reverse cholesterol transport (99). Reverse lipid transport would be a better description of this process since PC is also reversibly transported in this process.

1.3.1.3 PC and bile formation

Biliary PC secretion is dependent on ABCB4, which is an ATP-binding cassette transporter (23). Biliary PC is a major component of bile micelles. Bile micelles facilitate dietary fat digestion in the intestine. However, fat absorption in the intestine was not affected by a deficiency of biliary PC in *Abcb4*$^{-/-}$ mice (100), even though another component of bile micelles, biliary cholesterol, was also lacking due to ABCB4-deficiency (23). ABCB4-deficiency did not affect biliary secretion of bile acids (23). Thus, deficiency in biliary PC secretion caused cholestasis in both mice models and humans (23,101).

1.3.1.4 PC and cell signaling

PC is also a precursor for cell signaling (102). Several signaling pathways are involved with PC itself or PC metabolites. PC is a precursor for intracellular messengers such as diacylglycerol (102) and ceramide after the conversion of PC into sphingomyelin (103). For example, PC-specific phospholipase C (PC-PLC) hydrolyzes PC into phosphocholine and diacylglycerol, and thereby diacylglycerol stimulates protein kinase C (PKC) -involved signaling (102). The catabolic products of PC, lysoPC (by PLA_2) and phosphatidic acid (by PLD) are both signals of receptor-specific signaling (102). PC is also the precursor of signaling lipids, platelet-activating factor and sphingosylphosphorylcholine (21,103-105). Phosphocholine and/or GPC may be involved in the regulatory mechanism via initiating cell signaling (33).

1.3.2 Acetylcholine: neurotransmitter

Acetylcholine is a neurotransmitter synthesized from choline and acetyl-CoA catalyzed by choline acetyltransferase (7). Neurons that synthesize and release acetylcholine are termed cholinergic neurons. When an action potential reaches the terminus of a presynaptic neuron, a voltage-gated calcium channel is opened. The influx of calcium ions stimulates the exocytosis of presynaptic vesicles containing acetylcholine, which is thereby released into the synaptic cleft. Once released, acetylcholine must be removed rapidly in order to allow repolarization to take place. Acetylcholine is hydrolyzed by the enzyme, acetylcholinesterase, to yield acetate and choline.

1.3.3 CDP-choline: memory capability

In several European countries and Asia, citicoline (CDP-choline) is a frequently prescribed drug for cognitive and memory impairment (10). CDP-choline accelerates recovery from traumatic coma and restores walking ability. Studies suggest that citicoline may protect cell membranes by accelerating PC production; may increase acetylcholine synthesis; improves mental performance in patients with Alzheimer's disease; and even improves memory in elderly patients with memory deficits (10). CDP-choline administration may improve ability to learn and memory (10,106). However, in North America, clinical application of citicoline is still pending by FDA (www.fda.gov).

1.3.4 Betaine: osmotic regulation and methyl donor for methionine biosynthesis

Osmotic regulation of betaine is vital in plants. In animals, higher activity of choline oxidase found in kidney suggested that betaine might also play critical roles in osmotic regulation. This idea is supported by the finding of transporters that transport betaine into kidney medulla (12,73-75). In the liver betaine is an important donor of methyl groups for methionine biosynthesis (76). With a sufficient supply of dietary methionine, the methionine biosynthetic pathway through choline oxidation may be minimal.

1.4 Choline metabolism and liver

Liver possesses the unique endogenous pathway of choline biosynthesis, since the only quantitatively significant PEMT activity was found in the liver (19,54). Liver is also important for lipid secretion via PC-enclosed lipoproteins (VLDL and preβ-HDL), which requires newly synthesized PC (19,107). Lipoproteins have two major functions: one is transporting fat to adipose tissues for storage via VLDL particles; and the other is to deliver peripheral cholesterol back to liver via HDL particles and finally excrete cholesterol into bile. Hepatic PC is secreted into bile to form micelles to promote fat digestion. In addition, liver is the most abundant tissue of choline (13). Thus, liver is the most active organ for choline/PC metabolism. For this reason, this project is mainly focused on the choline metabolism in the liver.

1.5 Choline deficiency

Choline deficiency is not only a symptom in human nutrition but also a powerful tool for research in choline metabolism.

1.5.1 Physiological situations of choline deficiency

Since healthy humans are deficient in choline only during starvation, pregnancy and lactation, studies on choline as an important nutrient have been centered on experimental animals fed a choline-deficient (CD) diet (5,8,108,109). In addition, constant intake of alcohol also causes choline deficiency along with a deficiency of other nutrients (110). Patients with hepatic cirrhosis might also suffer choline deficiency (8,111).

1.5.2 Artificial manipulations of choline deprivation

Unlike gene-deficiency (gene knockout), for a nutrient, it is impossible to achieve 100% deficiency. Thus, blockage of choline acquisition pathways was referred to as choline deficiency. The most frequently used method for generating choline deficiency is feeding animals a CD diet to deprive dietary intake of choline. In 1997, colleagues from D. Vance's lab developed *Pemt*$^{-/-}$ mice to eliminate endogenous choline biosynthesis (56,61). Wild-type mice and rats fed a CD diet and *Pemt*$^{-/-}$ mice fed a normal chow diet behaved normally (56,61,112,113). The blockage of all choline acquisition pathways was achieved by feeding *Pemt*$^{-/-}$ mice a CD diet (61). I shall refer to this as "complete choline deprivation" rather than choline deficiency.

1.5.3 Choline deficiency and liver disorders

Major pathological problems associated with choline deficiency are fatty liver and hepatic dysfunction (2-8). Dietary choline deficiency does not cause liver damage in wild-type mice and rats (61,113). Only when both choline acquisition pathways are blocked (*Pemt*$^{-/-}$ plus CD diet) does liver damage occur (61), which is a unique model of "complete choline deprivation". Complete choline deprivation is lethal, as demonstrated by CD-*Pemt*$^{-/-}$ mice which die of acute liver failure and severe steatohepatitis within 4 ~ 5 days (61). Mice or rats fed a choline- and methionine-deficient (MCD) diet mimic the model of CD-*Pemt*$^{-/-}$ mice to reduce the endogenous biosynthesis of hepatic PC or choline. Since *S*-adenosylmethionine (AdoMet) is a substrate for PEMT and made from methionine (12), dietary deprivation of methionine attenuates the PEMT pathway from depleting the substrate. However, as compared with acute steatohepatitis in CD-*Pemt*$^{-/-}$ mice, it took ~3 months for MCD-wild type mice to developed into similar steatohepatitis (114,115). This probably results from non-complete blockage of the PEMT pathway, since methionine can also be made *de novo* from betaine or methyltetrahydrofolate with homocysteine. Although a short-term (3 weeks to 3 months) of dietary choline deficiency could be compensated by up-regulation of the PEMT pathway (112,113), very long-term (one year) of dietary choline deficiency induced liver tumors, which is believed to result from multiple factors such as increased lipid peroxidation and free radicals (3,116-118).

1.5.4 Choline deficiency and other disorders

Animals fed a choline-deficient diet for a long-term might also develop growth retardation, renal dysfunction and hemorrhage, or bone abnormalities (3,5,7,8); however, most of these studies were performed with a low-methionine diet. Thus, these disorders might result from more severe choline deprivation rather that dietary choline-deficiency alone.

1.6 Thesis objective

Choline is an important nutrient in the diet of animals. Nevertheless, choline deprivation is not lethal in rodents and humans so it has never been clear that choline is essential for mammalian life despite claims that choline is an essential nutrient (4,8). Since animals can acquire choline from both diet and *de novo* biosynthesis via the PEMT pathway, "complete choline deprivation" can only be achieved by eliminating both choline acquisition pathways, that is, feeding *Pemt*$^{-/-}$ mice a choline-deficient (CD) diet. Only under complete choline deprivation, were we able to address whether or not choline is an essential nutrient. As CD-*Pemt*$^{-/-}$ mice died rapidly within 4~5 days, we were not able to illustrate the mechanism of lethality from complete choline deprivation. Therefore, we attempted to prolong the life of CD-*Pemt*$^{-/-}$ mice via blockage of one choline depleting pathway, biliary PC secretion. By constructing a mouse model that lacks both PEMT and ABCB4, we were able to illustrate the mechanism of adaptation to choline deprivation in CD-*Abcb4*$^{-/-}$/*Pemt*$^{-/-}$ mice and thereby the mechanism of lethality of complete choline deprivation in CD-*Pemt*$^{-/-}$ mice. Therefore, the ultimate goal of this thesis is to further demonstrate the importance of choline by illustrating how mice adapt to choline deprivation and which finally leads to the formulation of the "choline balance theory". That is, there is a balance between gain and loss of choline that determines the survival of choline-containing organisms. Besides classical adaptations to choline deprivation such as up-regulation of PEMT, I attempt to demonstrate the existence of several new adaptations to choline deprivation, including choline recycling, maintenance of membrane integrity via maintenance of PC/PE ratio, choline redistribution and choline storage.

PE biosynthesis is composed of the CDP-ethanolamine pathway, PS decarboxylation and sphingosine-1-phosphate lyation. Using the technique of RNA interference (RNAi), I attempt to distinguish the difference among these pathways of PE biosynthesis.

PEMT has been suggested to be a potential tumor suppressor. This thesis will present studies to explore the importance of PEMT in hepatocarcinogenesis by comparing *Pemt*$^{+/+}$ and *Pemt*$^{-/-}$ mice.

To characterize subcellular functions of PEMT, especially PEMT1 in the ER, colleagues from the D. Vance laboratory have been tormented for ~20 years to produce an antibody against PEMT1. This thesis will also describe several attempts to produce an anti-PEMT1 antibody and potential modifications of PEMT1 proteins.

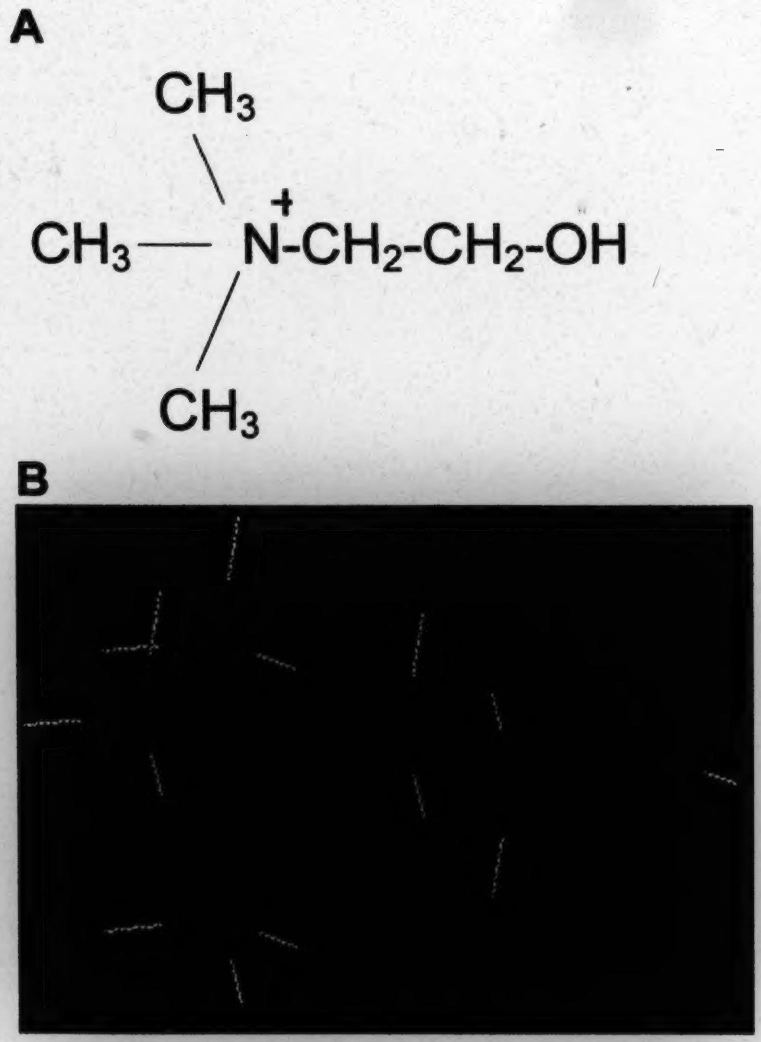
A
CH3
CH3
N-CH2-CH2-OH
+
CH3
B

Fig. 1.1 Structure of choline

(A) Chemical structure of choline; **(B)** 3-D structure of choline. Hydrogen, white; Oxygen, red; Carbon, grey; Nitrogen, blue. Adopted from http://www.natuurlijkerwijs.com/choline3d.htm.

Fig. 1.2 Choline homeostasis

A, in animals, there are two choline acquisition pathways, including dietary choline intake and endogenous biosynthesis from phosphatidylethanolamine (PE) methylation pathway catalyzed by PE *N*-methyltransferase (PEMT), which is the only endogenous pathway for choline biosynthesis (green lines). The only catabolic pathway of choline is the oxidation of choline to betaine, which is catalyzed by choline oxidase and betaine aldehyde dehydrogenase. Two depletion pathways of choline are biliary secretion of PC and choline oxidation (red lines). In addition, PC can be secreted in very low density lipoprotein (VLDL) and brought into liver via high density lipoproteins (HDL). The conversion of free choline into acetylcholine is catalyzed by acetylcholine synthase and acetylcholine hydrolysis catalyzed by acetylcholine esterase. P-choline, phosphocholine; GPC, glycerophosphocholine; CT, CTP:phosphocholine cytidylyltransferase; PEMT, phosphatidylethanolamine *N*-methyltransferase; MDR2, multiple drug resistant protein 2; PC, phosphatidylcholine; PE, phosphatidylethanolamine; AdoMet, *S*-adenosylmethionine; Met, methionine; SM, sphingomyelin; LysoPC, lysophosphatidylcholine. **B**, intestinal choline balance. Biliary PC accounts for ~90% of total choline uptake in the intestine and the rest of 10% is from dietary choline. Over 95% of biliary choline is re-absorbed by intestine and the rest of 5% is excreted in the feces.

A

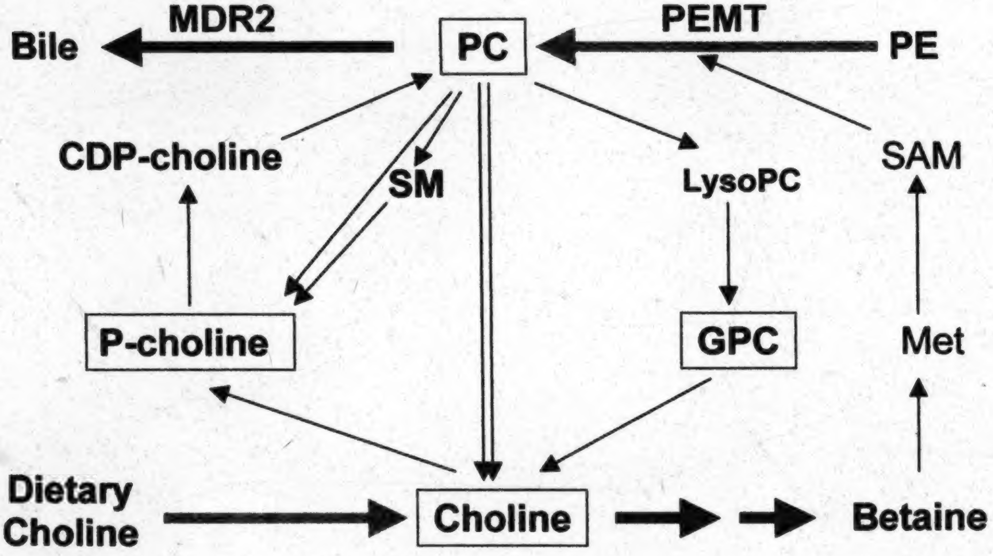

MDR2
PEMT
Bile
PC
PE
CDP-choline
SM
LysoPC
SAM
P-choline
GPC
Met
Dietary Choline
Choline
Betaine

B

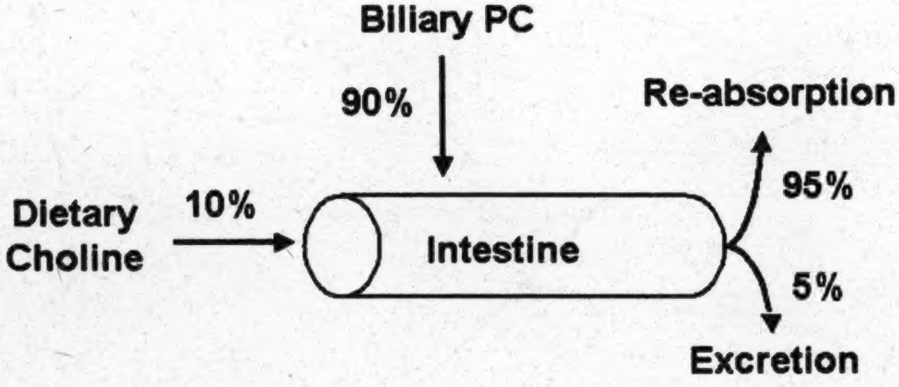

Biliary PC
90%
Re-absorption
95%
Dietary Choline
10%
Intestine
5%
Excretion

References

1. Strecker, A. Uber eingige neue Bestandtheile der Schweinegalle. (1862) *Ann Chem Pharmacie* **183**, 964-965

2. Best, C. H., and Huntsman, M. E. The effects of the components of lecithine upon deposition of fat in the liver. (1932) *Journal of Physiology-London* **75**, 405-412

3. Best, C. H., Lucas, C. C., and Ridout, J. H. The lipotropic factors. (1954) *Ann N Y Acad Sci* **57**, 646-653

4. Zeisel, S. H., Da Costa, K. A., Franklin, P. D., Alexander, E. A., Lamont, J. T., Sheard, N. F., and Beiser, A. Choline, an essential nutrient for humans. (1991) *Faseb J* **5**, 2093-2098

5. Zeisel, S. H., and Blusztajn, J. K. Choline and human nutrition. (1994) *Annu Rev Nutr* **14**, 269-296

6. Zeisel, S. H. Choline. A nutrient that is involved in the regulation of cell proliferation, cell death, and cell transformation. (1996) *Adv Exp Med Biol* **399**, 131-141

7. Blusztajn, J. K. Choline, a vital amine. (1998) *Science* **281**, 794-795

8. Zeisel, S. H. Choline: an essential nutrient for humans. (2000) *Nutrition* **16**, 669-671

9. Adibhatla, R. M., and Hatcher, J. F. Cytidine 5'-diphosphocholine (CDP-choline) in stroke and other CNS disorders. (2005) *Neurochem Res* **30**, 15-23

10. Fioravanti, M., and Yanagi, M. Cytidinediphosphocholine (CDP-choline) for cognitive and behavioural disturbances associated with chronic cerebral disorders in the elderly. (2005) *Cochrane Database Syst Rev*, CD000269

11. Abdelmalek, M. F., Angulo, P., Jorgensen, R. A., Sylvestre, P. B., and Lindor, K. D. Betaine, a promising new agent for patients with nonalcoholic steatohepatitis: results of a pilot study. (2001) *Am J Gastroenterol* **96**, 2711-2717

12. Vance, D. E. *Phospholipid biosynthesis in eukaryotes.* (2002) in *Biochemistry of lipids, lipoproteins and membranes* (Vance, D. E., J. E. Vance, ed), pp. 205-232, Elsevier, New York

13. Zeisel, S. H., Mar, M. H., Howe, J. C., and Holden, J. M. Concentrations of choline-containing compounds and betaine in common foods. (2003) *J Nutr* **133**, 1302-1307

14. Sundler, R., and Akesson, B. Regulation of phospholipid biosynthesis in isolated rat hepatocytes. Effect of different substrates. (1975) *J. Biol. Chem.* **250**, 3359-3367

15. DeLong, C. J., Shen, Y.-J., Thomas, M. J., and Cui, Z. Molecular distinction of phosphatidylcholine synthesis between the CDP-choline pathway and phosphatidylethanolamine methylation pathway. (1999) *J. Biol. Chem.* **274**, 29683-29688

16. Reo, N. V., Adinehzadeh, M., and Foy, B. D. Kinetic analyses of liver phosphatidylcholine and phosphatidylethanolamine biosynthesis using (13)C NMR spectroscopy. (2002) *Biochim Biophys Acta* **1580**, 171-188.

17. Agellon, L. B., Walkey, C. J., Vance, D. E., Kuipers, F., and Verkade, H. J. The unique acyl chain specificity of biliary phosphatidylcholines in mice is independent of their biosynthetic origin in the liver. (1999) *Hepatology* **30**, 725-729

18. Tso, P., and Fujimoto, K. The absorption and transport of lipids by the small intestine. (1991) *Brain Res Bull* **27**, 477-482

19. Vance, D. E. *Biochemistry of lipids, lipoproteins and membranes* (2002) in *Biochemistry of Lipids, Lipoprotein and Membranes, 4th edition.* (Vance, D. E., J. E. Vance, ed), pp. 205-232, Elsevier, New York

20. Waite, M. Phospholipases, enzymes that share a substrate class. (1990) *Adv Exp Med Biol* **279**, 1-22

21. Snyder, F., Lee, T., and Wykle, R. L. *Ether-linked lipids and their bioactive species.* (2002) in *Biochemistry of lipids, lipoproteins and membranes* (Vance, D. E., J. E. Vance, ed), pp. 223-262, Elsevier, New York

22. Kuipers, F., Oude Elferink, R. P., Verkade, H. J., and Groen, A. K. Mechanisms and (patho)physiological significance of biliary cholesterol secretion. (1997) *Subcell Biochem* **28**, 295-318

23. Smit, J. J., Schinkel, A. H., Oude Elferink, R. P., Groen, A. K., Wagenaar, E., van Deemter, L., Mol, C. A., Ottenhoff, R., van der Lugt, N. M., van Roon, M. A., and et al. Homozygous disruption of the murine mdr2 P-

glycoprotein gene leads to a complete absence of phospholipid from bile and to liver disease. (1993) *Cell* **75**, 451-462

24. Borgstrom, B. (1976) *Phospholipid absorption*. Lipid absorption (Rommel, K., H. Goebell, R. Bohmer, Ed.), MTP Press Ltd., London
25. Robins, S. J. Recirculation and reutilization of micellar bile lecithin. (1975) *Am J Physiol* **229**, 598-602
26. Okuda, T., and Haga, T. High-affinity choline transporter. (2003) *Neurochem Res* **28**, 483-488
27. Lockman, P. R., and Allen, D. D. The transport of choline. (2002) *Drug Dev Ind Pharm* **28**, 749-771
28. Okuda, T., and Haga, T. Functional characterization of the human high-affinity choline transporter. (2000) *FEBS Lett* **484**, 92-97
29. Kamath, A. V., Darling, I. M., and Morris, M. E. Choline uptake in human intestinal Caco-2 cells is carrier-mediated. (2003) *J Nutr* **133**, 2607-2611
30. Aoyama, C., Ohtani, A., and Ishidate, K. Expression and characterization of the active molecular forms of choline/ethanolamine kinase-alpha and -beta in mouse tissues, including carbon tetrachloride-induced liver. (2002) *Biochem J* **363**, 777-784
31. Aoyama, C., Liao, H., and Ishidate, K. Structure and function of choline kinase isoforms in mammalian cells. (2004) *Prog Lipid Res* **43**, 266-281
32. Aoyama, C., Yamazaki, N., Terada, H., and Ishidate, K. Structure and characterization of the genes for murine choline/ethanolamine kinase isozymes alpha and beta. (2000) *J Lipid Res* **41**, 452-464

33. Kiss, Z. Regulation of mitogenesis by water-soluble phospholipid intermediates. (1999) *Cell Signal* **11**, 149-157

34. Lacal, J. C. Choline kinase: a novel target for antitumor drugs. (2001) *IDrugs* **4**, 419-426

35. Rodriguez-Gonzalez, A., Ramirez de Molina, A., Benitez-Rajal, J., and Lacal, J. C. Phospholipase D and choline kinase: their role in cancer development and their potential as drug targets. (2003) *Prog Cell Cycle Res* **5**, 191-201

36. Shaulian, E., and Karin, M. AP-1 as a regulator of cell life and death. (2002) *Nat Cell Biol* **4**, E131-136

37. Aoyama, C., Ishidate, K., and Vance, D. E. *unpublished results*

38. Kent, C. Regulatory enzymes of phosphatidylcholine biosynthesis: a personal perspective. (2005) *Biochim Biophys Acta* **1733**, 53-66

39. Jackowski, S., and Fagone, P. CTP: Phosphocholine cytidylyltransferase: paving the way from gene to membrane. (2005) *J Biol Chem* **280**, 853-856

40. Wang, L., Magdaleno, S., Tabas, I., and Jackowski, S. Early embryonic lethality in mice with targeted deletion of the CTP:phosphocholine cytidylyltransferase alpha gene (Pcyt1a). (2005) *Mol Cell Biol* **25**, 3357-3363

41. Jacobs, R. L., Devlin, C., Tabas, I., and Vance, D. E. Targeted deletion of hepatic CTP:phosphocholine cytidylyltransferase alpha in mice decreases

plasma high density and very low density lipoproteins. (2004) *J Biol Chem* **279**, 47402-47410

6

42. Jamil, H., Yao, Z. M., and Vance, D. E. Feedback regulation of CTP:phosphocholine cytidylyltransferase translocation between cytosol and endoplasmic reticulum by phosphatidylcholine. (1990) *J Biol Chem* **265**, 4332-4339
43. Fiscus, W. G., and Schneider, W. C. The role of phospholipids in stimulating phosphorylcholine cytidyltransferase activity. (1966) *J Biol Chem* **241**, 3324-3330
44. Feldman, D. A., and Weinhold, P. A. CTP:phosphorylcholine cytidylyltransferase from rat liver. Isolation and characterization of the catalytic subunit. (1987) *J Biol Chem* **262**, 9075-9081
45. Cornell, R. B. Regulation of CTP:phosphocholine cytidylyltransferase by lipids. 1. Negative surface charge dependence for activation. (1991) *Biochemistry* **30**, 5873-5880
46. Clement, J. M., and Kent, C. CTP:phosphocholine cytidylyltransferase: insights into regulatory mechanisms and novel functions. (1999) *Biochem Biophys Res Commun* **257**, 643-650
47. Walkey, C. J., Kalmar, G. B., and Cornell, R. B. Overexpression of rat liver CTP:phosphocholine cytidylyltransferase accelerates phosphatidylcholine synthesis and degradation. (1994) *J Biol Chem* **269**, 5742-5749
48. Sugimoto, H., Okamura, K., Sugimoto, S., Satou, M., Hattori, T., Vance, D. E., and Izumi, T. Sp1 is a co-activator with Ets-1, and net is an important

repressor of the transcription of CTP: Phosphocholine cytidylyltransferase alpha. (2005) *J Biol Chem* in press

49. Wright, M. M., and McMaster, C. R. PC and PE synthesis: mixed micellar analysis of the cholinephosphotransferase and ethanolaminephosphotransferase activities of human choline/ethanolamine phosphotransferase 1 (CEPT1). (2002) *Lipids* **37**, 663-672

50. Henneberry, A. L., and McMaster, C. R. Cloning and expression of a human choline/ethanolaminephosphotransferase: synthesis of phosphatidylcholine and phosphatidylethanolamine. (1999) *Biochem J* **339 (Pt 2)**, 291-298

51. McMaster, C. R., and Bell, R. M. CDP-choline:1,2-diacylglycerol cholinephosphotransferase. (1997) *Biochim Biophys Acta* **1348**, 100-110

52. Ridgway, N. D., and Vance, D. E. Purification of phosphatidylethanolamine N-methyltransferase from rat liver. (1987) *J Biol Chem* **262**, 17231-17239

53. Ridgway, N. D., and Vance, D. E. Phosphatidylethanolamine N-methyltransferase from rat liver. (1992) *Methods Enzymol* **209**, 366-374

54. Cui, Z., Vance, J. E., Chen, M. H., Voelker, D. R., and Vance, D. E. Cloning and expression of a novel phosphatidylethanolamine N-methyltransferase. A specific biochemical and cytological marker for a unique membrane fraction in rat liver. (1993) *J Biol Chem* **268**, 16655-16663

55. Walkey, C. J., Cui, Z., Agellon, L. B., and Vance, D. E. Characterization of the murine phosphatidylethanolamine N-methyltransferase-2 gene. (1996) *J Lipid Res* **37**, 2341-2350

56. Walkey, C. J., Donohue, L. R., Bronson, R., Agellon, L. B., and Vance, D. E. Disruption of the murine gene encoding phosphatidylethanolamine N-methyltransferase. (1997) *Proc Natl Acad Sci U S A* **94**, 12880-12885

57. Shields, D. J., Agellon, L. B., and Vance, D. E. Structure, expression profile and alternative processing of the human phosphatidylethanolamine N-methyltransferase (PEMT) gene. (2001) *Biochim Biophys Acta* **1532**, 105-114

58. Shields, D. J., Altarejos, J. Y., Wang, X., Agellon, L. B., and Vance, D. E. Molecular dissection of the S-adenosylmethionine-binding site of phosphatidylethanolamine N-methyltransferase. (2003) *J Biol Chem* **278**, 35826-35836

59. Shields, D. J., Lehner, R., Agellon, L. B., and Vance, D. E. Membrane topography of human phosphatidylethanolamine N-methyltransferase. (2003) *J Biol Chem* **278**, 2956-2962

60. Shields, D. J., Lingrell, S., Agellon, L. B., Brosnan, J. T., and Vance, D. E. Localization-independent regulation of homocysteine secretion by phosphatidylethanolamine N-methyltransferase. (2005) *J Biol Chem* **280**, 27339-27344

61. Walkey, C. J., Yu, L., Agellon, L. B., and Vance, D. E. Biochemical and evolutionary significance of phospholipid methylation. (1998) *J Biol Chem* **273**, 27043-27046

62. Noga, A. A., Stead, L. M., Zhao, Y., Brosnan, M. E., Brosnan, J. T., and Vance, D. E. Plasma homocysteine is regulated by phospholipid methylation. (2003) *J Biol Chem* **278**, 5952-5955

63. Noga, A. A., Zhao, Y., and Vance, D. E. An unexpected requirement for phosphatidylethanolamine N-methyltransferase in the secretion of very low density lipoproteins. (2002) *J Biol Chem* **277**, 42358-42365

64. Noga, A. A., and Vance, D. E. A gender-specific role for phosphatidylethanolamine N-methyltransferase-derived phosphatidylcholine in the regulation of plasma high density and very low density lipoproteins in mice. (2003) *J Biol Chem* **278**, 21851-21859

65. Wilton, D. C., and Waite, M. *Phospholipases* (2002) in *Biochemistry of lipids, lipoproteins and membranes* (Vance, D. E., J. E. Vance, ed), pp. 291-314, Elsevier, New York

66. Hirabayashi, T., and Shimizu, T. Localization and regulation of cytosolic phospholipase A(2). (2000) *Biochim Biophys Acta* **1488**, 124-138

67. Ventura, C., and Maioli, M. Protein kinase C control of gene expression. (2001) *Crit Rev Eukaryot Gene Expr* **11**, 243-267

68. Jenkins, G. M., and Frohman, M. A. Phospholipase D: a lipid centric review. (2005) *Cell Mol Life Sci*

69. Wang, P., Anthes, J. C., Siegel, M. I., Egan, R. W., and Billah, M. M. Existence of cytosolic phospholipase D. Identification and comparison with membrane-bound enzyme. (1991) *J Biol Chem* **266**, 14877-14880

70. Foster, D. A., and Xu, L. Phospholipase d in cell proliferation and cancer. (2003) *Mol Cancer Res* **1**, 789-800

71. Vance, J. E., and Vance, D. E. Phospholipid biosynthesis in mammalian cells. (2004) *Biochem Cell Biol* **82**, 113-128

72. Vance, J. E. Molecular and cell biology of phosphatidylserine and phosphatidylethanolamine metabolism. (2003) *Prog Nucleic Acid Res Mol Biol* **75**, 69-111

73. Yamauchi, A., Uchida, S., Kwon, H. M., Preston, A. S., Robey, R. B., Garcia-Perez, A., Burg, M. B., and Handler, J. S. Cloning of a Na(+)- and Cl(-)-dependent betaine transporter that is regulated by hypertonicity. (1992) *J Biol Chem* **267**, 649-652

74. Handler, J. S., and Kwon, H. M. Regulation of the myo-inositol and betaine cotransporters by tonicity. (1996) *Kidney Int* **49**, 1682-1683

75. Kempson, S. A., and Montrose, M. H. Osmotic regulation of renal betaine transport: transcription and beyond. (2004) *Pflugers Arch* **449**, 227-234

76. Barak, A. J., Beckenhauer, H. C., and Tuma, D. J. Betaine, ethanol, and the liver: a review. (1996) *Alcohol* **13**, 395-398

77. Huang, S., and Lin, Q. Functional expression and processing of rat choline dehydrogenase precursor. (2003) *Biochem Biophys Res Commun* **309**, 344-350

78. Schneider, W. J., and Vance, D. E. Effect of choline deficiency on the enzymes that synthesize phosphatidylcholine and phosphatidylethanolamine in rat liver. (1978) *Eur J Biochem* **85**, 181-187

79. Li, Z., Agellon, L. B., and Vance, D. E. Phosphatidylcholine homeostasis and liver failure. (2005) *J Biol Chem*

80. Vance, J. E., and Vance, D. E. Metabolic insights into phospholipid function using gene-targeted mice. (2005) *J Biol Chem* **280**, 10877-10880

81. Ruetz, S., and Gros, P. Phosphatidylcholine translocase: a physiological role for the mdr2 gene. (1994) *Cell* **77**, 1071-1081

82. Ruetz, S., and Gros, P. Enhancement of Mdr2-mediated phosphatidylcholine translocation by the bile salt taurocholate. Implications for hepatic bile formation. (1995) *J Biol Chem* **270**, 25388-25395

83. Elferink, R. O. Cholestasis. (2003) *Gut* **52 Suppl 2**, ii42-48

84. Lammert, F., Wang, D. Q., Hillebrandt, S., Geier, A., Fickert, P., Trauner, M., Matern, S., Paigen, B., and Carey, M. C. Spontaneous cholecysto- and hepatolithiasis in Mdr2-/- mice: a model for low phospholipid-associated cholelithiasis. (2004) *Hepatology* **39**, 117-128

85. Kok, T., Bloks, V. W., Wolters, H., Havinga, R., Jansen, P. L., Staels, B., and Kuipers, F. Peroxisome proliferator-activated receptor alpha (PPARalpha)-mediated regulation of multidrug resistance 2 (Mdr2) expression and function in mice. (2003) *Biochem J* **369**, 539-547

86. Cullis, P. R., Fenske, D. B., and Hope, M. J. *Physical properties and functional roles of lipids in membranes.* (1996) in *Biochemistry of lipids, lipoproteins and membranes* (Vance, D. E., J. E. Vance, ed), pp. 1-34, Elsevier, New York

87. Schmidt, E., and Schmidt, F. W. Enzyme release. (1987) *J Clin Chem Clin Biochem* **25**, 525-540

88. Kristensen, S. R. Mechanisms of cell damage and enzyme release. (1994) *Dan Med Bull* **41**, 423-433

89. Lenaz, G. The role of lipids in the structure and function of membranes. (1979) *Subcell Biochem* **6**, 233-343

90. Schachter, D. Fluidity and function of hepatocyte plasma membranes. (1984) *Hepatology* **4**, 140-151

91. Sikorski, A. F., Hanus-Lorenz, B., Jezierski, A., and Dluzewski, A. R. Interaction of membrane skeletal proteins with membrane lipid domain. (2000) *Acta Biochim Pol* **47**, 565-578

92. Edidin, M. Lipids on the frontier: a century of cell-membrane bilayers. (2003) *Nat Rev Mol Cell Biol* **4**, 414-418

93. Abel, S., Smuts, C. M., de Villiers, C., and Gelderblom, W. C. Changes in essential fatty acid patterns associated with normal liver regeneration and the progression of hepatocyte nodules in rat hepatocarcinogenesis. (2001) *Carcinogenesis* **22**, 795-804

94. Haque, M. E., McIntosh, T. J., and Lentz, B. R. Influence of lipid composition on physical properties and peg-mediated fusion of curved and

uncurved model membrane vesicles: "nature's own" fusogenic lipid bilayer. (2001) *Biochemistry* **40**, 4340-4348

95. Michalak, K., Bobrowska, M., Bialkowska, K., Szopa, J., and Sikorski, A. F. Interaction of erythrocyte spectrin with some nonbilayer phospholipids. (1994) *Gen Physiol Biophys* **13**, 57-62

96. Diakowski, W., and Sikorski, A. F. Brain spectrin interacts with membrane phospholipids. (1994) *Acta Biochim Pol* **41**, 153-154

97. Diakowski, W., Prychidny, A., Swistak, M., Nietubyc, M., Bialkowska, K., Szopa, J., and Sikorski, A. F. Brain spectrin (fodrin) interacts with phospholipids as revealed by intrinsic fluorescence quenching and monolayer experiments. (1999) *Biochem J* **338 (Pt 1)**, 83-90

98. Vance, J. E. *Assembly and secretion of lipoproteins* (2002) in *Biochemistry of lipids, lipoproteins and membranes* (Vance, D. E., J. E. Vance, ed), pp. 505-526, Elsevier, New York

99. Fielding, P. E., and Fielding, C. J. *Dynamics of lipoprotein transport in the human circulatory system* (2002) in *Biochemistry of lipids, lipoproteins and membranes* (Vance, D. E., J. E. Vance, ed), pp. 527-552, Elsevier, New York

100. Voshol, P. J., Minich, D. M., Havinga, R., Elferink, R. P., Verkade, H. J., Groen, A. K., and Kuipers, F. Postprandial chylomicron formation and fat absorption in multidrug resistance gene 2 P-glycoprotein-deficient mice. (2000) *Gastroenterology* **118**, 173-182

101. Jacquemin, E. Role of multidrug resistance 3 deficiency in pediatric and adult liver disease: one gene for three diseases. (2001) *Semin Liver Dis* **21**, 551-562

102. McPhail, L. C. *Glycolipids in signal transduction* (2002) in *Biochemistry of lipids, lipoproteins and membranes* (Vance, D. E., J. E. Vance, ed), pp. 315-340, Elsevier, New York

103. Merrill Jr., A. H., and Sandhoff, K. *Sphingolipids: metabolism and cell signaling* (2002) in *Biochemistry of lipids, lipoproteins and membranes* (Vance, D. E., J. E. Vance, ed), pp. 373-408, Elsevier, New York

104. Seufferlein, T., and Rozengurt, E. Sphingosylphosphorylcholine activation of mitogen-activated protein kinase in Swiss 3T3 cells requires protein kinase C and a pertussis toxin-sensitive G protein. (1995) *J Biol Chem* **270**, 24334-24342

105. Spiegel, S., and Milstien, S. Sphingolipid metabolites: members of a new class of lipid second messengers. (1995) *J Membr Biol* **146**, 225-237

106. Agut, J., and Ortiz, J. A. Age-related changes in memory and their pharmacologic modulation. (1991) *Ann N Y Acad Sci* **640**, 295-297

107. Vance, J. E., and Vance, D. E. Lipoprotein assembly and secretion by hepatocytes. (1990) *Annu Rev Nutr* **10**, 337-356

108. Kuksis, A., and Mookerjea, S. Choline. (1978) *Nutr Rev* **36**, 201-207

109. Zeisel, S. H., Mar, M. H., Zhou, Z., and da Costa, K. A. Pregnancy and lactation are associated with diminished concentrations of choline and its metabolites in rat liver. (1995) *J Nutr* **125**, 3049-3054

110. Sinclair, H. M. Nutritional aspects of alcohol consumption. (1972) *Proc Nutr Soc* **31**, 117-123

111. Chawla, R. K., Wolf, D. C., Kutner, M. H., and Bonkovsky, H. L. Choline may be an essential nutrient in malnourished patients with cirrhosis. (1989) *Gastroenterology* **97**, 1514-1520

112. Cui, Z., and Vance, D. E. Expression of phosphatidylethanolamine N-methyltransferase-2 is markedly enhanced in long term choline-deficient rats. (1996) *J Biol Chem* **271**, 2839-2843

113. Yao, Z. M., Jamil, H., and Vance, D. E. Choline deficiency causes translocation of CTP:phosphocholine cytidylyltransferase from cytosol to endoplasmic reticulum in rat liver. (1990) *J Biol Chem* **265**, 4326-4331

114. Weltman, M. D., Farrell, G. C., and Liddle, C. Increased hepatocyte CYP2E1 expression in a rat nutritional model of hepatic steatosis with inflammation. (1996) *Gastroenterology* **111**, 1645-1653

115. Koteish, A., and Mae Diehl, A. Animal models of steatohepatitis. (2002) *Best Pract Res Clin Gastroenterol* **16**, 679-690

116. Perera, M. I., Betschart, J. M., Virji, M. A., Katyal, S. L., and Shinozuka, H. Free radical injury and liver tumor promotion. (1987) *Toxicol Pathol* **15**, 51-59

117. Zeisel, S. H., da Costa, K. A., Albright, C. D., and Shin, O. H. Choline and hepatocarcinogenesis in the rat. (1995) *Adv Exp Med Biol* **375**, 65-74

118. Albright, C. D., Liu, R., Mar, M. H., Shin, O. H., Vrablic, A. S., Salganik, R. I., and Zeisel, S. H. Diet, apoptosis, and carcinogenesis. (1997) *Adv Exp Med Biol* **422**, 97-107

Chapter 2

Choline is an Essential Nutrient

--- Adaptation to Choline Deprivation I: Choline Recycling

This chapter was published in *The Journal of Biological Chemistry*, 2005.

2.1 Introduction

Choline is an important nutrient in the diet of animals (1-6). Nevertheless, choline deprivation is not lethal in rodents and humans so it has never been clear that choline is essential for mammalian life despite claims that choline is an essential nutrient (3,6). Pathological problems associated with dietary choline deficiency are fatty liver and hepatic dysfunction (1-6). Choline can be converted to phosphatidylcholine (PC) via the CDP-choline pathway or can be oxidized to betaine (Fig. 2.1). In liver, PC can also be generated via methylation of phosphatidylethanolamine (PE) by the enzyme PE *N*-methyltransferase (PEMT). PC accounts for ~95% of choline-containing compounds in the liver; others include sphingomyelin, lysoPC, glycerophosphocholine (GPC), phosphocholine and choline. PC can be catabolized by phospholipase A_2 (PLA_2), C, D and phosphatidylserine synthase 1 or can be converted to sphingomyelin. A quantitatively important fate of hepatic PC is secretion into bile, mediated by a PC-specific flippase, multi-drug resistant protein 2 (MDR2 in mice, MDR3 in humans, also called ABCB4), in hepatocyte canalicular membranes (Fig. 2.1) (7).

PEMT has an important role in hepatic PC biosynthesis. Additionally, PEMT coupled to PC catabolism is the only pathway for endogenous choline biosynthesis in animals. Insight into the essential role for PEMT came from studies in *Pemt*$^{-/-}$ mice. Whereas wild-type mice fed a choline-deficient (CD) diet developed mild fatty liver, mice that lacked PEMT exhibited liver failure within 3 days and died at 4~5 days (8). *Pemt*$^{-/-}$ mice fed a CD diet are also a unique model for "complete" choline deprivation since choline can neither be acquired from the diet nor made endogenously.

Because complete choline deprivation is rapidly lethal in CD-*Pemt*$^{-/-}$ mice, a study of metabolic adaptations to a complete lack of choline is not feasible. However, development of a new mouse model provided us with an opportunity to investigate adaptive mechanisms triggered by complete choline deprivation. The liver of a 20 g mouse contains ~20 mg of PC and secretes ~23 mg of PC into bile each day (9). Since livers from *Pemt*$^{-/-}$ mice lose ~50% of their hepatic PC when fed a CD diet for 3 days (8), we speculated that the rapid liver failure in *Pemt*$^{-/-}$ mice fed a CD diet was due to rapid depletion of hepatic PC by export into bile. To test this hypothesis we have bred *Pemt*$^{-/-}$ mice with mice lacking ABCB4. Remarkably, *Abcb4*$^{-/-}$/*Pemt*$^{-/-}$ mice live for at least 90 days when fed a CD diet. Development of the CD-*Abcb4*$^{-/-}$/*Pemt*$^{-/-}$ mouse model enabled us to demonstrate that choline is an essential nutrient.

2.2 Materials and Methods

2.2.1 Animals

Abcb4$^{-/-}$/*Pemt*$^{-/-}$ mice were produced by breeding *Pemt*$^{-/-}$ mice (C57BL/6; 129/J background) (10) with *Abcb4*$^{-/-}$ mice (FVB; 129/J background) (7). The mice were fed a choline-deficient (CD) diet, a semi-synthetic diet without choline (*ICN*, Cat#0290138710) or a choline-supplemented (CS) diet (a CD diet containing 0.4% (w/w) choline chloride). At the age of 10 to 12 weeks, *Pemt*$^{-/-}$ and *Abcb4*$^{-/-}$/*Pemt*$^{-/-}$ mice were fed a CS diet for 24 h and then switched to a CD diet for 3 to 90 days. Mice were fasted for 12 h before sacrifice. Four to eight mice of each gender were used for each time point in all experiments and assays were performed in duplicate. All data are given as means ± S.D.

2.2.2 Genotyping

As PCR templates, genomic DNA from tails of mice was extracted with a DNeasy Tissue Kit (*Qiagen*). Specific PCR reactions were used to distinguish between wild type and knockout alleles containing a neomycin resistance gene (*neo*^{r}) (Fig. 2.2). Primer sequences: 1, for *Pemt* gene, forward primer (F): 5'-GAGCGCAATGGTACTCACCACATTCC, reverse primer (R): 5'-GATCTTGTCTTCAGAGCCACAG; 2, for *Pemt* knockout allele, F: 5'-GAGCGCAATGGTACTCACCACATTCC, R: 5'-CTCGACGTTGTCGAAG; 3, for *Abcb4* gene, F: 5'-GCTGAGATGGATCTTGAG, R: 5'-GTCGAGTAGCCAGATGATGG; 4, for *Abcb4* knockout allele, F: 5'-CGGCGAGGATCTCGTCGTGACCCA, R: 5'-GCGATACCGTAAAGCACGAGGAAG.

2.2.3 Sample collections

Murine livers were frozen in liquid N_2 after dissection. Blood was collected by cardiac puncture with instruments pretreated with EDTA. Plasma was separated by centrifugation at 2,000 rpm for 20 min in a refrigerated bench top centrifuge. Bile was collected from the intact gallbladders. All samples were stored at -70°C before use.

2.2.4 Preparation of primary hepatocytes

Pemt$^{-/-}$ mice and *Abcb4*$^{-/-}$/*Pemt*$^{-/-}$ mice were fed a choline-supplemented (CS) diet for 24 h. The *Pemt*$^{-/-}$ mice were then fed the CD diet for 2 days (CD2) and the *Abcb4*$^{-/-}$/*Pemt*$^{-/-}$ mice were fed the CD diet for 3 (CD3) or 21 (CD21) days. Hepatocytes were prepared (11) and cultured (12) in CS medium (Dulbecco's modified Eagle's medium + 17 % fetal bovine serum) or CD medium (Dulbecco's modified Eagle's medium without choline + 17 % delipidated fetal bovine serum). Three preparations of hepatocytes were used in each experiment.

2.2.5 Enzyme assays

Plasma aspartate and alanine aminotransferase (AST/ALT) activities were measured with a GPT/GOT Kit (*Sigma,* catalog # P505).

Choline oxidase activity was determined by incubation of [^{3}H]choline with mitochondria isolated as the pellet obtained after centrifugation of liver homogenates at 12,000 x g for 15 min (13). [^{3}H]betaine in the aqueous phase was separated by TLC after lipid extraction.

Choline kinase activity was measured in liver homogenates (14) in incubations with [^{3}H]choline and the product, [^{3}H]phosphocholine, was separated from choline by TLC.

CTP:phosphocholine cytidylyltransferase activity was assayed in both liver homogenates and membrane fractions (100,000 x g pellet) (15).

Phospholipase A_2 (PLA_2) activity was measured in liver homogenates and primary hepatocytes with PED6 (*N*-((6-(2,4-dinitrophenyl)amino)hexanoyl)-2-(4,4-difluoro- 5,7-dimethyl-4-bora-3a,4a-diaza-*s*-indacene-3-pentanoyl) -1-hexadecanoyl-*sn*-glycero-3-phosphoethanolamine, triethylammonium salt, *Molecular Probes*), a self-quenching BODIPY-fluorescent analog of PE and a substrate specific for PLA_2 (16). Hepatocytes were incubated with PED6 liposomes for 2 h and visualized by fluorescence microscopy.

Phospholipases C and D activities were measured in liver homogenates with [^{3}H]PC as substrate (17).

2.2.6 Analyses of lipids and choline metabolites

Livers were homogenized with a Polytron homogenizer in 5 vol of homogenizing buffer [10 mM Tris-HCl, pH 7.2, containing 150 mM NaCl, 1 mM EDTA, 1 mM dithiothreitol, 1 mM phenylmethylsulfonyl fluoride, 1:100 protease inhibitors cocktail (*Sigma*, P8340)]. The homogenates were centrifuged for 5 min at 600 × g and supernatants were collected. Protein was quantified by the method of Bradford (18). Total lipids were extracted from liver homogenates, plasma and bile by the method of Bligh & Dyer (19). Phospholipids were separated by high performance liquid chromatography (HPLC) and quantified with an electron-light scattering detector (20). Phosphatidyldimethylethanolamine was used as an internal standard for quantification. The aqueous phase from lipid extractions was collected and lyophilized. Aqueous choline metabolites were separated by thin-layer chromatography, subjected to acid hydrolysis, and quantified with Phospholipids B kit (*Wako*) (21,22).

2.2.7 Tracing PC metabolism

[^{3}H]Glycerol or [^{3}H]choline was added to culture media to trace PC metabolism in cultured primary hepatocytes from *Abcb4*$^{-/-}$/*Pemt*$^{-/-}$ mice. Primary hepatocytes were incubated for 2 h with the radiolabeled substrate, then the radiolabel was chased for 2 h. The rates of PC synthesis and degradation were calculated as previously described (23,24). PC biosynthetic rate = increase in dpm in [^{3}H]PC/mg protein from [^{3}H]choline between the end of the pulse and after 2 h of chase divided by [2 h x the nmole of phosphocholine/mg protein at the beginning of the pulse]. PC degradation rate = decrease in dpm in [^{3}H]PC/mg protein derived from [^{3}H]glycerol between the end of the pulse and after 2 h of chase divided by [2 h x nmole of PC/mg protein]. The relative rates are presented as a comparison between CS and CD hepatocytes. Formation of [^{3}H]PC from [^{3}H]GPC was monitored by incubation of 1 x 10^6 primary cultured hepatocytes from *Abcb4*$^{-/-}$/*Pemt*$^{-/-}$ mice with 60 mmol/l [^{3}H]GPC for 2 h in CS or CD medium.

2.2.8 Western blotting for c-Jun

Fifty μg proteins of liver homogenates were separated by 10% SDS-PAGE and blotted with an anti-c-Jun antibody. PDI blotting was used as a protein loading control.

2.2.9 *In vivo* injection of c-Jun antisense DNA

Phosphorothioated c-Jun antisense DNA, 5'-T*T*C*C*ATCTTTGCAG*T*C*A*T-3' (*, phosphorothioated bond) was synthesized by *IDT* (Integrated DNA Technologies). *Abcb4*$^{-/-}$/*Pemt*$^{-/-}$ mice were injected once intraperitoneally (i.p.) with 5 μg antisense DNA/kg mouse body weight in 200 μl saline. Then mice were fed a CD diet for 3 days. The control mice were injected with 200 μl saline. Mice were fasted for 12 h before sacrifice.

Three mice of each gender were used for each time point in all experiments and assays were performed in duplicate.

2.3 Results

2.3.1 Biliary secretion of PC is lethal in CD-*Pemt*$^{-/-}$ mice

To understand why complete choline deprivation is lethal (i.e., why *Pemt*$^{-/-}$ mice die from choline deprivation), *Pemt*$^{-/-}$ mice and *Abcb4*$^{-/-}$/*Pemt*$^{-/-}$ mice were fed a CD diet for 3 days. No liver damage was observed in *Abcb4*$^{-/-}$/*Pemt*$^{-/-}$ mice as indicated by a low level of the hepatic enzymes ALT and AST in plasma (Fig. 2.3). Hepatic total choline-containing metabolites, including PC, in *Abcb4*$^{-/-}$/*Pemt*$^{-/-}$ mice were decreased by only ~20% compared with the >50% decrease in CD-*Pemt*$^{-/-}$ mice after 3 days of the CD diet (Fig. 2.4A, B). Biliary PC levels were negligible in *Abcb4*$^{-/-}$/*Pemt*$^{-/-}$ mice (Fig. 2.5) whereas CD-*Pemt*$^{-/-}$ mice continuously depleted hepatic PC for 3 days via biliary secretion (Fig. 2.5 insert). Since ~60% of hepatic PC is excreted via biliary secretion each day (25,26), we conclude that the lethality of choline deprivation in *Pemt*$^{-/-}$ mice emanates primarily from rapid depletion of hepatic PC via biliary secretion.

When *Abcb4*$^{-/-}$/*Pemt*$^{-/-}$ mice were fed the CD diet for 21 days, total choline-containing compounds in the liver decreased by ~50% and remained at this level for 3 months (Fig. 2.4A), even though there was neither endogenous synthesis of choline via PEMT nor any dietary choline. Thus, adaptation to choline deprivation directed *Abcb4*$^{-/-}$/*Pemt*$^{-/-}$ mice into a new state of PC homeostasis.

2.3.2 Enhanced PC metabolism in CD-*Abcb4*$^{-/-}$/*Pemt*$^{-/-}$ mice, but not in CD-*Pemt*$^{-/-}$ mice

To preserve PC levels in mice fed the CD diet, we expected that the activity of phospholipases, especially PLA_2, which is quantitatively the most important enzyme for PC catabolism (27), would decrease. Indeed, PLA_2 activity was decreased ~ 50% in livers of CD-*Pemt*$^{-/-}$ mice after 3 days (Fig. 2.6A). In contrast, hepatic PLA_2 activity was increased ~ 3-fold in CD-*Abcb4*$^{-/-}$/*Pemt*$^{-/-}$ mice (Fig. 2.6A). That this was PLA_2 activity was further indicated by inhibition of the activity with a PLA_2-specific inhibitor, arachidonoyl trifluoromethyl ketone (ATK) (Fig. 2.6A). PLA_2 activity was also assayed in cultured hepatocytes derived from CD-*Pemt*$^{-/-}$ mice and CD-*Abcb4*$^{-/-}$/*Pemt*$^{-/-}$ mice (Fig. 2.6B). Hepatocytes were incubated with a PLA_2-specific substrate, PED6 (16), a derivative of PE containing a fluorescence-labeled fatty acid at the *sn-2* position and a modified head-group that quenches fluorescence from the fatty acid. When the fatty acid is cleaved from the lipid by PLA_2, fluorescence is detectable. Fig. 2.6B shows that feeding the CD diet for 3 days increased PLA_2 activity in hepatocytes from CD-*Abcb4*$^{-/-}$/*Pemt*$^{-/-}$ mice but not from CD-*Pemt*$^{-/-}$ mice. The activities of phospholipases C and D were decreased in livers of *Pemt*$^{-/-}$ mice fed the CD diet for 3 days whereas in the livers of CD-*Abcb4*$^{-/-}$/*Pemt*$^{-/-}$ mice there was an initial decrease in these activities followed by a return to normal levels (Fig. 2.6C). These data demonstrate that the capacity for PC degradation via PLA_2 was significantly increased in *Abcb4*$^{-/-}$/*Pemt*$^{-/-}$ mice fed the CD diet.

2.3.3 Choline metabolites are channeled towards PC biosynthesis

PC metabolism generates sphingomyelin, phosphatidylserine, lysoPC, GPC, phosphocholine and choline. No significant change in levels of hepatic sphingomyelin, phosphatidylserine or lysoPC was observed upon feeding the CD diet to either *Abcb4*$^{-/-}$/*Pemt*$^{-/-}$ mice or *Pemt*$^{-/-}$ mice whereas hepatic choline and GPC levels decreased significantly in *Pemt*$^{-/-}$ mice (Fig. 2.4C and 2.4D). The quantitatively more important hepatic choline metabolite, phosphocholine, decreased dramatically in CD-*Pemt*$^{-/-}$ mice by 3 days (Fig. 2.4C), but did not decline significantly for at least 90 days in CD-*Abcb4*$^{-/-}$/*Pemt*$^{-/-}$ mice (Fig. 2.4D). Thus, choline and phosphocholine were preserved for PC biosynthesis in CD-*Abcb4*$^{-/-}$/*Pemt*$^{-/-}$ mice.

The only pathway for catabolism of choline is oxidation to betaine (Fig. 2.1). Choline oxidase was almost completely inactivated by choline deprivation for 3 days in both *Pemt*$^{-/-}$ and *Abcb4*$^{-/-}$/*Pemt*$^{-/-}$ mice (Fig. 2.7). In contrast, the activity of choline kinase was initially stimulated ~ 2-fold in *Abcb4*$^{-/-}$/*Pemt*$^{-/-}$ mice after 3 days of CD diet then gradually declined (Fig. 2.8). Choline kinase is not considered to be rate-limiting for PC biosynthesis via the CDP-choline pathway

(28). Instead, CTP:phosphocholine cytidylyltransferase (CT) is the rate-limiting enzyme (Fig. 1A). CT activity increased ~ 3-fold when *Abcb4$^{-/-}$/Pemt$^{-/-}$* mice were fed the CD diet for 21 days and this level of CT activity was maintained for at least 90 days (Fig. 2.9A). The activity of the membrane-associated form of CT (the active form) was similarly increased by the CD diet (Fig. 2.9B). These data demonstrate that *Abcb4$^{-/-}$/Pemt$^{-/-}$* mice adjust their metabolism to ensure that available choline is channeled towards PC biosynthesis.

2.3.4 Adaptation to complete choline deprivation --- choline recycling

Since the above data suggest that *Abcb4$^{-/-}$/Pemt$^{-/-}$* mice adapt their hepatic metabolism of PC in response to the CD diet, we investigated this adjustment further in intact hepatocytes. [^{3}H]Glycerol and [^{3}H]choline were used to trace PC metabolism in primary hepatocytes isolated from *Abcb4$^{-/-}$/Pemt$^{-/-}$* mice. Fig. 2.10 indicates that both the biosynthesis and degradation of PC were increased in response to the CD diet. Fig. 2.7 and Fig. 2.10 demonstrate that complete choline deprivation in CD-*Abcb4$^{-/-}$/Pemt$^{-/-}$* mice activates choline production by increasing PC degradation and inhibiting choline oxidation. Thus, choline recycling was initiated and enhanced. In addition to these compensatory mechanisms, PC was further preserved in *Abcb4$^{-/-}$/Pemt$^{-/-}$* mice during choline deprivation by an increased incorporation of GPC into PC (Fig. 2.11), indicating that choline recycling is enhanced to conserve the levels of total choline-containing metabolites. Enhanced choline recycling, therefore, allows the utilization of choline more efficiently when PC levels drop to 50% during choline deprivation.

2.3.5 A new choline homeostasis — life and death

The rapid decline in hepatic total choline-containing metabolites in CD-*Pemt*$^{-/-}$ mice was incompatible with life beyond 4 to 5 days (29). However, a more gradual reduction in choline-containing metabolites provided sufficient time for *Abcb4*$^{-/-}$/*Pemt*$^{-/-}$ mice to adapt to the stress of choline deprivation. A minimum threshold of total choline-containing metabolites in the liver for survival is suggested to be ~110 nmol/mg protein (Fig. 2.4A). The level of total choline-containing compounds in *Pemt*$^{-/-}$ mice fed a CD diet for 3 days fell below this baseline. Thus, the CD-*Pemt*$^{-/-}$ mice faced a severe choline deficiency whereas the CD-*Abcb4*$^{-/-}$/*Pemt*$^{-/-}$ mice were able to establish a new choline homeostasis, thereby conserving sufficient amounts of choline metabolites for viability (Fig. 2.12A, B). After 3 days of the CD diet a turning point between life and death was reached. This threshold was critically dependent on the phosphocholine levels but not other choline-containing metabolites (Fig. 2.12A, B).

2.3.6 Exploring regulatory mechanisms of adaptation to choline deprivation

Adaptation to choline deprivation is achieved by choline recycling, however, the regulatory mechanism(s) for choline recycling is not clear. Our preliminary data suggest that c-Jun, as a regulator of cell life and death (30), could be a promising candidate involved in this process, since examination of the putative regulatory elements in the promoters for choline kinase α, CTα and PLA_2 showed the presence of an AP1 site, which interacts with c-Jun homodimer or cJun/c-Fos heterodimer. Moreover, c-Jun has been shown to alter the expression of the mRNA for choline kinase (31). We found a striking increase in the amount of immunoreactive c-Jun in the liver of *Abcb4*$^{-/-}$/*Pemt*$^{-/-}$ mice after initiation of the CD diet (Fig. 2.13). Injection of c-Jun antisense DNA into *Abcb4*$^{-/-}$/*Pemt*$^{-/-}$ mice successfully interrupted the adaptative response of c-Jun during choline deprivation, since liver damage was significantly induced in CD-*Abcb4*$^{-/-}$/*Pemt*$^{-/-}$ mice with the treatment of c-Jun antisense as compared with the control of CD-*Abcb4*$^{-/-}$/*Pemt*$^{-/-}$ mice (Fig. 2.14). c-Jun is involved in a stress-driven signalling. Choline deprivation is a stress for mice. However, it would be worthwhile in future studies to determine why the response to this stress only occurred in CD-*Abcb4*$^{-/-}$/*Pemt*$^{-/-}$ mice but not in CD-*Pemt*$^{-/-}$ mice.

In addition, phosphocholine and/or glycerophosphocholine may also be key regulators during this adaptation, since certain studies suggested that phosphocholine and/or glycerophosphocholine might be involved in a regulatory mechanism via initiating cell signaling (32). Moreover, the maintenance of the relative phosphocholine level is probably an important issue to be further addressed in the future, since the relative phosphocholine level might be more valuable in evaluating different choline homeostasis as compared to the net level of phosphocholine as addressed before.

2.4 Discussion

The data from these experiments provide unambiguous evidence that choline is an essential nutrient in animals. Liver failure in *Pemt*$^{-/-}$ mice fed the CD diet results from continued secretion of PC into bile during a time when PC biosynthesis is severely curtailed. The rapidity with which PC levels decrease in *Pemt*$^{-/-}$ mice apparently allows no time for the mice to adapt to the crisis in PC biosynthesis. Unexpectedly, the levels of PC also decreased in *Abcb4*$^{-/-}$/*Pemt*$^{-/-}$ mice fed the CD diet for 21 days even though these mice no longer secrete PC into bile. The decrease in PC can be explained by the 3-fold increase in PLA_2 activity within the first 21 days of the CD diet. Importantly, the decrease in PC occurs more gradually in CD-*Abcb4*$^{-/-}$/*Pemt*$^{-/-}$ mice allowing them to adapt to the decrease in PC biosynthesis by maintaining the pool of phosphocholine, a substrate for CT, the rate-limiting enzyme in PC biosynthesis.

PEMT plays an important role in PC and choline homeostasis in individual organisms. Rodents do not have significant PEMT activity before birth (33). Moreover, *Pemt*$^{-/-}$ mice develop normally and have a normal life-span (29,34). Thus, dietary choline is adequate for life independent of PEMT. However, PEMT compensates for the lack of dietary choline (35). PEMT, therefore, becomes critical when dietary choline is not adequate as may occur during starvation, pregnancy or lactation. PEMT is also important because it contributes to the total pool of choline in the biosphere. Plants make choline by methylation of phosphoethanolamine (36) and yeast synthesize choline from both methylation of PE and methylation of phosphoethanolamine (37). Mammals obtain choline from their diet and from the PEMT pathway. Therefore, all choline in nature is ultimately derived from the methylation of ethanolamine in the form of PE or phosphoethanolamine.

Fig. 2.15 summarizes the adaptations that facilitate survival of CD-*Abcb4*$^{-/-}$/*Pemt*$^{-/-}$ mice. By eliminating the loss of PC into bile, these mice are able to implement significant changes in PC and choline metabolism. Notably, the oxidation of choline to betaine is markedly curtailed and choline kinase and CT activities are increased to ensure re-utilization of choline for PC biosynthesis. Another adaptation is that PLA_2 activity and PC catabolism are increased to ensure an ample supply of phosphocholine for PC biosynthesis. The gradual reduction of hepatic PC in *Abcb4*$^{-/-}$/*Pemt*$^{-/-}$ mice fed the CD diet provided sufficient time for regulatory mechanisms to be triggered and for adaptation to the stress of choline deprivation. The conversion of choline into PC via choline recycling generates a large reserve pool of choline that can be readily accessible at times of high demand, which may explain why rodents and humans do not die from dietary choline deficiency.

Several choline metabolites have been used in clinical therapy. For example, citicoline (CDP-choline) is used to treat brain disorders such as cognitive and memory impairment and stroke (38,39). Betaine is used to treat patients with non-alcoholic steatohepatitis (40). However, the mechanisms behind these treatments are still unclear. Our studies provide new clues about choline and PC homeostasis that might help elucidate the mechanisms for these treatments. Moreover, our results might lead to more potent therapeutics for these disorders.

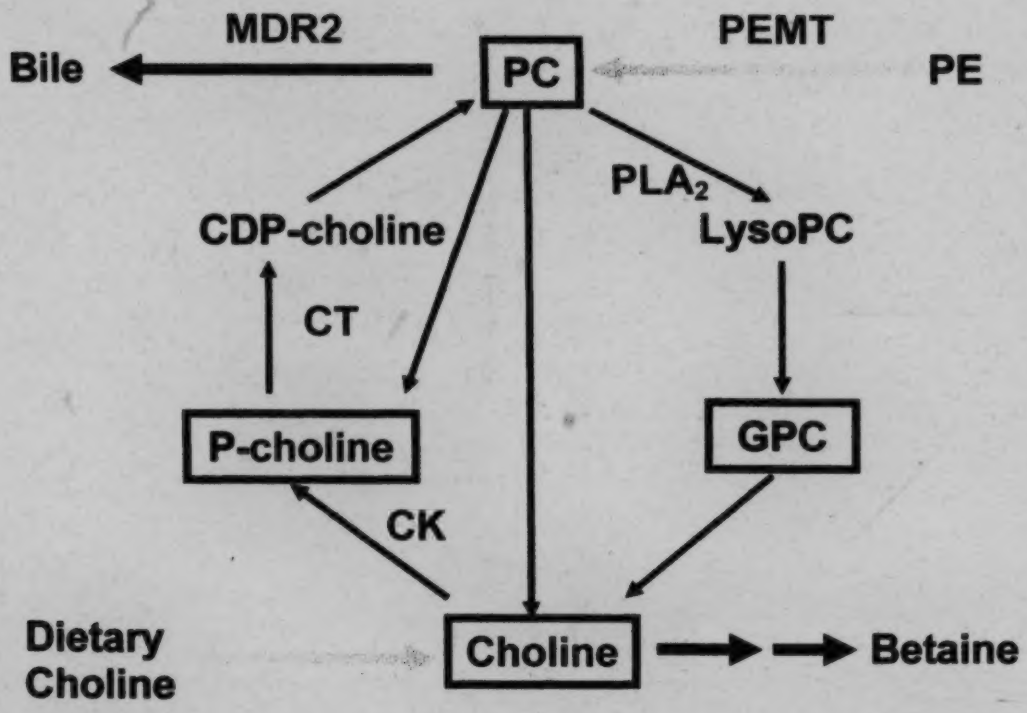
MDR2
PEMT
Bile
PC
PE
PLA$_2$
CDP-choline
LysoPC
CT
P-choline
GPC
CK
Dietary Choline
Choline
Betaine

Fig. 2.1 Choline homeostasis in liver

P-choline, phosphocholine; GPC, glycerophosphocholine; PLA$_2$, phospholipase A$_2$; CT, CTP:phosphocholine cytidylyltransferase; CK, choline kinase; PEMT, phosphatidylethanolamine *N*-methyltransferase; MDR2, multiple drug resistant protein 2; PC, phosphatidylcholine. P-choline in PC can be used for sphingomyelin biosynthesis. PC can be secreted in very low density lipoproteins and delivered to liver by high density lipoproteins.

Fig. 2.2 Genotyping of *Pemt*$^{-/-}$ and *Abcb4*$^{-/-}$/*Pemt*$^{-/-}$ mice

(A & B) show the wild type and knockout alleles for *Pemt* and *Abcb4* genes. Genomic DNA was extracted from mice tails as templates and specific PCR reactions were used to distinguish between wild type and targeted alleles containing a neomycin resistance gene (*neo*^{r}). The specific primer pairs used are presented in Materials and Methods and are located as shown by the arrows. **(C)** Lanes 1 – 4 are for specific PCR detection of the *Pemt* gene, *Pemt* knockout allele, *Abcb4* gene and *Abcb4* knockout allele respectively.

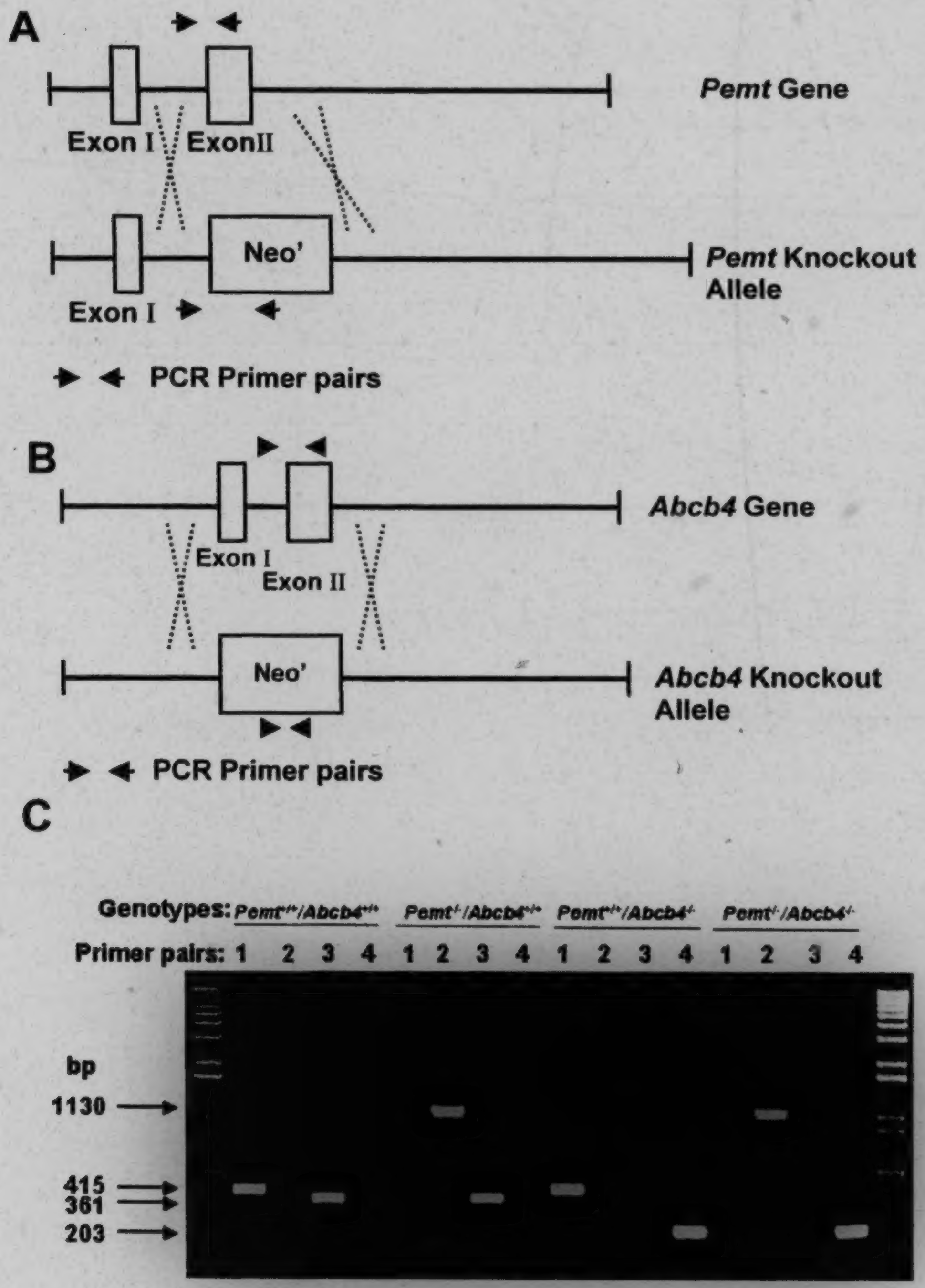
A
Pemt Gene
Exon I
ExonII
Neo'
Pemt Knockout Allele
Exon I
PCR Primer pairs
B
Abcb4 Gene
Exon I
Exon II
Neo'
Abcb4 Knockout Allele
PCR Primer pairs
C
Genotypes: Pemt+/+/Abcb4+/+ Pemt-/-/Abcb4+/+ Pemt+/+/Abcb4-/- Pemt-/-/Abcb4-/-
Primer pairs: 1 2 3 4 1 2 3 4 1 2 3 4 1 2 3 4
bp
1130
415
361
203

Fig. 2.3 Liver damage was assessed by measurement of plasma alanine/aspartate aminotransferase (ALT/AST) activity

Plasma samples were collected from *Pemt*$^{-/-}$ mice and *Abcb4*$^{-/-}$/*Pemt*$^{-/-}$ mice fed the choline-supplemented (CS) diet for 24 h (0 day) then transferred to the choline-deficient (CD) diet for 3 to 90 days. Plasma ALT/AST activity was measured at day –1, 0, 1, 2, 3, 6, 9, 14, 21 and 90. Mice were fed a normal chow diet until day –1. **(A)** plasma ALT activity; **(B)** plasma AST activity.

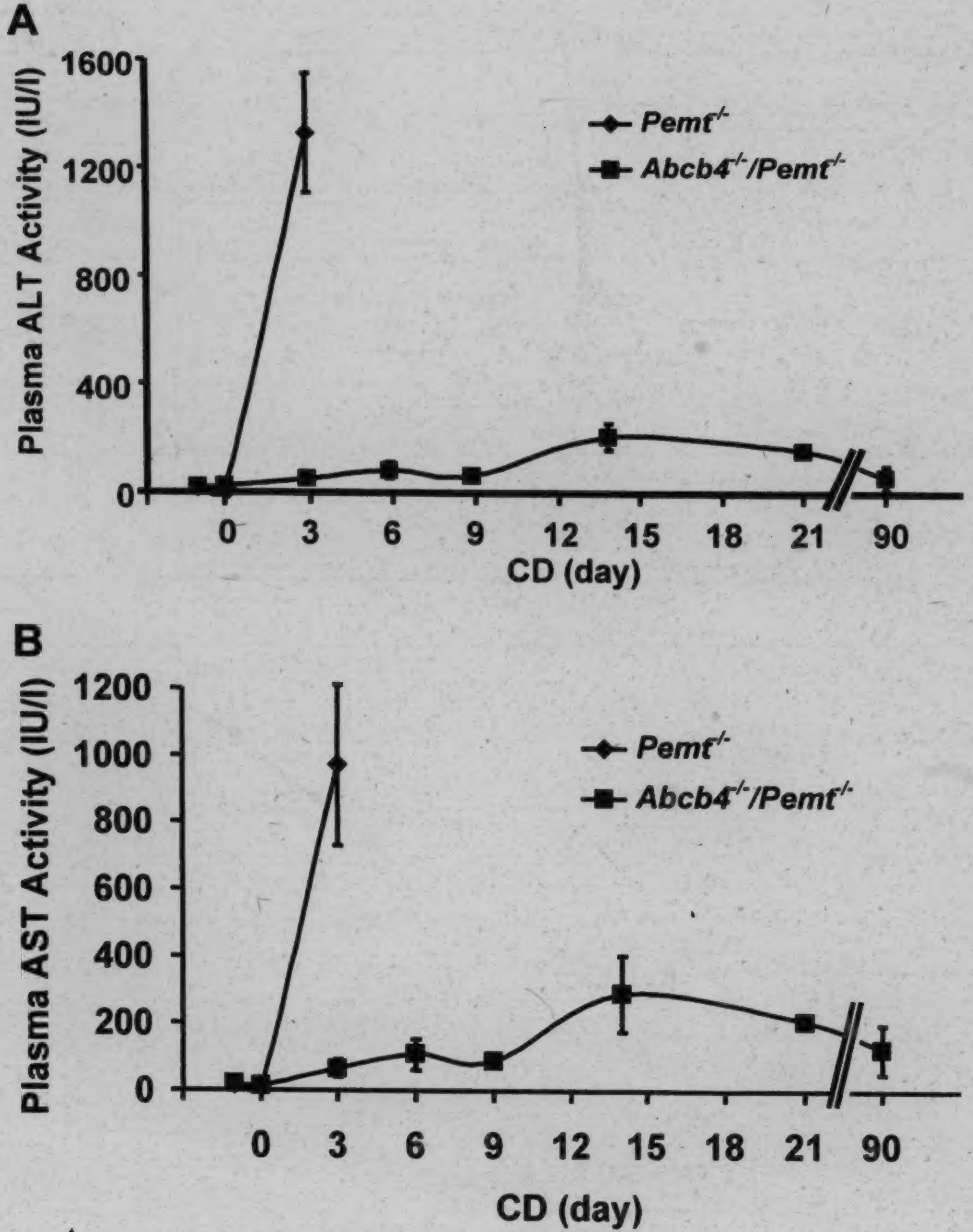
A
Plasma ALT Activity (IU/l)
1600
1200
800
400
0
Pemt-/-
Abcb4-/-/Pemt-/-
0
3
6
9
12
15
18
21
90
CD (day)
B
Plasma AST Activity (IU/l)
1200
1000
800
600
400
200
0
Pemt-/-
Abcb4-/-/Pemt-/-
0
3
6
9
12
15
18
21
90
CD (day)

Fig. 2.4 Hepatic total choline-containing metabolites (PC, sphingomyelin, lysoPC, glycerophosphocholine, phosphocholine and choline)

Liver samples were collected from *Pemt*$^{-/-}$ mice and *Abcb4*$^{-/-}$/*Pemt*$^{-/-}$ mice fed the choline-supplemented (CS) diet for 24 h (0 day) then transferred to the choline-deficient (CD) diet for 3 to 90 days. **(A)** the amount of total choline-containing metabolites in the liver; **(B)** hepatic PC levels; **(C)** water-soluble choline metabolites in the liver of *Pemt*$^{-/-}$ mice; **(D)** water-soluble choline metabolites in the liver of *Pemt*$^{-/-}$/*Abcb4*$^{-/-}$ mice. P-choline, phosphocholine; GPC, glycerophosphocholine. *, $p < 0.05$; **, $p < 0.01$.

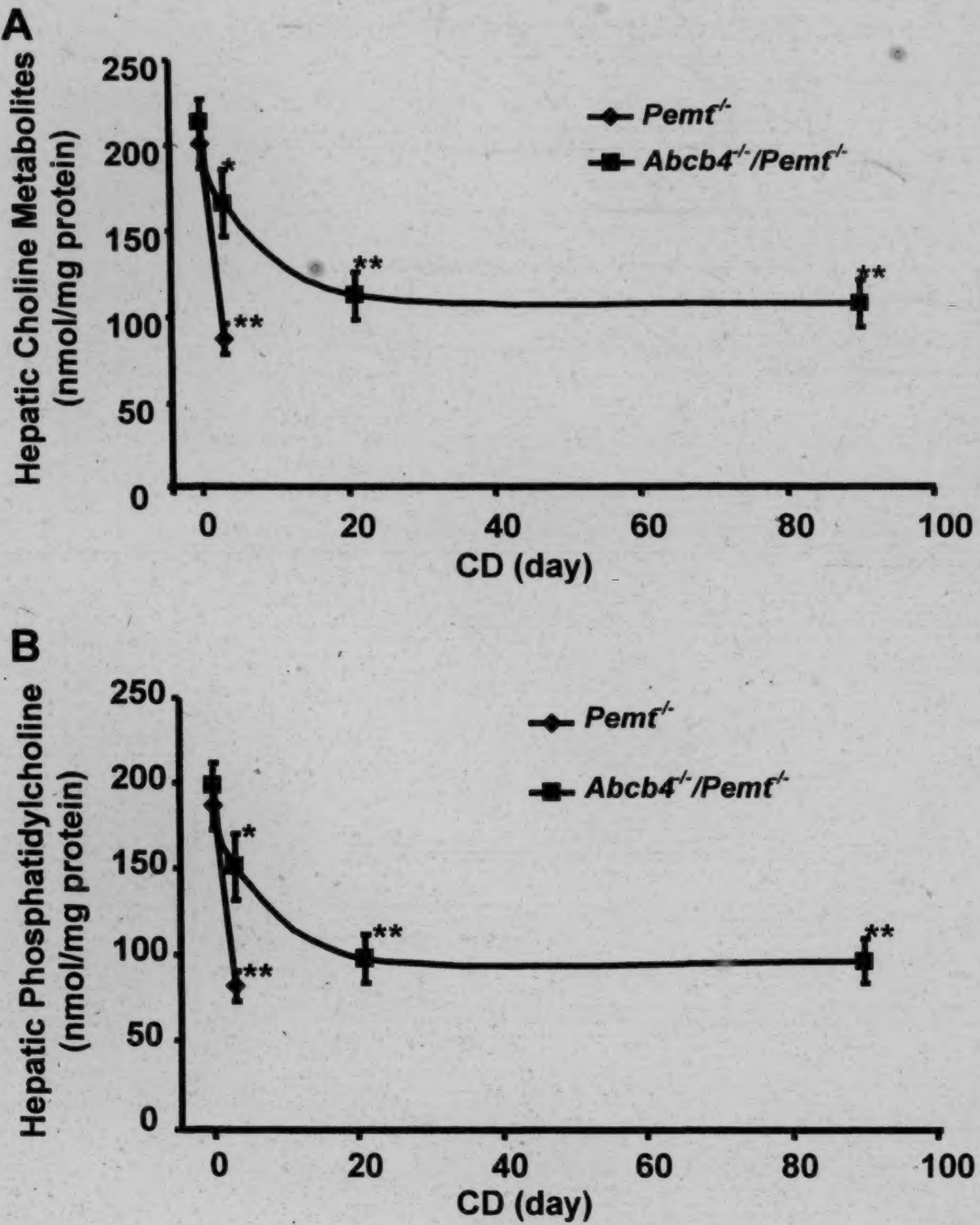
A
Hepatic Choline Metabolites (nmol/mg protein)
250
200
150
100
50
0
0
20
40
60
80
100
CD (day)
Pemt-/-
Abcb4-/-/Pemt-/-
*
**
**
**
B
Hepatic Phosphatidylcholine (nmol/mg protein)
250
200
150
100
50
0
0
20
40
60
80
100
CD (day)
Pemt-/-
Abcb4-/-/Pemt-/-
*
**
**
**

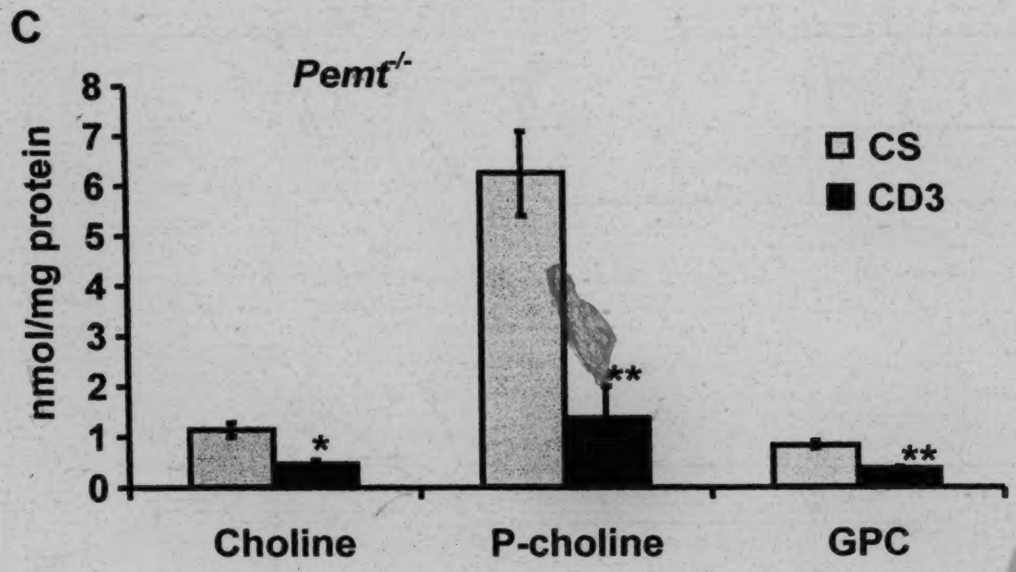
C
Pemt-/-
nmol/mg protein
8
7
6
5
4
3
2
1
0
CS
CD3
*
**
**
Choline
P-choline
GPC

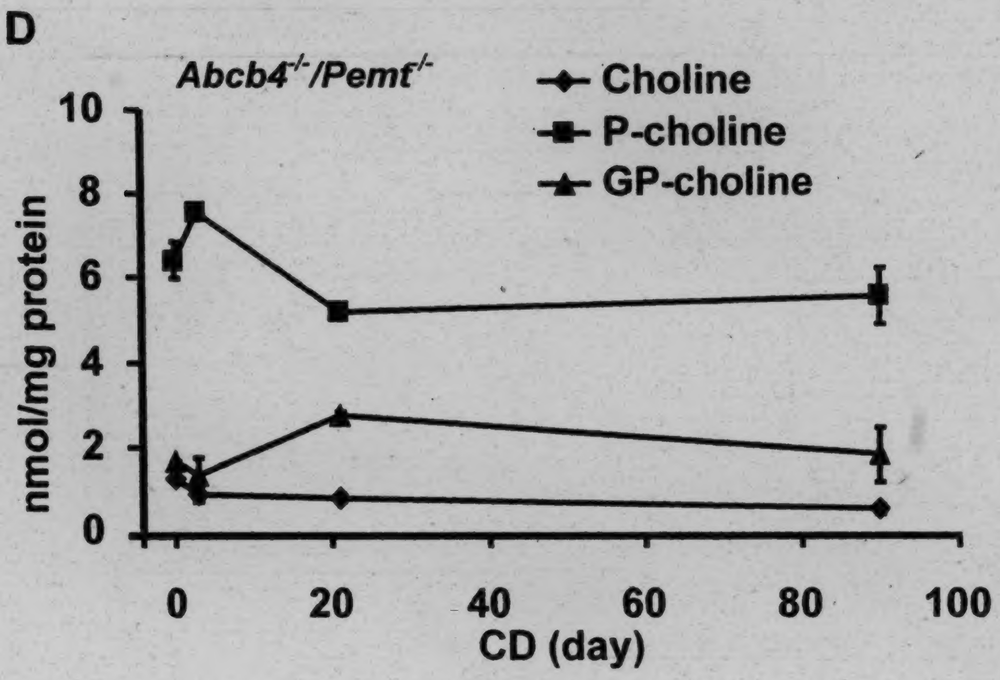
D
Abcb4-/-/Pemt-/-
Choline
P-choline
GP-choline
nmol/mg protein
10
8
6
4
2
0
0
20
40
60
80
100
CD (day)

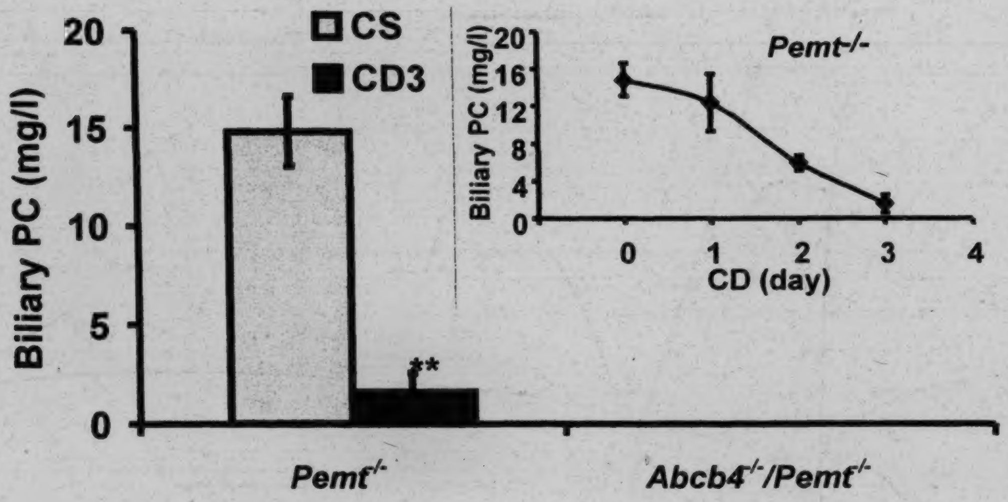

Fig. 2.5 The amount of biliary PC

Bile samples were collected from *Pemt*$^{-/-}$ mice and *Abcb4*$^{-/-}$/*Pemt*$^{-/-}$ mice fed the choline-supplemented (CS) diet for 24 h (0 day) then transferred to the choline-deficient (CD) diet for 3 to 90 days. Biliary PC was not detectable in *Pemt*$^{-/-}$/*Abcb4*$^{-/-}$ mice. No significant change in the volume of bile was observed in both models. Insert shows the change of biliary PC in *Pemt*$^{-/-}$ mice each day during 3 days of CD (CD3).

Fig. 2.6 Hepatic PC catabolism is enhanced by the CD diet in *Abcb4$^{-/-}$/Pemt$^{-/-}$* mice but not in *Pemt$^{-/-}$* mice

(A) PLA$_2$ activity was measured in liver homogenates with a PLA$_2$–specific substrate, PED6 (a self-quenching fluorescent analog of PE). Lower panel: ATK (50 μM), a specific inhibitor of PLA$_2$, was added to some samples as indicated. **(B)** PLA$_2$ activity was assessed by incubation of PD6 with primary hepatocytes from *Pemt$^{-/-}$* mice and *Abcb4$^{-/-}$/Pemt$^{-/-}$* mice fed the choline-supplemented (CS) diet for 24 h and transferred to the choline-deficient (CD) diet for 2 or 21 days. **(C)** Hepatic phospholipase C (PLC) and D (PLD) activities. Liver samples were collected from *Pemt$^{-/-}$* mice and *Abcb4$^{-/-}$/Pemt$^{-/-}$* mice fed a choline-supplemented (CS) diet for 24 h (0 day) and then switched to a choline-deficient (CD) diet for 3, 21 or 90 days. [^{3}H-choline]phosphatidylcholine was used for PLC and PLD assays with liver homogenates.

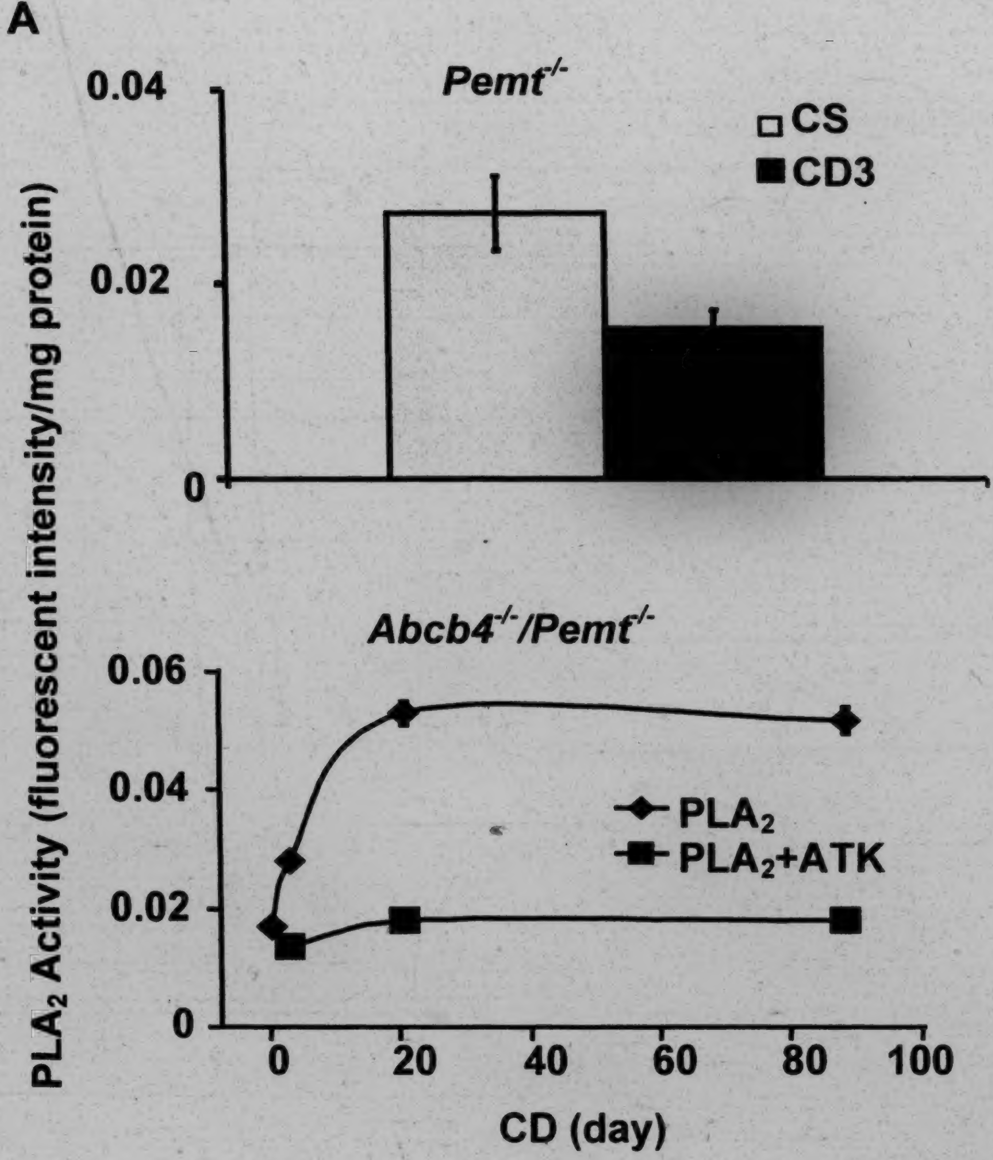
A
Pemt$^{-/-}$
0.04
0.02
0
□ CS
■ CD3
PLA$_2$ Activity (fluorescent intensity/mg protein)
Abcb4$^{-/-}$/Pemt$^{-/-}$
0.06
0.04
0.02
0
PLA$_2$
PLA$_2$+ATK
0
20
40
60
80
100
CD (day)

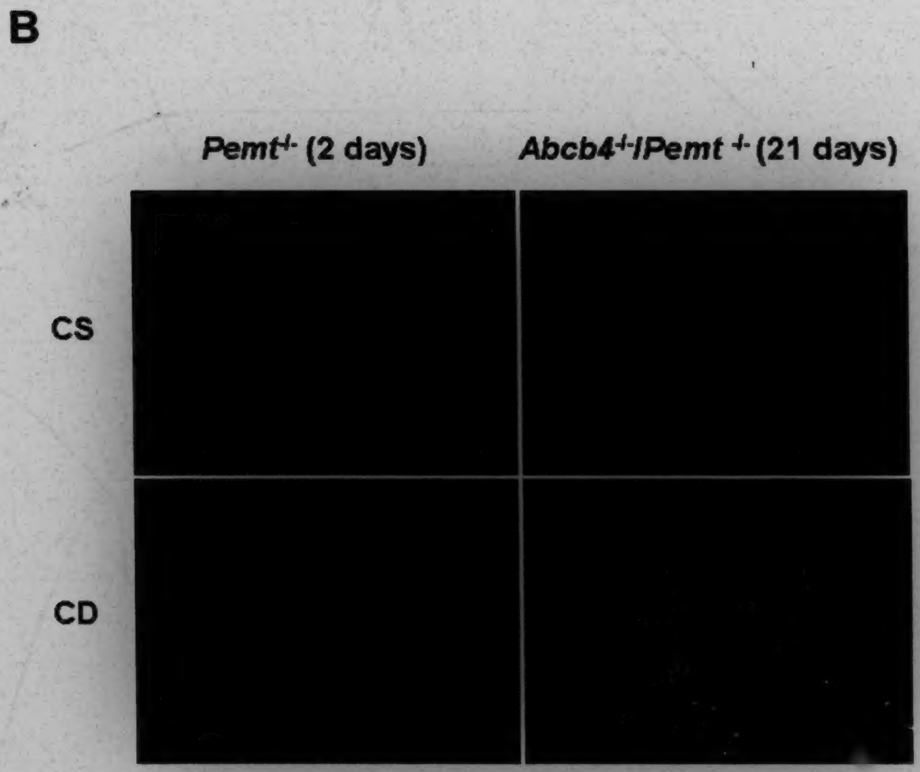
B
Pemt-/- (2 days)
Abcb4-/-/*Pemt* -/- (21 days)
CS
CD

C

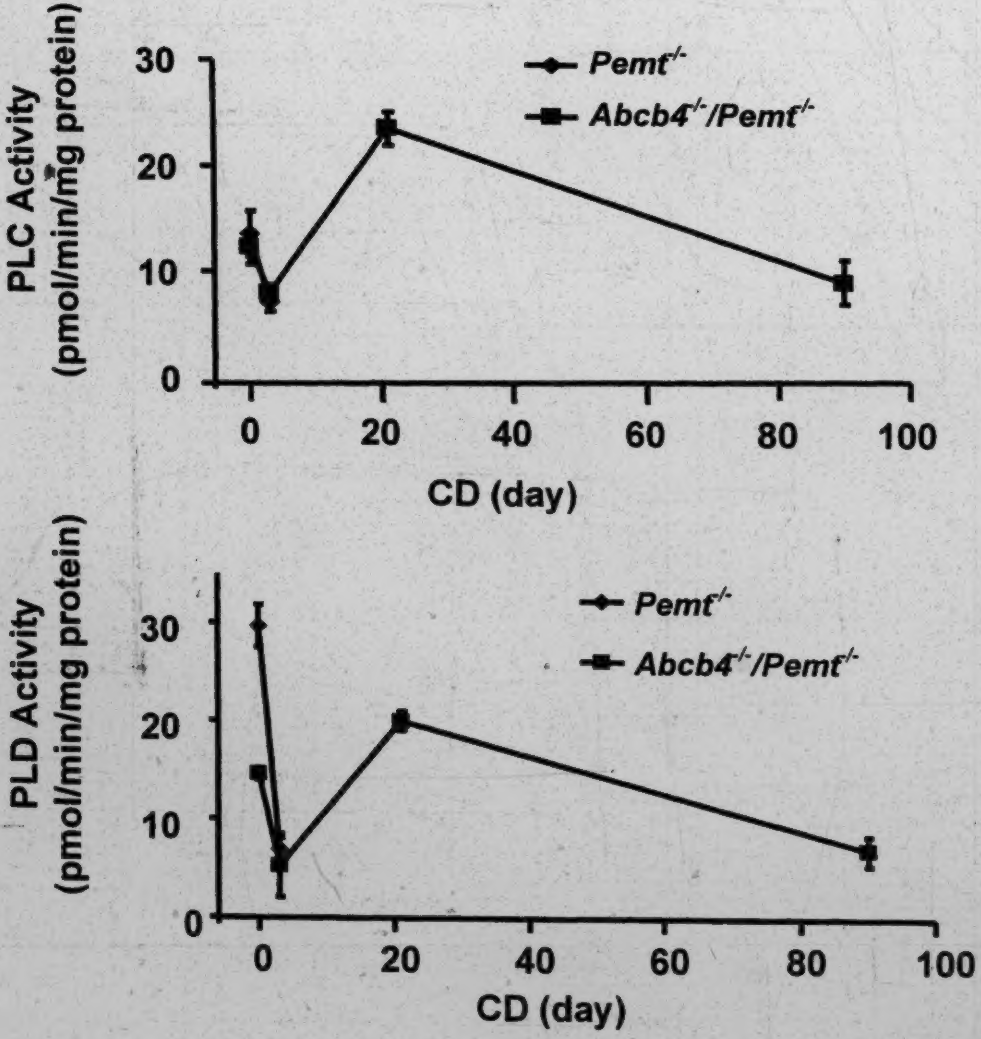
PLC Activity
(pmol/min/mg protein)
30
20
10
0
0
20
40
60
80
100
CD (day)
Pemt-/-
Abcb4-/-/Pemt-/-
PLD Activity
(pmol/min/mg protein)
30
20
10
0
0
20
40
60
80
100
CD (day)
Pemt-/-
Abcb4-/-/Pemt-/-

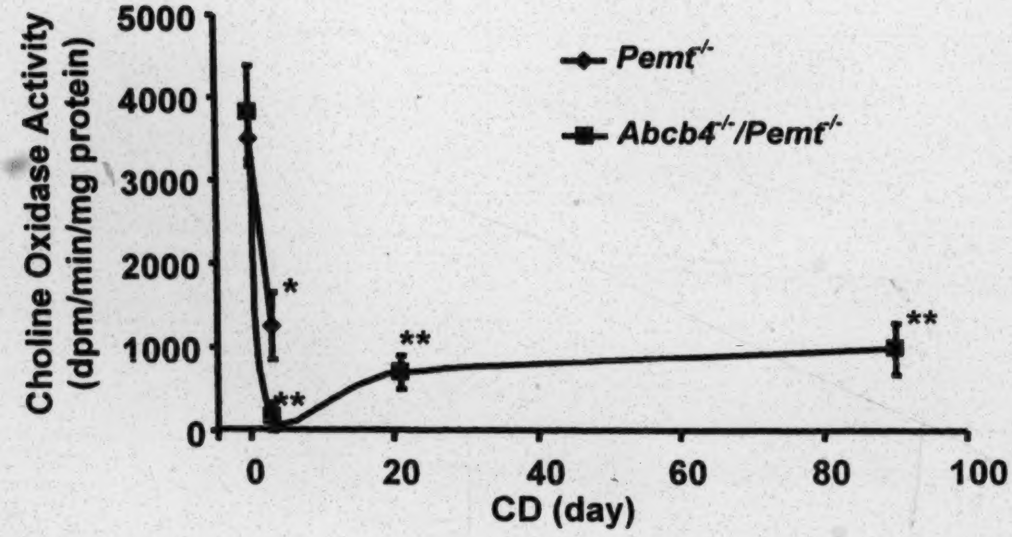

Fig. 2.7 Choline oxidase activity was curtailed in livers of both *Pemt$^{-/-}$* mice and *Abcb4$^{-/-}$/Pemt$^{-/-}$* mice

Liver samples were collected from *Pemt$^{-/-}$* mice and *Abcb4$^{-/-}$/Pemt$^{-/-}$* mice fed the choline-supplemented (CS) diet for 24 h (0 day) then transferred to the choline-deficient (CD) diet for 3 to 90 days. Choline oxidase activity was determined by incubation of [^{3}H]choline with crude mitochondrial fractions isolated as the pellet obtained after centrifugation of liver homogenates at 12,000 x g for 15 min.

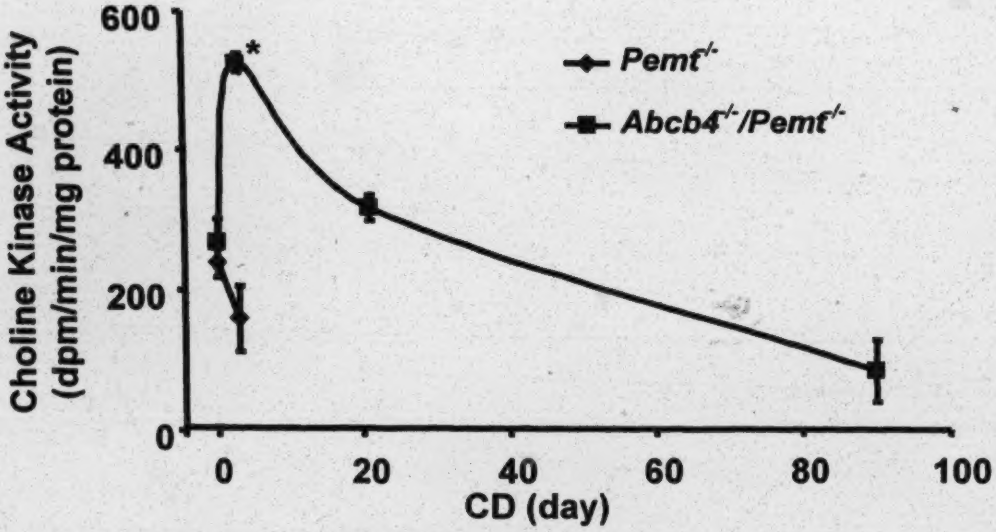

Fig. 2.8 Choline kinase activity in liver homogenates

Liver samples were collected from *Pemt*$^{-/-}$ mice and *Abcb4*$^{-/-}$/*Pemt*$^{-/-}$ mice fed the choline-supplemented (CS) diet for 24 h (0 day) then transferred to the choline-deficient (CD) diet for 3 to 90 days. Choline kinase activity was measured in liver homogenates by incubating with [^{3}H]choline and then separating [^{3}H]phosphocholine by TLC.

Fig. 2.9 CTP:phosphocholine cytidylyltransferase (CT) activity assays

Liver samples were collected from *Pemt*$^{-/-}$ mice and *Abcb4*$^{-/-}$/*Pemt*$^{-/-}$ mice fed the choline-supplemented (CS) diet for 24 h (0 day) then transferred to the choline-deficient (CD) diet for 3 to 90 days. CT activity was assayed in both liver homogenates **(A)** and membrane fractions (100,000 x g pellet) **(B)**.

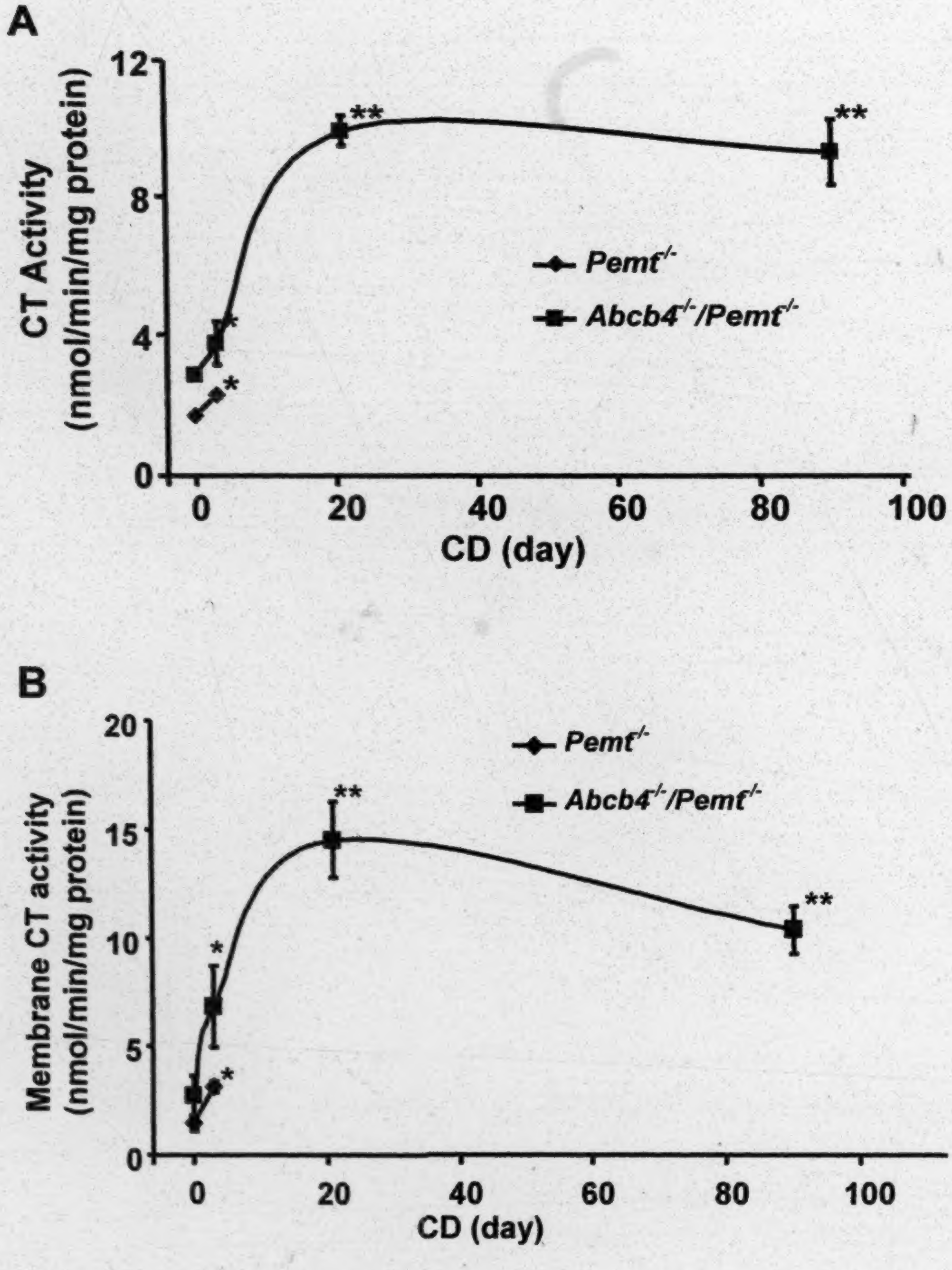
A
CT Activity
(nmol/min/mg protein)
0
4
8
12
0
20
40
60
80
100
CD (day)
*
*
**
**
Pemt-/-
Abcb4-/-/Pemt-/-
B
Membrane CT activity
(nmol/min/mg protein)
0
5
10
15
20
0
20
40
60
80
100
CD (day)
*
*
**
**
Pemt-/-
Abcb4-/-/Pemt-/-

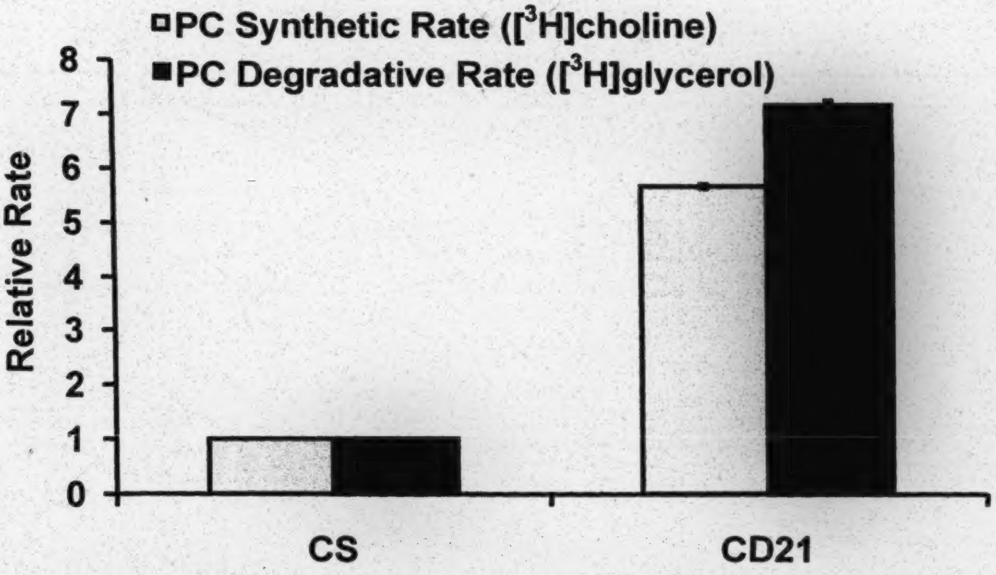

Fig. 2.10 PC biosynthesis and degradation in intact hepatocytes of *Abcb4$^{-/-}$/Pemt$^{-/-}$* mice

Incorporation of [^{3}H]glycerol or [^{3}H]choline into [^{3}H]phosphatidylcholine in primary cultured hepatocytes was performed with *Abcb4$^{-/-}$/Pemt$^{-/-}$* mice during choline deprivation. *Abcb4$^{-/-}$/Pemt$^{-/-}$* mice were fed a choline-supplemented (CS) diet for 24 h and switched to a choline-deficient (CD) diet for 21 days (CD21). The rates of PC synthesis and degradation were calculated with data from pulse-chase labeling of primary cultured hepatocytes from *Abcb4$^{-/-}$/Pemt$^{-/-}$* mice with [^{3}H]glycerol or [^{3}H]choline. *Abcb4$^{-/-}$/Pemt$^{-/-}$* mice were fed a choline-supplemented (CS) diet for 24 h and switched to a choline-deficient (CD) diet for 21 days (CD21). The relative rate was based on the comparison between CS and CD groups.

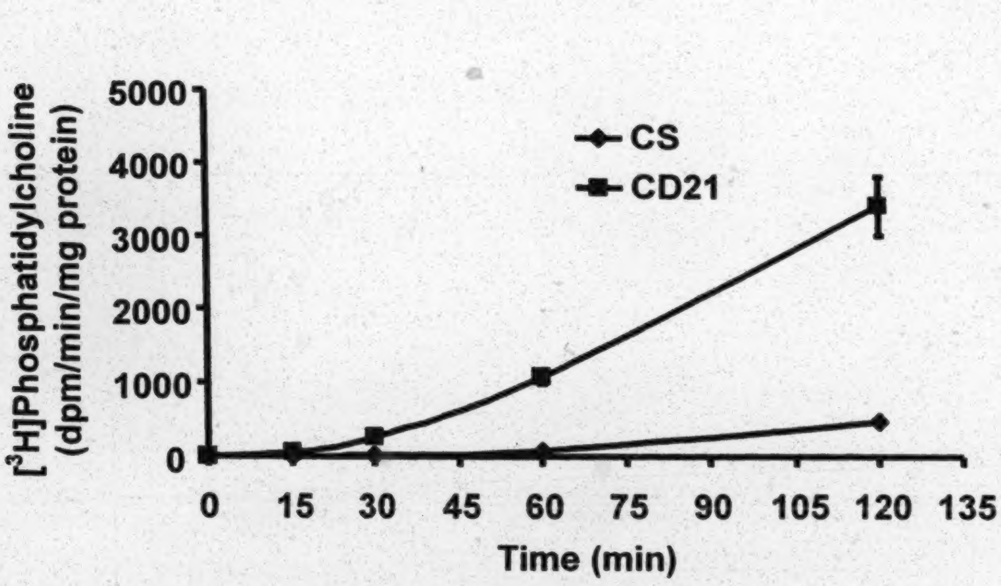

Fig. 2.11 Incorporation of [^{3}H]glycerophosphocholine ([^{3}H]GPC) into [^{3}H]phosphatidylcholine in primary cultured hepatocytes of *Abcb4$^{-/-}$/Pemt$^{-/-}$* mice during choline deprivation

Abcb4$^{-/-}$/Pemt$^{-/-}$ mice were fed a choline-supplemented (CS) diet for 24 h and switched to a choline-deficient (CD) diet for 21 days (CD21). Primary cultured hepatocytes isolated from *Abcb4$^{-/-}$/Pemt$^{-/-}$* mice were incubated with [^{3}H]GPC for 2 h. Then total lipids were extracted and separated by TLC. [3H]PC was collected and counted with a scintillation counter.

Fig. 2.12 Relative amounts of water-soluble choline metabolites as a percentage of the mass of total choline-containing metabolites (%)

(A) Relative amounts of water-soluble choline metabolites (%) in the liver of *Pemt*$^{-/-}$ mice. **(B)** Relative amounts of water-soluble choline metabolites (%) in the liver of *Abcb4*$^{-/-}$/*Pemt*$^{-/-}$ mice. P-choline, phosphocholine; GP-choline, glycerophosphocholine.

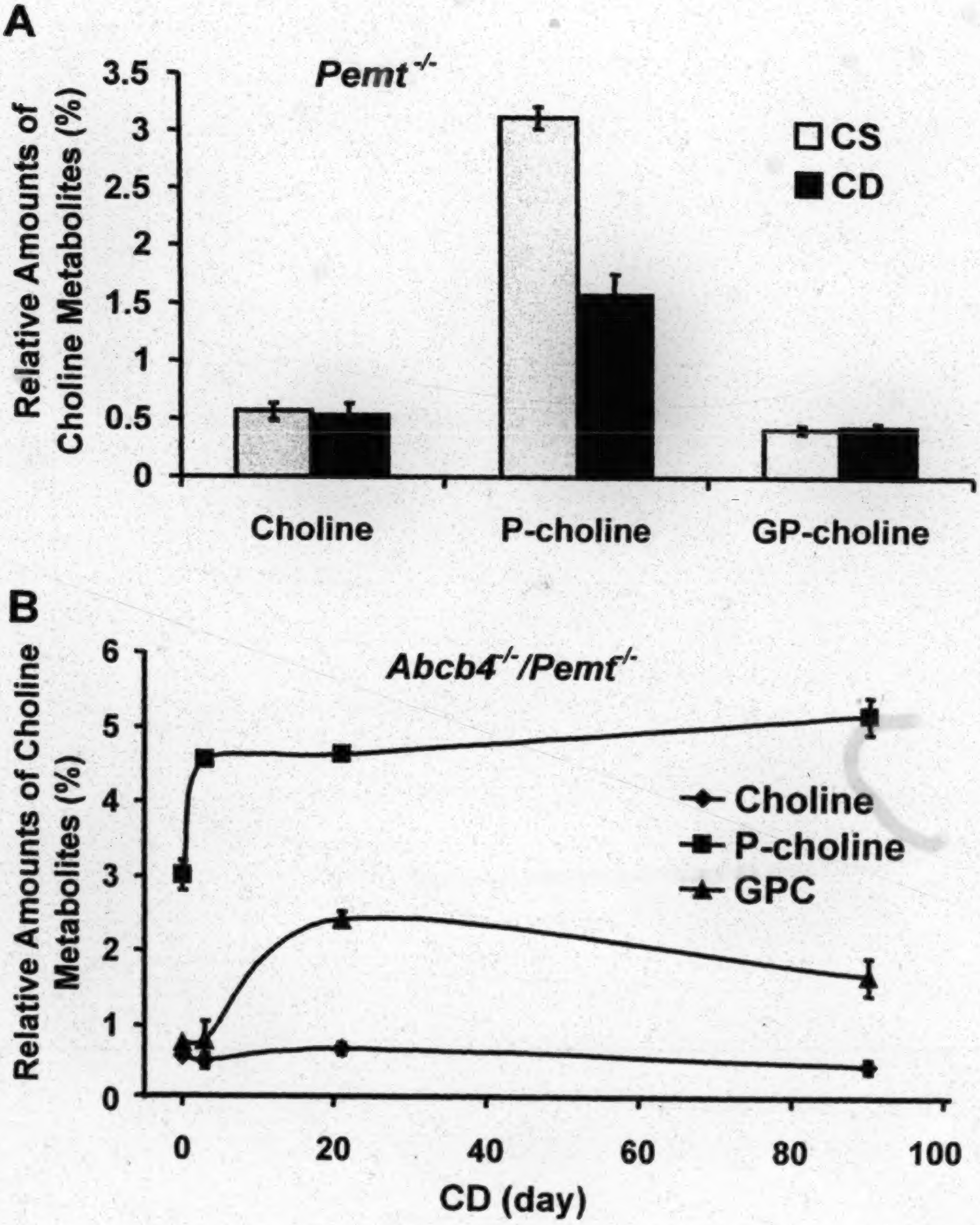
A
Pemt$^{-/-}$
Relative Amounts of Choline Metabolites (%)
3.5
3
2.5
2
1.5
1
0.5
0
☐ CS
■ CD
Choline
P-choline
GP-choline
B
Abcb4$^{-/-}$/Pemt$^{-/-}$
Relative Amounts of Choline Metabolites (%)
6
5
4
3
2
1
0
◆ Choline
■ P-choline
▲ GPC
0
20
40
60
80
100
CD (day)

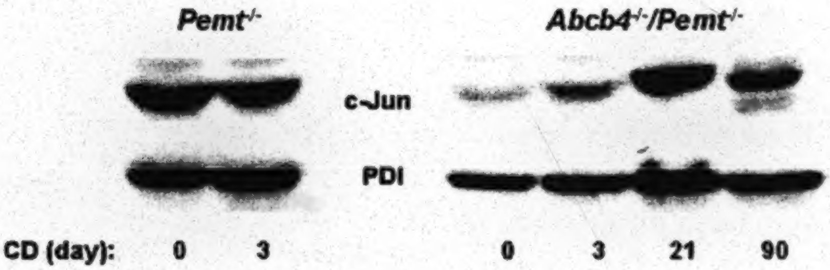

Fig. 2.13 Expression of c-Jun was increased in *Abcb4*$^{-/-}$/*Pemt*$^{-/-}$ mice during choline deprivation, but not in *Pemt*$^{-/-}$ mice

Liver samples were collected from *Pemt*$^{-/-}$ mice and *Abcb4*$^{-/-}$/*Pemt*$^{-/-}$ mice fed a choline-supplemented (CS) diet for 24 h (0 day) and then switched to a choline-deficient (CD) diet for 3, 21 or 90 days. Fifty μg proteins from liver homogenates were separated by 10% SDS-PAGE and blotted with an anti-c-Jun antibody (*Santa Cruz*). Four mice were used for each group in the experiment with each sample assayed in triplicate.

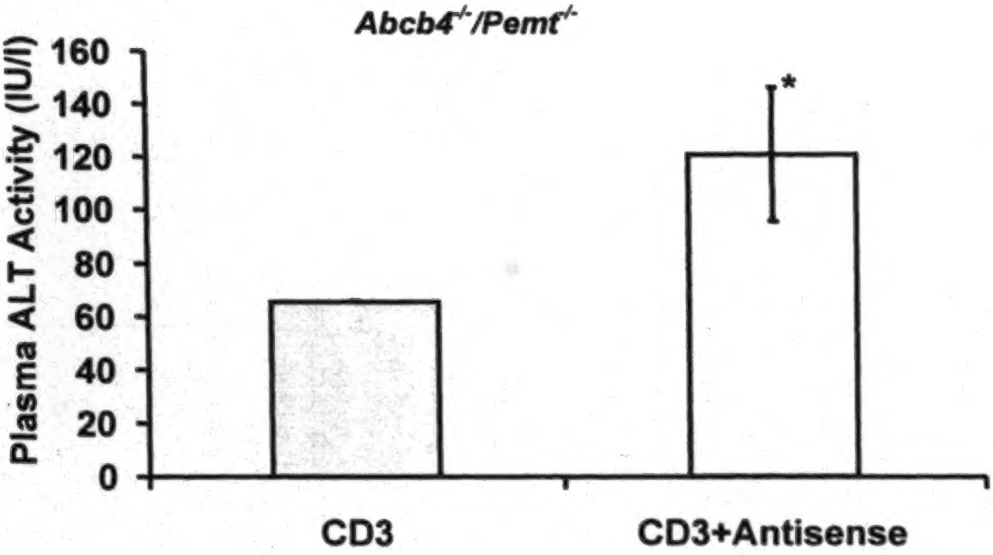

Fig. 2.14 c-Jun antisense blocked the adaptive response to choline deprivation in *Abcb4*$^{-/-}$/*Pemt*$^{-/-}$ mice

Abcb4$^{-/-}$/*Pemt*$^{-/-}$ mice were injected once intraperitoneally (i.p.) with 5 μg antisense DNA/kg mouse body weight in 200 μl saline. Then mice were fed a CD diet for 3 days. The control mice were injected with 200 μl saline. Liver damage occurred as indicated by increased plasma ALT activity after the treatment of c-Jun antisense.

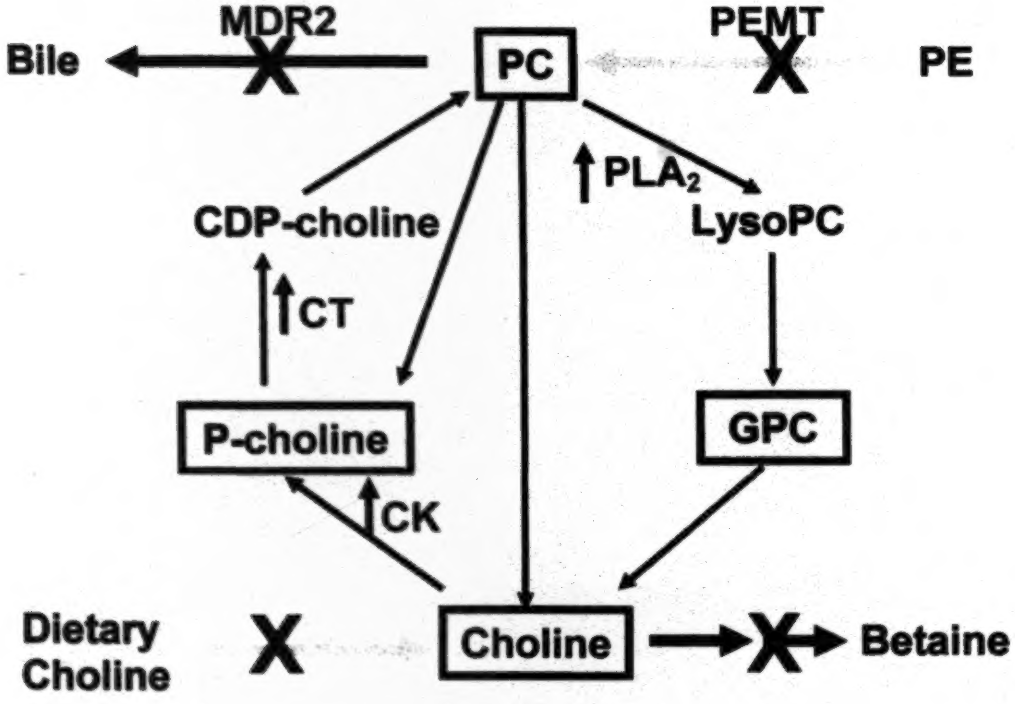
MDR2
Bile
PC
PEMT
PE
CDP-choline
PLA2
LysoPC
CT
P-choline
GPC
CK
Dietary Choline
Choline
Betaine

Fig. 2.15 Choline recycling pathways

P-choline, phosphocholine; GPC, glycerophosphocholine; PLA_2, phospholipase A_2; CT, CTP:phosphocholine cytidylyltransferase; CK, choline kinase; MDR2, multiple drug resistant protein 2.

References

1. Best, C. H., and Huntsman, M. E. The effects of the components of lecithine upon deposition of fat in the liver. (1932) *Journal of Physiology-London* **75**, 405-412
2. Best, C. H., Lucas, C. C., and Ridout, J. H. The lipotropic factors. (1954) *Ann N Y Acad Sci* **57**, 646-653
3. Zeisel, S. H., Da Costa, K. A., Franklin, P. D., Alexander, E. A., Lamont, J. T., Sheard, N. F., and Beiser, A. Choline, an essential nutrient for humans. (1991) *Faseb J* **5**, 2093-2098
4. Zeisel, S. H., and Blusztajn, J. K. Choline and human nutrition. (1994) *Annu Rev Nutr* **14**, 269-296
5. Blusztajn, J. K. Choline, a vital amine. (1998) *Science* **281**, 794-795
6. Zeisel, S. H. Choline: an essential nutrient for humans. (2000) *Nutrition* **16**, 669-671
7. Smit, J. J., Schinkel, A. H., Oude Elferink, R. P., Groen, A. K., Wagenaar, E., van Deemter, L., Mol, C. A., Ottenhoff, R., van der Lugt, N. M., van Roon, M. A., and et al. Homozygous disruption of the murine mdr2 P-glycoprotein gene leads to a complete absence of phospholipid from bile and to liver disease. (1993) *Cell* **75**, 451-462
8. Walkey, C. J., Yu, L., Agellon, L. B., and Vance, D. E. Biochemical and evolutionary significance of phospholipid methylation. (1998) *J Biol Chem* **273**, 27043-27046

9. Kuipers, F., Oude Elferink, R. P., Verkade, H. J., and Groen, A. K. Mechanisms and (patho)physiological significance of biliary cholesterol secretion. (1997) *Subcell Biochem* **28**, 295-318

10. Walkey, C. J., Donohue, L. R., Bronson, R., Agellon, L. B., and Vance, D. E. Disruption of the murine gene encoding phosphatidylethanolamine N-methyltransferase. (1997) *Proc Natl Acad Sci U S A* **94**, 12880-12885

11. Klaunig, J. E., Goldblatt, P. J., Hinton, D. E., Lipsky, M. M., Chacko, J., and Trump, B. F. Mouse liver cell culture. I. Hepatocyte isolation. (1981) *In Vitro* **17**, 913-925

12. Klaunig, J. E., Goldblatt, P. J., Hinton, D. E., Lipsky, M. M., and Trump, B. F. Mouse liver cell culture. II. Primary culture. (1981) *In Vitro* **17**, 926-934

13. Schneider, W. J., and Vance, D. E. Effect of choline deficiency on the enzymes that synthesize phosphatidylcholine and phosphatidylethanolamine in rat liver. (1978) *Eur J Biochem* **85**, 181-187

14. Weinhold, P. A., and Rethy, V. B. The separation, purification, and characterization of ethanolamine kinase and choline kinase from rat liver. (1974) *Biochemistry* **13**, 5135-5141

15. Yao, Z. M., Jamil, H., and Vance, D. E. Choline deficiency causes translocation of CTP:phosphocholine cytidylyltransferase from cytosol to endoplasmic reticulum in rat liver. (1990) *J Biol Chem* **265**, 4326-4331

16. Farber, S. A., Pack, M., Ho, S. Y., Johnson, I. D., Wagner, D. S., Dosch, R., Mullins, M. C., Hendrickson, H. S., Hendrickson, E. K., and Halpern,

M. E. Genetic analysis of digestive physiology using fluorescent phospholipid reporters. (2001) *Science* **292**, 1385-1388

17. Krug, E. L., and Kent, C. Assay for phospholipase C. (1981) *Methods Enzymol* **72**, 347-351
18. Bradford, M. M. A rapid and sensitive method for the quantitation of microgram quantities of protein utilizing the principle of protein-dye binding. (1976) *Anal Biochem* **72**, 248-254
19. Bligh, E. G., and Dyer, W. J. A rapid method of total lipid extraction and purification. (1959) *Can J Biochem Physiol* **37**, 911-917
20. McCluer, R. H., Ullman, M. D., and Jungalwala, F. B. HPLC of glycosphingolipids and phospholipids. (1986) *Adv Chromatogr* **25**, 309-353
21. Pritchard, P. H., and Vance, D. E. Choline metabolism and phosphatidylcholine biosynthesis in cultured rat hepatocytes. (1981) *Biochem J* **196**, 261-267
22. Hise, M. K., and Mansbach, C. M., 2nd. Determination of intracellular choline levels by an enzymatic assay. (1983) *Anal Biochem* **135**, 78-82
23. Brindle, N. P. J., and Ontko, J. A. Suppression of triglyceride secretion by epinephrine in isolated rat hepatocytes. (1986) *Biochem. Biophys. Res. Commun.* **141**, 191-197
24. Ko, K. W., Cook, H. W., and Vance, D. E. Reduction of phosphatidylcholine turnover in a Nb 2 lymphoma cell line after prolactin

treatment. A novel mechanism for control of phosphatidylcholine levels in cells. (1986) *J Biol Chem* **261**, 7846-7852

25. Borgstrom, B. *Phospholipid absorption* (1976) in *Lipid absorption: Biochemical and clinical aspects* (Rommel, K. G., H.; Bohmer, R., ed), pp. 65-72, MTP Press, Ltd., London

26. Robins, S. J. Recirculation and reutilization of micellar bile lecithin. (1975) *Am J Physiol* **229**, 598-602

27. Waite, M. Phospholipases, enzymes that share a substrate class. (1990) *Adv Exp Med Biol* **279**, 1-22

28. Vance, D. E. *Phospholipid biosynthesis in eukaryotes* (2002) in *Biochemistry of Lipids, Lipoproteins and Membranes* (Vance, J. E., ed), pp. 205-232, Elsevier Science, Amsterdam

29. Walkey, C. J., Yu, L., Agellon, L. B., and Vance, D. E. Biochemical and evolutionary significance of phospholipid methylation. (1998) *J. Biol. Chem.* **273**, 27043-27046

30. Shaulian, E., and Karin, M. AP-1 as a regulator of cell life and death. (2002) *Nat Cell Biol* **4**, E131-136

31. Aoyama, C., Ishidate, K., and Vance, D. E. unpublished results. *unpublished results*

32. Kiss, Z. Regulation of mitogenesis by water-soluble phospholipid intermediates. (1999) *Cell Signal* **11**, 149-157

33. Cui, Z., Shen, Y.-J., and Vance, D. E. Inverse correlation bewteen expression of phosphatidylethanolamine N-methyltransferase-2 and

growth rate of perinatal rat livers. (1997) *Biochim. Biophys. Acta* **1346**, 10-16

34. Vance, D. E., Walkey, C. J., and Cui, Z. Phosphatidylethanolamine N-methyltransferase from liver. (1997) *Biochim. Biophys. Acta* **1348**, 142-150

35. Cui, Z., and Vance, D. E. Expression of phosphatidylethanolamine N-methyltransferase-2 is markedly enhanced in long term choline-deficient rats. (1996) *J. Biol. Chem.* **271**, 2839-2843

36. Datko, A. H., and Mudd, S. H. Phosphatidylcholine Synthesis - Differing Patterns in Soybean and Carrot. (1988) *Plant Physiology* **88**, 854-861

37. Voelker, D. R. New perspectives on the regulation of intermembrane glycerophospholipid traffic. (2003) *J Lipid Res* **44**, 441-449

38. Fioravanti, M., and Yanagi, M. Cytidinediphosphocholine (CDP-choline) for cognitive and behavioural disturbances associated with chronic cerebral disorders in the elderly. (2005) *Cochrane Database Syst Rev*, CD000269

39. Adibhatla, R. M., and Hatcher, J. F. Cytidine 5'-diphosphocholine (CDP-choline) in stroke and other CNS disorders. (2005) *Neurochem Res* **30**, 15-23

40. Abdelmalek, M. F., Angulo, P., Jorgensen, R. A., Sylvestre, P. B., and Lindor, K. D. Betaine, a promising new agent for patients with nonalcoholic steatohepatitis: results of a pilot study. (2001) *Am J Gastroenterol* **96**, 2711-2717

Chapter 3

The Ratio of PC to PE is a Key Regulator of Membrane Integrity
--- Adaptation to Choline Deprivation II: Maintenance of Membrane Integrity via Maintenance of PC/PE Ratio

3.1 Introduction

A fundamental function of phospholipids in cells is to form membrane barriers. However, the reason membrane bilayers have a defined phospholipid composition is not clear. Phosphatidylcholine (PC) and phosphatidylethanolamine (PE) are two major phospholipids that are asymmetrically distributed in the plasma membrane bilayer where the majority of PC is localized to the outer leaflet whereas PE is enriched in the inner leaflet (*1*). PC homeostasis in the liver consists of PC anabolism and catabolism as well as PC uptake and secretion (Fig. 3.1). Hepatic PC is made from the CDP-choline pathway and via PE *N*-methyltransferase (PEMT), which converts PE to PC via 3 methylation reactions (2). PC secretion into bile is mediated by a PC-specific flippase, multiple drug resistant protein 2 (MDR2, ABCB4), in the hepatic canalicular membrane (3). Mice lacking PEMT are outwardly normal until they are fed a choline-deficient (CD) diet, after which rapid liver failure ensues *(4)*. However, mice lacking both ABCB4 and PEMT are resistant to the rapid liver failure exhibited by CD-*Pemt*$^{-/-}$ mice, and survive for at least 3 months when fed the CD diet (5). PE is made in mammalian cells from ethanolamine via the CDP-ethanolamine pathway or the decarboxylation of phosphatidylserine.

The release of hepatic alanine/aspartate aminotransferases (ALT/AST) into plasma is a well-known indicator of liver damage, since it is well-acknowledged that cellular contents will be released from liver cells upon cell damage. However, the mechanisms involved in the loss of membrane integrity during this process is unclear. Here, we report that a decrease in PC/PE ratio causes the loss of membrane integrity and induces cell damage and steatohepatitis in mice models.

3.2 Materials and Methods

3.2.1 Animals see 2.2.1

In choline re-feeding experiments, after fed a CD diet for 3 days, *Pemt*$^{-/-}$ mice were fed a CS diet for an additional 4 days.

3.2.2 Genotyping see 2.2.2

3.2.3 Sample collections see 2.2.3

3.2.4 Preparation of primary hepatocytes

Primary hepatocytes were isolated from *Pemt*$^{-/-}$ and *Abcb4*$^{-/-}$/*Pemt*$^{-/-}$ mice fed a choline-supplemented (CS) diet for 24 h and then switched to a choline-deficient (CD). *Pemt*$^{-/-}$ mice were fed a CD diet for 2 days and *Abcb4*$^{-/-}$/*Pemt*$^{-/-}$ mice were fed a CD diet for 3 or 21 days. Hepatocytes were cultured on a CS Dulbecco's modified Eagle's medium (DMEM) containing 4 mg/l choline or CD medium (DMEM without choline). Ethanolamine (4 mg/l) was added to both CS and CD medium. Three preparations of hepatocytes were used in each expeiment.

3.2.5 Lipid Analyses

Livers were homogenized with a Polytron homogenizer in 5 vol of 10 mM Tris-HCl, pH 7.2, 150 mM NaCl, 1 mM EDTA, 1 mM dithiothreitol, 1 mM phenylmethylsulfonyl fluoride, 1:100 proteinase inhibitor cocktail (*Sigma*, Cat#P8340). The homogenates were centrifuged for 5 min at 600 × g and the supernatants were collected. Protein concentration was quantified by the method of Bradford (6). Total lipids were extracted from liver homogenates by the method of Bligh & Dyer (7). Phospholipids were separated by high performance liquid chromatography and quantified with an electron-light scattering detector (8). Phosphatidyldimethylethanolamine was used as an internal standard for quantification. Neutral lipids including triacylglycerol, cholesterol and cholesteryl ester were measured by gas chromatography (9).

3.2.6 Enzyme assays

Plasma aspartate/alanine aminotransferases (AST/ALT) were assayed with a GPT/GOT Kit (*Sigma*, Cat#P505).

CTP:phosphoethanolamine cytidylyltransferase (ET) activity was measured in total cell homogenates (10). The substrate for the ET assay, [^{3}H]phosphoethanolamine, was made from [^{3}H]ethanolamine by phosphorylation with choline/ethanolamine kinase (10).

Phospholipase A_2 (PLA_2) activities were assayed in liver homogenates and primary hepatocytes with PED6 ((*N*-(6-(2,4-dinitrophenyl)amino)hexanoyl)-2-(4,4-difluoro-5,7-dimethyl-4-bora-3a,4a-diaza-*s*-indacene-3-pentanoyl)-1-hexadecanoyl-*sn*-glycero-3-phosphoethanolamine, triethylammonium salt, *Molecular Probes*), a self-quenching fluorescent analog of PE and a PLA_2-specific substrate (11). The specificity of increase in PLA_2 activity was further demonstrated by *in vitro* assay with 50 μmol/l PLA_2 inhibitors, BEL (bromoenol lactoe, an iPLA2-specific inhibitor) (12) and ATK (inhibits both $iPLA_2$ and $cPLA_2$) (13).

3.2.7 Preparation of hepatic plasma membranes and assessment of purity

Hepatocytes were incubated with colloidal silica and plasma membranes purified through differential centrifugation (14,15). Purity of plasma membrane fractions was assessed by enrichment of the plasma membrane marker (5'-nucleotidase) and degree of contamination by endoplasmic reticulum (NADPH-cytochrome C reductase) (16). Specific activities of 5'-nucleotidase in plasma membrane fractions and total liver homogenates were 56.4 and 3.8 μmol/h/mg protein, respectively. Specific activities of NADPH-cytochrome C reductase in plasma membrane fractions and total liver homogenates were 0.4 and 48.5 nmol/min/mg protein, respectively.

3.2.8 Assay of plasma membrane fluidity and potential

Membrane fluidity in the plasma membrane of hepatocytes was assessed by incubation of hepatocytes with 1-(4-trimethylammoniumphenyl)-6-phenyl-1,3,5-hexatriene *p*-tolunesulfonate (TMA-DPH) (*Molecular Probes*) at 4°C for 10 min and subsequently analyzed with a fluorometer within one min. The fluorescent polarization value was calculated with a formula of p = (F parallel-F perpendicular)/ (F parallel + F perpendicular) (17).

Membrane potential was assayed by incubation of hepatocytes with bis-(1,3-dibutylbarbituric acid)trimethine oxonol (DiBAC4(3)) (*Molecular Probes*) at 4°C for 30 min and subsequently analyzed with a fluorimeter within one min. Fluorescent intensity per cell number is presented (18).

3.2.9 Detection of PE on the cell surface of hepatocytes

Primary cultured hepatocytes were incubated with biotinylated PE-specific binding peptide, Ro98-019 (from Dr. Masato Umeda, Kyoto University), at 4°C for 30 min and subsequently with fluorescein isothiocyante (FITC) conjugated streptavidin (*Molecular Probes*) for 30 min. Fluorescence was visualized under a fluorescent microscope (19). Propidium iodide was added into the incubation buffer to identify viable cells. Fluorescent intensity of FITC (PE-binding) per cell number was quantified by flow cytometry. Four mice were used for each group in the experiment with each sample assayed in triplicate.

3.2.10 Measurement of PE synthesis and degradation

Primary hepatocytes from *Abcb4*$^{-/-}$/*Pemt*$^{-/-}$ mice were incubated with [^{3}H]glycerol for 2 h and then chased for 2 h. The rates of PE synthesis and degradation were calculated with the formula described previously (20). PE biosynthetic rate = dpm in PE at end of the pulse/mg protein divided by 2 h x the nmole of phosphoethanolamine/mg protein at the beginning of the pulse. PE degradation rate = decrease in dpm in PE between the end of the pulse and 2 h of chase/mg protein divided by 2 h x nmole of PE/mg protein. The relative rates are presented as a comparison between CS and CD groups.

3.2.11 Assays of VLDL-PC secretion and HDL-PC uptake rate

(i) VLDL-PC secretion assay: CS or CD hepatocytes from *Pemt*$^{-/-}$ and *Abcb4*$^{-/-}$/*Pemt*$^{-/-}$ mice were labeled with [^{3}H]choline for 2 h and then chased for 2 h. Cell culture medium was harvested and VLDL particles in the medium were isolated via sucrose gradient centrifugation (21,22). Total lipids were extracted by the Bligh & Dyer method (7) and [^{3}H]PC was separated by thin-layer chromatography (TLC). The rate of VLDL-PC secretion (dpm/h/1 × 10^6 cells) was calculated from 4 time points during the chase.

(ii) HDL-PC uptake assay: HDL particles were isolated from plasma of wild type mice via sucrose gradient centrifugation and pre-incubated with fluorescence-labeled PC, BODIPY-PC (*Molecular Probes*) (21,22). Primary cultured hepatocytes were incubated with [BODIPY-PC]HDL for 2 h. Cells were washed 3 times before measurement. Intracellular fluorescent intensity was measured by a fluorimeter. The rate of HDL-PC uptake (fluorescent intensity/h/1 × 10^6 cells) was calculated from 4 time points during 2 h of incubation.

3.2.12 Permeability assays of large unilamellar vesicles (LUVs)

Hepatic PC and PE (Avanti) were used to make LUVs at the PC/PE ratios of 0.5, 1.0, 1.5 and 2.0. PC + PE were mixed with sphingomyelin and cholesterol in a ratio of 86:1:9. Lipids were hydrated in Tris-HCl buffer (pH 9.0) with 50 mM calcein (*Molecular Probes*), a concentration at which the fluorescence of calcein is highly quenched. LUVs were prepared with an extruder (*Lipex Biomembranes*) and 100 nm Nuclepore filters at 55°C (23,24). LUVs were separated from released calcein by chromatography over a Sephadex G-75 column. The diameter of LUVs was measured by a light-scattering photometer and was controlled to 100 nm (23,24). The permeability assay was based on the measurement of the fluorescence of calcein accompanying its dequenching upon release from LUVs in Tris-HCl buffer (pH 7.4). The fluorescent intensity corresponding to 100% leakage was determined by adding 10% Triton X-100 to fully solubilize LUVs (23,24).

3.2.13 RNA interference (RNAi) of ET in cultured hepatocytes

RNAi sequence, 5'-AAGCACAACTGTGACTTCTCT-3', targeted to the mRNA of ET was inserted into p*Silencer* 4.1-CMV vectors (*Ambion*) to produce ETi vectors. A control sequence of ETi, 5'-AATCACAGCTATCACTGCTCT-3', was inserted into p*Silencer* 4.1-CMV vectors to produce an ETi control vector. Lipofectamine™ 2000 (*Invitrogen*) was used as carrier for transfection. ETi and control vectors were co-transfected with GFP vectors (ratio, 4:1) into cultured hepatocytes isolated from CD-*Pemt*$^{-/-}$ mice for 24 or 48 h. Hepatic RNA was extracted and mRNA levels of ET were quantified by SYBR Green assays via real-time PCR. Cyclophilin mRNA level was measured as the control. After transfection for 20 or 44 h, cells were incubated with fresh medium and cultured for 4 h. The cell culture medium was collected and assayed for ALT activity.

3.2.14 Inhibition of PE catabolism by arachidonyl trifluoromethyl ketone (ATK)

Primary hepatocytes were isolated from the livers of chow-fed *Abcb4*$^{-/-}$ */Pemt*$^{-/-}$ mice and cultured in medium that contained 17% delipidated FBS in DMEM that was choline-deficient (CD). The medium was replaced every 2 h in the first 8 h during cell culture to remove any secreted PC since PC secreted into medium might be reused. Arachidonyl trifluoromethyl ketone (ATK), a PLA_2-specific inhibitor (50 μmol/l) was added into the CD medium to block the degradation of phospholipids (including PE) for 24 or 48 h. After treatment for 20 or 44 h, cells were changed to fresh medium and cultured for 4 h after which cell culture medium was collected and assayed for ALT activity.

3.2.15 *In vivo* injection of ETi

Chow diet-fed *Pemt*$^{-/-}$ mice were hydrodynamically injected with control or ETi vectors (50mg/kg) in 1 ml saline in 5 sec at 0, 8 and 24 h. Mice were fasted for 12 h before sacrifice.

3.2.16 Histological and pathological Analysis

Liver tissues were fixed in 10% formalin. Liver sections were stained with hemotoxylin and eosin by the Department of Laboratory Medicine and Pathology, University of Alberta Hospital. The slides were visualized under light microscopy with 400 X magnification. Steatohepatitis was evaluated for inflammation by a pathologist using a standardized system (25).

3.3 Results

3.3.1 Liver failure is associated with a decreased ratio of PC to PE.

3.3.1.1 Hepatic low PC/PE ratios correlate with liver damage

Rapid depletion of hepatic PC by 50% via biliary secretion was originally suggested as the cause of severe liver failure in CD-*Pemt*$^{-/-}$ mice (4). However, CD-*Abcb4*$^{-/-}$/*Pemt*$^{-/-}$ mice also have a ~50% reduction in hepatic PC (Fig. 3.2A) without liver failure. Hepatic accumulation of triacylglycerol was observed in both CD-*Pemt*$^{-/-}$ mice and CD-*Abcb4*$^{-/-}$/*Pemt*$^{-/-}$ mice (Table 3.1). Thus, the liver damage is independent of the decrease in hepatic PC and fat accumulation.

An important difference between *Pemt*$^{-/-}$ mice and *Abcb4*$^{-/-}$/*Pemt*$^{-/-}$ mice is the PE content during choline deprivation. In CD-*Abcb4*$^{-/-}$/*Pemt*$^{-/-}$ mice, hepatic PC and PE decreased to a similar extent (Fig. 3.2A). In contrast, in CD-*Pemt*$^{-/-}$ mice, hepatic PE was unchanged while PC decreased by 50% (Fig. 3.2A). Thus, the PC to PE ratio decreased by 57% in CD-*Pemt*$^{-/-}$ mice but by only 17% in CD-*Abcb4*$^{-/-}$/*Pemt*$^{-/-}$ mice (Fig. 3.2B). The decrease in PC/PE ratio in CD-*Pemt*$^{-/-}$ mice coincided with an increased plasma level of alanine aminotransferase (ALT) (Fig. 3.3). The strong correlation (r = 0.95) between the PC/PE ratio and plasma ALT activity (Fig. 3.4) suggests that the liver failure in

CD-*Pemt*$^{-/-}$ mice might be associated with a decreased PC/PE ratio. Amounts of hepatic cholesterol (Table 3.1) and sphingomyelin (Fig. 3.2A), major plasma membrane lipids (Table 3.1), did not change in either murine model fed the CD diet. Moreover, the hepatic PC/PE ratio was unaffected in wild-type mice fed the CD diet for up to 21 days (Fig. 3.5A) and no liver damage was observed, although hepatic PC and PE levels both decreased by ~28% (Fig. 3.5B).

3.3.1.2 Plasma membrane PC/PE ratios correlate with hepatocyte damage

One possible explanation for the liver damage is that the plasma bile acid level was increased which would be detrimental to plasma membrane integrity. However, plasma bile acid levels were not increased in either CD-*Pemt*$^{-/-}$ or CD-*Abcb4*$^{-/-}$/*Pemt*$^{-/-}$ mice (Table 3.1). Another explanation for the liver damage is that alterations in phospholipid levels in the plasma membrane decreased the integrity of the plasma membrane. Therefore, plasma membranes were isolated from hepatocytes of CD-*Pemt*$^{-/-}$ and *CD-Abcb4*$^{-/-}$/*Pemt*$^{-/-}$ mice and the concentrations of PC, PE and SM were determined (Fig. 3.6A). We found a similar change of the PC/PE ratio as observed in total liver homogenates (Fig. 3.6B, 3.2 B). A high correlation (r = 0.97) was observed between the PC/PE ratio in the plasma membrane and plasma ALT activity (Fig. 3.6C). Neither the genotype nor the CD diet affected the plasma membrane level of SM (Fig. 3.6A). Although the amounts of PC in the livers of *Pemt*$^{-/-}$ mice decreased by ~50%, the amount of the majority of total lipids in the hepatocyte plasma membrane was not significantly affected by genotype or the choline content in the diet (Table 3.1).

3.3.1.3 Hepatic PC/PE ratios correlate with membrane fluidity

A change in membrane fluidity has been suggested to cause variations in membrane integrity and functions of membrane proteins (26). We, therefore, assessed the fluidity of hepatocyte plasma membranes using a fluorescent probe, 1-(4-trimethylammoniumphenyl)-6-phenyl-1,3,5-hexatriene *p*-toluenesulfonate (TMA-DPH) and found that membrane fluidity was higher in CD- compared to CS-*Pemt*$^{-/-}$ mice (Fig. 3.7) and correlated with the decrease in the PC/PE ratio (Fig. 3.6B).

3.3.1.4 Increased PE exposure on the cell surface in CD-*Pemt*$^{-/-}$ hepatocytes

Since the PC/PE ratio is strikingly lower in CD-*Pemt*$^{-/-}$ mice than in CD-*Abcb4*$^{-/-}$/*Pemt*$^{-/-}$ mice we postulated that more PE would be exposed on the cell surface of CD-*Pemt*$^{-/-}$ hepatocytes. Figs. 3.8 shows a striking increase in surface exposure of PE in hepatocytes from *Pemt*$^{-/-}$ mice fed the CD diet for 2 days, but no change in the *Abcb4*$^{-/-}$/*Pemt*$^{-/-}$ mice fed the CD diet for 21 days.

3.3.1.5 Hypothetical mechanism for liver failure in CD-*Pemt*$^{-/-}$ mice

The data suggest a strong link between liver damage and the PC/PE ratio in the plasma membrane. We hypothesize that the physical change in membrane structure induced by increased PE exposure on the cell surface causes a loss of membrane integrity (Fig. 3.9). An increased content of the cone-shaped, non-bilayer-forming lipid, PE, in the outer monolayer of the plasma membrane, may result in the formation of structures that are not as closely packed as those formed by PC which has a cylindrical shape (27,28). The maintenance of a normal PC/PE ratio of ~ 1.5 to 1.8 in the livers of CD-*Pemt*$^{-/-}$/*Abcb4*$^{-/-}$ would, therefore, favor retention of membrane integrity whereas a ratio of < 1.0 in CD-*Pemt*$^{-/-}$ mice would result in disruption of membrane integrity.

3.3.2 The mechanism of the maintenance of PC/PE ratio in CD-*Pemt*$^{-/-}$/*Abcb4*$^{-/-}$ mice

3.3.2.1 Increased PE catabolism causes the decrease in hepatic PE levels in CD-*Pemt*$^{-/-}$/*Abcb4*$^{-/-}$ mice

The major difference in our two murine models during choline deprivation is regulation of PE levels. We investigated the reason for the decline in PE in the CD-*Pemt*$^{-/-}$/*Abcb4*$^{-/-}$ mice. [^{3}H]Glycerol was used to trace PE metabolism by pulse-chase labeling experiments in primary hepatocytes. As seen in Fig. 3.10, the rate [^{3}H]glycerol incorporation into PE was ~1.8 times higher in CD compared to CS hepatocytes. In contrast the catabolism of [^{3}H]PE was enhanced ~3-fold. Thus, the decreased content of PE in CD-*Pemt*$^{-/-}$/*Abcb4*$^{-/-}$ mice likely resulted from an imbalance between PE biosynthesis and degradation.

3.3.2.2 Different fates for PC removal lead to altered PE metabolism and adaptation to choline deprivation

The levels of hepatic PC decreased in both mouse models. Hepatic PC can be decreased by secretion into bile, lipoprotein secretion and catabolism. We have attributed the rapid decline in hepatic PC in CD-*Pemt*$^{-/-}$ mice to the elimination of PC into bile (5). Since there was no secretion of PC into bile of CD-*Pemt*$^{-/-}$/*Abcb4*$^{-/-}$ mice, we investigated the mechanism for the decrease of PC in the CD-*Pemt*$^{-/-}$/*Abcb4*$^{-/-}$ mice. The amount of hepatic PC obtained from HDL uptake is similar to the amount of PC secreted in VLDL (22). The rate of VLDL-PC secretion was decreased by choline deprivation in hepatocytes of both murine models after choline deprivation (Fig. 3.11A), but HDL-PC uptake rate did not change (Fig. 3.11B). Thus, liver did not exhibit increased PC loss via lipoprotein metabolism in the two murine models during choline deprivation. A likely mechanism for the decrease in PC content in *Pemt*$^{-/-}$/*Abcb4*$^{-/-}$ hepatocytes is increased catabolism. We previously found that phospholipase A_2 (PLA_2) activity and PC degradation are up-regulated in CD-*Pemt*$^{-/-}$/*Abcb4*$^{-/-}$ mice, but not in CD-*Pemt*$^{-/-}$ mice (Chapter 2) (5). Moreover, the activities of both calcium-dependent PLA_2 ($cPLA_2$) and calcium-independent PLA_2 ($iPLA_2$) are enhanced in CD-*Pemt*$^{-/-}$/*Abcb4*$^{-/-}$ hepatocytes (Fig. 3.12), but not in CD-*Pemt*$^{-/-}$ hepatocytes (Fig. 3.12). The observed increase of *in vitro* PLA_2 activity in CD-*Pemt*$^{-/-}$/*Abcb4*$^{-/-}$ hepatocytes was prevented by the PLA_2 inhibitors, BEL (an $iPLA_2$-specific inhibitor) and ATK (an inhibitor of both $iPLA_2$ and $cPLA_2$) (Fig. 3.12). Thus, confirming that the activity being measured was PLA_2. Rapid depletion of hepatic PC resulted from constant bile secretion of PC in CD-*Pemt*$^{-/-}$ mice (5) whereas the loss of hepatic PC in CD-*Pemt*$^{-/-}$/*Abcb4*$^{-/-}$ mice can be attributed to increased PC catabolism. Thus, CD-*Pemt*$^{-/-}$/*Abcb4*$^{-/-}$ mice maintain the PC/PE ratio and membrane integrity in hepatocyte plasma membranes, escape liver failure and adapt to choline deprivation by balancing PC catabolism with enhanced PE catabolism (Fig. 3.13).

3.3.3 The ratio of PC to PE is a key regulator of membrane integrity

3.3.3.1 PC/PE ratios influence membrane integrity of large unilamellar vesicles (LUVs)

Our data suggest that a decrease in the PC/PE ratio led to loss of membrane integrity. To test this idea, we made large unilamellar vesicles (LUVs) of different PC/PE ratios. The LUVs contained a fluorescent molecule, calcein, in a quenched state entrapped in the vesicles. Fluorescence is observed only when calcein fluorescence is de-quenched upon leakage from the vesicles. Consistent with our hypothesis, a decrease in the PC/PE ratio enhanced release of calcein from LUVs (Fig. 3.14) indicating that the low PC/PE ratio in CD-*Pemt*$^{-/-}$ hepatocytes might be responsible for increased membrane permeability.

3.3.3.2 Knockdown of PE biosynthesis in CD-*Pemt*$^{-/-}$ hepatocytes increases PC/PE ratio and attenuates cell damage

In another approach to test the importance of the PC/PE ratio for membrane integrity, we hypothesized that liver failure in CD-*Pemt*$^{-/-}$ mice occurred because PE biosynthesis did not decrease in response to choline deprivation. The activity of CTP:phosphoethanolamine cytidylyltransferase (ET, or PCYT2) was the same in *Pemt*$^{-/-}$ and *Abcb4*$^{-/-}$/*Pemt*$^{-/-}$ murine hepatocytes and did not change upon feeding the animals the CD diet (Fig. 3.15), suggesting that the rate of PE biosynthesis from the CDP-ethanolamine pathway was independent of the genotype of the mice. We next investigated whether or not liver damage would be reduced in CD-*Pemt*$^{-/-}$ murine hepatocytes when PE synthesis was attenuated via inhibition of ET. To test this idea, we performed RNA interference (RNAi) using a vector targeted to ET (ETi). Hepatocytes were prepared from *Pemt*$^{-/-}$ mice fed a CD diet for 2 days. Four h after plating, the hepatocytes were transfected with a vector encoding green fluorescent protein (GFP) and either the control vector, or the ETi vector for 24 h or 48 h. ETi effectively decreased the mRNA level (71% after 24 h and 75% after 48 h) and activity for ET by 55% after 24 h and 37% after 48 h (Fig. 3.16A, B) and decreased the concentration of PE by 25% after 24 h and 45% after 48 h (Fig. 3.17), with a corresponding increase in the PC/PE ratio by 25% after 24 h and 62% after 48 h (Fig. 3.18A). When hepatocytes incubated with ETi for 24 h were incubated with [^{3}H]ethanolamine for 2 h (Fig. 3.19A) and 24 h (Fig. 3.19B), incorporation of label into PE was reduced by 36 % and 46% respectively. The increased PC/PE ratio correlated with both a decreased exposure of PE on the hepatocyte surface (Fig. 3.20) and decreased leakage of ALT into the medium (Fig. 3.18B). Thus, in hepatocytes from CD-*Pemt*$^{-/-}$ mice, inhibition of PE biosynthesis increases the PC/PE ratio and decreases membrane integrity.

3.3.3.3 Inhibition of PE degradation in CD-*Abcb4*$^{-/-}$/*Pemt*$^{-/-}$ hepatocytes causes decreased PC/PE ratios and induces cell damage

In an alternative approach to alter hepatocyte permeability, we increased the PE content of hepatocytes from CD-*Abcb4*$^{-/-}$/*Pemt*$^{-/-}$ mice. The hepatocytes were cultured in CD medium and the CD medium was replaced every 2 h during the first 8 h of cell culture to remove hepatic PC. An inhibitor of PLA_2 (arachidonyl trifluoromethyl ketone, ATK) was added into CD medium to block PC and PE degradation. Fig. 3.21 shows that the presence of the PLA_2 inhibitor lowered the PC/PE ratio and increased the release of ALT after 24 or 48 h. Thus, attenuation of PE catabolism in CD-*Abcb4*$^{-/-}$/*Pemt*$^{-/-}$ hepatocytes decreased the PC/PE ratio and increased hepatocyte damage.

3.3.4 Is PC/PE ratio a critical regulator in developing steatosis into steatohepatitis?

3.3.4.1 CD-*Pemt*$^{-/-}$ mice developed steatohepatitis but CD-*Pemt*$^{-/-}$/*Abcb4*$^{-/-}$ mice developed steatosis

Both CD-*Pemt*$^{-/-}$ mice and CD-*Pemt*$^{-/-}$/*Abcb4*$^{-/-}$ mice showed increased liver weight and ratios of liver weight to body weight but the CD diet did not affect body weight (Fig. 3.22A, B, C). When *Pemt*$^{-/-}$ mice were fed the CD diet they died of fulminant hepatic failure with panlobular macrovesicular steatosis, prominent hepatocyte ballooning, Mallories hyaline and panacinar inflammation (pan lobular steatohepatitis, all zones) (Fig. 3.3, 3.23, 3.24, Table 3.1) (4). In contrast, *Abcb4*$^{-/-}$/*Pemt*$^{-/-}$ mice developed zone 3 microvesicular steatosis after being fed the CD diet for 3 days, and macrovesicular steatosis in all zones without lobular inflammation by 21 days (Fig. 3.3, 3.23, 3.24, Table 3.1). Glucose and insulin levels in plasma were normal in CD-*Pemt*$^{-/-}$/*Abcb4*$^{-/-}$ mice, but decreased levels of both plasma glucose and insulin suggested that insulin insensitivity might occur in CD-*Pemt*$^{-/-}$ mice (Fig. 3.25A, B). Thus, these two mouse models are pure steatosis or steatohepatitis without diabetes.

3.3.4.2 Hepatic PC/PE ratios correlate with the degree of steatohepatitis

Multiple 'hit' models have been proposed for the pathogenesis of non-alcoholic fatty liver disease but no distinct mechanism has been shown to convert steatosis into steatohepatitis (29,30). The PC/PE ratio is a potential candidate for this process since the difference between steatosis and non-alcoholic steatohepatitis (NASH) is hepatocellular injury in the latter, typified by ballooning degeneration, and the resulting lobular inflammation (29,30).

From these two models, we found that the decrease of PC/PE ratio correlated with the increased degrees of steatohepatitis, but not steatosis. In the other words, variations of the PC/PE ratio were correlated with status of liver damage, but not fat accumulation. Further support for the involvement of the PC/PE ratio in steatosis is that when wild-type mice were fed the CD diet for 21 days, steatosis developed but the PC/PE ratio was not changed and no liver damage occurred regardless of the reduction of hepatic PC level (Fig. 3.5, 3.26).

3.3.4.3 Increased PC/PE ratios reverse steatohepatitis

In *Pemt*$^{-/-}$ mice, a choline-supplemented diet reversed the liver damage caused by choline deficiency (31). The severe steatohepatitis in CD-*Pemt*$^{-/-}$ mice was markedly attenuated, and the PC/PE ratio returned to normal when *Pemt*$^{-/-}$ mice were fed choline (Fig. 3.27). Moreover, normalization of the PC level coincided with reversal of panlobular macrovesicular fat to normal as indicated by histology and hepatic TG levels. (Fig. 3.23, 3.24, 3.27).

3.3.4.4 Increased PC/PE ratios reverse steatohepatitis, but not steatosis

In *in vitro* analyses, we found that ETi increases the PC/PE ratio and attenuates cell damage in CD-*Pemt*$^{-/-}$ hepatocytes by decreasing the amount of PE. (Fig. 3.17, 3.18). To determine if a similar result were observed in mice, we injected the ETi vector via the tail-vein into CD-*Pemt*$^{-/-}$ mice using a hydrodynamic protocol that results in efficient delivery of the vector to the liver (32,33). Mice were injected 3 times over a 24 h period, then fed the CD diet for 2 days prior to sacrifice. The ETi prevented the steatohepatitis but not the steatosis (Fig. 3.23, 3.28A, B, C). The PC/PE ratio in the liver was increased by the ETi injections but the PC level did not change (Fig. 3.28D, E), consistent with the idea that fat accumulation in the liver depends on hepatic PC levels. These data suggest that an increased PC/PE ratio *in vivo* can reverse steatohepatitis, but not steatosis. However, an increased amount of hepatic PC can attenuate steatosis.

3.3 Discussion

In combination, these studies suggest that the PC/PE ratio is a critical modulator of membrane integrity. A gradual decrease in hepatic PC in CD-wild-type and CD-*Pemt*$^{-/-}$/*Abcb4*$^{-/-}$ mice provides sufficient time for PC and PE metabolism to be modified so that a normal PC/PE ratio is maintained and liver failure is prevented. An adaptation to choline deprivation in CD-*Abcb4*$^{-/-}$/*Pemt*$^{-/-}$ mice is triggered during choline deprivation, that is, the maintenance of membrane integrity via the maintenance of PC/PE ratio to escape liver failure. This adaptation was also displayed in wild-type mice fed the CD diet. On the other hand, in CD-*Pemt*$^{-/-}$ mice, the PC content decreased too rapidly for metabolic adjustments to be made. Consequently, the PC/PE ratio decreased and liver damage occurred. Our results also explain, for the first time, how ALT/AST can be released outside hepatocytes during liver damage. Support for our hypothesis comes from studies in which choline deprivation similarly decreased the amount of PC, but not PE, in PC12 cells resulting in cell death (34). Moreover, an increased level of PE but not PC, promoted cell damage of heart myocytes as indicated by the leakage of the cytosolic enzyme lactate dehydrogenase (35). Our results also suggest that when the PC/PE ratio decreased below ~1.0 in liver, membrane integrity is impaired.

A well-acknowledged model of non-alcoholic steatohepatitis (NASH) is to feed mice or rats a methionine-deficient and choline-deficient (MCD) diet, which has been intensely studied in the past few decades (30,36). Although no previous reports have noted a correlation between the PC/PE ratio and steatohepatitis, livers from these animals had a decreased content of PC levels but no change in the amount of PE. Therefore, the PC/PE ratio was decreased (37-39). Livers from MCD murine models have a reduced endogenous rate of PC and choline biosynthesis and mimic CD-*Pemt*$^{-/-}$ mice. Since *S*-adenosylmethionine (AdoMet) is derived from methionine and is a substrate of PEMT (28), dietary deprivation of methionine attenuates the PEMT pathway. Although liver failure and steatohepatitis occurred within 3 days in CD-*Pemt*$^{-/-}$ mice, a similar degree of steatohepatitis did not develop until ~3 months in MCD mice (30,36), probably because the PEMT pathway was incompletely blocked in MCD mice. Moreover, methionine can be made *de novo* from betaine or methyltetrahydrofolate (40). In addition, gradual development of steatohepatitis in MCD-wild type mice also indicates that the flux of remaining SAM into PC resulted in gradual reduction of hepatic PC. Therefore, the PC/PE ratio was decreased gradually (3 months) in MCD-wild type mice as compared with acute (3 days) reduction of the PC/PE ratio in CD-*Pemt*$^{-/-}$ mice (37-39).

The current data strongly support the hypothesis that a decreased ratio of PC/PE is very important for the evolution of steatosis into steatohepatitis. A decreased PC/PE ratio adversely affects membrane integrity, resulting in liver damage. However, the question remains whether or not the change in the PC/PE ratio initiaties inflammation or is the end point of inflammation. A decreased PC/PE ratio correlates with decreased membrane potential of hepatocyte plasma membranes (Fig. 3.29). The change of membrane potential was suggested to be the initial reason for inflammation since ion flow (such as calcium and radicals) are altered during the change of membrane potential. In addition, loss of membrane integrity not only leads to the release of cellular contents, but also increases the influx of extracellular contents including cytokines. C-reactive protein (CRP) is one of the acute phase proteins that increases during systemic inflammation. The activation of CRP is initiated by the binding of phosphocholine on the cell surface (41). A disturbed membrane bilayer appears to be necessary for binding of CRP and decreased PC/PE ratio in cell membranes led to increased binding of CRP to membrane and activated the alternative complement pathway (42). Therefore, a decreased PC/PE ratio might initiate inflammation.

Elevated plasma ALT/AST activity is a hallmark of human liver disorders. The factors that promote hepatocyte damage and inflammation in the progression of steatosis to steatohepatitis have yet to be resolved. It will be of great interest to determine whether the PC/PE ratio is decreased in patients with non-alcoholic fatty liver disease and alcoholic liver disease. The mouse models used in our study might be helpful for determining what regulates the transition from steatosis to steatohepatitis. From pilot experiments on human liver disorders, we did find significant reductions of hepatic PC/PE ratio in alcoholic cirrhotic livers (decrease 46.4%) and primary biliary cirrhotic livers (decrease 46.0%) as compared with healthy human livers, although cirrhosis is the final stage of severe steatohepatitis. Our results not only provide a clue to the mechanisms involved in the development of steatohepatitis, but also suggest that boosting hepatic PC levels and/or reducing the hepatic PE level might ameliorate steatohepatitis.

Table 3.1 Factors potentially influencing membrane integrity

Plasma bile acids were analyzed with kits from Sigma. Neutral lipids in liver homogenates and plasma membrane were extracted and analyzed by gas-liquid chromatography-flame ionization detector. TG, triacylglycerol; Ch, cholesterol; PL, phospholipid; Memb., membrane; CS, choline supplemented; CD, choline-deficient for 3 or 21 days.

	Pemt$^{-/-}$, CS	*Pemt*$^{-/-}$, CD3	*Abcb4*$^{-/-}$/ *Pemt*$^{-/-}$, CS	*Abcb4*$^{-/-}$/ *Pemt*$^{-/-}$ CD21
Hepatic TG (µg/mg protein)	105.3 ± 41.9	578.9 ± 122.5*	17.3 ± 9.2	962.2 ± 171.7*
Hepatic Ch (nmol/mg protein)	14.9 ± 0.9	15.4 ± 2.9	14.2 ± 2.3	17.2 ± 2.2
Plasma Memb. Ch (nmol/mg protein)	158.7 ± 14.2	173.3 ± 1.3	146.4 ± 15.3	177.5 ± 12.6
Plasma Memb. Total Lipids (PL + Ch) (nmol/mg protein)	431.3 ± 23.7	431.2 ± 28.3	413.7 ± 17.3	380.3 ± 9.6
Plasma Bile Acids (µmol/l)	101.5 ± 41.9	131.9 ± 42.5	117.6 ± 52.1	57.8 ± 9.7

*, $p<0.05$; Data = mean ± SD.

Fig. 3.1 Phosphatidylcholine (PC) homeostasis in the liver

There are four acquisition pathways indicated by green arrows. 1) 70% of PC biosynthesis in the liver is derived from the CDP-choline pathway; 2) 30% of PC biosynthesis is from phosphatidylethanolamine (PE) via the phosphatidylethanolamine *N*-methyltransferase (PEMT) pathway; 3) PC can also be derived from reacylation of lysoPC; 4) high density lipoprotein and low density lipoprotein (HDL and LDL) transport not only neutral lipids into liver, but also phospholipids (mainly PC). PC provides choline for sphingomyelin (SM) synthesis and is a precursor of phosphatidylserine (PS). A major loss of hepatic PC is from biliary secretion mediated by multiple drug resistant protein 2 (MDR2, ABCB4). In addition to PC degradation by phospholipases, hepatic PC can also be secreted as an important component of very low-density lipoprotein (VLDL) and HDL.

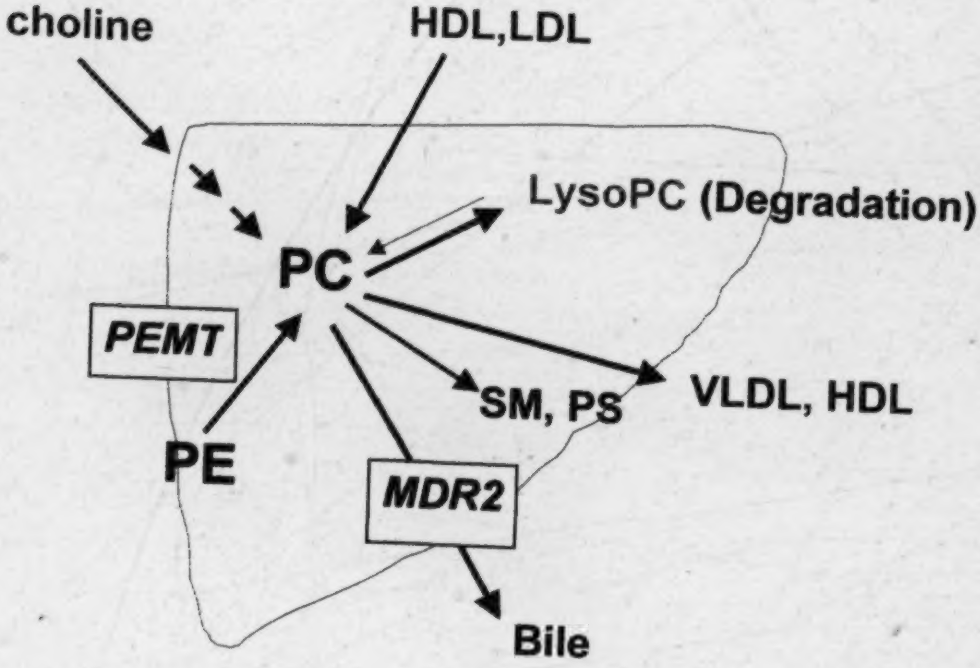
choline
HDL,LDL
LysoPC (Degradation)
PC
PEMT
PE
SM, PS
VLDL, HDL
MDR2
Bile

Fig. 3.2 Hepatic phospholipid compositions

Pemt$^{-/-}$ mice and *Abcb4*$^{-/-}$/*Pemt*$^{-/-}$ mice were fed a choline-supplemented (CS) diet for 24 h and then switched to a choline-deficient (CD) diet for 3 (CD3) or 21 (CD21) days. **(A)** Levels of PC, PE and sphingomyelin (SM) in liver homogenates. *, $P < 0.05$; **, $P < 0.001$ comparing CS to CD groups. **(B)** Molar ratio of PC to PE in CS compared to CD mice. *, $P < 0.05$; **, $P < 0.001$.

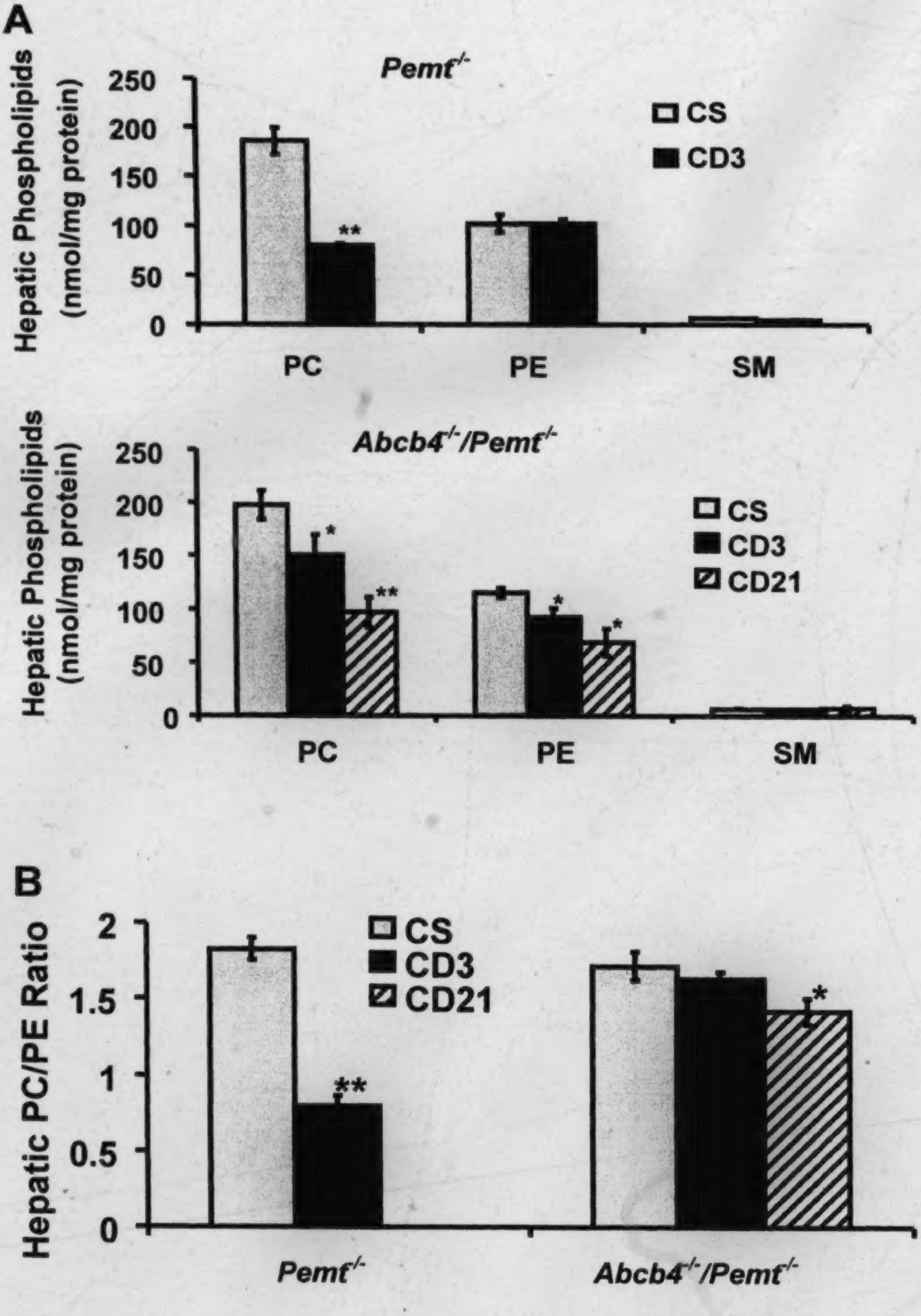
A
Pemt-/-
Hepatic Phospholipids (nmol/mg protein)
250
200
150
100
50
0
CS
CD3
**
PC
PE
SM
Abcb4-/-/Pemt-/-
Hepatic Phospholipids (nmol/mg protein)
250
200
150
100
50
0
CS
CD3
CD21
*
**
*
*
PC
PE
SM
B
Hepatic PC/PE Ratio
2
1.5
1
0.5
0
CS
CD3
CD21
**
*
Pemt-/-
Abcb4-/-/Pemt-/-

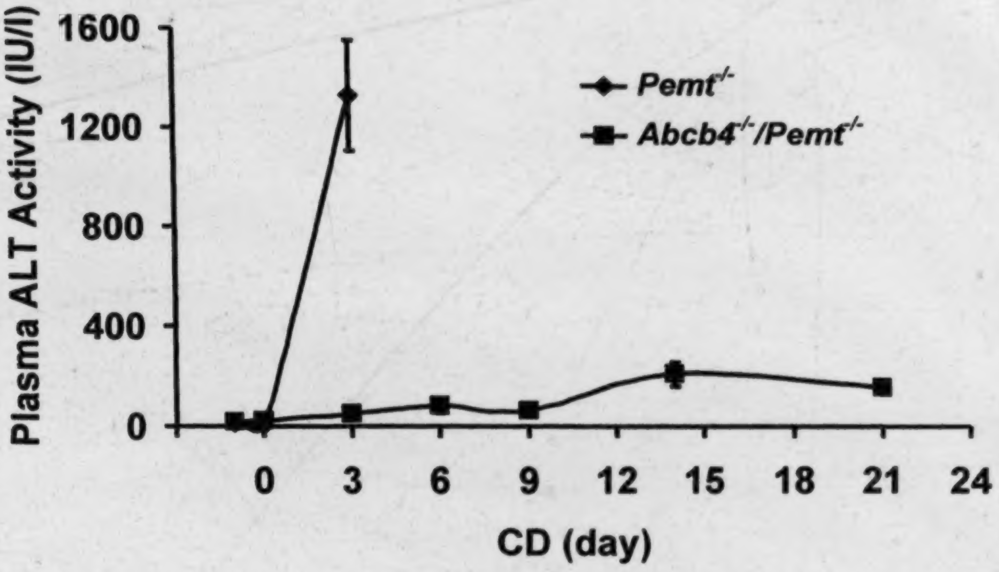

Fig. 3.3 CD-*Abcb4*$^{-/-}$/*Pemt*$^{-/-}$ mice are resistant to liver failure, but not CD-*Pemt*$^{-/-}$ mice

Plasma samples were collected from *Pemt*$^{-/-}$ mice and *Abcb4*$^{-/-}$/*Pemt*$^{-/-}$ mice fed the choline-supplemented (CS) diet for 24 h (0 day) then transferred to the choline-deficient (CD) diet for 3 to 21 days. Plasma ALT activity was measured at day –1, 0, 1, 2, 3, 6, 9, 14 and 21. Mice were fed a normal chow diet until day –1.

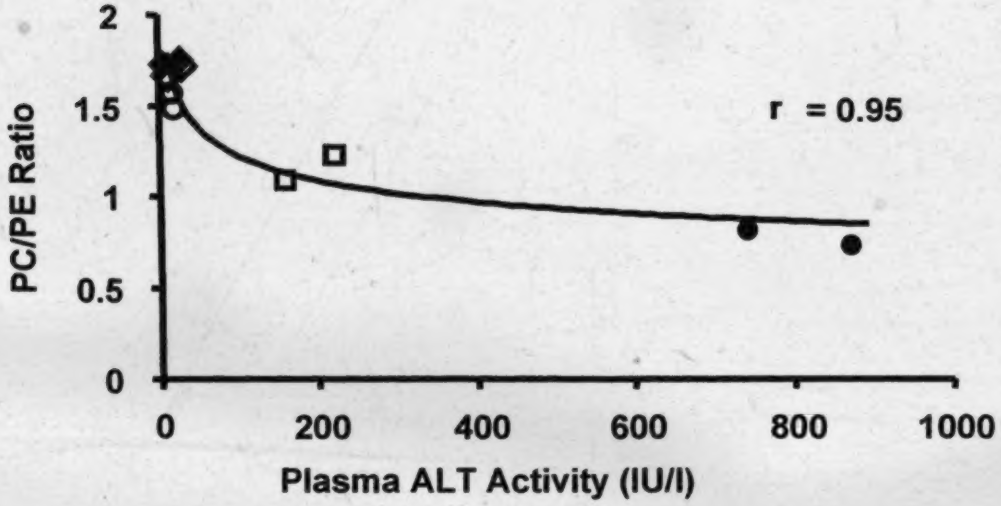

Fig. 3.4 Hepatic PC/PE ratios correlate with liver damage

Correlation between hepatic PC/PE ratio and plasma ALT activity. Data are means from CS-*Pemt*$^{-/-}$ mice (◆), CS-*Abcb4*$^{-/-}$/*Pemt*$^{-/-}$ mice (◇), CD3-*Abcb4*$^{-/-}$/*Pemt*$^{-/-}$ mice (O), CD21-*Abcb4*$^{-/-}$/*Pemt*$^{-/-}$ mice (□) and CD3-*Pemt*$^{-/-}$ mice (•).

Fig. 3.5 The PC/PE ratio is maintained without liver damage in CD-*Pemt*$^{+/+}$ mice

Pemt$^{+/+}$ mice (wild type) were fed a choline-supplemented (CS) diet for 24 h (0 day) and then switched to a choline-deficient (CD) diet for 3 (CD3) or 21 (CD21) days. **(A)** The PC/PE ratio in CD-wild type mice. **(B)** The amount of hepatic PC and PE as a function of days on a CD diet. Plasma ALT activities were 19.5 ± 4.5, 36 ± 3 and 39 ± 13 IU/l in CS-wild type, CD3-wild type and CD21-wild type mice, respectively.

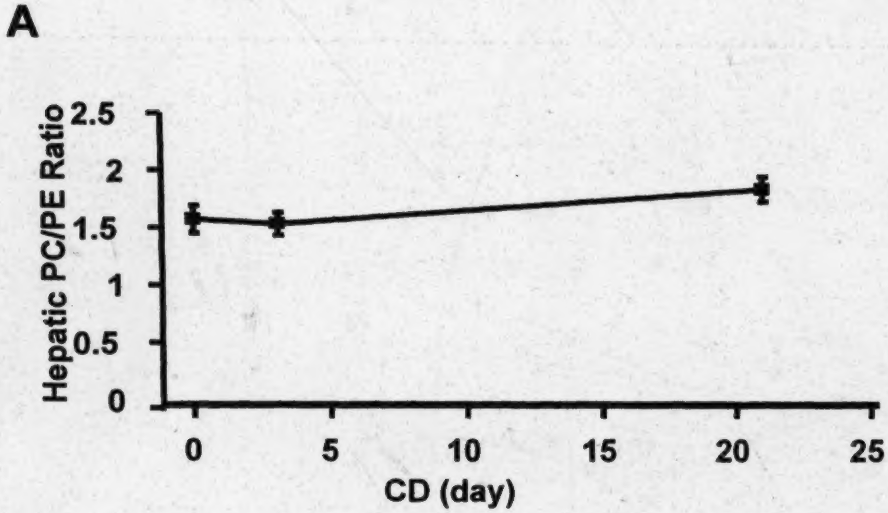
A
Hepatic PC/PE Ratio
2.5
2
1.5
1
0.5
0
0
5
10
15
20
25
CD (day)

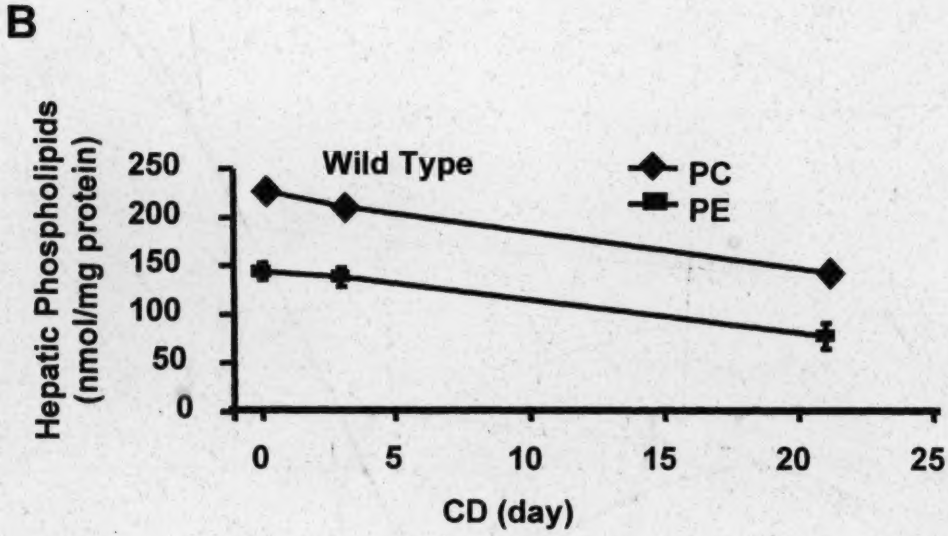
B
Hepatic Phospholipids (nmol/mg protein)
Wild Type
PC
PE
250
200
150
100
50
0
0
5
10
15
20
25
CD (day)

Fig. 3.6 Plasma membrane PC/PE ratios correlate with hepatocyte damage

(A) Amounts of phospholipids in the plasma membrane of hepatocytes from 3 preparations of *Pemt*$^{-/-}$ mice and *Abcb4*$^{-/-}$/*Pemt*$^{-/-}$ mice fed a choline-supplemented (CS) diet for 24 h and then switched to a choline-deficient (CD) diet for 2, 3 or 21 (CD2, CD3 or CD21) days. *, $P < 0.05$; **, $P < 0.01$ for CS vs CD mice. **(B)** The PC/PE ratio in the plasma membrane of hepatocytes. *, $P < 0.05$; **, $P < 0.01$ comparing CS to CD groups. §, *Pemt*$^{-/-}$ mice were fed the CD diet for 2 days and *Abcb4*$^{-/-}$/*Pemt*$^{-/-}$ mice were fed the CD diet for 3 days. **(C)** Correlation between plasma membrane PC/PE ratios and plasma ALT activity. Data were means from CS-*Pemt*$^{-/-}$ mice (◆), CS-*Abcb4*$^{-/-}$/*Pemt*$^{-/-}$ mice (◇), CD3-*Abcb4*$^{-/-}$/*Pemt*$^{-/-}$ mice (○), CD21-*Abcb4*$^{-/-}$/*Pemt*$^{-/-}$ mice (□) and CD2-*Pemt*$^{-/-}$ mice (•).

A

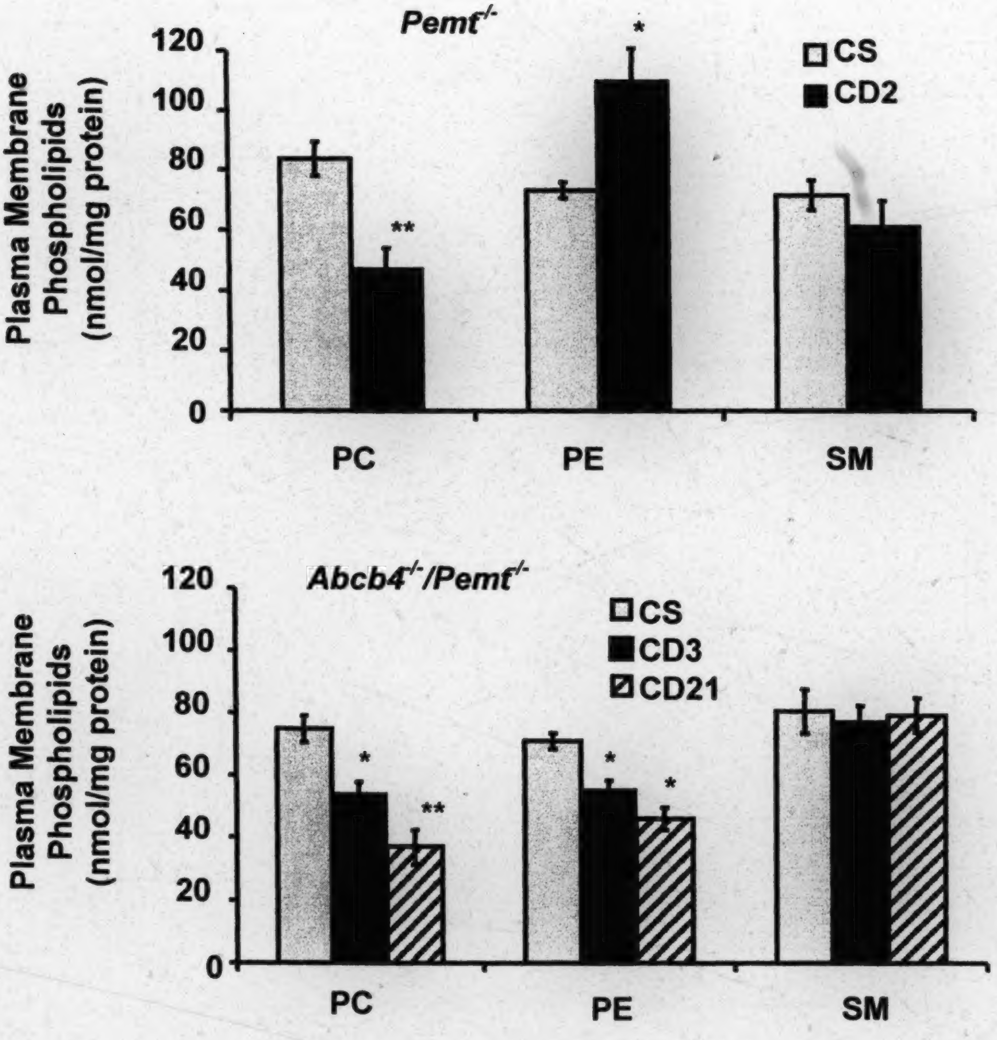
Pemt-/-
Plasma Membrane Phospholipids (nmol/mg protein)
120
100
80
60
40
20
0
CS
CD2
**
*
PC
PE
SM
Abcb4-/-/Pemt-/-
Plasma Membrane Phospholipids (nmol/mg protein)
120
100
80
60
40
20
0
CS
CD3
CD21
*
**
*
*
PC
PE
SM

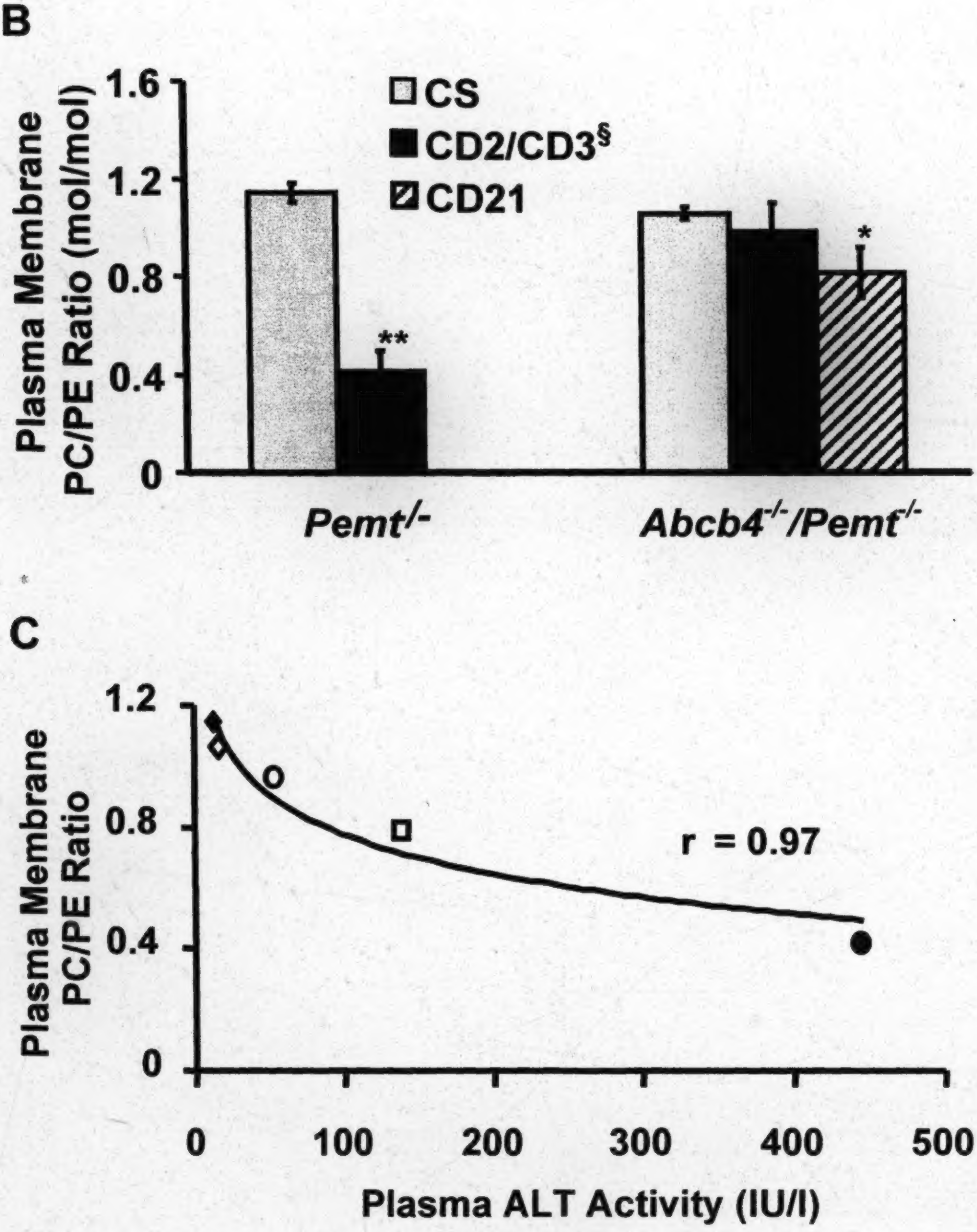
B
Plasma Membrane PC/PE Ratio (mol/mol)
1.6
1.2
0.8
0.4
0
□ CS
■ CD2/CD3§
▨ CD21
**
*
Pemt-/-
Abcb4-/-/Pemt-/-
C
Plasma Membrane PC/PE Ratio
1.2
0.8
0.4
0
r = 0.97
0
100
200
300
400
500
Plasma ALT Activity (IU/l)

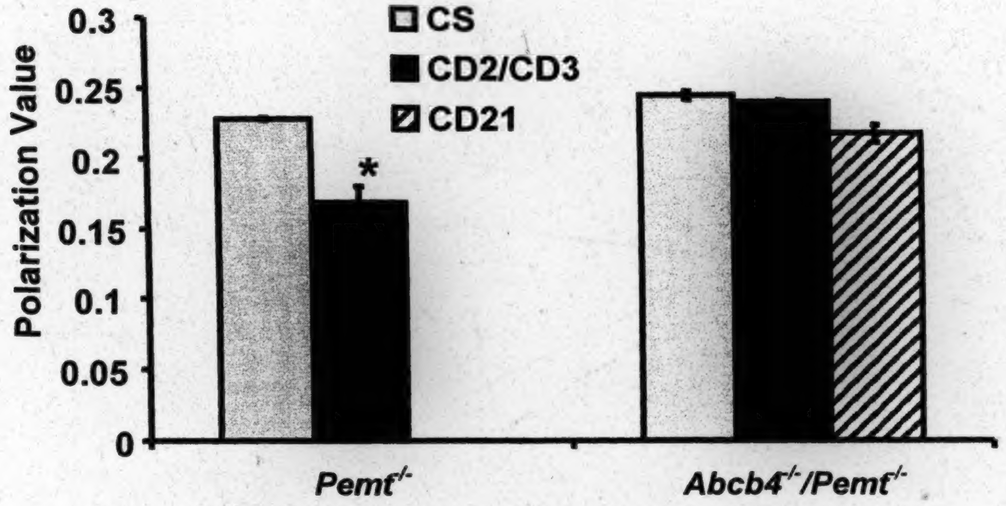

Fig. 3.7 Hepatic PC/PE ratios correlate with membrane fluidity.

Membrane fluidity was assayed with 1-(4-trimethylammoniumphenyl)-6-phenyl-1,3,5-hexatriene *p*-toluenesulfonate (TMA-DPH). Primary hepatocytes were isolated from *Pemt*$^{-/-}$ and *Abcb4*$^{-/-}$/*Pemt*$^{-/-}$ mice fed a choline-supplemented (CS) diet for 24 h and then switched to a choline-deficient (CD) diet. *Pemt*$^{-/-}$ mice were fed a CD diet for 2 days and *Abcb4*$^{-/-}$/*Pemt*$^{-/-}$ mice were fed a CD diet for 3 or 21 days. Hepatocytes were incubated with TMA-DPH at 4°C for 10 min and subsequently analyzed with a fluorimeter within one min. The fluorescent polarization value was calculated with a formula of p = (F parallel – F perpendicular)/(F parallel + F perpendicular). Three mice were used for each group in the experiment with each sample assayed in triplicate. *, $P < 0.05$.

Fig. 3.8 PE on the cell surface

Primary hepatocytes were prepared from *Pemt*$^{-/-}$ and *Abcb4*$^{-/-}$/*Pemt*$^{-/-}$ mice fed a choline-supplemented (CS) diet for 24 h and then switched to a choline-deficient (CD) diet. *Pemt*$^{-/-}$ mice were fed a CD diet for 2 days and *Abcb4*$^{-/-}$/*Pemt*$^{-/-}$ mice were fed a CD diet for 3 or 21 days. After plating for 4 h, hepatocytes were incubated with biotinylated PE-specific binding peptide, Ro98-019, at 4°C for 30 min and subsequently with FITC conjugated streptavidin for 30 min. Fluorescence was visualized under a fluorescent microscope **(A).** Propidium iodide was added into the incubation buffer to identify viable cells. Fluorescent intensity of FITC (PE-binding) per cell number was quantified by flow cytometry **(B).** Four mice were used for each group in the experiment with each sample assayed in triplicate. * $P < 0.01$ for CS compared to CD-fed mice.

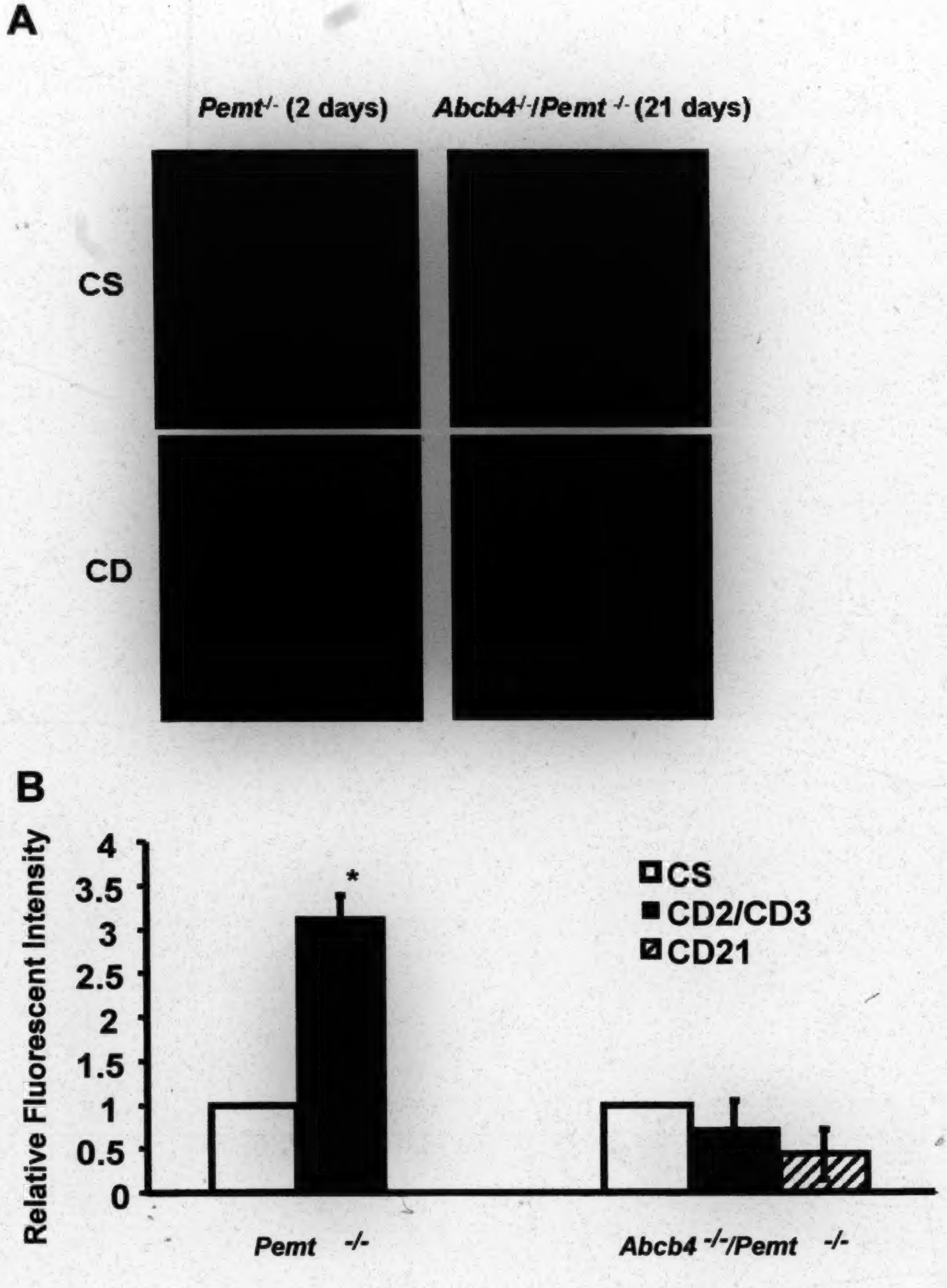
A
Pemt-/- (2 days)
Abcb4-/-/Pemt-/- (21 days)
CS
CD
B
Relative Fluorescent Intensity
0
0.5
1
1.5
2
2.5
3
3.5
4
*
☐ CS
■ CD2/CD3
▨ CD21
Pemt -/-
Abcb4 -/-/Pemt -/-

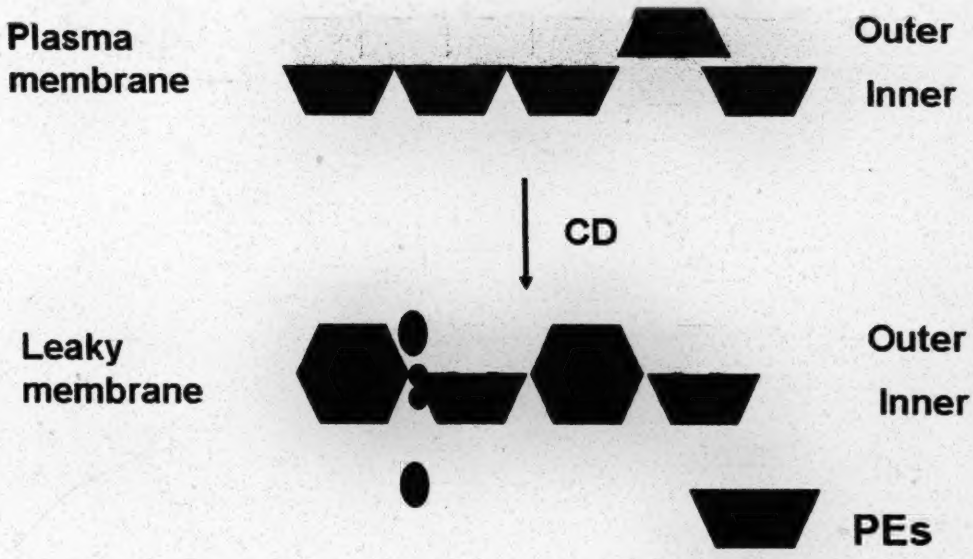
Plasma
membrane
Outer
Inner
CD
Leaky
membrane
Outer
Inner
PEs

Fig. 3.9 Hypothetical mechanism for liver failure in CD-*Pemt*$^{-/-}$ mice.

PCs form cylindrical structures (green) and PEs form conical structures (red). Cellular contents (blue) are released when membrane becomes leaky.

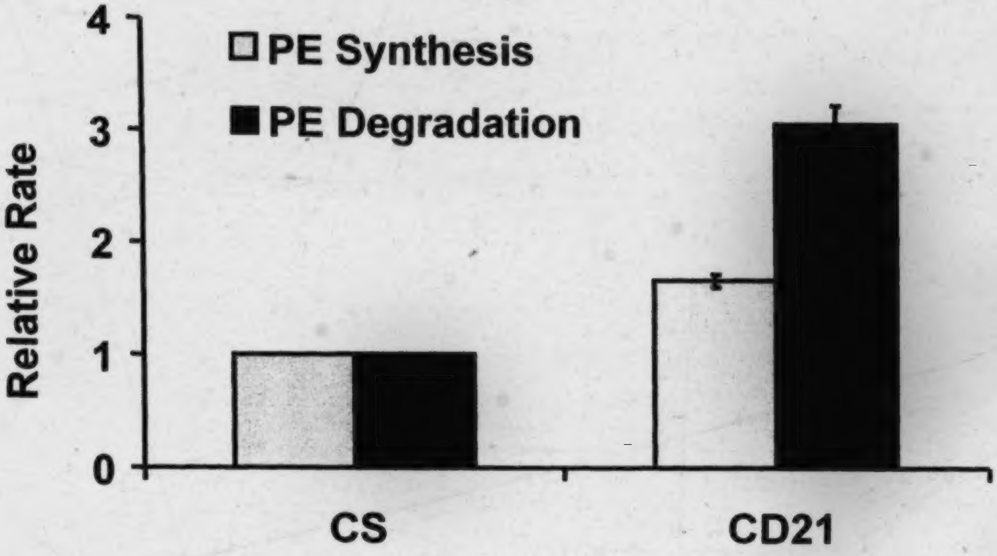

Fig. 3.10 Increased PE catabolism causes the decrease in hepatic PE level in CD-*Pemt*$^{-/-}$/*Abcb4*$^{-/-}$ mice

The rates of PE synthesis and degradation estimated from pulse-chase labeling with [^{3}H]glycerol of primary cultured hepatocytes from *Abcb4*$^{-/-}$/*Pemt*$^{-/-}$ mice. *Abcb4*$^{-/-}$/*Pemt*$^{-/-}$ mice were fed a choline-supplemented (CS) diet for 24 h and switched to a choline-deficient (CD) diet for 21 days (CD21). Relative rates were based on comparisons between CS and CD groups.

Fig. 3.11 VLDL-PC secretion and HDL-PC uptake by hepatocytes

Pemt$^{-/-}$ and *Abcb4*$^{-/-}$/*Pemt*$^{-/-}$ mice were fed a choline-supplemented (CS) diet for 24 h and then switched to a choline-deficient (CD) diet for 2 (*Pemt*$^{-/-}$) or 21 (*Abcb4*$^{-/-}$/*Pemt*$^{-/-}$) days. **(A)** VLDL-PC secretion assay: hepatocytes were labeled with [^{3}H]choline for 2 h and then chased for 2 h. Cell culture medium was collected at the end of the chase and PC in VLDL particles isolated. **(B)** HDL-PC uptake assay: murine HDL particles were pre-incubated with fluorescence-labeled PC, BODIPY-PC. Primary cultured hepatocytes were incubated with (BODIPY-PC) HDL for 2 h. Intracellular fluorescent intensity was measured as HDL-PC.

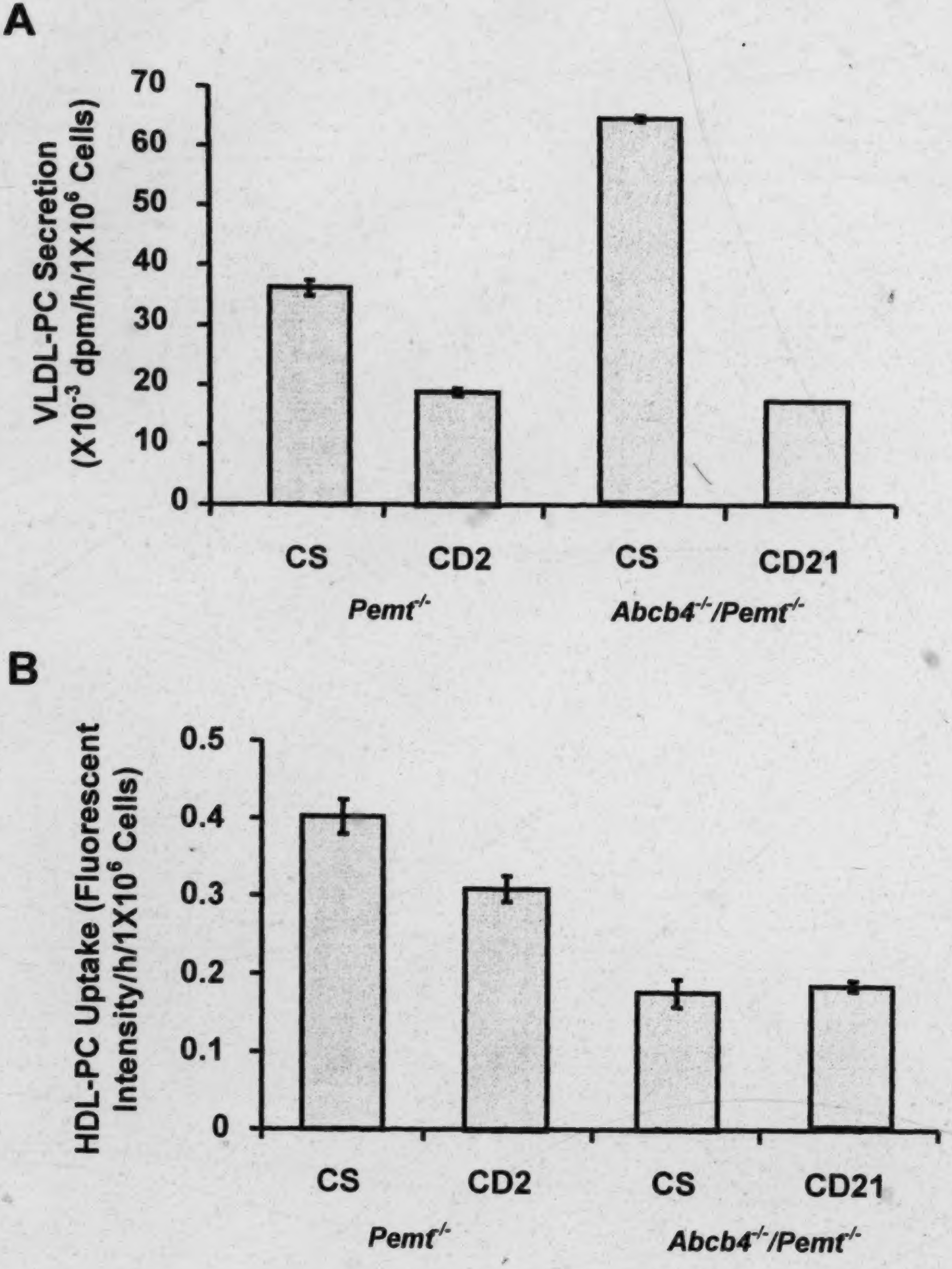
A
VLDL-PC Secretion
(X10^{-3} dpm/h/1X10^{6} Cells)
70
60
50
40
30
20
10
0
CS
CD2
CS
CD21
Pemt$^{-/-}$
Abcb4$^{-/-}$/Pemt$^{-/-}$
B
HDL-PC Uptake (Fluorescent
Intensity/h/1X10^{6} Cells)
0.5
0.4
0.3
0.2
0.1
0
CS
CD2
CS
CD21
Pemt$^{-/-}$
Abcb4$^{-/-}$/Pemt$^{-/-}$

Fig. 3.12 PLA_2 activity is enhanced in CD-*Abcb4$^{-/-}$/Pemt$^{-/-}$* mice, but not in CD-*Pemt$^{-/-}$* mice

In vitro assays were performed in liver homogenates from *Pemt$^{-/-}$* and *Abcb4$^{-/-}$/Pemt$^{-/-}$* mice of calcium-dependent PLA_2 ($cPLA_2$) and calcium-independent PLA2 ($iPLA_2$) activities with PED6 (a self-quenching fluorescent substrate for PLA_2). The specificity of increase in PLA_2 activity was further demonstrated by *in vitro* assay with 50 μmol/l PLA_2 inhibitors, BEL (an iPLA2-specific inhibitor) and ATK (inhibits both $iPLA_2$ and $cPLA_2$).

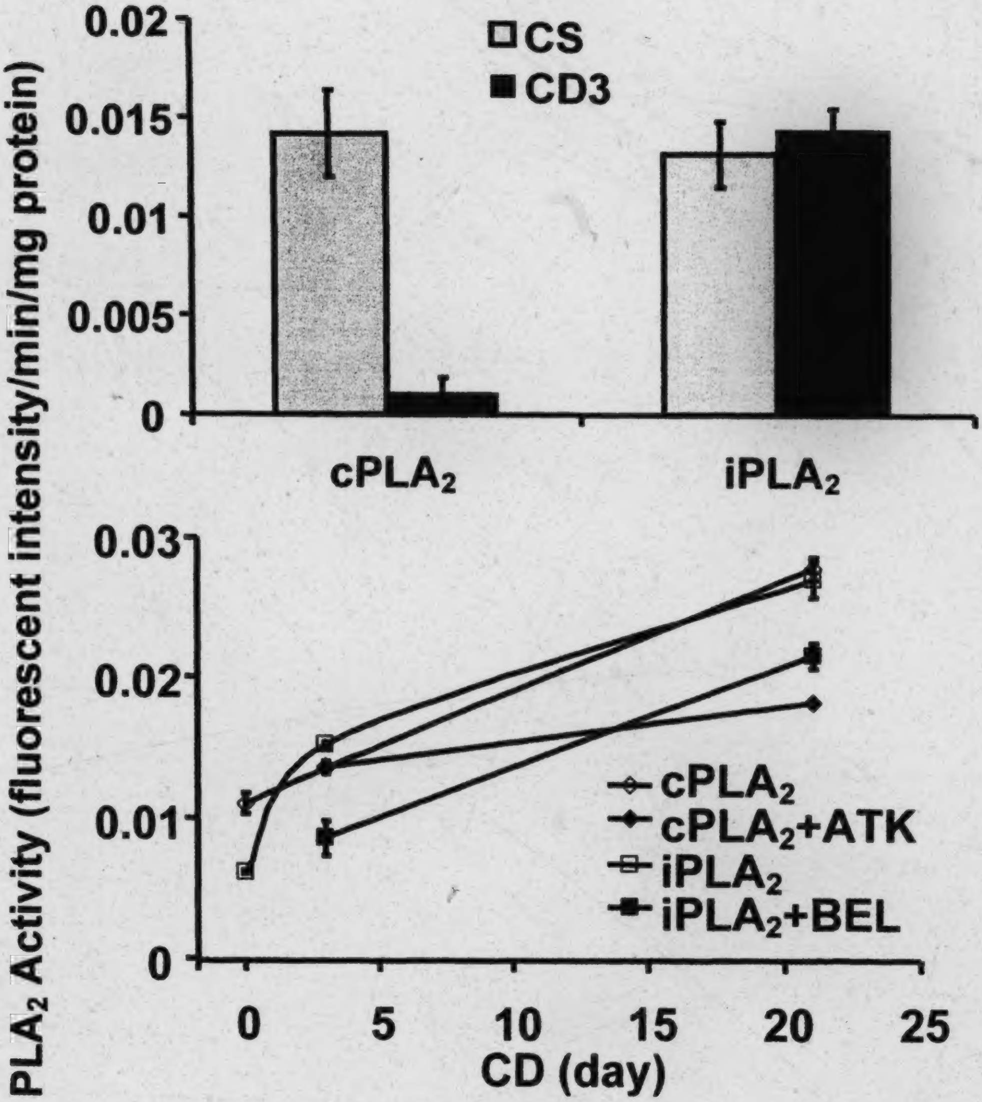

PLA$_2$ Activity (fluorescent intensity/min/mg protein)
0.02
0.015
0.01
0.005
0
□ CS
■ CD3
cPLA$_2$
iPLA$_2$
0.03
0.02
0.01
0
cPLA$_2$
cPLA$_2$+ATK
iPLA$_2$
iPLA$_2$+BEL
0
5
10
15
20
25
CD (day)

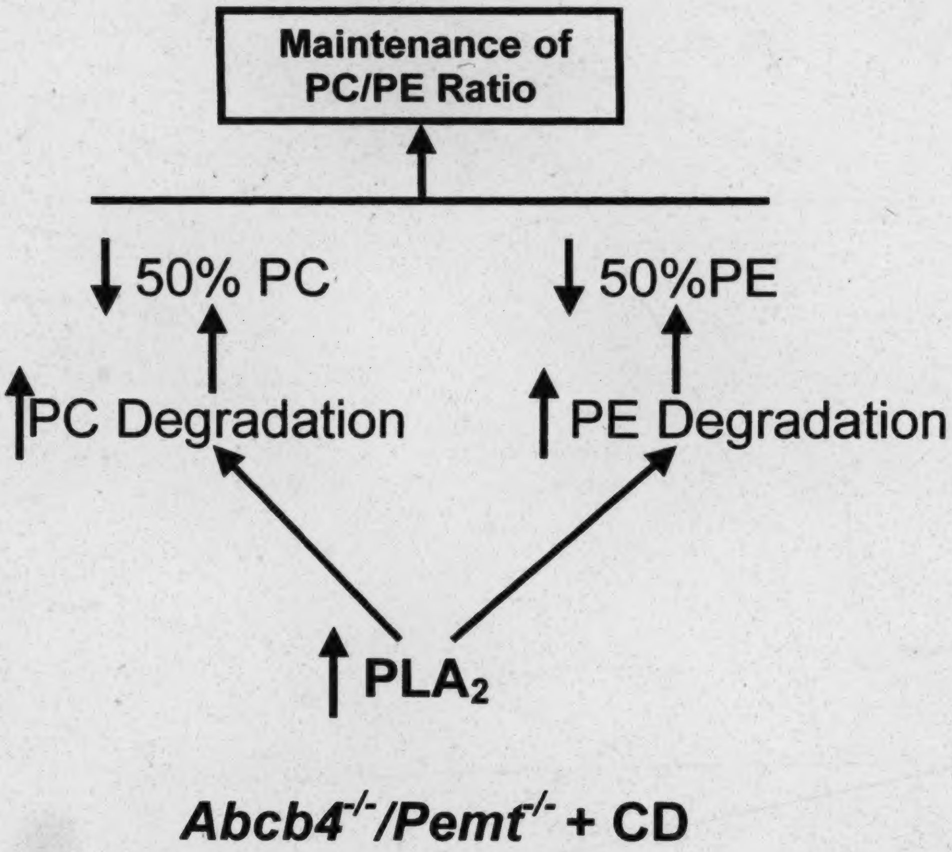
Maintenance of PC/PE Ratio
↓ 50% PC
↓ 50%PE
↑ PC Degradation
↑ PE Degradation
↑ PLA$_2$
Abcb4$^{-/-}$/Pemt$^{-/-}$ + CD

Fig. 3.13 Proposed scheme for the maintenance of PC/PE ratios in CD-*Abcb4$^{-/-}$/Pemt$^{-/-}$* mice

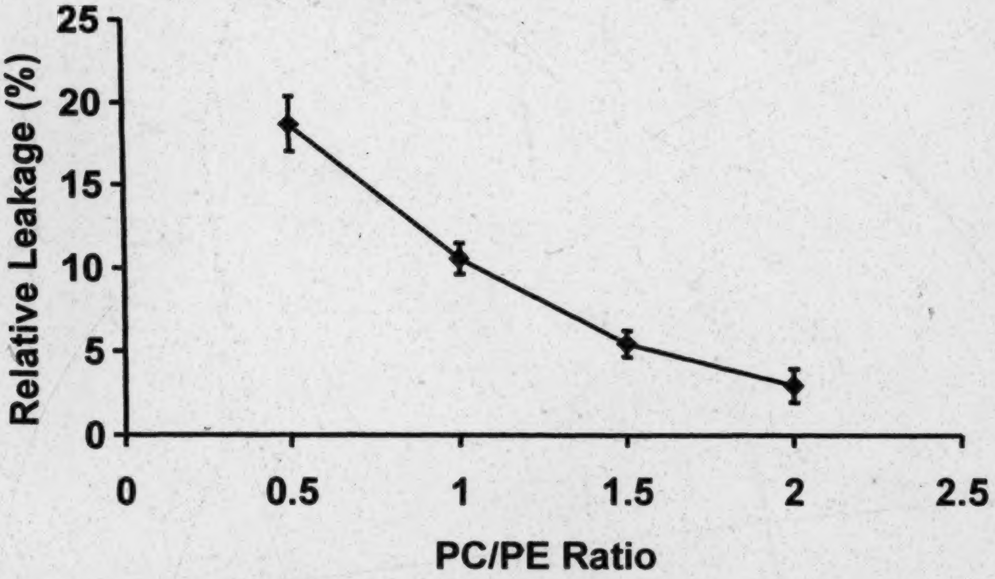

Fig. 3.14 PC/PE ratios influence membrane integrity of large unilamellar vesicles (LUVs)

Permeability assays of LUVs with different PC/PE ratios. LUVs of 100 nm were prepared at PC/PE ratios of 0.5 to 2.0. The ratio of hepatic PC + PE, sphingomyelin and cholesterol were kept constant at 86:1:9. Leakage was based on the measurement of the release of entrapped calcein. n=3.

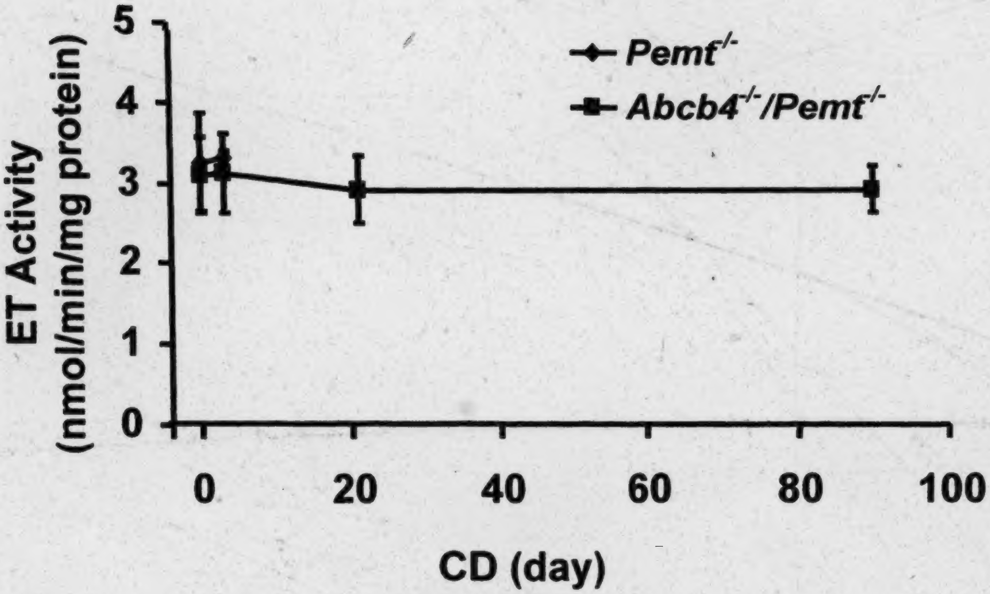

Fig. 3.15 Choline deprivation does not affect hepatic ET activity

Liver samples were collected from *Pemt*$^{-/-}$ mice and *Abcb4*$^{-/-}$/*Pemt*$^{-/-}$ mice fed a choline-supplemented (CS) diet for 24 h (0 day) and then switched to a choline-deficient (CD) diet for 3, 21 or 90 days. Liver homogenates were assayed for ET activity with CTP and [^{3}H]phosphoethanolamine as substrates. The production rate of [^{3}H]CDP-ethanolamine during 15 min was calculated as ET activity. Four mice were used for each time point in the experiment with each sample assayed in duplicate.

Fig. 3.16 Knockdown of PE biosynthesis in CD-*Pemt*$^{-/-}$ hepatocytes by ETi

ETi vectors were co-transfected with GFP vectors (ratio, 4:1) into cultured hepatocytes isolated from CD-*Pemt*$^{-/-}$ mice for 24 or 48 h. The control cells were transfected with RNAi control vectors and GFP vectors (ratio, 4:1). **(A)** Relative mRNA level of ET. Hepatocyte mRNA was extracted and quantified via quantitative PCR. Relative values were obtained from comparison between ET and cyclophilin. **(B)** ET activity was measured in total cell homogenates. ** $P < 0.01$. ***, $P < 0.001$.

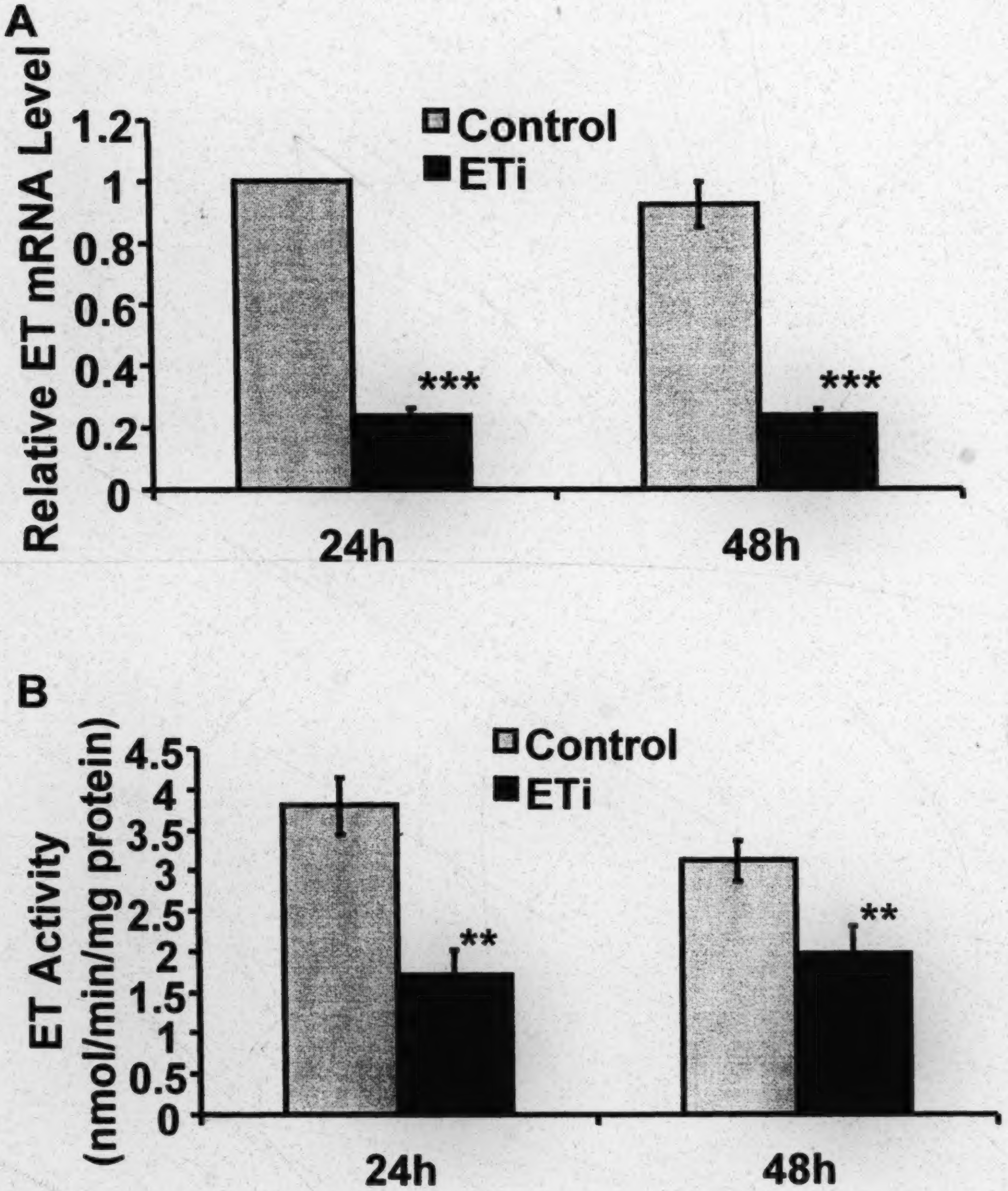
A
Relative ET mRNA Level
1.2
1
0.8
0.6
0.4
0.2
0
▨ Control
■ ETi
***
***
24h
48h
B
ET Activity (nmol/min/mg protein)
4.5
4
3.5
3
2.5
2
1.5
1
0.5
0
▨ Control
■ ETi
**
**
24h
48h

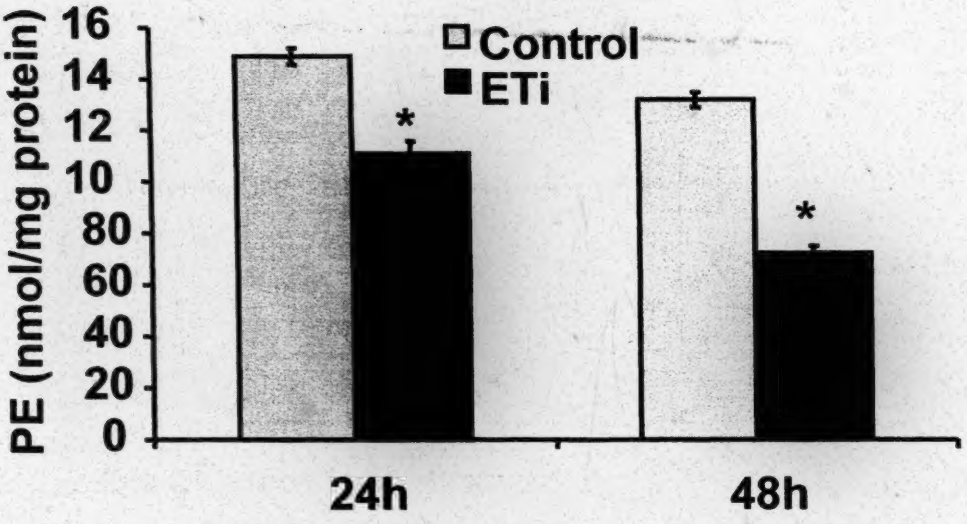

Fig. 3.17 ETi decreases PE levels in hepatocytes

ETi vectors were co-transfected with green fluorescent protein (GFP) vectors (ratio, 4:1) for 24 or 48 h into hepatocytes isolated from *Pemt*$^{-/-}$ mice fed a CD diet for 2 days. The hepatocytes were harvested and PE was extracted by the Bilgh and Dyer method and analyzed by HPLC.

Fig. 3.18 ETi increases PC/PE ratio and attenuates cell damage

ETi vectors were co-transfected with green fluorescent protein (GFP) vectors (ratio, 4:1) for 24 or 48 h into hepatocytes isolated from *Pemt*$^{-/-}$ mice fed a CD diet for 2 days. The medium was replaced with fresh medium for an additional 4 h. Alanine aminotransferase (ALT) activity in the medium was measured as an indicator of cell damage. *, $P < 0.05$.

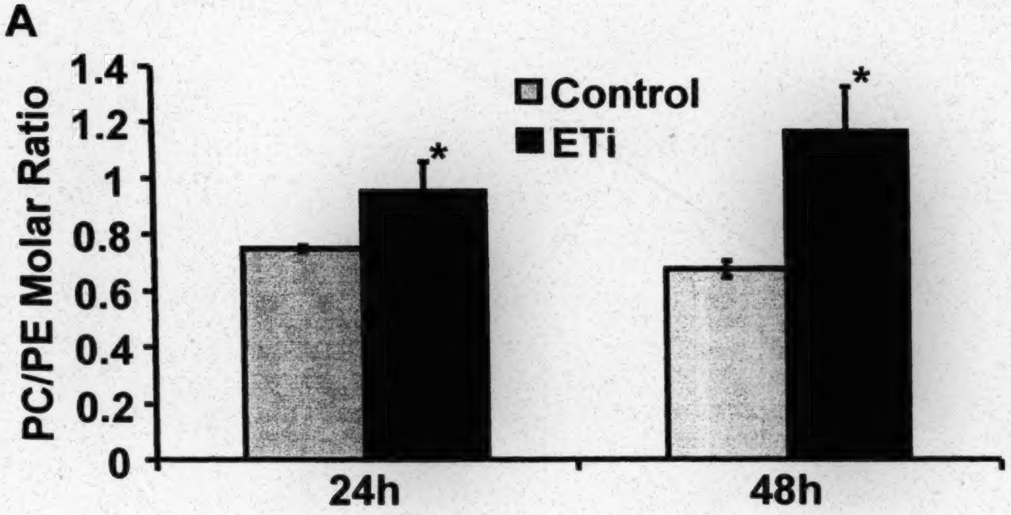
A
PC/PE Molar Ratio
1.4
1.2
1
0.8
0.6
0.4
0.2
0
Control
ETi
*
*
24h
48h

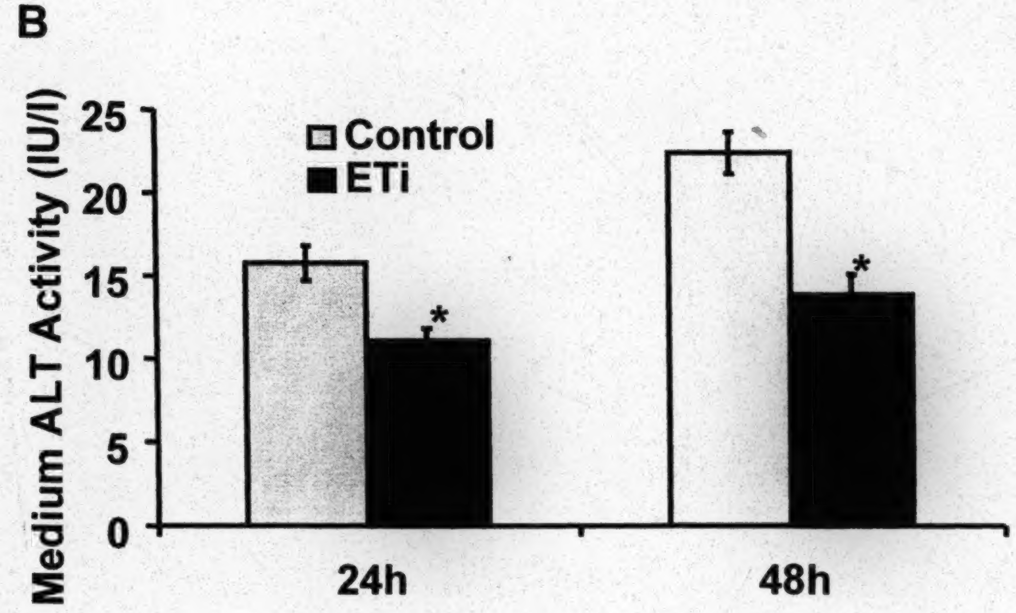
B
Medium ALT Activity (IU/l)
25
20
15
10
5
0
Control
ETi
*
*
24h
48h

Fig. 3.19 ETi attenuates the incorporation of [^{3}H]ethanolamine into [^{3}H]PE

(A) Hepatocytes from CD-*Pemt*$^{-/-}$ mice after transfection with ETi for 24 h were labeled with [^{3}H]ethanolamine for up to 2 h. n=3. **(B)** Hepatocytes were labeled with [^{3}H]ethanolamine for 24 h since the start of transfection. *, $P < 0.05$.

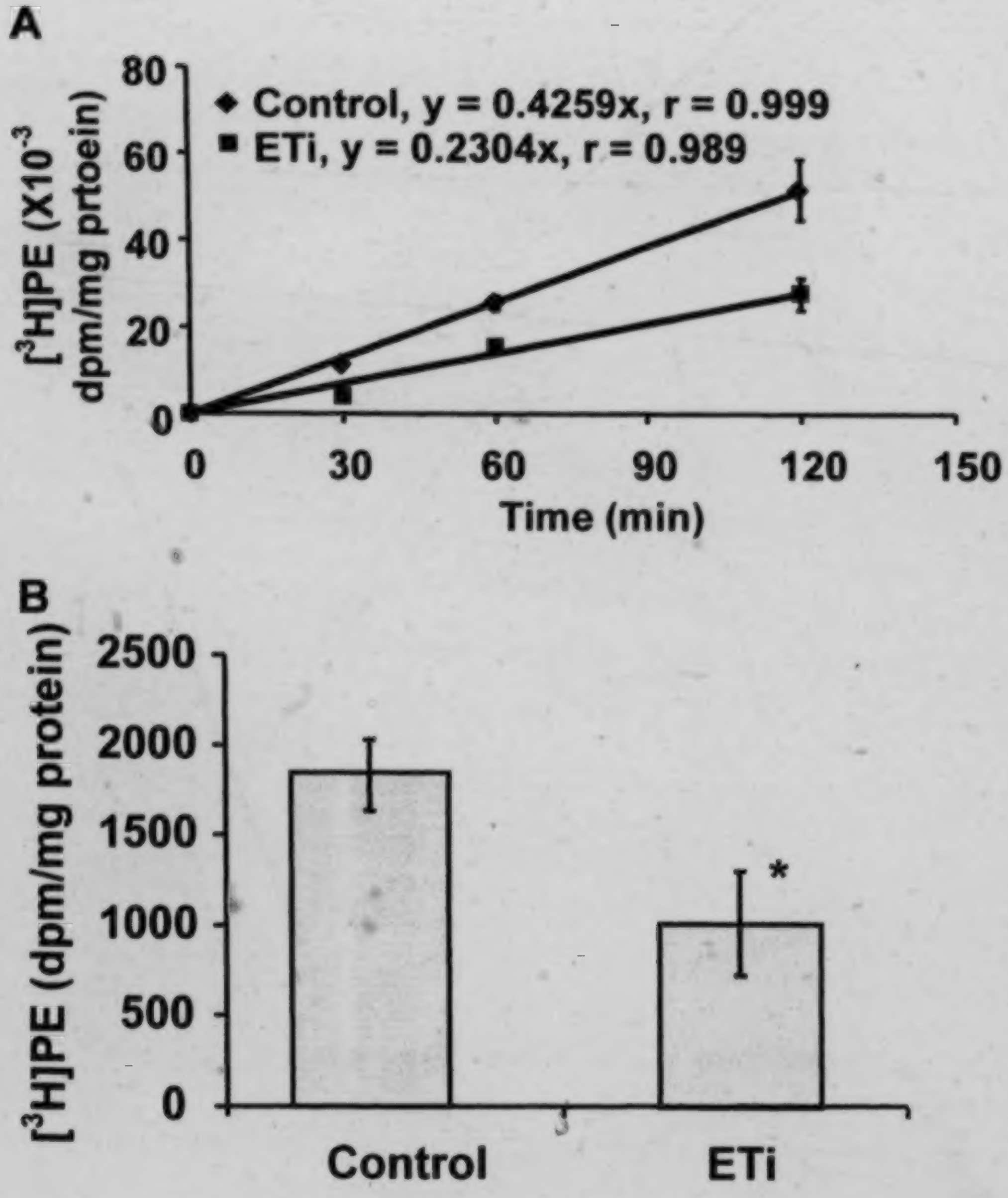
A
[3H]PE (X10-3 dpm/mg prtoein)
80
60
40
20
0
Control, y = 0.4259x, r = 0.999
ETi, y = 0.2304x, r = 0.989
0
30
60
90
120
150
Time (min)
B
[3H]PE (dpm/mg protein)
2500
2000
1500
1000
500
0
*
Control
ETi

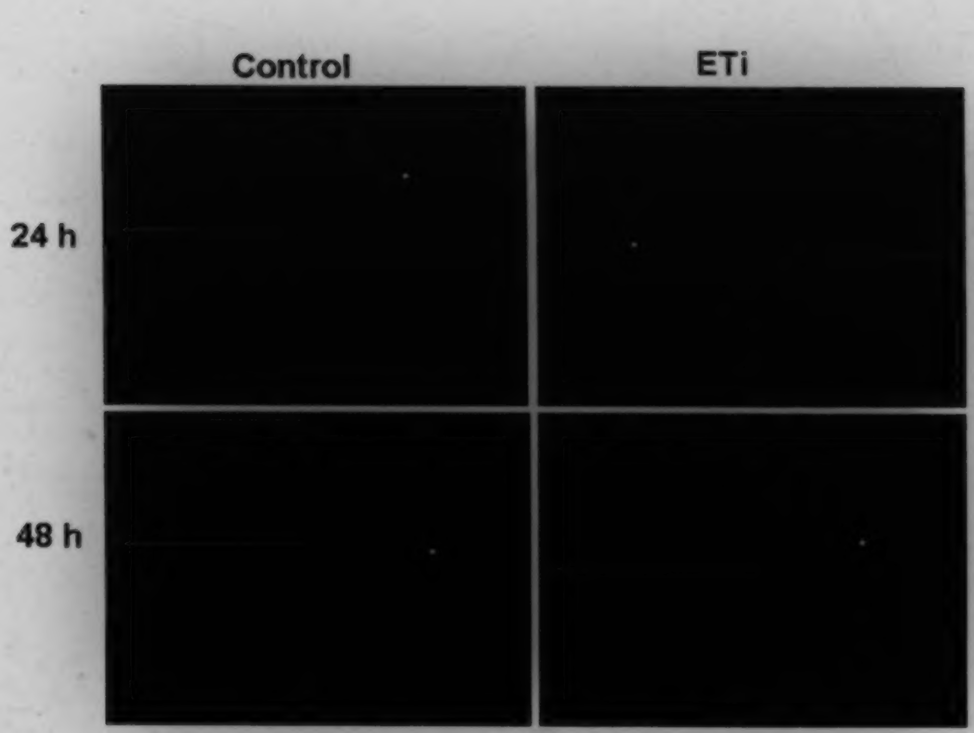

Fig. 3.20 PE exposure on the cell surface after ETi

After transfection for 24 or 48 h, hepatocytes from CD-*Pemt*$^{-/-}$ mice were incubated with biotinylated PE-specific binding peptide, Ro98-019, at 4°C for 30 min and subsequently with Texas Red®-conjugated streptavidin for 30 min. GFP fluorescence (green); PE-binding fluorescence (red), n=3.

Fig. 3.21 Attenuation of PE catabolism induces cell damage in CD-*Abcb4*$^{-/-}$/*Pemt*$^{-/-}$ murine hepatocytes

Arachidonyl trifluoromethyl ketone (ATK), a PLA$_2$-specific inhibitor was added to CD medium (CD+ATK) for 24 h and 48 h. The medium was replaced with fresh medium every 2 h during the first 8 h of cell culture to remove hepatic PC. After an additional 4 h of culture with fresh medium, ALT activity in the medium was measured as an indicator of cell damage and the PC/PE ratio was calculated. n=3. *, $P < 0.01$.

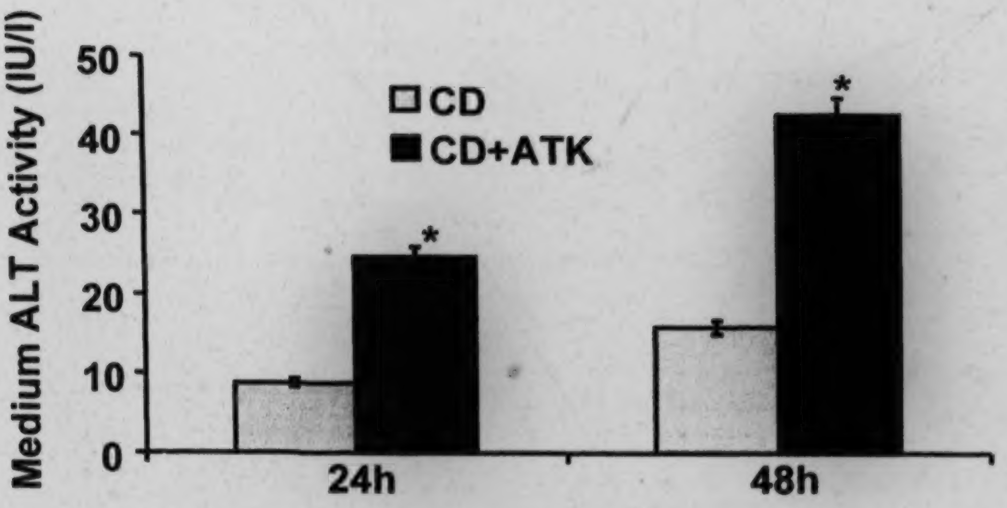
Medium ALT Activity (IU/l)
50
40
30
20
10
0
□ CD
■ CD+ATK
*
*
24h
48h

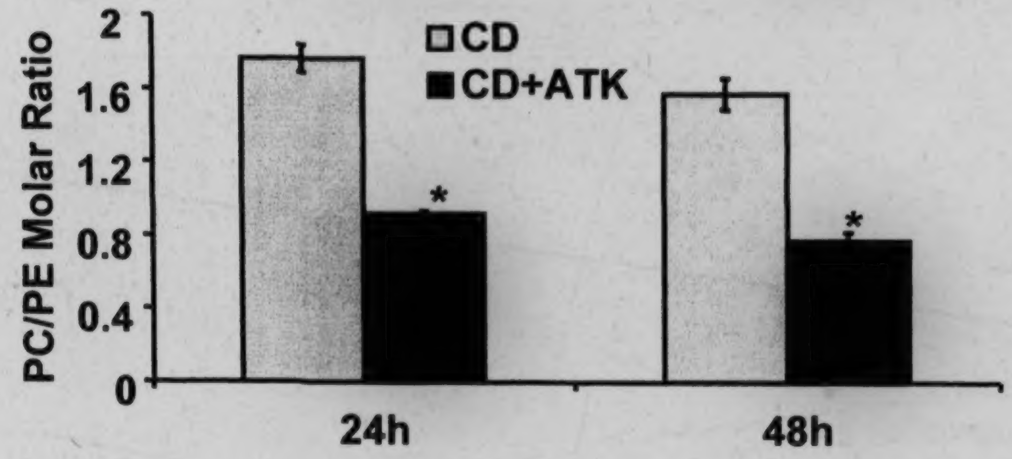
PC/PE Molar Ratio
2
1.6
1.2
0.8
0.4
0
□ CD
■ CD+ATK
*
*
24h
48h

Fig. 3.22 Liver weight (LW) and body weight (BW)

Pemt$^{-/-}$ mice and *Abcb4*$^{-/-}$/*Pemt*$^{-/-}$ mice were fed a choline-supplemented (CS) diet for 24 h and then switched to a choline-deficient (CD) diet for 3 to 90 days. The mice were weighed before sacrifice then the livers were removed and weighed.

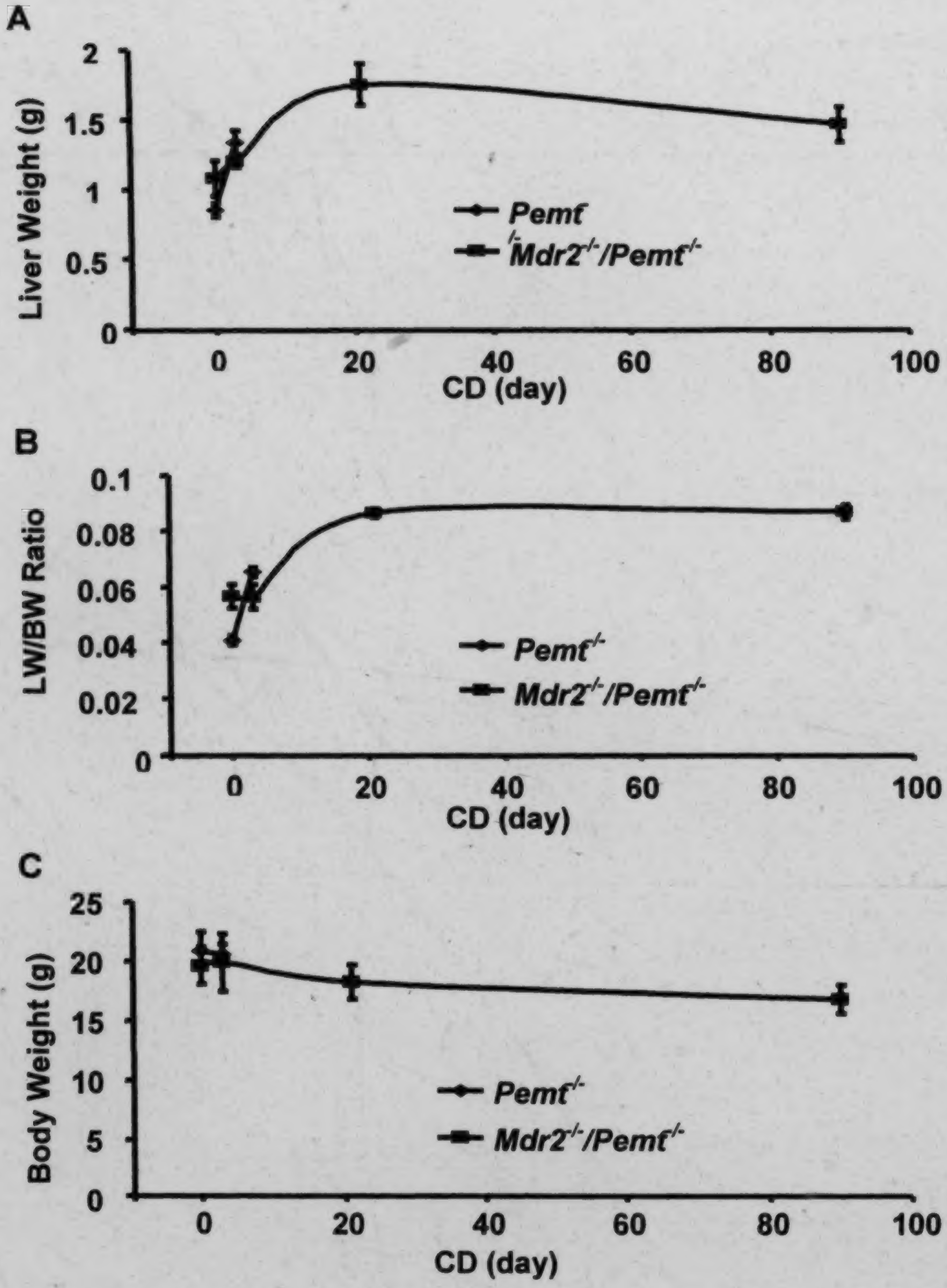
A
Liver Weight (g)
2
1.5
1
0.5
0
0
20
40
60
80
100
CD (day)
Pemt-/-
Mdr2-/-/Pemt-/-
B
LW/BW Ratio
0.1
0.08
0.06
0.04
0.02
0
0
20
40
60
80
100
CD (day)
Pemt-/-
Mdr2-/-/Pemt-/-
C
Body Weight (g)
25
20
15
10
5
0
0
20
40
60
80
100
CD (day)
Pemt-/-
Mdr2-/-/Pemt-/-

Fig. 3.23 Liver photos

Pemt$^{-/-}$ mice and *Abcb4*$^{-/-}$/*Pemt*$^{-/-}$ mice were fed a choline-supplemented (CS) diet for 24 h and then switched to a choline-deficient (CD) diet for 3 (CD3) or 21 (CD21) days. In choline re-feeding experiments, after fed a CD diet for 3 days, *Pemt*$^{-/-}$ mice were fed a CS diet for an additional 4 days (CD3+CS4). Chow diet-fed *Pemt*$^{-/-}$ mice were hydrodynamically injected with control or ETi vectors (50mg/kg) in 1ml saline at the time points of 0, 8 and 24 h. Mice were fasted for 12 h before sacrifice (ETi).

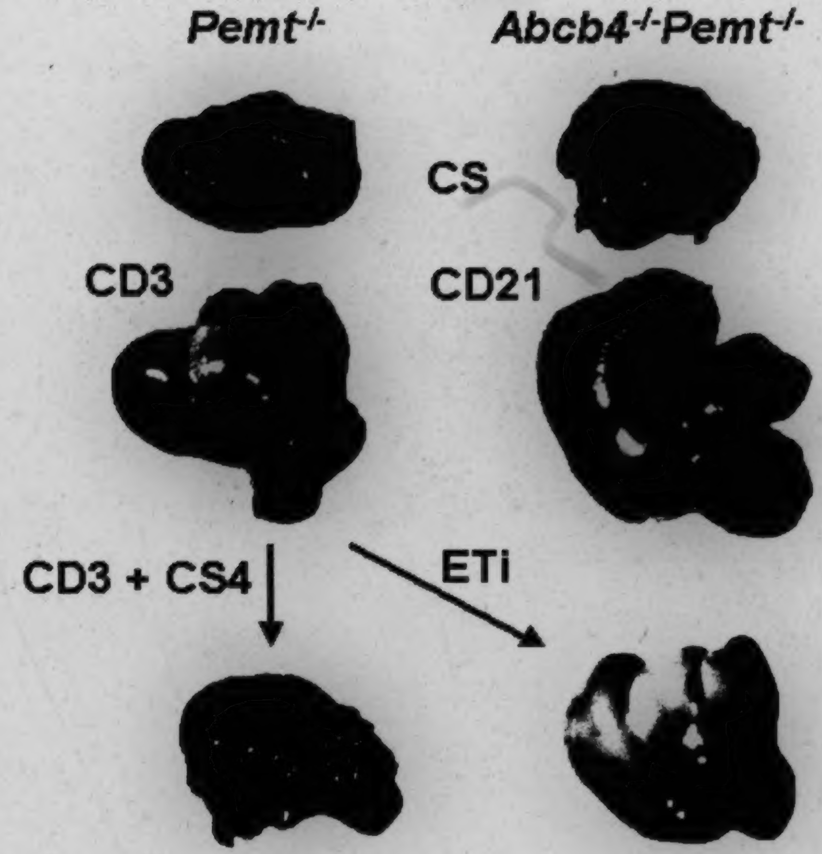
$Pemt^{-/-}$
$Abcb4^{-/-}Pemt^{-/-}$
CS
CD3
CD21
CD3 + CS4
ETi

Fig. 3.24 Liver histology by hemotoxylin and eosin staining

Pemt$^{-/-}$ mice and *Abcb4*$^{-/-}$/*Pemt*$^{-/-}$ mice were fed a choline-supplemented (CS) diet for 24 h and then switched to a choline-deficient (CD) diet for 3 (CD3) or 21 (CD21) days. CD3-*Pemt*$^{-/-}$ mice were fed a CS diet for 4 days (CD3 + CS4). Liver tissues were fixed in 10% formalin. Liver sections were stained with hemotoxylin and eosin by the Department of Laboratory Medicine and Pathology, University of Alberta Hospital. The slides were visualized under light microscopy with 400 X magnification.

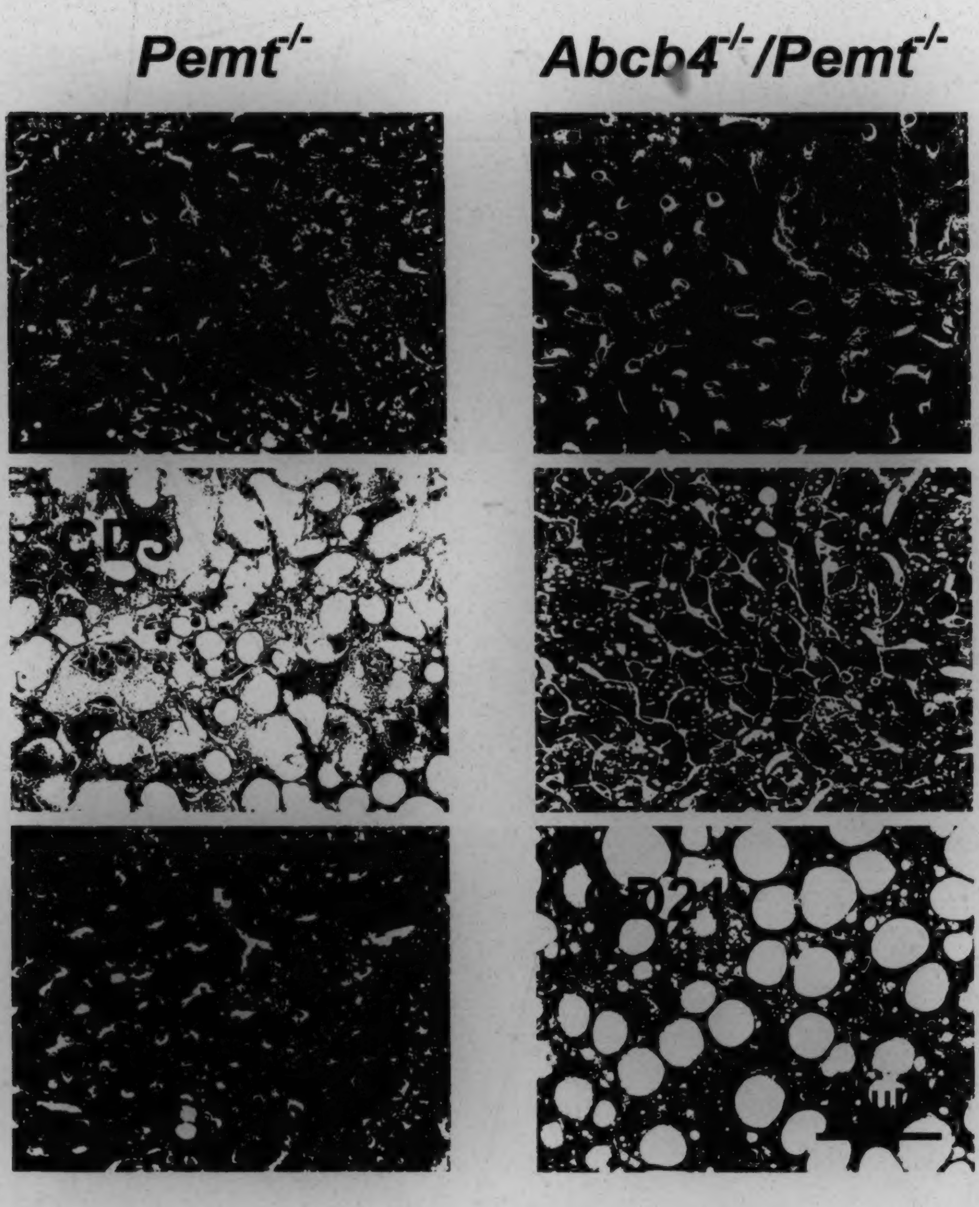
Pemt$^{-/-}$
Abcb4$^{-/-}$/*Pemt*$^{-/-}$
CD3
D21

Fig. 3.25 Plasma levels of glucose and insulin

Plasma samples were collected from *Pemt*$^{-/-}$ mice and *Abcb4*$^{-/-}$/*Pemt*$^{-/-}$ mice fed the choline-supplemented (CS) diet for 24 h (0 day) then transferred to the choline-deficient (CD) diet for 3 to 21 days. Plasma glucose and insulin were measured with chemical kits from Sigma and Alpco respectively.

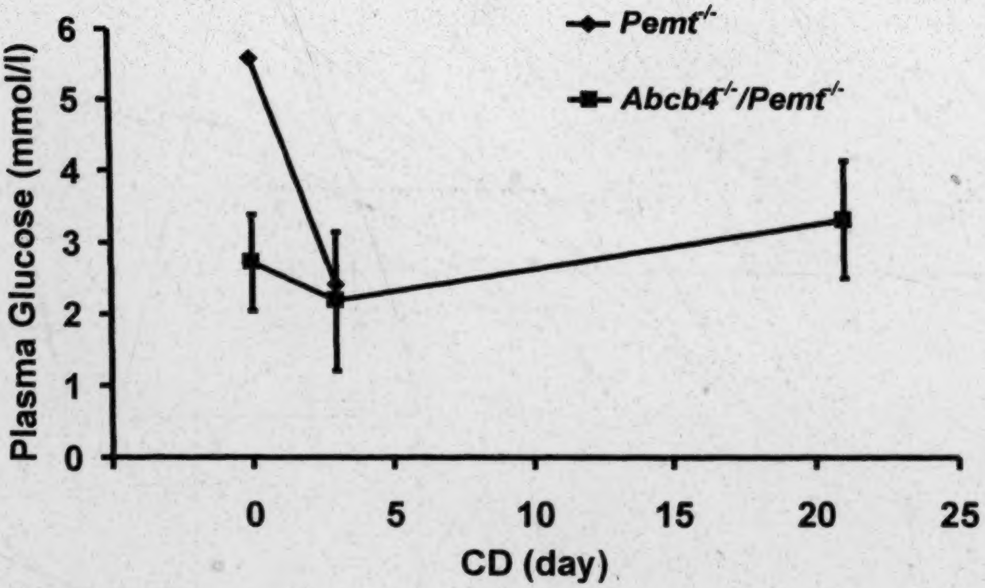
Pemt-/-
Abcb4-/-/Pemt-/-
Plasma Glucose (mmol/l)
6
5
4
3
2
1
0
0
5
10
15
20
25
CD (day)

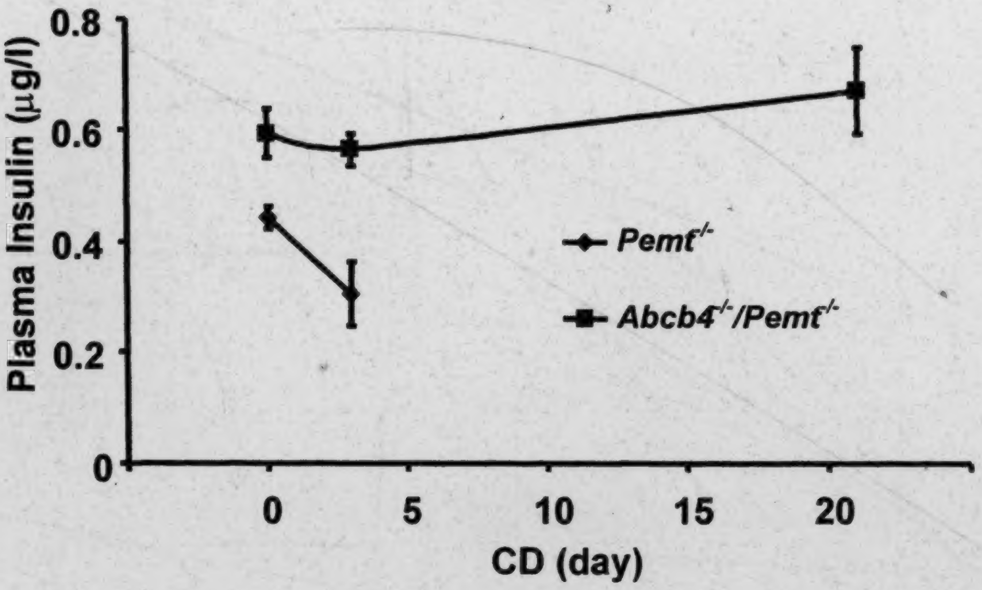
Plasma Insulin (µg/l)
0.8
0.6
0.4
0.2
0
Pemt-/-
Abcb4-/-/Pemt-/-
0
5
10
15
20
CD (day)

Fig. 3.26 Liver histology by hemotoxylin and eosin staining

Wild-type mice were fed a choline-supplemented (CS) diet for 24 h and then switched to a choline-deficient (CD) diet for 3 (CD3) or 21 (CD21) days. Liver tissues were fixed in 10% formalin. Liver sections were stained with hemotoxylin and eosin by the Department of Laboratory Medicine and Pathology, University of Alberta Hospital. The slides were visualized under light microscopy with 400 X magnification.

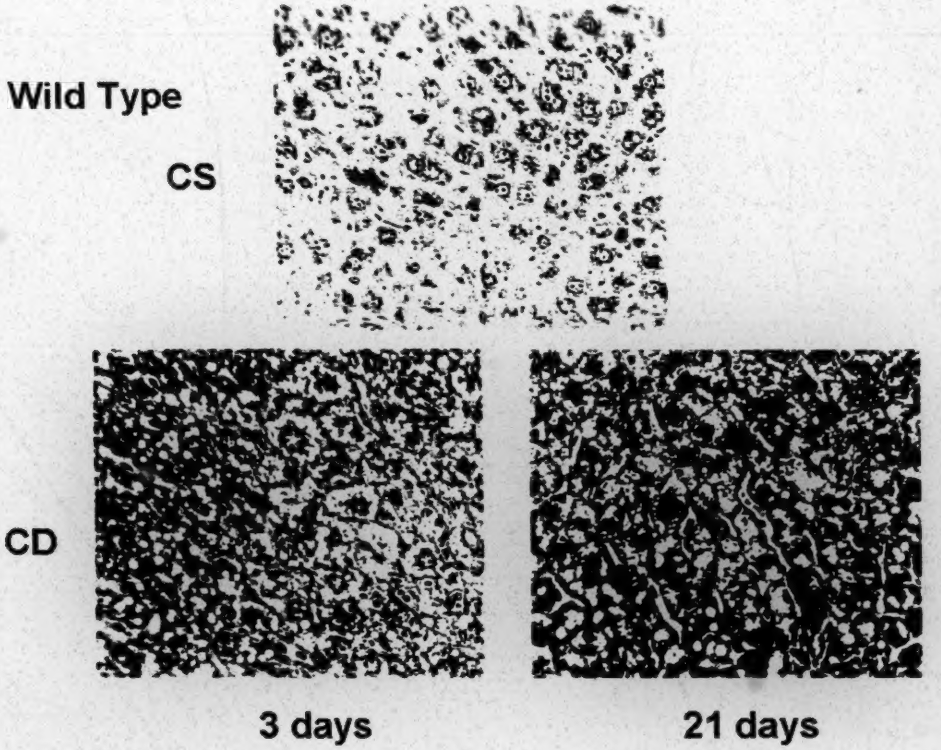
Wild Type
CS
CD
3 days
21 days

Fig. 3.27 Choline re-feeding reverses both hepatitis and steatosis in CD-*Pemt*$^{-/-}$ mice

Pemt$^{-/-}$ mice were fed a choline-supplemented (CS) diet for 24 h and then switched to a choline-deficient (CD) diet for 3 (CD3) days. CD3-*Pemt*$^{-/-}$ mice were fed a CS diet for 4 days (CD3 + CS4). **(A)** Liver PC and PE levels. **(B)** Hepatic PC/PE molar ratios. **(C)** Liver damage as assessed by plasma alanine aminotransferase (ALT) activity. **(D)** Liver TG levels.

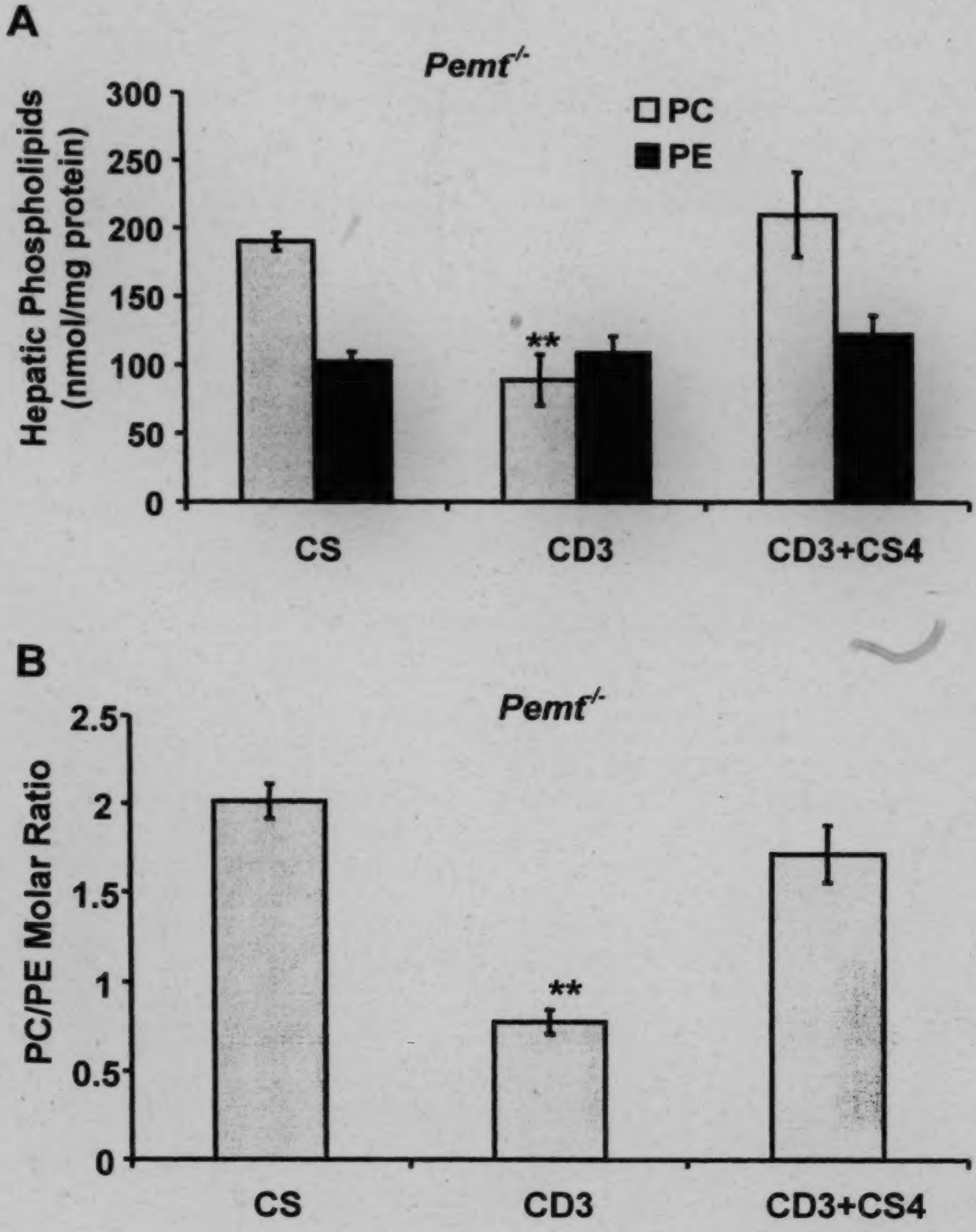
A
Pemt-/-
Hepatic Phospholipids (nmol/mg protein)
300
250
200
150
100
50
0
☐ PC
■ PE
**
CS
CD3
CD3+CS4
B
Pemt-/-
PC/PE Molar Ratio
2.5
2
1.5
1
0.5
0
**
CS
CD3
CD3+CS4

C

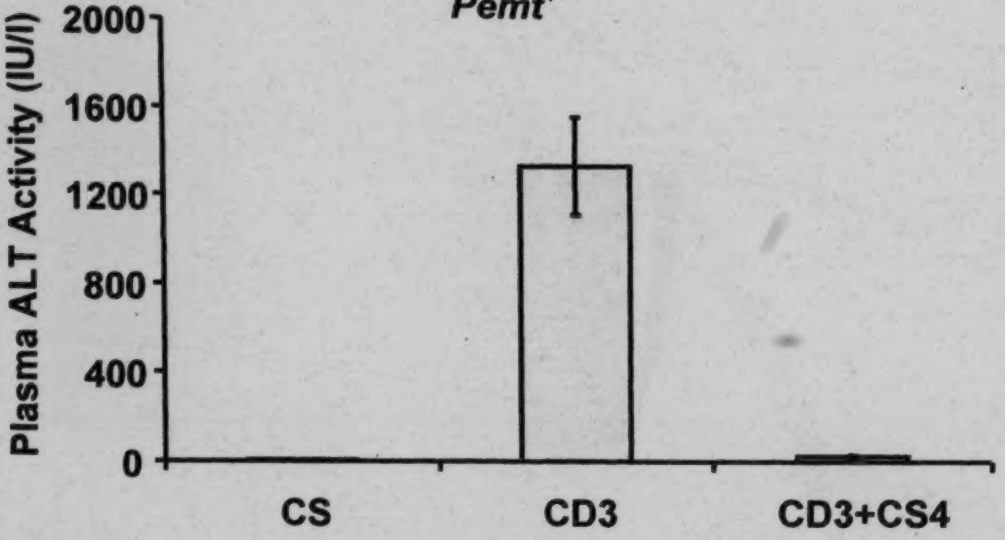

Pemt-/-
Plasma ALT Activity (IU/l)
2000
1600
1200
800
400
0
CS
CD3
CD3+CS4

D

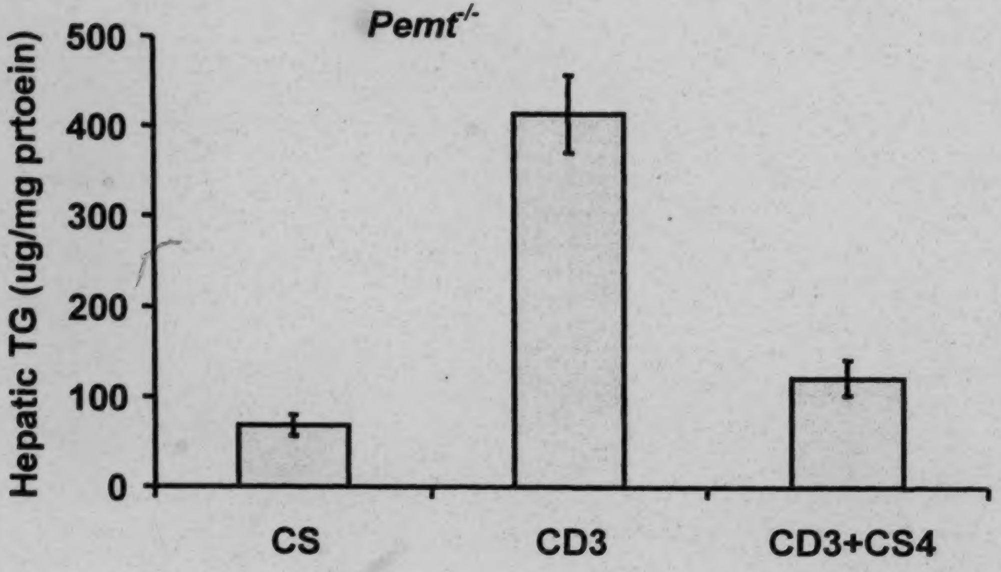

Pemt-/-
Hepatic TG (ug/mg prtoein)
500
400
300
200
100
0
CS
CD3
CD3+CS4

Fig. 3.28 Increased PC/PE ratio reversed hepatitis, but not steatosis

After 3 injections of Control or ETi vectors (ETi) (50 mg/kg), *Pemt*$^{-/-}$ mice were fed a choline-deficient (CD) diet for 2 days. n=3. **(A)** Liver histology by hemotoxylin and eosin staining. **(B)** Liver damage as assessed by plasma alanine aminotransferase (ALT) activity. **(C)** Liver TG levels. **(D)** Liver PC and PE levels. **(E)** Hepatic PC/PE molar ratios. *, $P < 0.05$; **, $P < 0.01$.

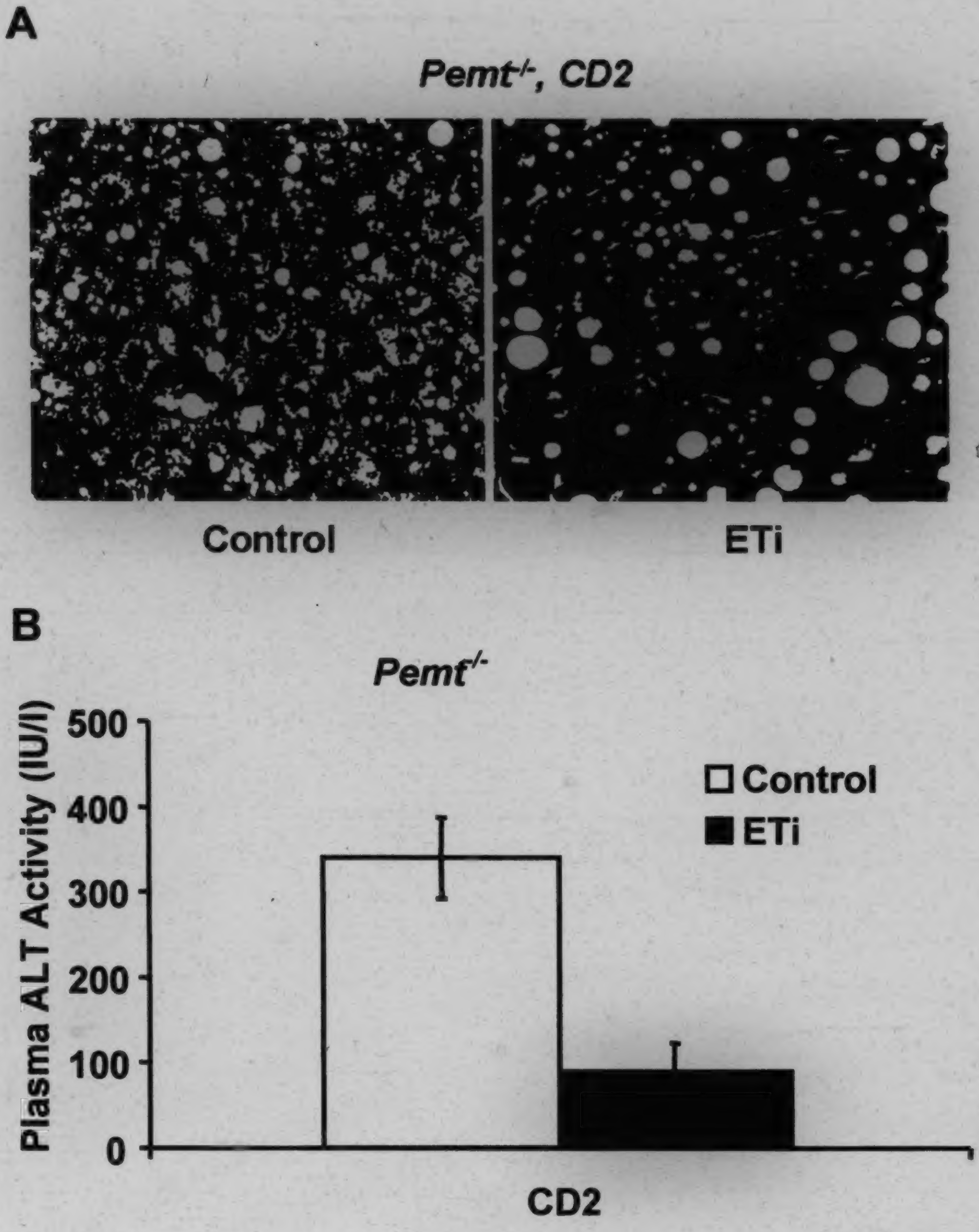
A
Pemt-/-, CD2
Control
ETi
B
Pemt-/-
Plasma ALT Activity (IU/l)
500
400
300
200
100
0
□ Control
■ ETi
CD2

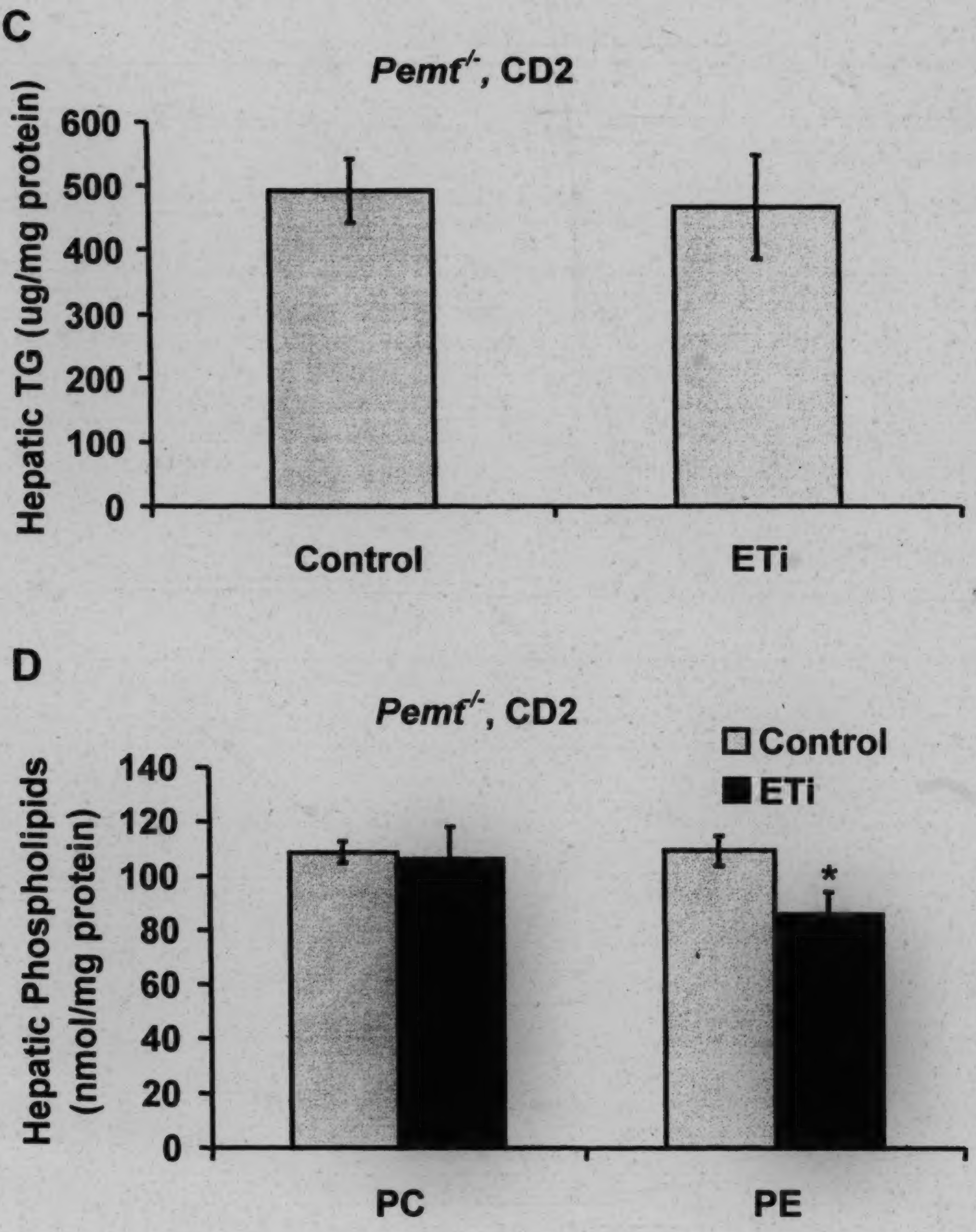
C
Pemt-/-, CD2
Hepatic TG (ug/mg protein)
600
500
400
300
200
100
0
Control
ETi
D
Pemt-/-, CD2
☐ Control
■ ETi
Hepatic Phospholipids (nmol/mg protein)
140
120
100
80
60
40
20
0
*
PC
PE

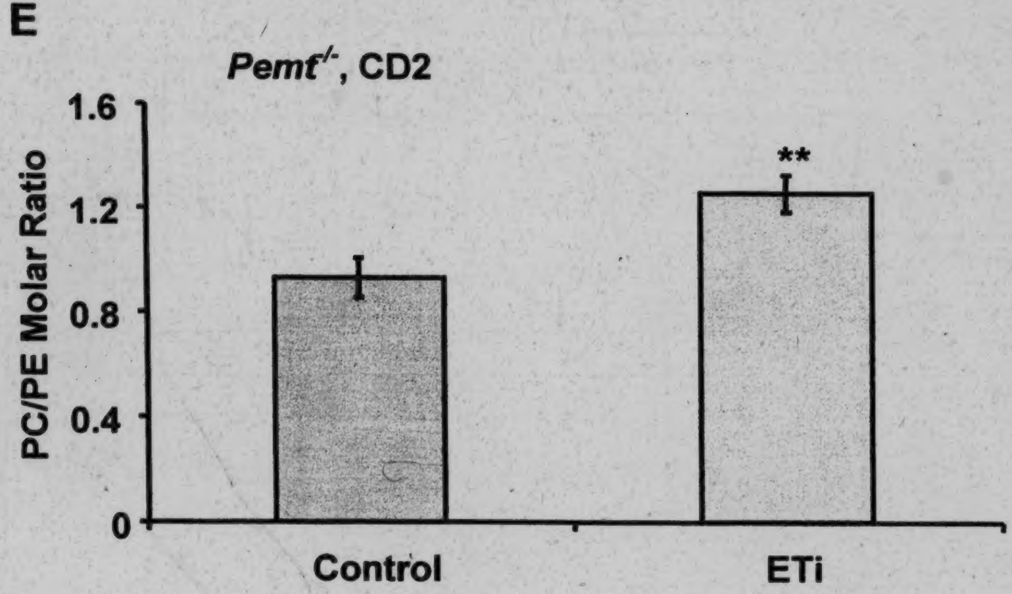
E
Pemt-/-, CD2
PC/PE Molar Ratio
1.6
1.2
0.8
0.4
0
**
Control
ETi

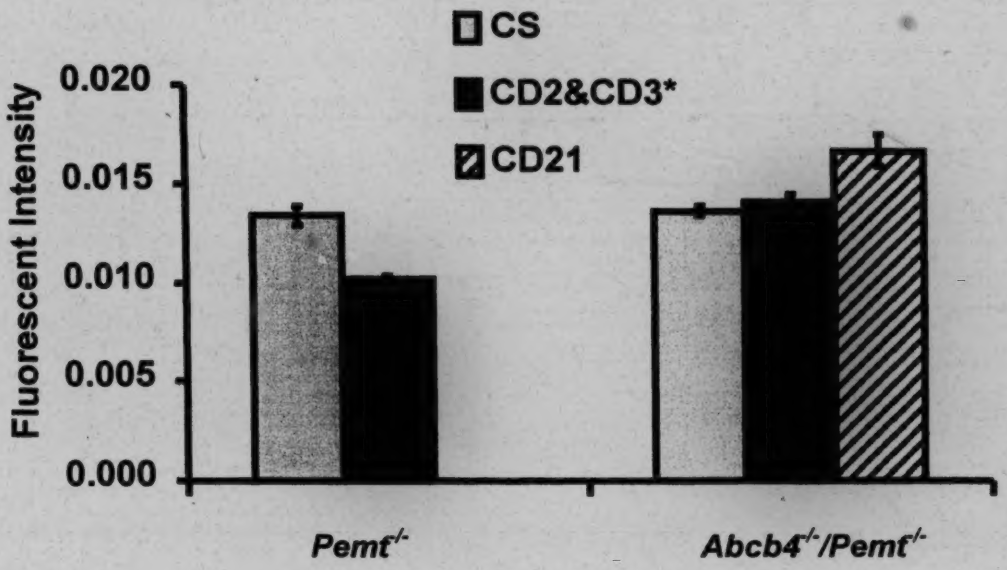

Fig. 3.29 Plasma membrane potentials of hepatocytes

Primary hepatocytes were isolated from *Pemt*$^{-/-}$ and *Abcb4*$^{-/-}$/*Pemt*$^{-/-}$ mice fed a choline-supplemented (CS) diet for 24 h and then switched to a choline-deficient (CD) diet. *Pemt*$^{-/-}$ mice were fed a CD diet for 2 days and *Abcb4*$^{-/-}$/*Pemt*$^{-/-}$ mice were fed a CD diet for 3 or 21 days. Membrane potential was assayed by incubation hepatocytes with bis-(1,3-dibutylbarbituric acid)trimethine oxonol (DiBAC4(3)) at 4°C for 30 min and subsequently analyzed with a fluorimeter within one min. Fluorescent intensity per cell number is displayed.

References

1. Devaux, P. F. Static and dynamic lipid asymmetry in cell membranes. (1991) *Biochemistry* **30**, 1163-1173
2. Vance, D. E. *Phospholipid biosynthesis in eukaryotes.* (2002) in *Biochemistry of lipids, lipoproteins and membranes* (Vance, D. E., J. E. Vance, ed), pp. 205-232, Elsevier, New York
3. Smit, J. J., Schinkel, A. H., Oude Elferink, R. P., Groen, A. K., Wagenaar, E., van Deemter, L., Mol, C. A., Ottenhoff, R., van der Lugt, N. M., van Roon, M. A., and et al. Homozygous disruption of the murine mdr2 P-glycoprotein gene leads to a complete absence of phospholipid from bile and to liver disease. (1993) *Cell* **75**, 451-462
4. Walkey, C. J., Yu, L., Agellon, L. B., and Vance, D. E. Biochemical and evolutionary significance of phospholipid methylation. (1998) *J Biol Chem* **273**, 27043-27046
5. Li, Z., Agellon, L. B., and Vance, D. E. Phosphatidylcholine homeostasis and liver failure. (2005) *J Biol Chem*, In press
6. Bradford, M. M. A rapid and sensitive method for the quantitation of microgram quantities of protein utilizing the principle of protein-dye binding. (1976) *Anal Biochem* **72**, 248-254
7. Bligh, E. G., and Dyer, W. J. A rapid method of total lipid extraction and purification. (1959) *Can J Biochem Physiol* **37**, 911-917

8. McCluer, R. H., Ullman, M. D., and Jungalwala, F. B. HPLC of glycosphingolipids and phospholipids. (1986) *Adv Chromatogr* **25**, 309-353

9. Lohninger, A., Preis, P., Linhart, L., Sommoggy, S. V., Landau, M., and Kaiser, E. Determination of plasma free fatty acids, free cholesterol, cholesteryl esters, and triacylglycerols directly from total lipid extract by capillary gas chromatography. (1990) *Anal Biochem* **186**, 243-250

10. Tijburg, L. B., Vermeulen, P. S., and van Golde, L. M. Ethanolamine-phosphate cytidylyltransferase. (1992) *Methods Enzymol* **209**, 258-263

11. Farber, S. A., Pack, M., Ho, S. Y., Johnson, I. D., Wagner, D. S., Dosch, R., Mullins, M. C., Hendrickson, H. S., Hendrickson, E. K., and Halpern, M. E. Genetic analysis of digestive physiology using fluorescent phospholipid reporters. (2001) *Science* **292**, 1385-1388

12. Hazen, S. L., Zupan, L. A., Weiss, R. H., Getman, D. P., and Gross, R. W. Suicide inhibition of canine myocardial cytosolic calcium-independent phospholipase A2. Mechanism-based discrimination between calcium-dependent and -independent phospholipases A2. (1991) *J Biol Chem* **266**, 7227-7232

13. Street, I. P., Lin, H. K., Laliberte, F., Ghomashchi, F., Wang, Z., Perrier, H., Tremblay, N. M., Huang, Z., Weech, P. K., and Gelb, M. H. Slow- and tight-binding inhibitors of the 85-kDa human phospholipase A2. (1993) *Biochemistry* **32**, 5935-5940

treatment. A novel mechanism for control of phosphatidylcholine levels in cells. (1986) *J Biol Chem* **261**, 7846-7852

21. Chung, B. H., Wilkinson, T., Geer, J. C., and Segrest, J. P. Preparative and quantitative isolation of plasma lipoproteins: rapid, single discontinuous density gradient ultracentrifugation in a vertical rotor. (1980) *J Lipid Res* **21**, 284-291

22. Jeong, T., Schissel, S. L., Tabas, I., Pownall, H. J., Tall, A. R., and Jiang, X. Increased sphingomyelin content of plasma lipoproteins in apolipoprotein E knockout mice reflects combined production and catabolic defects and enhances reactivity with mammalian sphingomyelinase. (1998) *J Clin Invest* **101**, 905-912

23. Allen, T. M., Ryan, J. L., and Papahadjopoulos, D. Gangliosides reduce leakage of aqueous-space markers from liposomes in the presence of human plasma. (1985) *Biochim Biophys Acta* **818**, 205-210

24. Haque, M. E., McIntosh, T. J., and Lentz, B. R. Influence of lipid composition on physical properties and peg-mediated fusion of curved and uncurved model membrane vesicles: "nature's own" fusogenic lipid bilayer. (2001) *Biochemistry* **40**, 4340-4348

25. Batts, K. P., and Ludwig, J. Chronic hepatitis. An update on terminology and reporting. (1995) *Am J Surg Pathol* **19**, 1409-1417

26. Lang, F., Busch, G. L., Ritter, M., Volkl, H., Waldegger, S., Gulbins, E., and Haussinger, D. Functional significance of cell volume regulatory mechanisms. (1998) *Physiol Rev* **78**, 247-306

27. Dowhan, W., M. Bogdanov. 2002) in *Biochemistry of lipids, lipoproteins and membranes, 4th edition.* (Vance, D. E., J. E. Vance, ed), pp. 1-36, Elsevier, New York

28. Vance, D. E. *Biochemistry of lipids, lipoproteins and membranes* (2002) in *Biochemistry of Lipids, Lipoprotein and Membranes, 4th edition.* (Vance, D. E., J. E. Vance, ed), pp. 205-232, Elsevier, New York

29. Koteish, A., and Diehl, A. M. Animal models of steatosis. (2001) *Semin Liver Dis* **21**, 89-104

30. Koteish, A., and Mae Diehl, A. Animal models of steatohepatitis. (2002) *Best Pract Res Clin Gastroenterol* **16**, 679-690

31. Waite, K. A., Cabilio, N. R., and Vance, D. E. Choline deficiency-induced liver damage is reversible in Pemt(-/-) mice. (2002) *J Nutr* **132**, 68-71

32. Song, Y. K., Liu, F., Zhang, G., and Liu, D. Hydrodynamics-based transfection: simple and efficient method for introducing and expressing transgenes in animals by intravenous injection of DNA. (2002) *Methods Enzymol* **346**, 92-105

33. Kobayashi, N., Matsui, Y., Kawase, A., Hirata, K., Miyagishi, M., Taira, K., Nishikawa, M., and Takakura, Y. Vector-based in vivo RNA interference: dose- and time-dependent suppression of transgene expression. (2004) *J Pharmacol Exp Ther* **308**, 688-693

34. Yen, C. L., Mar, M. H., and Zeisel, S. H. Choline deficiency-induced apoptosis in PC12 cells is associated with diminished membrane

phosphatidylcholine and sphingomyelin, accumulation of ceramide and diacylglycerol, and activation of a caspase. (1999) *Faseb J* **13**, 135-142

35. Post, J. A., Bijvelt, J. J., and Verkleij, A. J. Phosphatidylethanolamine and sarcolemmal damage during ischemia or metabolic inhibition of heart myocytes. (1995) *Am J Physiol* **268**, H773-780
36. Weltman, M. D., Farrell, G. C., and Liddle, C. Increased hepatocyte CYP2E1 expression in a rat nutritional model of hepatic steatosis with inflammation. (1996) *Gastroenterology* **111**, 1645-1653
37. Beare-Rogers, J. L. Liver phospholipids of rats fed a choline-deficient diet supplemented with choline or methionine. (1971) *Lipids* **6**, 649-651
38. Lyman, R. L., Sheehan, G., and Tinoco, J. Phosphatidylethanolamine metabolism in rats fed a low methionine, choline-deficient diet. (1973) *Lipids* **8**, 71-79
39. Yost, R. W., Chander, A., and Fisher, A. B. Differential response of lung and liver of juvenile rats to choline deficiency. (1985) *J Appl Physiol* **59**, 738-742
40. Finkelstein, J. D., and Martin, J. J. Methionine metabolism in mammals. Adaptation to methionine excess. (1986) *J Biol Chem* **261**, 1582-1587
41. Gewurz, H., Mold, C., Siegel, J., and Fiedel, B. C-reactive protein and the acute phase response. (1982) *Adv Intern Med* **27**, 345-372
42. Mold, C. Effect of membrane phospholipids on activation of the alternative complement pathway. (1989) *J Immunol* **143**, 1663-1668

Chapter 4

Choline Channeling from Peripheral Tissues to Brain and Liver --- Adaptation to Choline Deprivation III: Choline Redistribution

4.1 Introduction

Choline is an essential nutrient for humans and animals (1-3). Complete choline deprivation is lethal, which is attributed to severe liver failure (3,4). However, when biliary secretion of PC was blocked, mice (*Abcb4*$^{-/-}$/*Pemt*$^{-/-}$) showed an adaptive response to choline deprivation, choline recycling (Chapter 2) (3). Although the level of total choline-containing metabolites in the liver decreased ~50% after 21 days of choline-deficient (CD) diet in *Abcb4*$^{-/-}$/*Pemt*$^{-/-}$ mice as compared with choline-supplemented (CS) mice, the level of total choline-containing metabolites was then maintained for at least 3 months as the result of recycling choline and curtailing choline oxidation (3). There is another possibility for this adaptation besides choline recycling, which is choline redistribution. Choline oxidation, as the only catabolic pathway of choline, was maintained at a low level in CD-*Abcb4*$^{-/-}$/*Pemt*$^{-/-}$ mice during choline deprivation (Fig. 2.7) (3). Thus, liver might receive choline from extrahepatic tissues to compensate the loss from choline oxidation.

No obvious change was observed in organs other than liver during choline deprivation in CD-*Pemt*$^{-/-}$ mice (4). Like liver, brain is also an important organ for choline metabolism, requiring considerable amount of choline as acetylcholine for neurotransmission (5). Previously we found that CD-*Pemt*$^{-/-}$ mice were under severe choline deficiency whereas CD-*Abcb4*$^{-/-}$/*Pemt*$^{-/-}$ mice were able to establish a new choline homeostasis with a ~50% lower level of total choline-containing metabolites than CS-*Abcb4*$^{-/-}$/*Pemt*$^{-/-}$ mice (3). Although the two mouse models were under different situations of choline deficiency, the brains in both models did not show any obvious damage during choline deprivation. Hence, the brain might not face choline deficiency and might obtain choline from peripheral tissues. Therefore, choline redistribution might be initiated as another adaptation to choline deprivation.

4.2 Materials and Methods

4.2.1 Animals see 2.2.1

4.2.2 Plasma S100β protein assay

The brain protein S100β when found in the plasma is a marker of brain damage (6,7). Sandwich enzyme-linked immunosorbent assay (ELISA) was performed for measurement of plasma S100β protein level. Polyclonal anti-S100β protein antibody (*Santa Cruz*) was used as both catching and detecting antibodies. The secondary antibody was conjugated with horseradish peroxidase (HRP) and 3, 3', 5, 5'-tetramethylbenzidine (TMB) (*Sigma*) was used for color developing. Brain homogenates (1:100 dilution) were used as a positive control.

4.2.3 Assay for total choline-containing metabolites

Liver or brain homogenates were assayed for total choline-containing metabolites with Phospholipids B kit (*Wako*) based on the release of free choline by phospholipase D and choline oxidation by choline oxidase.

4.2.4 Lipid analysis see 2.2.6

4.2.5 Choline oxidase assay see 2.2.5

4.2.6 Western blotting for choline high-affinity transporter (CHT)

Fifty μg of protein from liver and brain homogenates were separated by 10% SDS-PAGE and blotted with an anti-CHT antibody (*Santa Cruz*). S100β protein blotting was used as a protein loading control for brain analysis. Protein disulfide isomerase (PDI) blotting was used as a protein loading control for liver analysis.

4.2.7 *In vivo* injection of [^{3}H]choline

Pemt$^{-/-}$ and *Abcb4*$^{-/-}$/*Pemt*$^{-/-}$ mice were fed a CS diet for 24 h and then switched to a CD diet for 3 or 21 days. 100 μCi [^{3}H]choline in 100 μl saline was injected into mice (~20 g) via the tail-vein. Mice were sacrificed after 1 h or 24 h of injection. Total radioactivity in the whole tissue was measured and all assayed tissues included brain, liver, intestine, kidney, heart, lung and muscle, as well as plasma. Total muscle weight was based on the muscle/body weight index (8). Total plasma volume was estimated as 2 ml in a 20 g mouse (9). Four mice were in each group and assayed in duplicate. Data from different mice were normalized to a mouse of 20 g body weight for comparison.

4.3 Results

4.3.1 No brain damage occurred during choline deprivation.

The brain protein S100β when found in the plasma is a marker of brain damage (6,7). We found that no S100β proteins was detectable in plasma of CS- and CD-*Pemt*$^{-/-}$ mice or *Abcb4*$^{-/-}$*/Pemt*$^{-/-}$ mice, which indicated that no brain damage was found in both CD-*Pemt*$^{-/-}$ mice and CD-*Abcb4*$^{-/-}$*/Pemt*$^{-/-}$ mice (plasma S100β proteins levels in 1:100 diluted brain homogenates: 0.84 fluorescent intensity as a positive control; no S100β protein was detectable in plasma of wild type mice as a negative control). We also checked genomic DNA of brain and did not find any DNA ladder fragments, which suggested that no apoptosis occurred in the brain during choline deprivation.

4.3.2 Brain did not exhibit choline deficiency.

The level of total choline-containing metabolites in brain homogenates was analyzed with Phospholipids B kit (Wako). No significant change of total choline-containing metabolites was found in the brain of both *Pemt*$^{-/-}$ mice and *Abcb4*$^{-/-}$/*Pemt*$^{-/-}$ mice after CD feeding (Fig. 4.1A). As the major choline-containing metabolite, PC levels did not change significantly in brains of both mouse models during choline deprivation (Fig. 4.1B). Interestingly, we found that brain still maintained high activities of choline oxidase in both models during choline deprivation (Fig. 4.2). Choline oxidation is the only catabolic pathway of choline (10).

We found that the expression of CHT in brains showed a minor increase after choline deprivation, but not in livers (Fig. 4.3). Choline high-affinity transporter is under feedback regulation by acetylcholine level that is dependent on the pool size of total choline-containing metabolites in brain (11). In contrast, we found that plasma free choline level did not decline significantly (Fig. 4.4A) even though the level of plasma PC dramatically decreased (Fig. 4.4B). Thus, brains in both mouse models were still able to acquire sufficient choline during choline deprivation.

4.3.3 Choline distribution and redistribution during choline deprivation

To trace the distribution and redistribution of choline during choline deprivation, [^{3}H]choline was injected through a tail-vein into both *Pemt*$^{-/-}$ mice and *Abcb4*$^{-/-}$/*Pemt*$^{-/-}$ mice under CS and CD diets. Two time points were used to collect organs, 1 h and 24 h after injection. Total radioactivity in each whole tissue was calculated on the basis of a 20 g mouse body weight. The sum of radioactivity in all selected tissues was the combination of total radioactivity from brain, liver, intestine, kidney, heart, lung and muscle, plus plasma. Potential choline redistributions among tissues are summarized in Fig. 4.5.

From the sum of radioactivity in all selected tissues, we found that in both mouse models, the CD diet caused increased uptake of [^{3}H]choline by comparing CS and CD mice after 1 h of injection with [^{3}H]choline ($p<0.01$) (Fig. 4.6A, B). After 24 h of injection with [^{3}H]choline, increased uptake of choline was only found in CD-*Abcb4*$^{-/-}$/*Pemt*$^{-/-}$ mice ($p<0.05$) but not in CD-*Pemt*$^{-/-}$ mice as compared with CS mice (Fig. 4.6 A, B). Total radioactivity in both CS- and CD-*Abcb4*$^{-/-}$/*Pemt*$^{-/-}$ mice from 1 h to 24 h was higher than that in CS- and CD-*Pemt*$^{-/-}$ mice. Therefore, selected tissues in CD-*Abcb4*$^{-/-}$/*Pemt*$^{-/-}$ mice were able to incorporate more choline in total during choline deprivation compared to CD-*Pemt*$^{-/-}$ mice. Since, without biliary PC re-absorption (> 95%) and redistribution (12-14), choline uptake in all tissues might be up-regulated. However, when biliary PC redistribution was involved, choline uptake in all tissues only increased in CS-*Pemt*$^{-/-}$ mice but not in CD-*Pemt*$^{-/-}$ mice from 1 h to 24 h (Fig. 4.6A).

As seen in Fig. 4.7, in CS-*Pemt*$^{-/-}$ mice, after 1 h of injection with [^{3}H]choline, the majority of choline labeling was found in intestine, kidney, muscle and liver. After 24 h, labeling in intestine ($p<0.001$) and muscle ($p<0.05$) was increased. When choline was deprived from the diet, after 1 h of injection with

[^{3}H]choline, the majority of choline labeling was still found in intestine, kidney, muscle and liver in CD-*Pemt*$^{-/-}$ mice. However, after 24 h, labeling in most of tissues did not change except that decreased labeling was found in kidney ($p<0.01$) and increased labeling in liver ($p<0.05$) and heart ($p<0.01$) from 1 h to 24 h in CD-*Pemt*$^{-/-}$ mice. Since total injection of [^{3}H]choline was the same in all CD-*Pemt*$^{-/-}$ mice, the alternations of labeling found in kidney, liver and heart suggested that choline was redistributed from 1 h to 24 h in CD-*Pemt*$^{-/-}$ mice and increased labeling in heart and liver might result from the decreased labeling in kidney and/or unevaluated tissues. By comparing CS-*Pemt*$^{-/-}$ mice and CD-*Pemt*$^{-/-}$ mice, we found that initial uptake of choline (1 h labeling) was up-regulated during choline deprivation, especially reflected in intestine ($p<0.001$) and muscle ($p<0.05$). However, both intestine ($p<0.01$) and kidney ($p<0.05$) showed significant reduction of labeling whereas both liver ($p<0.05$) and heart ($p<0.01$) showed increased radioactivity from CS to CD after 24 h of labeling in *Pemt*$^{-/-}$ mice (Fig. 4.7). Meanwhile, the sum of radioactivity showed no significant change from CS to CD after 24 h of labeling in *Pemt*$^{-/-}$ mice (Fig. 4.6A). Thus, these results suggested that choline redistribution was initiated by choline deprivation. The donors of this choline redistribution might be intestine and kidney, and the acceptors of choline were liver and heart. However, we still cannot exclude unevaluated tissues that might contribute to this choline redistribution.

When biliary PC secretion was eliminated (*Abcb4*$^{-/-}$) (bililary PC is the major source of choline in normal animals, >90%) (12,14), dietary choline became the only source of choline other than via PEMT. Thus, choline uptake and distribution might change in this case. In CS-*Abcb4*$^{-/-}$/*Pemt*$^{-/-}$ mice, most choline labeling was found in the liver after 1 h of labeling, whereas after 24 h, labeling in liver was dramatically decreased ($p<0.01$) whereas labeling in intestine ($p<0.01$), muscle ($p<0.001$) and brain ($p<0.05$) was increased significantly (Fig. 4.8). Since the sum of radioactivity in CS-*Abcb4*$^{-/-}$/*Pemt*$^{-/-}$ mice also increased significantly ($p<0.01$) from 1 h to 24 h labeling (Fig. 4.6B), we were not able to distinguish which tissue, either unevaluated tissues or liver, might have contributed to the increased labeling in intestine, muscle and brain (Fig. 4.8). In CD-*Abcb4*$^{-/-}$/*Pemt*$^{-/-}$ mice, most of the choline labeling was found in the intestine, kidney, muscle and liver after 1 h of labeling, whereas after 24 h, labeling was significantly decreased in intestine ($p<0.05$) and kidney ($p<0.05$) but increased in liver ($p<0.05$), muscle ($p<0.001$), heart ($p<0.05$), lung ($p<0.05$) and brain ($p<0.05$) (Fig. 4.8). Since the sum of radioactivity in all selected tissues did not change significantly from 1 h to 24 h labeling in CD-*Abcb4*$^{-/-}$/*Pemt*$^{-/-}$ mice (Fig. 4.6B), intestine and kidney might contribute their choline to liver, muscle, heart, lung and brain. By comparing CS- and CD-*Abcb4*$^{-/-}$/*Pemt*$^{-/-}$ mice at 1 h labeling, the CD diet caused increased uptake of choline in intestine ($p<0.001$), kidney ($p<0.001$) and muscle ($p<0.01$), and decreased uptake in liver ($p<0.01$) (Fig. 4.8). Even though the sum of radioactivity in all selected tissues was higher ($p<0.05$) in CD- compared to CS-*Abcb4*$^{-/-}$/*Pemt*$^{-/-}$ mice after 24 h of labeling (Fig. 4.6B), the radioactivity in muscles were significantly lower ($p<0.05$) in CD- compared to CS-*Abcb4*$^{-/-}$/*Pemt*$^{-/-}$ mice after 24 h of labeling. Thus, these results suggested that muscles made a significant contribution to choline redistribution during choline deprivation aside from plasma by comparing CD- to CS-*Abcb4*$^{-/-}$/*Pemt*$^{-/-}$ mice after 24 h of labeling ($p<0.05$) (Fig. 4.8). Unlike the acute adaptation in CD-*Pemt*$^{-/-}$ mice, during long-term choline deprivation, muscles in CD-*Abcb4*$^{-/-}$/*Pemt*$^{-/-}$ mice might be donors in choline redistribution, which might be further supported by the observation of significant weight loss of extra hepatic tissues in CD-*Abcb4*$^{-/-}$/*Pemt*$^{-/-}$ mice (Table 4.1). In CD-*Abcb4*$^{-/-}$/*Pemt*$^{-/-}$ mice, choline redistribution benefited not only liver, but also intestine, kidney, heart and lung, since total radioactivity in these tissues were all increased from CS to CD after 24 h of labeling. Moreover, the sum of radioactivity in all selected tissues was higher in CD- compared to CS-*Abcb4*$^{-/-}$/*Pemt*$^{-/-}$ mice after 24 h of labeling ($p<0.05$) (Fig. 4.6B). The increase in radioactivity at 24 h in CD mice suggests that some unevaluated tissues might also contribute to choline redistribution during choline deprivation.

It was interesting that the radioactivity in brain did not show any significant change in both mouse models under a CS or CD diet (Fig. 4.7, 4.8).

Under normal conditions, liver may be the major organ for uptake of free choline, converting it into PC or lysoPC that are secreted into plasma for transport to extrahepatic tissues. This process was further supported by increased labeling in plasma PC, rather than free choline, from 1 h to 24 h labeling in both CS-mouse models ($p<0.01$) (Fig. 4.9). However, once mice were deprived of dietary choline, no difference in the ratio of PC to free choline was found from 1 h to 24 h labeling in both CD-mouse models, and even at 1 h of labeling, most of the radioactivity occurred in PC in both CD-mouse models (Fig. 4.9). This indicates that during choline deprivation, the conversion of free choline into PC was enhanced, which is consistent with our previous finding that CT was up-regulated during choline deprivation (3).

Since biliary PC accounts for >90% of total choline uptake in mammals (the rest from diet), the data obtained from comparing CS-*Pemt*$^{-/-}$ mice and CS-*Abcb4*$^{-/-}$/*Pemt*$^{-/-}$ mice at 1 h of labeling (Fig. 4.7, 4.8) suggest that dietary choline might be mainly delivered into liver in CS-*Abcb4*$^{-/-}$/*Pemt*$^{-/-}$ mice since no biliary choline was available, whereas biliary choline mainly into intestine, kidney and muscle in CS-*Pemt*$^{-/-}$ mice.

4.3.4 Liver was more active in choline uptake than brain.

From specific activity assays, in both CS-*Pemt*$^{-/-}$ mice and CS-*Abcb4*$^{-/-}$/*Pemt*$^{-/-}$ mice, brains showed increased uptake of choline by comparing the radioactivity from 1 h to 24 h ($p<0.05$) (Fig. 4.10A, C). However, liver showed the opposite results ($p<0.05$) (Fig. 4.10B, D), since PC synthesized in liver might be delivered to extrahepatic tissues, which is consistent with the observation that more PC occurred in plasma from 1 h to 24 h (Fig. 4.9). At 24 h of labeling, most choline was converted into PC and/or further metabolized. When mice were fed with the CD diet, both brain and liver showed increased uptake of choline from 1 h to 24 h in CD-*Abcb4*$^{-/-}$/*Pemt*$^{-/-}$ mice ($p<0.05$), but not in CD-*Pemt*$^{-/-}$ mice (Fig. 4.10). The total specific activity in livers from either mouse strain fed a CS or CD diet was much higher than that in brain (Fig. 4.10). This suggested that choline uptake in liver was more active than in brain, especially under dietary choline-deficiency.

4.4 Discussion

The level of total choline-containing metabolites in the brain was almost maintained during choline deprivation in both mouse models (Fig. 4.1), however, as we previously reported, the level of total choline-containing metabolites in the liver dropped to half (3) and the level of total choline-containing metabolites in the plasma to 10~20% during choline deprivation in both mouse models (Fig. 4.4B). Thus, decreased level of total choline-containing metabolites in the liver, but not in other organs during choline deprivation, suggests that liver is the most sensitive organ to respond to the stress of choline deprivation and that liver has the capability of down-regulation of choline homeostasis for survival (3). Moreover, liver is the only organ that producing choline (in the presence of PEMT) and delivering choline to other organs (15,16). It was interesting that brain still maintained higher activity of choline oxidase (Fig. 4.2) but liver down-regulated choline oxidation to a lower level in both mouse models during choline deprivation (Fig. 2.7). Combined all together, our data suggest that brain becomes an acceptor of choline during the whole period of choline deprivation. Liver becomes an acceptor of choline during the later phase of choline deprivation in CD-*Abcb4*$^{-/-}$/*Pemt*$^{-/-}$ mice. Whereas during the early phase of choline deprivation in CD-*Abcb4*$^{-/-}$/*Pemt*$^{-/-}$ mice liver acted as a donor of choline, since choline oxidation was curtailed at 3 days of CD-*Abcb4*$^{-/-}$/*Pemt*$^{-/-}$ mice (Fig. 2.7) whereas the level of total choline-containing metabolites still decreased in the first 21 days of choline deprivation (Fig. 2.4).

In other words, choline redistribution among organs occurred during choline deprivation. As we found previously, the survival of CD-*Abcb4*$^{-/-}$/*Pemt*$^{-/-}$ mice depended on the maintenance of the level of total choline-containing metabolites after 21 days of choline deprivation (3). Thus, it was not surprising that choline redistribution also directed extrahepatic choline into liver to maintain the minimal level of choline for life in CD-*Abcb4*$^{-/-}$/*Pemt*$^{-/-}$ mice from 21 to 90 days. Our results also suggest that intestine, kidney and muscle might donate their choline to liver and brain via choline redistribution.

How did brain maintain its total choline level so stable during choline deprivation? From *in vivo* labeling, we found that choline uptake in brain only accounted for a minor part of total choline uptake in whole body (Fig. 4.7, 4.8, 4.10). In addition, choline oxidation was still active in the brain of both mouse models during choline deprivation (Fig. 4.2), whereas the total level of choline-containing metabolites did not decease significantly in brains after both strains of mice were fed the CD diet (Fig. 4.1A). These results suggest that choline deprivation did not significantly affect choline metabolism in brain in both mouse models and brain must have obtained continuous supply of choline from peripheral tissues during choline deprivation. Thus, during choline deprivation, choline redistribution was initiated, which guaranteed a steady supply of choline to the brain. Sufficient free choline in the plasma and stable choline transporters guaranteed the level of total choline-containing metabolites in the brain during choline redistribution (Fig. 4.3, 4.4). Hence, it was feasible for mice to maintain the total level of choline-containing metabolites in their brains via choline redistribution to escape/adapt to choline deprivation.

Previous studies showed that apoptosis was induced in brain cells cultured in a CD medium (17). This suggested that choline is an essential component for brain. However, *in vivo*, brain actually did not exhibit choline deficiency when mice were under PEMT deficiency and/or dietary choline deficiency (Fig. 4.1). Even though CD-*Pemt*$^{-/-}$ mice died of severe liver failure during complete choline deprivation (3,4), the level of total choline-containing metabolites in brain did not decline significantly in CD-*Pemt*$^{-/-}$ mice (Fig. 4.1). These results indicated that when mice were under the stress of choline deprivation, a fine regulatory mechanism was triggered to protect some important organs (such as brain and liver) from choline deprivation while some other organs (such as muscle and intestine) might sacrifice their choline storage to brain and liver, so called choline redistribution (Fig. 4.5). Besides, mice could also down-regulate their choline level to the threshold to maintain a basic life. For example, CD-*Abcb4*$^{-/-}$/*Pemt*$^{-/-}$ mice can survive on the baseline of hepatic choline level (~110 nmol/mg protein, about half of that under the CS diet) during choline deprivation as reported before (3). No matter either acute adaptation in CD-*Pemt*$^{-/-}$ mice or chronic adaptation in CD-*Abcb4*$^{-/-}$/*Pemt*$^{-/-}$ mice, choline redistribution did contribute to adaptation to choline deprivation.

From Table 4.1, I found that body weight decreased unparalleled with increased liver weight in *Abcb4*$^{-/-}$/*Pemt*$^{-/-}$ mice and the ratio of liver weight to body weight increased dramatically during choline deprivation. Furthermore, the weight of extrahepatic tissues decreased significantly after 21 days of choline deprivation. These results support the idea that mice might have to sacrifice some tissues (such as muscles) to provide choline to liver and brain. This redistribution of choline may be beneficial for mice during a long-term of choline deprivation.

What mediates choline redistribution is also an intriguing question. Fig. 4.4 showed that choline deprivation did not profoundly affect plasma free choline level in *Pemt*$^{-/-}$ mice after 3 days. This data imply that under acute choline deprivation the liver might be more dependent on PC entering the liver than that plasma choline can compensate as a substrate for the CDP-choline pathway. In mice, the major uptake of PC by liver is from HDL particles. Therefore, choline redistribution might be mediated by HDL transportation.

The last question is what regulates this process of choline redistribution to adapt to choline deprivation. Our previous findings suggest that it could be c-Jun-involved signaling (Chapter 2), which will be the major focus in future studies.

Table 4.1 Body Weight and Liver Weight of *Abcb4*$^{-/-}$/*Pemt*$^{-/-}$ Mice

	CS	CD3	CD21	CD90
Body Weight (g)	19.63 ± 1.56	19.90 ± 1.40	18.25 ± 1.40	16.83 ± 1.19*
Liver Weight (g)	1.07 ± 0.12	1.2 ± 0.04	1.75 ± 0.15**	1.46 ± 0.12*
Liver Weight/Body Weight	0.056 ± 0.004	0.056 ± 0.004	0.086 ± 0.001**	0.087 ± 0.002**
Body Weight – Liver Weight (g)	18.02 ± 1.17	17.43 ± 1.62	16.36 ± 0.87*	16.21 ± 1.20*

Abcb4$^{-/-}$/*Pemt*$^{-/-}$ mice were fed a choline-supplemented (CS) diet for 24 h and then switched to a choline-deficient (CD) diet for 3, 21 or 90 days. *, $p < 0.05$; **, $p < 0.01$. *P* values were from comparison between CS and CD mice.

Fig. 4.1 Levels of total choline–containing metabolites and phosphatidylcholine (PC) in the brain are not affected by the choline-deficient (CD) diet

Pemt$^{-/-}$ and *Abcb4*$^{-/-}$/*Pemt*$^{-/-}$ mice were fed a CS diet for 24 h and then switched to a CD diet for 3 to 90 days. The level of total choline-containing metabolites was assayed with Phospholipids B kit (Wako). Brain PC level was measured by HPLC after lipid extraction. **(A)** The level of total choline-containing metabolites; **(B)** The level of PC in the brain.

A

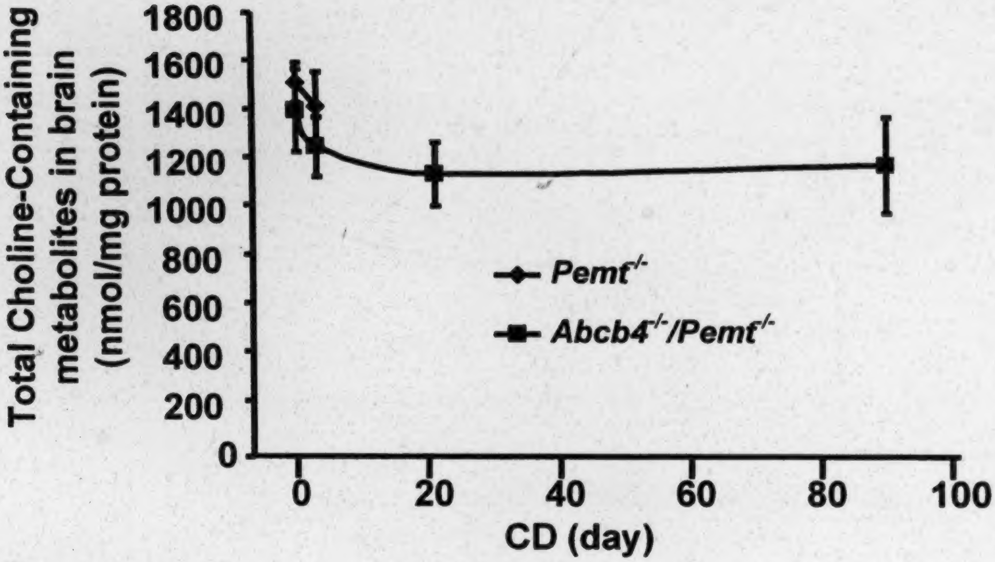
Total Choline-Containing metabolites in brain (nmol/mg protein)
1800
1600
1400
1200
1000
800
600
400
200
0
0
20
40
60
80
100
CD (day)
Pemt-/-
Abcb4-/-/Pemt-/-

B

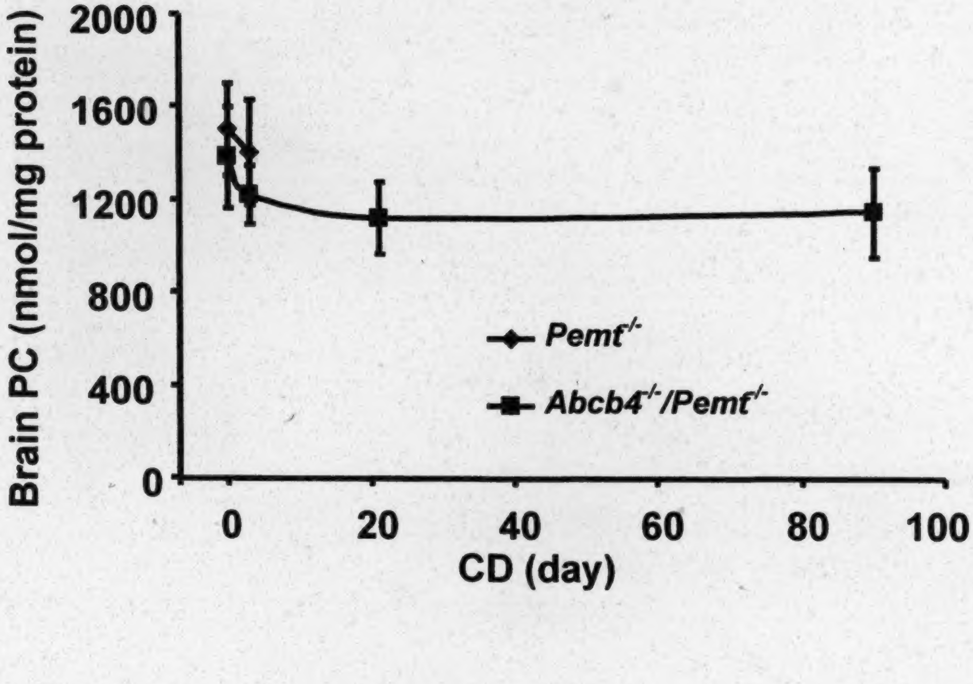
Brain PC (nmol/mg protein)
2000
1600
1200
800
400
0
0
20
40
60
80
100
CD (day)
Pemt-/-
Abcb4-/-/Pemt-/-

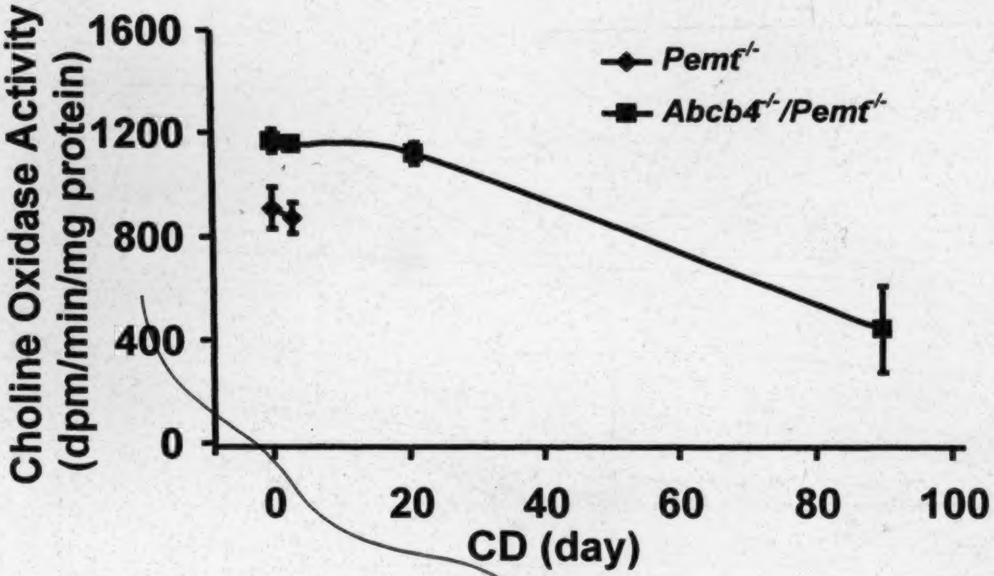

Fig. 4.2 Choline oxidation in the brain is still active during choline deprivation

Pemt$^{-/-}$ and *Abcb4*$^{-/-}$/*Pemt*$^{-/-}$ mice were fed a CS diet for 24 h and then switched to a CD diet for 3 to 90 days. Choline oxidase activity was determined by incubation of [^{3}H]choline with mitochondria isolated as the pellet obtained after centrifugation of liver homogenates at 12,000 x g for 15 min. [^{3}H]betaine was separated on TLC plates after lipid extraction.

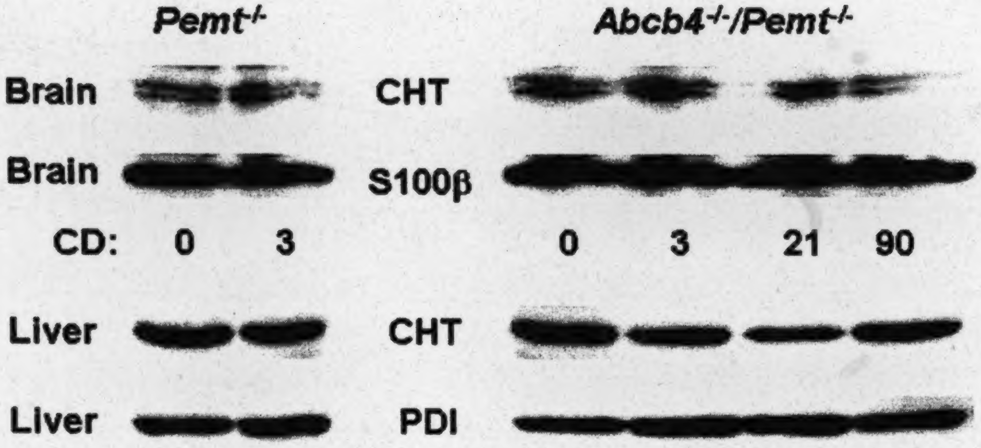
Pemt$^{-/-}$
Abcb4$^{-/-}$/*Pemt*$^{-/-}$
Brain
CHT
Brain
S100β
CD:
0
3
0
3
21
90
Liver
CHT
Liver
PDI

Fig. 4.3 Expression of choline high-affinity transporter (CHT) in the brain and liver.

Pemt$^{-/-}$ and *Abcb4*$^{-/-}$/*Pemt*$^{-/-}$ mice were fed a CS diet for 24 h and then switched to a CD diet for 3 to 90 days. Fifty μg proteins of liver and brain homogenates were separated by 10% SDS-PAGE and blotted with anti-CHT antibody. S100β protein blotting was used as protein loading control for brain analysis. PDI blotting was used as protein loading control for liver analysis.

Fig. 4.4 Plasma free choline levels did not decrease significantly on a CD diet whereas plasma PC was decreased markedly.

Plasma was collected from *Pemt*$^{-/-}$ and *Abcb4*$^{-/-}$/*Pemt*$^{-/-}$ mice fed a CS diet for 24 h and then switched to a CD diet for 3 to 90 days. The levels of free choline were assayed with choline oxidase. Plasma PC levels were measured by HPLC after lipid extraction. **(A)** The levels of free choline in the plasma; **(B)** Plasma PC levels.

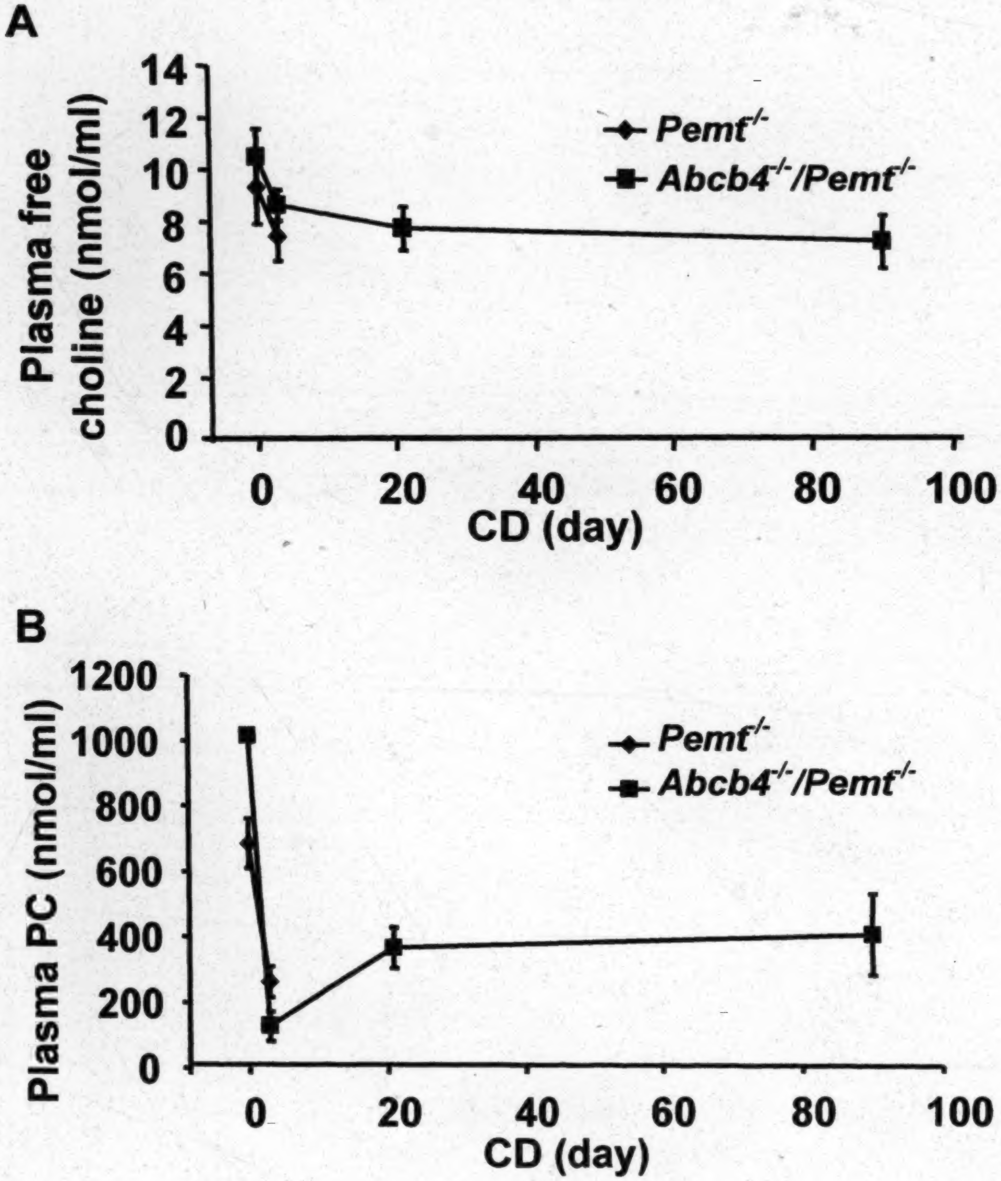
A
Plasma free choline (nmol/ml)
14
12
10
8
6
4
2
0
0
20
40
60
80
100
CD (day)
Pemt-/-
Abcb4-/-/Pemt-/-
B
Plasma PC (nmol/ml)
1200
1000
800
600
400
200
0
0
20
40
60
80
100
CD (day)
Pemt-/-
Abcb4-/-/Pemt-/-

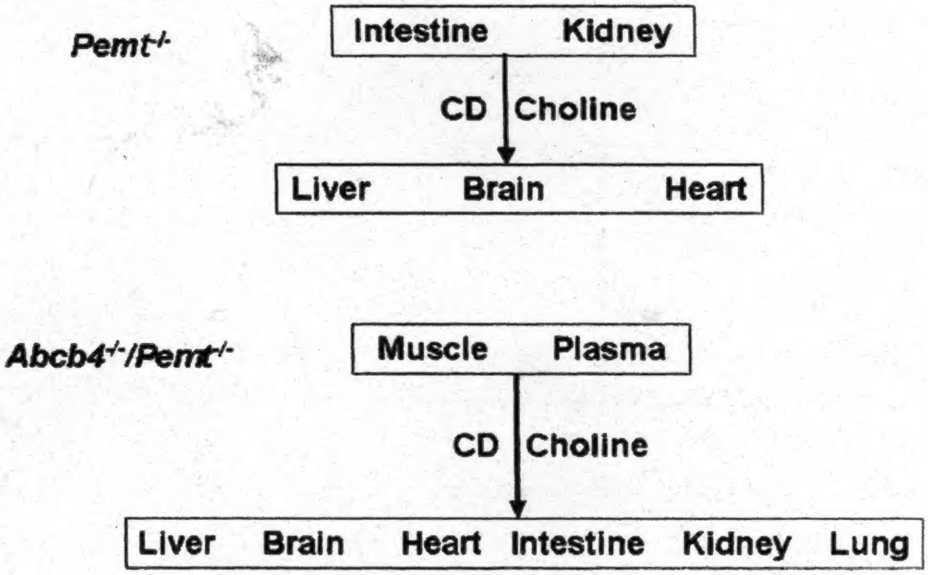
Pemt$^{-/-}$
Intestine
Kidney
CD
Choline
Liver
Brain
Heart
Abcb4$^{-/-}$/*Pemt*$^{-/-}$
Muscle
Plasma
CD
Choline
Liver
Brain
Heart
Intestine
Kidney
Lung

Fig. 4.5 Potential choline redistributions among tissues in *Pemt*$^{-/-}$ and *Abcb4*$^{-/-}$/*Pemt*$^{-/-}$ mice during choline deprivation

Fig. 4.6 Sum of total radioactivity in all tissues assayed

Pemt$^{-/-}$ and *Abcb4*$^{-/-}$/*Pemt*$^{-/-}$ mice were fed a CS diet for 24 h (CS) and then switched to a CD diet for 3 (CD3) or 21 (CD21) days. 100 μCi [^{3}H]choline in 100 μl saline was injected into mice via the tail-vein. Mice were sacrificed after 1 h or 24 h of injection. Total radioactivity in the whole tissue were measured and all assayed tissues included brain, liver, intestine, kidney, heart, lung and muscle, plus plasma. Data were presented as a 20 g mouse. Sum of total radioactivity in all tissues assayed in *Pemt*$^{-/-}$ mice **(A)** and *Abcb4*$^{-/-}$/*Pemt*$^{-/-}$ mice **(B)**.

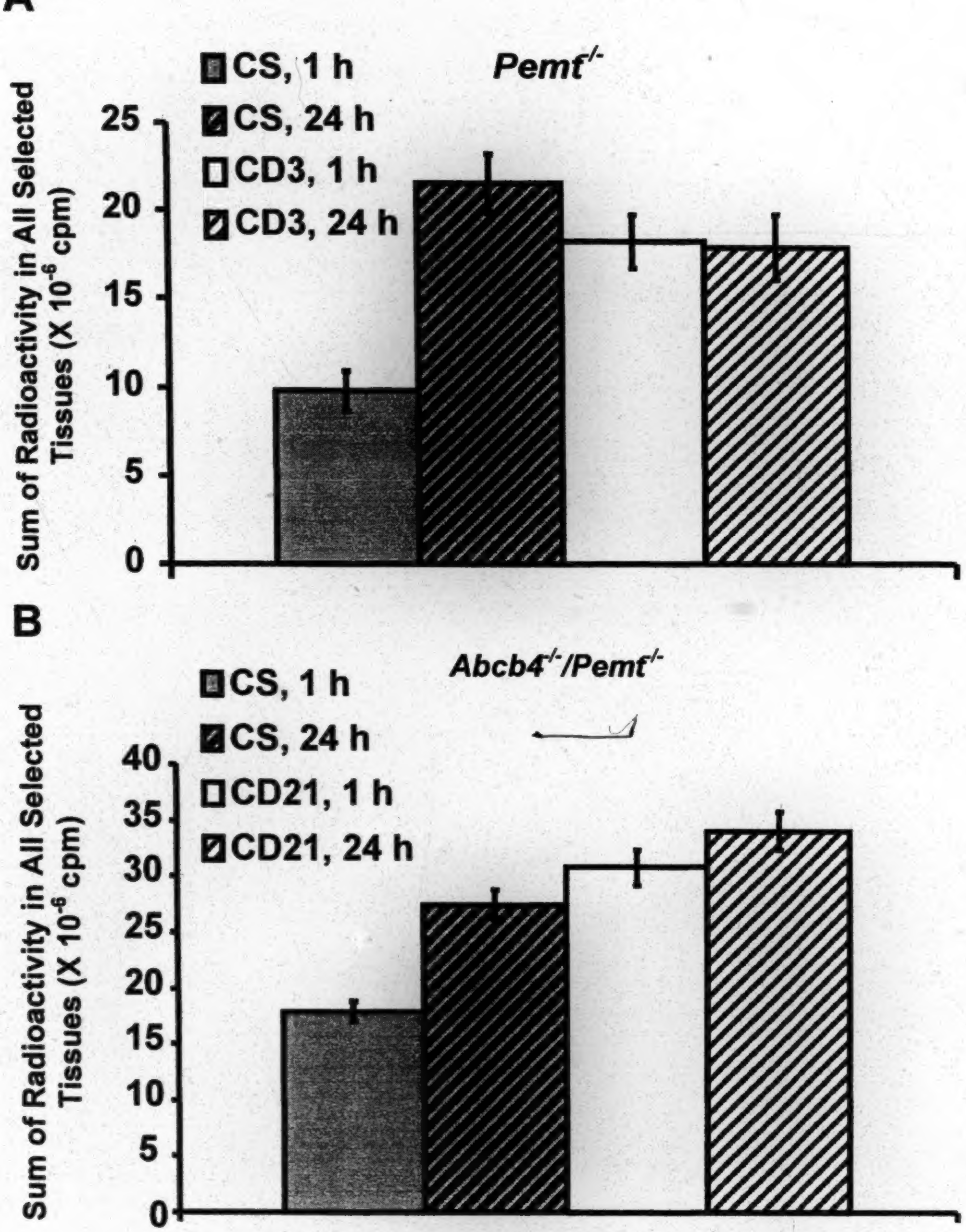
A
▨ CS, 1 h
▨ CS, 24 h
☐ CD3, 1 h
▨ CD3, 24 h
Pemt-/-
Sum of Radioactivity in All Selected Tissues (X 10-6 cpm)
25
20
15
10
5
0
B
▨ CS, 1 h
▨ CS, 24 h
☐ CD21, 1 h
▨ CD21, 24 h
Abcb4-/-/Pemt-/-
Sum of Radioactivity in All Selected Tissues (X 10-6 cpm)
40
35
30
25
20
15
10
5
0

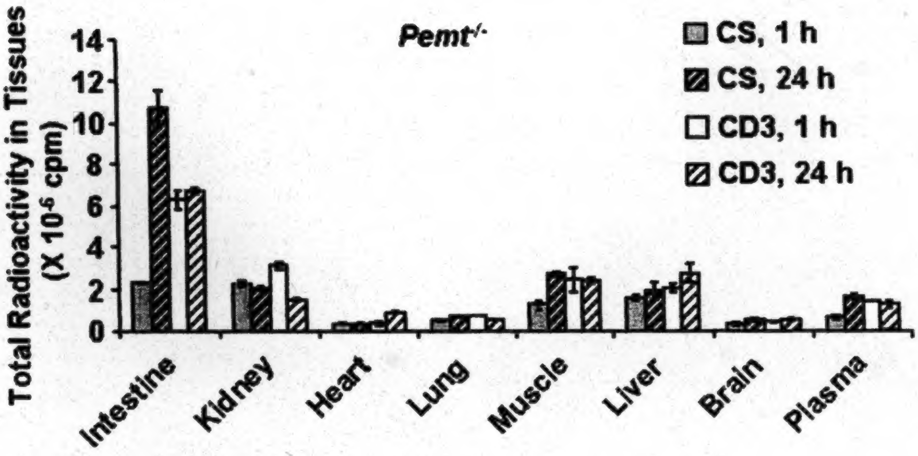

Fig. 4.7 Total radioactivity in the whole tissues of *Pemt*$^{-/-}$ mice.

Pemt$^{-/-}$ mice were fed a CS diet for 24 h (CS) and then switched to a CD diet for 3 (CD3) days. 100 μCi [^{3}H]choline in 100 μl saline was injected into mice via tail-vein. Mice were sacrificed after 1 h or 24 h of injection. Total radioactivity in the whole tissue were measured and all assayed tissues included brain, liver, intestine, kidney, heart, lung and muscle, plus plasma. Data were presented as a 20 g mouse.

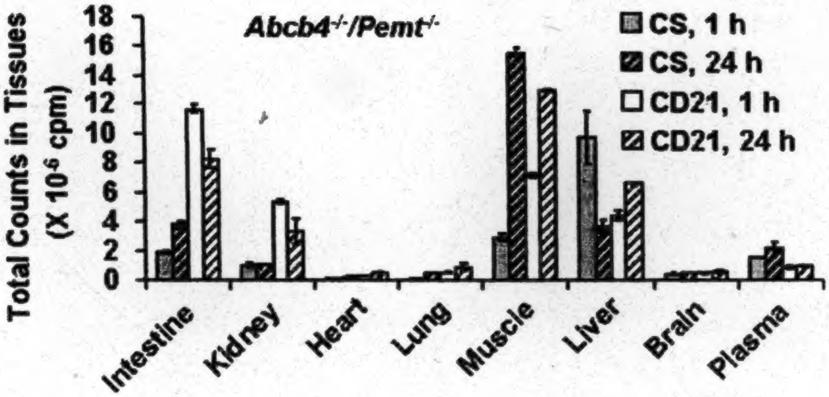

Fig. 4.8 Total radioactivity in the whole tissues of *Abcb4$^{-/-}$/Pemt$^{-/-}$* mice

Abcb4$^{-/-}$/Pemt$^{-/-}$ mice were fed a CS diet for 24 h (CS) and then switched to a CD diet for 21 (CD21) days. 100 μCi [^{3}H]choline in 100 μl saline was injected into mice via tail-vein. Mice were sacrificed after 1 h or 24 h of injection. Total radioactivity in the whole tissue were measured and all assayed tissues included brain, liver, intestine, kidney, heart, lung and muscle, plus plasma. Data were presented as a 20 g mouse.

Fig. 4.9 Distributions of [^{3}H]choline labeling in PC and free choline in the plasma

Pemt$^{-/-}$ and *Abcb4*$^{-/-}$/*Pemt*$^{-/-}$ mice were fed a CS diet for 24 h (CS) and then switched to a CD diet for 3 (CD3) or 21 (CD21) days. 100 μCi [^{3}H]choline in 100 μl saline was injected into mice via tail-vein. Mice were sacrificed after 1 h or 24 h of injection. Total radioactivity in the whole plasma were measured. Data are presented as 2 ml plasma in a 20 g mouse. PC and free choline were separated by thinner layer chromatography (TLC) after lipid extraction.

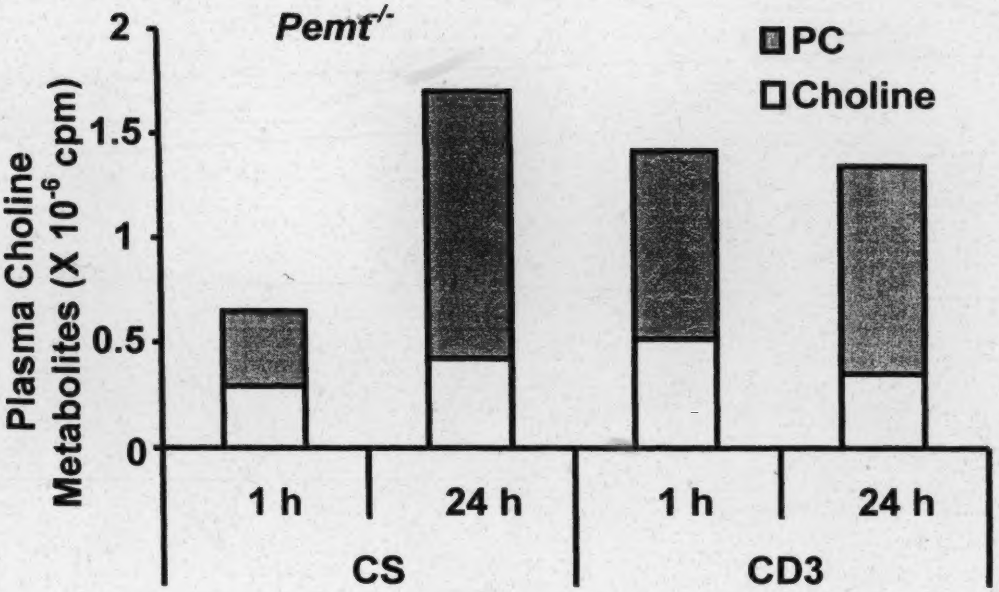
Pemt-/-
PC
Choline
Plasma Choline Metabolites (X 10-6 cpm)
2
1.5
1
0.5
0
1 h
24 h
1 h
24 h
CS
CD3

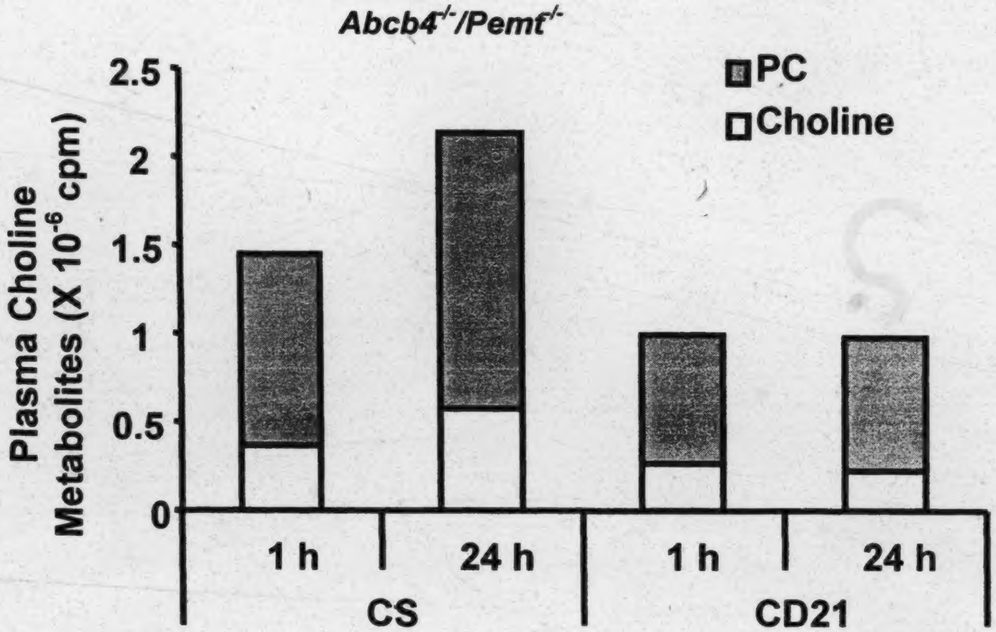
Abcb4-/-/Pemt-/-
PC
Choline
Plasma Choline Metabolites (X 10-6 cpm)
2.5
2
1.5
1
0.5
0
1 h
24 h
1 h
24 h
CS
CD21

Fig. 4.10 Specific activities of choline metabolites in brain and liver

Pemt$^{-/-}$ and *Abcb4*$^{-/-}$/*Pemt*$^{-/-}$ mice were fed a CS diet for 24 h (CS) and then switched to a CD diet for 3 (CD3) or 21 (CD21) days. 100 μCi [^{3}H]choline in 100 μl saline was injected into mice via tail-vein. Mice were sacrificed after 1 h or 24 h of injection. Total radioactivity in the whole tissue were measured. The level of total choline-containing metabolites was assayed with Phospholipids B kit (Wako). Data were presented for a 20 g mouse. Specific activities were calculated from total radioactivity/amount of total choline-containing metabolites. **(A)** Specific activities were assayed in the brain of *Pemt*$^{-/-}$ mice; **(B)** Specific activities were assayed in the liver of *Pemt*$^{-/-}$ mice; **(C)** Specific activities were assayed in the brain of *Abcb4*$^{-/-}$/*Pemt*$^{-/-}$ mice; **(D)** Specific activities were assayed in the liver of *Abcb4*$^{-/-}$/*Pemt*$^{-/-}$ mice.

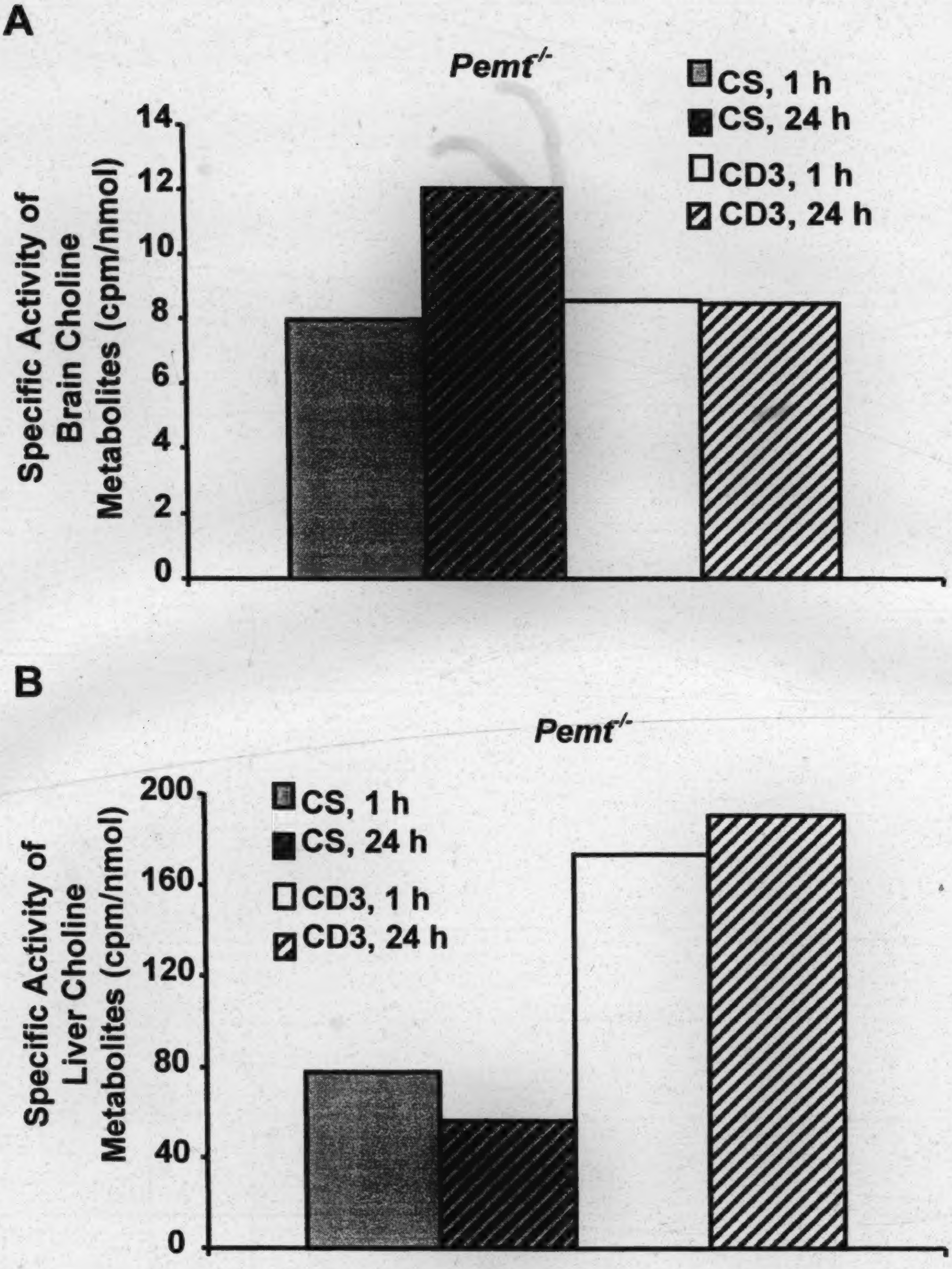
A
Pemt-/-
▨ CS, 1 h
■ CS, 24 h
☐ CD3, 1 h
▨ CD3, 24 h
Specific Activity of Brain Choline Metabolites (cpm/nmol)
14
12
10
8
6
4
2
0
B
Pemt-/-
▨ CS, 1 h
■ CS, 24 h
☐ CD3, 1 h
▨ CD3, 24 h
Specific Activity of Liver Choline Metabolites (cpm/nmol)
200
160
120
80
40
0

C

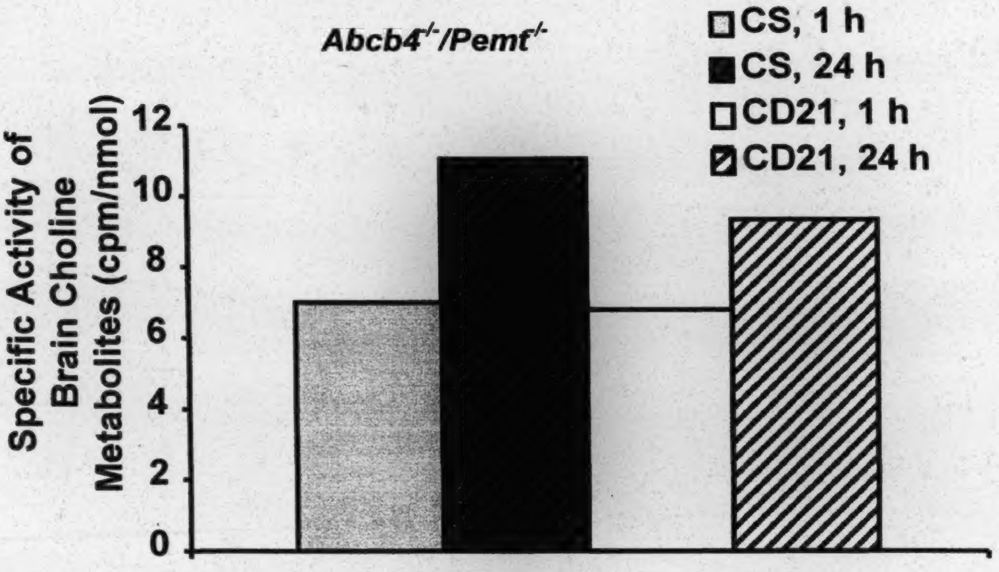

Abcb4-/-/Pemt-/-
▨ CS, 1 h
■ CS, 24 h
☐ CD21, 1 h
▨ CD21, 24 h
Specific Activity of Brain Choline Metabolites (cpm/nmol)
12
10
8
6
4
2
0

D

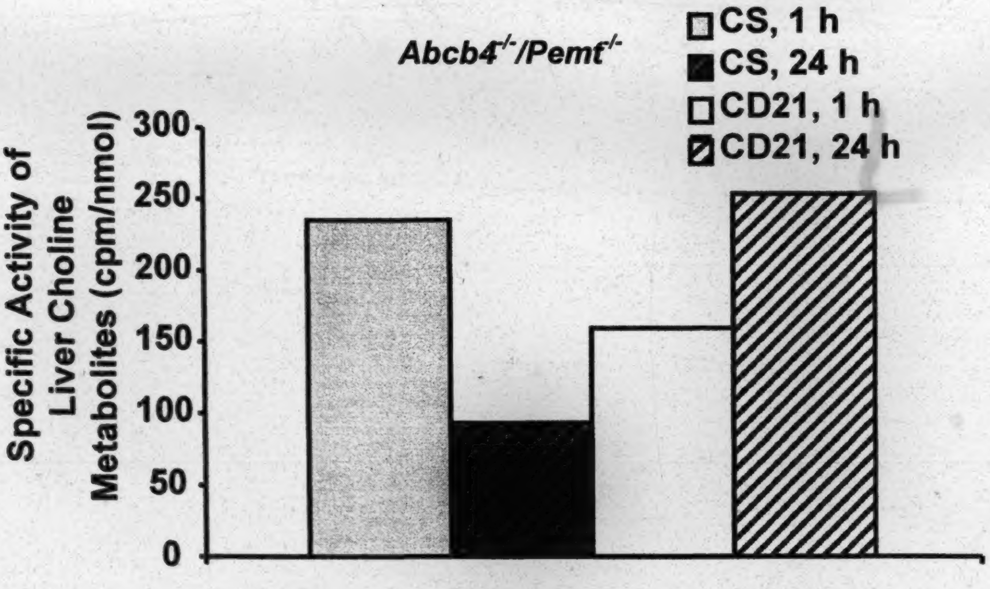

Abcb4-/-/Pemt-/-
▨ CS, 1 h
■ CS, 24 h
☐ CD21, 1 h
▨ CD21, 24 h
Specific Activity of Liver Choline Metabolites (cpm/nmol)
300
250
200
150
100
50
0

References

1. Best, C. H., and Huntsman, M. E. The effects of the components of lecithine upon deposition of fat in the liver. (1932) *Journal of Physiology-London* **75**, 405-412
2. Zeisel, S. H. Choline: an essential nutrient for humans. (2000) *Nutrition* **16**, 669-671
3. Li, Z., Agellon, L. B., and Vance, D. E. Phosphatidylcholine homeostasis and liver failure. (2005) *J Biol Chem*
4. Walkey, C. J., Yu, L., Agellon, L. B., and Vance, D. E. Biochemical and evolutionary significance of phospholipid methylation. (1998) *J Biol Chem* **273**, 27043-27046
5. Zeisel, S. H. Nutritional importance of choline for brain development. (2004) *J Am Coll Nutr* **23**, 621S-626S
6. Biberthaler, P., Mussack, T., Wiedemann, E., Kanz, K. G., Koelsch, M., Gippner-Steppert, C., and Jochum, M. Evaluation of S-100b as a specific marker for neuronal damage due to minor head trauma. (2001) *World J Surg* **25**, 93-97
7. Mussack, T., Biberthaler, P., Kanz, K. G., Heckl, U., Gruber, R., Linsenmaier, U., Mutschler, W., and Jochum, M. Immediate S-100B and neuron-specific enolase plasma measurements for rapid evaluation of primary brain damage in alcohol-intoxicated, minor head-injured patients. (2002) *Shock* **18**, 395-400

8. Lang, D. H., Sharkey, N. A., Lionikas, A., Mack, H. A., Larsson, L., Vogler, G. P., Vandenbergh, D. J., Blizard, D. A., Stout, J. T., Stitt, J. P., and McClearn, G. E. Adjusting data to body size: a comparison of methods as applied to quantitative trait loci analysis of musculoskeletal phenotypes. (2005) *J Bone Miner Res* **20**, 748-757

9. Bannerman, R. *Hematology* (1983) in *The Mouse in Biomedical Research* (Foster, H., Small, D., and Fox, J.G., ed) Vol. III, Academic Press, New York

10. Vance, D. E. *Phospholipid biosynthesis in eukaryotes.* (2002) in *Biochemistry of lipids, lipoproteins and membranes* (Vance, D. E., J. E. Vance, ed), pp. 205-232, Elsevier, New York

11. Sarter, M., and Parikh, V. Choline transporters, cholinergic transmission and cognition. (2005) *Nat Rev Neurosci* **6**, 48-56

12. Borgstrom, B. (1976) *Phospholipid absorption*. Lipid absorption (Rommel, K., H. Goebell, R. Bohmer, Ed.), MTP Press Ltd., London

13. Robins, S. J. Recirculation and reutilization of micellar bile lecithin. (1975) *Am J Physiol* **229**, 598-602

14. Tso, P., and Fujimoto, K. The absorption and transport of lipids by the small intestine. (1991) *Brain Res Bull* **27**, 477-482

15. Vance, J. E., and Vance, D. E. Lipoprotein assembly and secretion by hepatocytes. (1990) *Annu Rev Nutr* **10**, 337-356

16. Walkey, C. J., Donohue, L. R., Bronson, R., Agellon, L. B., and Vance, D. E. Disruption of the murine gene encoding phosphatidylethanolamine N-methyltransferase. (1997) *Proc Natl Acad Sci U S A* **94**, 12880-12885

17. Yen, C. L., Mar, M. H., and Zeisel, S. H. Choline deficiency-induced apoptosis in PC12 cells is associated with diminished membrane phosphatidylcholine and sphingomyelin, accumulation of ceramide and diacylglycerol, and activation of a caspase. (1999) *Faseb J* **13**, 135-142

Chapter 5

Mobilization of Extrahepatic Choline via Enhacing HDL-PC Efflux

--- Adaptation to choline deprivation IV: choline storage

5.1 Introduction

Choline is stored as a component of phosphatidylcholine (PC) in the membrane. PC accounts for > 95% of total choline-containing metabolites (1,2). Mice can survive at the basal level of total choline-containing metabolites (~50% of original level) during choline deprivation when choline is recycled (Chapter 2) (3) and redistributed (Chapter 4). In terms of choline redistribution, the donor tissues can also be treated as tissues of choline storage.

CD-*Pemt*$^{-/-}$ mice die of liver failure within 4~5 days (4). Acute lethality suggests that *Pemt*$^{-/-}$ mice failed to adapt to choline deprivation. However, it was intriguing to explore whether CD-*Pemt*$^{-/-}$ mice had an adaptive response to choline deprivation. We found that only female *Pemt*$^{-/-}$ mice showed successful adaptation to choline deprivation within the first day of choline deprivation. Both male and female mice showed adaptive response to choline deprivation through mobilization of choline stored in extrahepatic tissues, which was achieved by enhancing the efflux of high density lipoprotein-PC (HDL-PC). However, gender-specific requirement of HDL-PC by liver might determine gender-different adaptations to choline deprivation in CD-*Pemt*$^{-/-}$ mice. This acute adaptation to choline deprivation is named as choline storage.

5.2 Materials and Methods

5.2.1 Animals

Pemt$^{-/-}$ mice (C57BL/6; 129/J background) (5) were fed a choline-deficient (CD) diet, a semi-synthetic diet without choline (*ICN*, Cat#0290138710) or a choline-supplemented (CS) diet (a CD diet containing 0.4% (w/w) choline chloride). At the age of 10 to 12 weeks, *Pemt*$^{-/-}$ mice were fed a CS diet for 24 h (0 day) and then switched to a CD diet for 1, 2 or 3 days. Mice were fasted for 12 h before sacrifice. Four to eight mice of each gender were used for each time point in all experiments and assays were performed in duplicate. All data are given as means ± S.D.

5.2.2 Liver damage assays

Plasma samples were collected from *Pemt*$^{-/-}$ mice fed the choline-supplemented (CS) diet for 24 h (0 day) then transferred to the choline-deficient (CD) diet for 3 days. Plasma alanine/aspartate aminotransferase (ALT/AST) activities were measured with a GPT/GOT Kit (*Sigma*, catalog # P505) as indicators of liver damage. Plasma ALT/AST activity was measured at day 0, 1, 2 and 3.

5.2.3 Lipid analysis see 2.2.6

5.2.4 Profiles of choline-containing lipids in plasma lipoproteins

Blood was collected by cardiac puncture with instruments pretreated with EDTA. Plasma was separated by centrifugation at 2,000 rpm for 20 min in a refrigerated benchtop centrifuge. Fresh plasma samples were injected to fast-phase liquid chromatography (FPLC) for analysis of profiles of choline-containing lipids in lipoproteins. Plasma combined from at least three mice was used for FPLC analysis.

5.2.5 Treatment of mice with glybenclamide

Female *Pemt*$^{-/-}$ mice were fed a choline-supplemented (CS) diet containing glybenclamide (an inhibitor of ABCA1 mediated cholesterol and phospholipid efflux, from *Sigma*) (163 μg/g diet) for one day and then changed to a choline-deficient (CD) diet containg glybenclamide (163 μg/g diet) for one day. Female *Pemt*$^{-/-}$ mice were fed a CS or CD diet without glybenclamide as controls. Wild-type mice were fed a CS or CD diet with 163 μg/g glybenclamide as negative controls, and no liver damage was found.

5.2.6 Preβ HDL particles and ApoAI secretion from primary cultured hepatocytes

Male and Female *Pemt*$^{-/-}$ mice were fed the CS diet for one day and then switched to the CD diet for one day. Primary hepatocytes isolated from mice described in **2.2.4** were cultured in a CS or CD medium. After plating for 2 h, hepatocytes were changed to fresh medium without serum for 1 h. After that, hepatocytes were chased in a fresh medium for 2 h, then the medium was collected and concentrated through a centrifugation filter with pore size of 5,000 kD. The concentrated medium was separated on a 6% non-denatured PAGE (polyacrylamide gel electrophoresis) for analysis of preβ high density lipoprotein (preβ HDL) particles. Then proteins were transferred to a PVDF (polyvinylidene fluoride) membrane and blotted with an anti-ApoA1 antibody. Concentrated medium was also loaded and separated by 12% SDS-PAGE. Subsequently, total ApoAI proteins were measured by Western blotting.

Sandwich ELISA (enzyme-linked immunoabsorbent assay) was used for analyzing the amount of PC associated with ApoAI proteins. A 96-well plate was pre-incubated with anti-ApoAI antibody for 24 h at 4°C as a catching antibody. After incubation with concentrated medium, a detecting antibody, an anti-PC antibody (1:100) (from Dr. Masato Umeda) was used for measuring the amount of PC associated with ApoAI followed by a secondary antibody-conjugated with FITC (fluorescein isothiocyanate). Fluorescent intensity was measured with a fluorimeter.

5.3 Results

5.3.1 Gender-dependent response to choline deprivation in *Pemt*$^{-/-}$ mice

Analysis of liver damage markers, plasma ALT/AST activities, showed that when male *Pemt*$^{-/-}$ mice were fed the CD diet, liver damage was induced immediately after the CD feeding and increased constantly during three days of choline deprivation (Fig. 5.1). However, female *Pemt*$^{-/-}$ mice did not show any liver damage in the first day of the CD feeding and liver damage only occurred and increased after the first day of choline deprivation (Fig. 5.1). Thus, liver damage induced by choline deprivation in CD-*Pemt*$^{-/-}$ mice was delayed for one day in female mice compared to male mice (Fig. 5.1).

5.3.2 Gender-dependent difference in PC/PE ratios and PC levels in the liver

In Chapter 3, the PC/PE ratio is identified as a key regulator of membrane integrity and liver damage is induced by a decreased hepatic PC/PE ratio. Here, we provide additional evidence to support this conclusion. That is, gender-dependent status of liver damage in *Pemt*$^{-/-}$ mice during choline deprivation was compatible with the theory of hepatic PC/PE ratios. For example, on the first day of choline deprivation, female *Pemt*$^{-/-}$ mice did not show decreased PC/PE ratio, but male *Pemt*$^{-/-}$ mice did (Fig. 5.2 A) ($p<0.05$). No liver damage was induced in female *Pemt*$^{-/-}$ mice, but was in males (Fig. 5.1). When hepatic PC/PE ratios decreased in both male and female *Pemt*$^{-/-}$ mice, liver damage occurred and increased following continuous decrease in PC/PE ratios (Fig. 5.2A).

As addressed before, decreased PC/PE ratios in CD-*Pemt*$^{-/-}$ mice resulted from decreased PC levels and unchanged PE levels (Chapter 3). During 3 days of choline deprivation, there was no significant change in PE levels in livers of both male and female mice (Fig. 5.2B). Thus, the decrease in PC/PE ratios resulted from the change in PC levels.

5.3.3 Gender-dependent PC homeostasis in the liver

PC homeostasis in the liver consists of PC anabolism and catabolism as well as PC secretion and uptake (Fig. 3.1) (2). Biliary PC levels mirrored hepatic PC levels (Fig. 5.3, 5.2B) that indicated that biliary PC secretion was dependent on the pool size of hepatic PC. These results also suggest that down-regulation of biliary PC secretion might not be a successful means of adaptation to choline deprivation. Even though female *Pemt*$^{-/-}$ mice were able to maintain their hepatic PC levels for one day during choline deprivation (Fig. 5.2B), biliary PC secretion in female *Pemt*$^{-/-}$ mice was not down-regulated during the first day of choline deprivation (Fig. 5.3). Interestingly, female *Pemt*$^{-/-}$ mice showed obvious lower levels of plasma PC as compared with males when mice fed the CS diet (Fig. 5.4). Since most PC in plasma of mice is associated with HDL particles (6), it was not surprising to find that the difference in plasma PC levels was completely reflected by HDL-PC levels between female and male *Pemt*$^{-/-}$ mice (Fig. 5.5, 5.6). When *Pemt*$^{-/-}$ mice were fed the CD diet, female mice were able to increase their plasma PC levels through increasing HDL-PC levels (Fig. 5.4, 5.6), whereas male *Pemt*$^{-/-}$ mice were not (Fig. 5.4, 5.5). Since we found previously, HDL-PC uptake rate did not change in CD- compared to CS-*Pemt*$^{-/-}$ hepatocytes (Chapter 3), the increased HDL-PC levels in plasma might be from increased HDL-PC efflux from liver or other tissues.

5.3.4 Glybenclamide lowered HDL-PC and induced liver damage in female *Pemt*$^{-/-}$ mice

Glybenclamide (also called glyburide) is an inhibitor of HDL-PC/cholesterol efflux mediated by ABCA1 (7,8). When we fed glybenclamide (163 μg/g diet) to female CS- or CD-*Pemt*$^{-/-}$ mice, we found that glybenclamide effectively reduced HDL-PC and subsequently plasma PC levels were also decreased in female *Pemt*$^{-/-}$ mice when fed the CD diet for one day (CD+G) compared with female *Pemt*$^{-/-}$ mice fed the CS diet for one day (CS+G) (Fig. 5.7). Finally, hepatic PC levels decreased about 30% ($p<0.05$) and the PC/PE ratio decreased about 40% (Fig. 5.8A, B). The glybenclamide induced liver damage in female CD1-*Pemt*$^{-/-}$ mice (Fig. 5.9). However, glybenclamide did not induce any liver damage in female *Pemt*$^{-/-}$ mice when fed the CS diet for one day (Fig. 5.9) or in wild-type mice fed either the CS or CD diet for up to 2 days (plasma ALT activities in wild type mice fed glybenclamide of 163 μg/g diet for 2 days: 7.33 ± 0.89 IU/l).

5.3.5 Exploring the mechanisms of differential regulation of HDL-PC efflux

Primary hepatocytes isolated from male and female *Pemt*$^{-/-}$ mice fed the CS or CD diet were cultured to analyze hepatic PC efflux to ApoAI. Fig. 5.10 showed that hepatocytes only produced preβ HDL but not mature HDL. Dietary choline deprivation caused decreased formation of preβ HDL in both male and female *Pemt*$^{-/-}$ mice, even though the total amount of ApoAI secreted from hepatocytes was not changed significantly. The amount of PC associated with ApoAI was significantly reduced in both male and female *Pemt*$^{-/-}$ mice after choline deprivation (Fig. 5.11).

5.4 Discussion

The gender-dependent difference during choline deprivation was that female *Pemt*$^{-/-}$ mice showed a one-day delay of liver damage compared to male *Pemt*$^{-/-}$ mice. In addition, the reduction of hepatic PC, biliary PC and hepatic PC/PE ratio were similarly delayed for one-day in female CD-*Pemt*$^{-/-}$ mice compared with those in male CD-*Pemt*$^{-/-}$ mice. Thus, liver in female CD-*Pemt*$^{-/-}$ mice must have an alternative pathway to maintain PC since there was no dietary choline available for PC biosynthesis. Interestingly, we found that plasma

PC level increased in female *Pemt*$^{-/-}$ mice during the first day of choline deprivation, apparently mainly derived from increased HDL-PC. Liver is the major organ for reverse cholesterol transport in which the uptake of HDL-PC by liver is an important route for liver to obtain PC from peripheral tissues (9). When we used an ABCA1 inhibitor, glybenclamide (7,8), to block PC efflux to HDL particles, the one-day delay of liver damage in female *Pemt*$^{-/-}$ mice was eliminated. Therefore, the conclusion is that female *Pemt*$^{-/-}$ mice have a capability for adaptation to acute choline deprivation for one day via mobilizing PC stored in peripheral tissues through the HDL-reverse cholesterol transport pathway. This mobilization of peripheral PC ensures that the level of hepatic total choline-containing metabolites or PC is maintained in female *Pemt*$^{-/-}$ mice for one day during choline deprivation. This acute response to choline deprivation may occur in any animals when they are facing choline deprivation. The tissues as sources of HDL-PC efflux can also be treated as tissues of choline storage for acute adaptation to choline deprivation.

The most striking data from this experiment were that male *Pemt*$^{-/-}$ mice showed ~7-fold higher plasma PC levels than female *Pemt*$^{-/-}$ mice after fed a CS diet for 24 h. The majority of plasma PC is associated with HDL (6). When Albers et al (10) screened 15 different strains of mice fed a chow diet; they found male mice showed 10-60% higher level of plasma phospholipid (mainly PC) and 10-110% higher level of HDL-phospholipid (mainly HDL-PC) than female mice. C57BL/6J male mice, which have similar background to *Pemt*$^{-/-}$ mice

(C57BL/6J/129J), had 30% higher plasma phospholipid and HDL-phospholipid than female mice (10). Noga et al (11) reported that when fed the chow diet, male *Pemt*$^{-/-}$ mice showed 1.5-fold higher plasma PC level than female *Pemt*$^{-/-}$ mice. These results are similar to what Albers et al reported for wild type mice (10). It would be intriguing to explore why the deficiency of PEMT could enhance the gender difference in plasma PC and HDL-PC levels in the future studies. Moreover, there are two differences between my experiments and Noga's, which might account for enhanced difference in plasma PC levels between male and female *Pemt*$^{-/-}$ mice from my studies compared to Noga's. One is the diet, a CS diet in my experiments instead of a chow diet in Noga's. The other is the fasting period, 12 h in my experiments but overnight fasting (assumedly ~16 h) in Noga's.

Our results suggest that the reason why female *Pemt*$^{-/-}$ mice showed a one-day delay in hepatic choline deficiency during choline deprivation as compared to male *Pemt*$^{-/-}$ mice was due to a different capability of HDL-PC efflux from peripheral tissues. Possibly female *Pemt*$^{-/-}$ mice survive at a lower level of plasma PC and HDL-PC efflux than do male *Pemt*$^{-/-}$ mice under choline-supplemented conditions. Once choline deprivation was initiated, HDL-PC efflux and plasma PC levels in male *Pemt*$^{-/-}$ mice may already be saturated so that can not be up-regulated. In contrast, female *Pemt*$^{-/-}$ mice might have sufficient capability to increase their HDL-PC efflux to maintain hepatic PC levels and PC/PE ratios in order to prevent liver damage, which is an adaptive response to choline deprivation. This acute adaptation might be dependent on the capability of HDL-PC efflux. However, this adaptation only lasted for one day, which was not surprising because mice were under complete choline deprivation (*Pemt*$^{-/-}$ plus CD diet). Hence, those peripheral tissues as sources of HDL-PC efflux were also under choline deprivation. Undoubtedly, the most intriguing question is which tissue provided their PC to liver via HDL-PC. However, we can not answer this question, since it is still unclear which tissue(s) is the major place of mature HDL formation as well as HDL uptake (12,13). A current model is that hepatic PC is originally loaded onto ApoAI to form preβ HDL particles and then preβ HDL is delivered to peripheral tissues to receive cholesterol and transport it back to liver for disposal, so called reverse cholesterol transport (9,14,15). However, cholesterol efflux mediated by ABCA1 in peripheral tissues coordinates indispensably with PC efflux (9,16). Thus, preβ HDL receives both cholesterol and PC to form mature HDL particles. ABCA1 is expressed ubiquitously in all tissues (17), so it is hard to identify which tissue is the major one for HDL formation or HDL-PC efflux.

Why is there a gender difference in the capability of HDL-PC efflux in *Pemt*$^{-/-}$ mice? Noga et al. reported a gender-dependent expression of CT and PEMT in mice by *in vitro* assays (18), however, we did not find any gender-dependent difference in CT and PEMT activities in our wild-type mice and/or *Pemt*$^{-/-}$ mice (Table 5.1). Although no articles have reported gender-dependent difference of PC homeostasis *in vivo*, I hypothesize that male *Pemt*$^{-/-}$ mice have a different PC homeostasis than female *Pemt*$^{-/-}$ mice. Thus, male *Pemt*$^{-/-}$ mice may have a higher requirement for HDL-PC to maintain hepatic PC homeostasis. Once choline was deprived, there might be no capability for male *Pemt*$^{-/-}$ mice to further increase HDL-PC efflux from peripheral tissues. But this does not indicate that male *Pemt*$^{-/-}$ mice did not respond to choline deprivation, since male *Pemt*$^{-/-}$ mice maintained their high HDL-PC levels in plasma during the first day of choline deprivation (Fig. 5.4), even though hepatic PC significantly decreased at that time (Fig. 5.2B). Therefore, both male and female *Pemt*$^{-/-}$ mice showed an adaptive response to choline deprivation by enhancing HDL-PC efflux. However, a higher demand of HDL-PC for hepatic PC homeostasis in male *Pemt*$^{-/-}$ mice made it infeasible for the adaptation. Whereas lower demand of HDL-PC for hepatic PC homeostasis in female *Pemt*$^{-/-}$ mice allowed them to up-regulate HDL-PC efflux to adapt to choline deprivation. Thus, gender-dependent differences in *Pemt*$^{-/-}$ mice during choline deprivation might actually be differential adaptations to PC homeostasis. In fact, during the evolution, there is pressure for female to be resistant to choline deficiency such as lactation. This selective pressure renders female to have better homeostatic control over choline (PC) metabolism. This gender-specificity in hepatic PC homeostasis is also an adaptation to choline from evolution.

Two potential mechanisms are believed to enhance HDL-PC efflux (9,14-16). One is that lipid-poor preβ HDL particles are able to receive more lipids from peripheral tissues (14,15). The other is that increased ABCA1 expression in peripheral tissues can enhance HDL-PC efflux (16). Our results showed that choline deprivation caused the formation of poorly-lipidated preβ HDL particles from both male and female *Pemt*$^{-/-}$ hepatocytes (Fig. 5.10). This may answer why male *Pemt*$^{-/-}$ mice maintained higher HDL-PC efflux for the first day during choline deprivation and female *Pemt*$^{-/-}$ mice were able to up-regulate their HDL-PC efflux at the first day of choline deprivation (Fig. 5.4). From choline redistribution experiments (Chapter 4), intestine and kidney might be possible candidates for increased HDL-PC efflux via increased expression of ABCA1.These tissues showed increased loss of choline from CS to CD situations, which needs to be further studied in the future.

Table 5.1 Hepatic CT and PEMT activities in wild type and *Pemt*$^{-/-}$ mice

CT, CTP:phosphocholine cytidylyltransferase; mCT, membrane-bounded CT; PEMT, phosphatidylethanolamine *N*-methyltransferase. Data = mean ± SD.

		Total CT Activity (nmol/min/mg)	mCT Activity (nmol/min/mg)	PEMT Activity (nmol/min/mg)
Wild Type	Female	3.27 ± 0.56	2.21 ± 0.23	1.09 ± 0.19
Wild Type	Male	3.09 ± 0.11	2.23 ± 0.35	0.94 ± 0.06
Pemt$^{-/-}$	Female	1.44 ± 0.02	1.46 ± 0.03	0
Pemt$^{-/-}$	Male	1.58 ± 0.38	1.49 ± 0.09	0

Fig. 5.1 Liver damage assays

Plasma samples were collected from *Pemt*$^{-/-}$ mice fed the choline-supplemented (CS) diet for 24 h (0 day) then transferred to the choline-deficient (CD) diet for 1 to 3 days. Plasma alanine and aspartate aminotransferase (ALT/AST) activities were measured at day 0, 1, 2 and 3 as indicators of liver damage. **(A)** plasma ALT activity; **(B)** plasma AST activity. *, $p < 0.01$, from comparison between CS and CD mice.

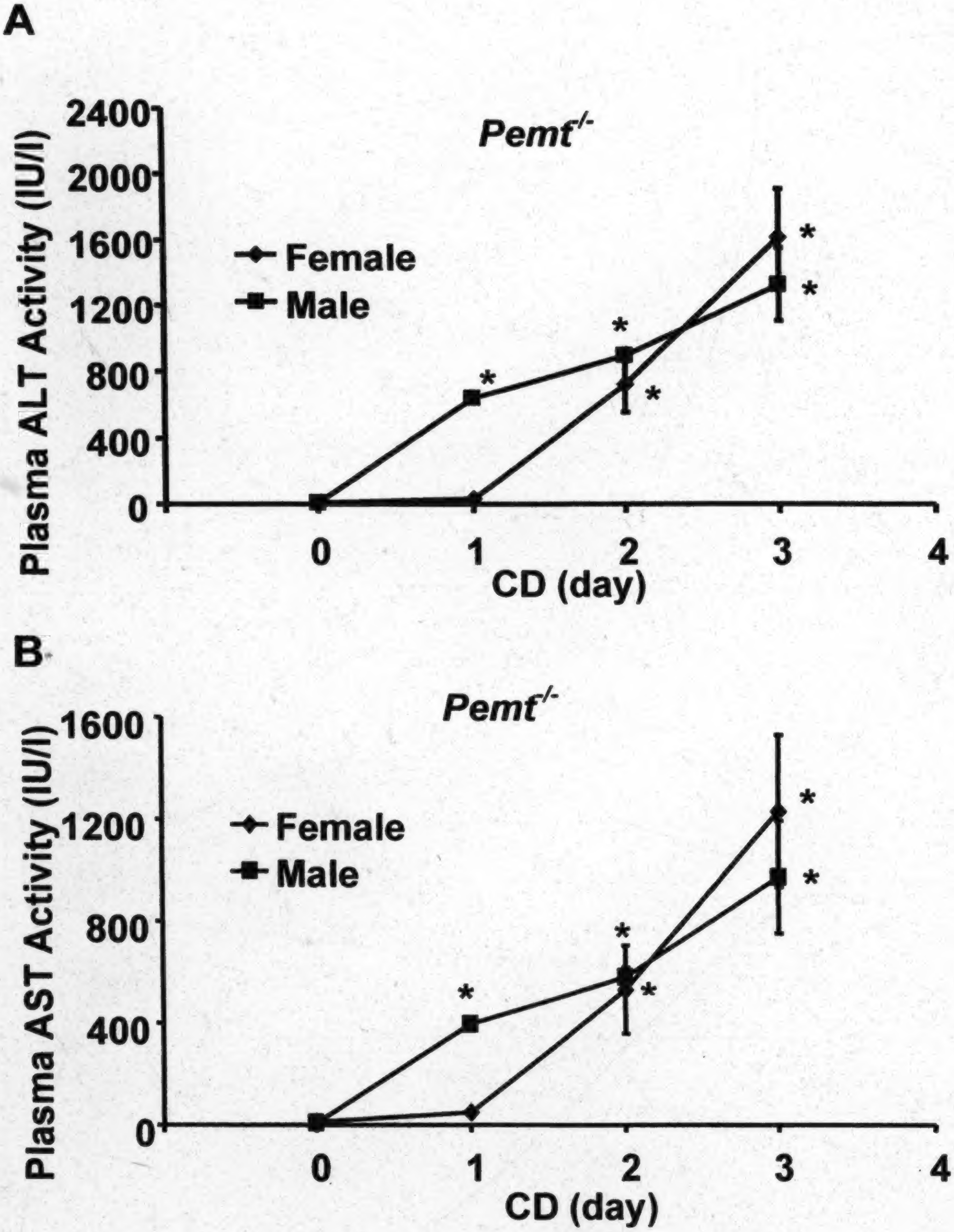
A
Pemt-/-
Plasma ALT Activity (IU/l)
2400
2000
1600
1200
800
400
0
Female
Male
*
*
*
*
*
0
1
2
3
4
CD (day)
B
Pemt-/-
Plasma AST Activity (IU/l)
1600
1200
800
400
0
Female
Male
*
*
*
*
*
0
1
2
3
4
CD (day)

Fig. 5.2 Hepatic phospholipid compositions

Pemt$^{-/-}$ mice were fed a choline-supplemented (CS) diet for 24 h and then switched to a choline-deficient (CD) diet for 1 to 3 days. **(A)** Molar ratio of PC to PE; **(B)** Levels of PC and PE in liver homogenates. *, $p < 0.05$.

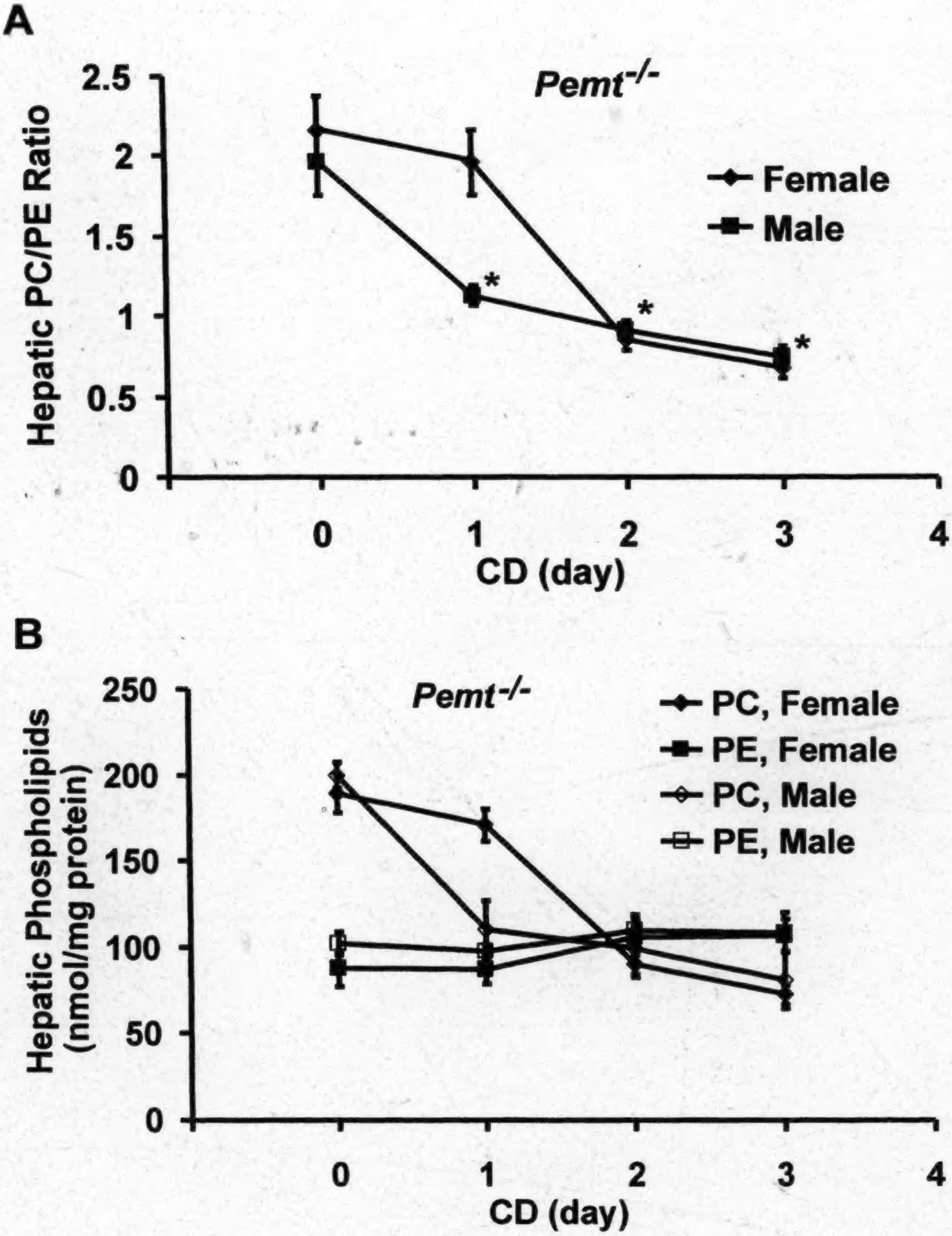
A
Pemt-/-
Hepatic PC/PE Ratio
2.5
2
1.5
1
0.5
0
0
1
2
3
4
CD (day)
Female
Male
*
*
*
B
Pemt-/-
Hepatic Phospholipids (nmol/mg protein)
250
200
150
100
50
0
0
1
2
3
4
CD (day)
PC, Female
PE, Female
PC, Male
PE, Male

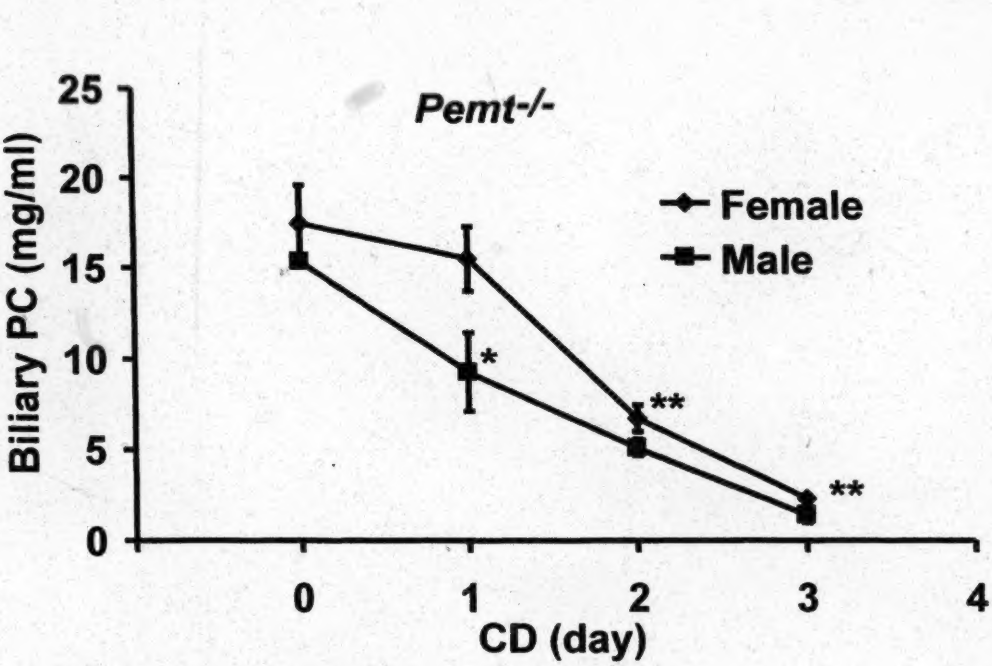

Fig. 5.3 The amount of biliary PC

Bile samples were collected from *Pemt*$^{-/-}$ mice fed the choline-supplemented (CS) diet for 24 h (0 day) then transferred to the choline-deficient (CD) diet for 1-3 days. Total lipids in bile were extracted with the Bligh & Dyer method and PC was separated and measured by HPLC as addressed in the Methods. *, $p < 0.05$; **, $p < 0.01$. P values from comparison between CS and CD mice.

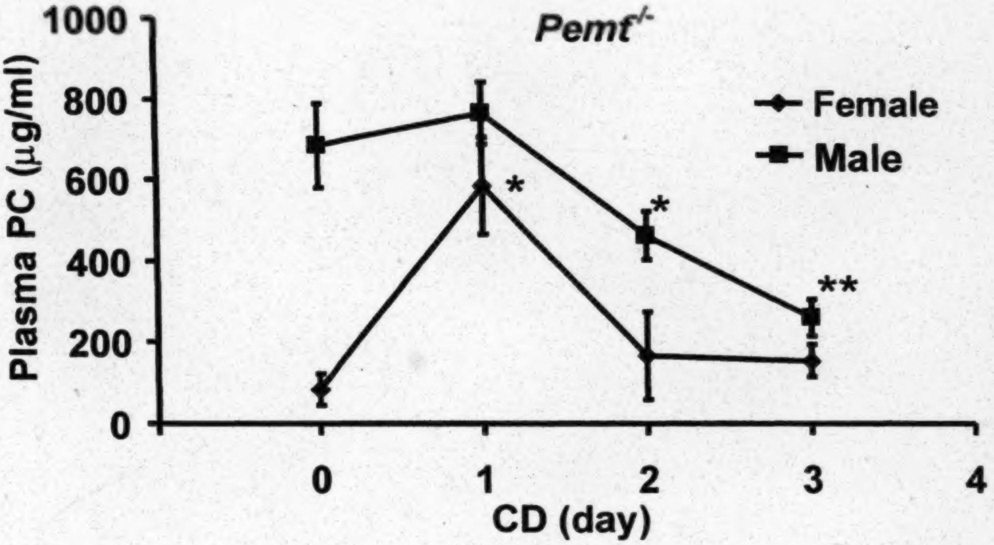

Fig. 5.4 The amount of plasma PC

Plasma samples were collected from *Pemt*$^{-/-}$ mice (n=4 for each gender) fed the choline-supplemented (CS) diet for 24 h (0 day) then transferred to the choline-deficient (CD) diet for 1 to 3 days. Total lipids in plasma were extracted with the Bligh & Dyer method and PC was separated and measured by HPLC as addressed in the Methods. *, $p<0.05$; **, $p<0.01$.

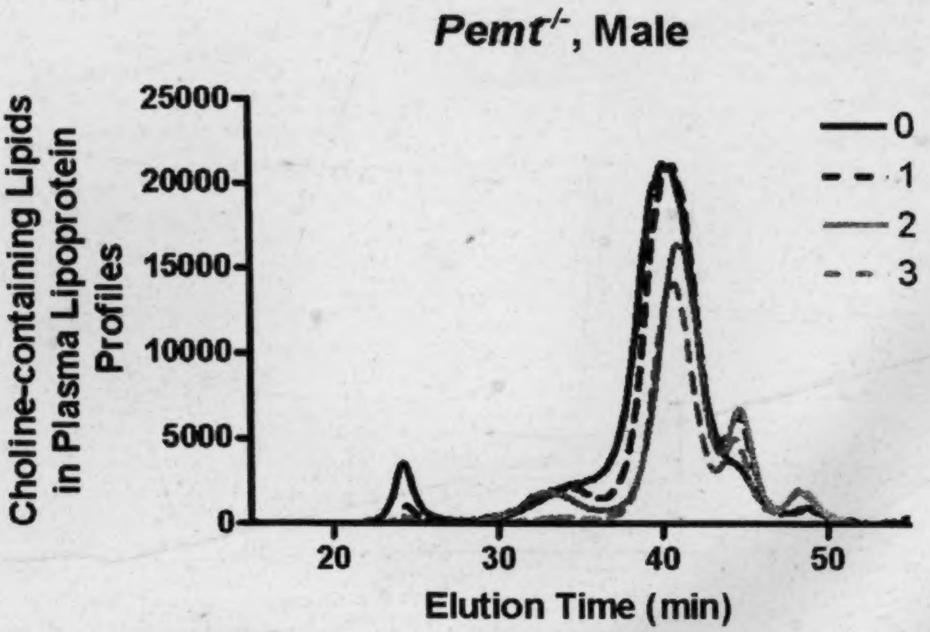

Fig. 5.5 Profiles of choline-containing lipids in plasma lipoproteins

Fresh plasma samples were applied with fast-phase liquid chromatography (FPLC) analysis for profiles of choline-containing lipids in lipoproteins. Plasma samples were collected from *Pemt*$^{-/-}$ mice fed the choline-supplemented (CS) diet for 24 h (0 day) then transferred to the choline-deficient (CD) diet for 1 to 3 days. Plasma was combined from at least three male *Pemt*$^{-/-}$ mice for each sample.

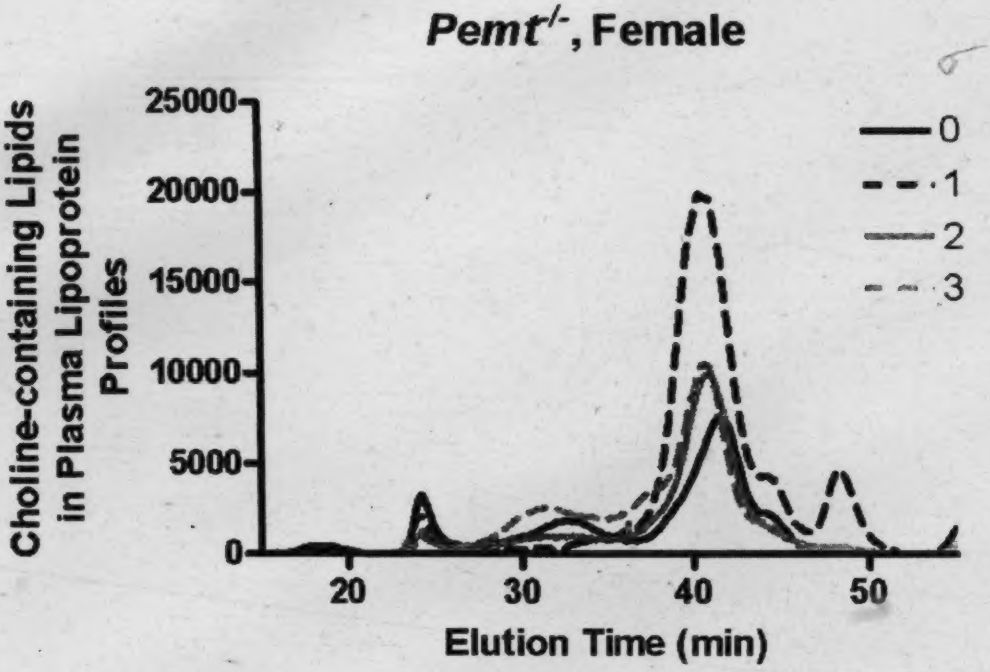

Fig. 5.6 Profiles of choline-containing lipids in plasma lipoproteins

Fresh plasma samples were applied with fast-phase liquid chromatography (FPLC) analysis for profiles of choline-containing lipids in lipoproteins. Plasma samples were collected from *Pemt*$^{-/-}$ mice fed the choline-supplemented (CS) diet for 24 h (0 day) then transferred to the choline-deficient (CD) diet for 1 to 3 days. Plasma combined from at least three female *Pemt*$^{-/-}$ mice was used for each sample.

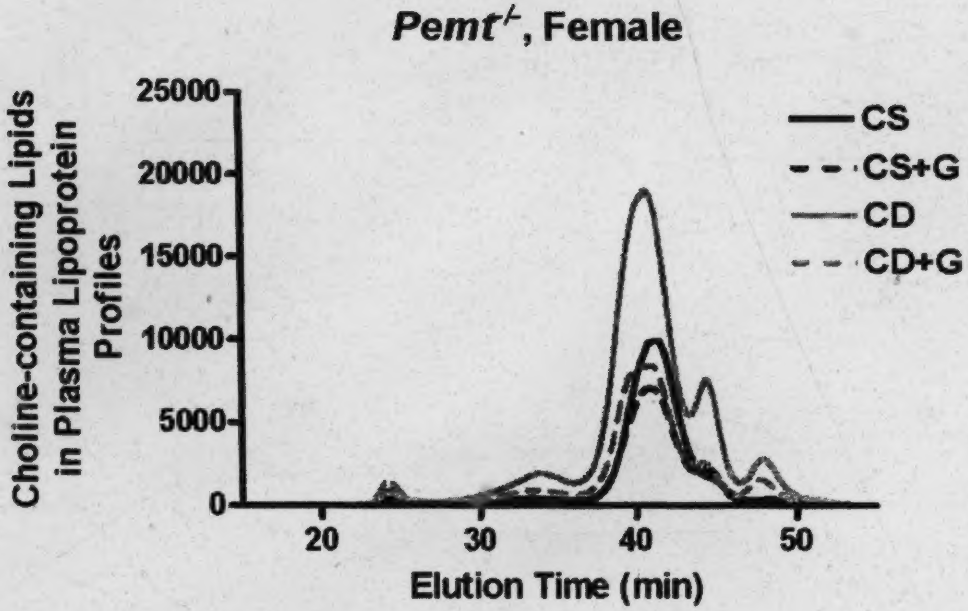

Fig. 5.7 Profiles of choline-containing lipids in plasma lipoproteins after glybenclamide treatment

Female *Pemt*$^{-/-}$ mice were fed a choline-supplemented (CS) diet containing glybenclamide of 163 μg/g body weight for one day (CS+G) and then changed to a choline-deficient (CD) diet containing glybenclamide of 163 μg/g body weight for one day (CD+G). Female *Pemt*$^{-/-}$ mice were fed a CS or CD diet without glybenclamide for one day as controls (CS and CD). Fresh plasma samples were applied for fast-phase liquid chromatography (FPLC) analysis profiles of choline-containing lipids in lipoproteins. Plasma combined from at least three female *Pemt*$^{-/-}$ mice was used for each FPLC analysis.

Fig. 5.8 Hepatic phospholipid compositions after glybenclamide treatment

Female *Pemt*$^{-/-}$ mice were fed a choline-supplemented (CS) diet containing glybenclamide of 163 μg/g body weight for one day (CS1) and then changed to a choline-deficient (CD) diet containaing glybenclamide of 163 μg/g body weight for one day (CD1). Female *Pemt*$^{-/-}$ mice were fed a CS or CD diet without glybenclamide as controls. **(A)** Levels of PC and PE in liver homogenates; **(B)** Molar ratio of PC to PE. *, $P < 0.05$; **, $P < 0.001$ comparing CS to CD groups.

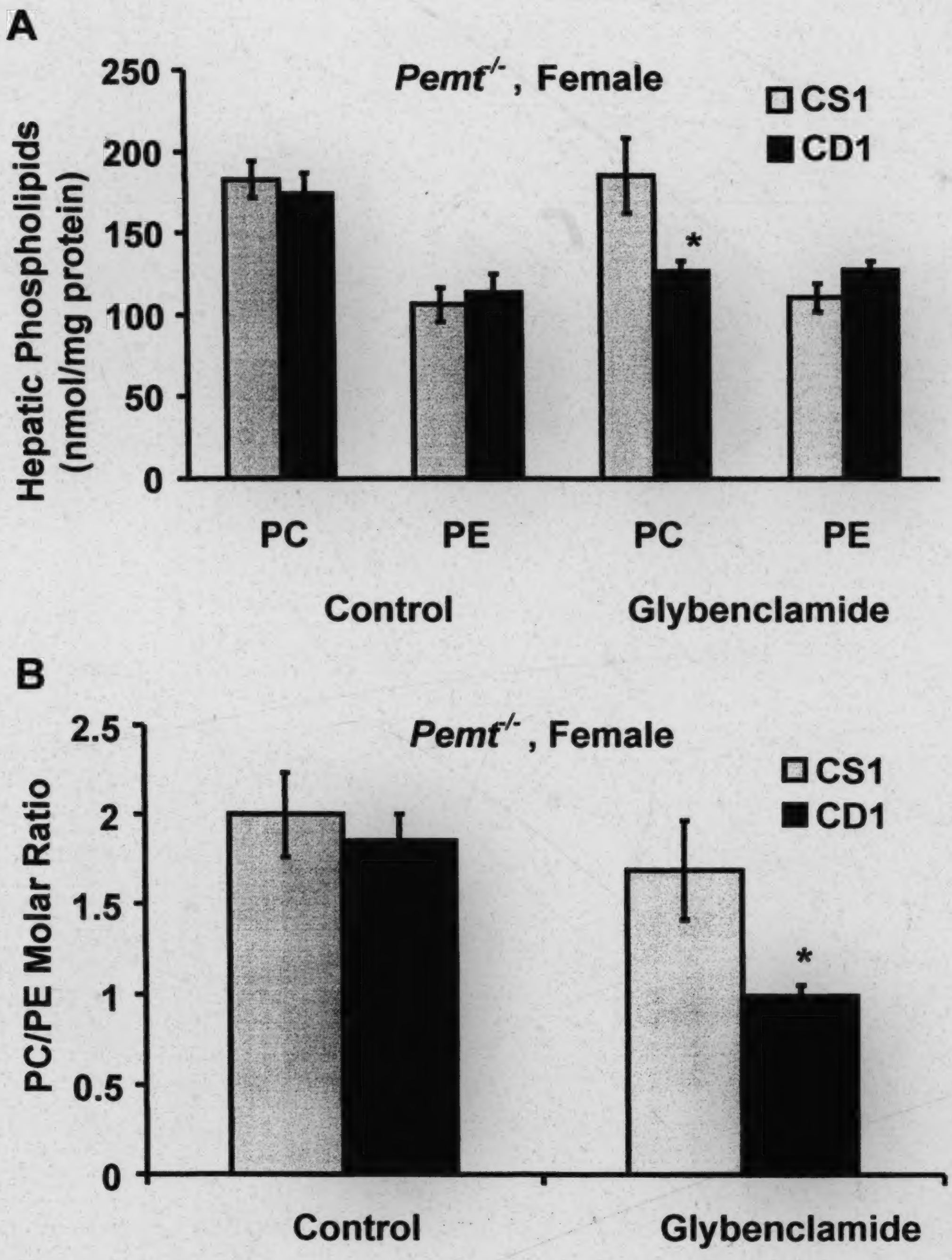
A
Pemt-/- , Female
Hepatic Phospholipids (nmol/mg protein)
250
200
150
100
50
0
□ CS1
■ CD1
*
PC
PE
PC
PE
Control
Glybenclamide
B
Pemt-/- , Female
PC/PE Molar Ratio
2.5
2
1.5
1
0.5
0
□ CS1
■ CD1
*
Control
Glybenclamide

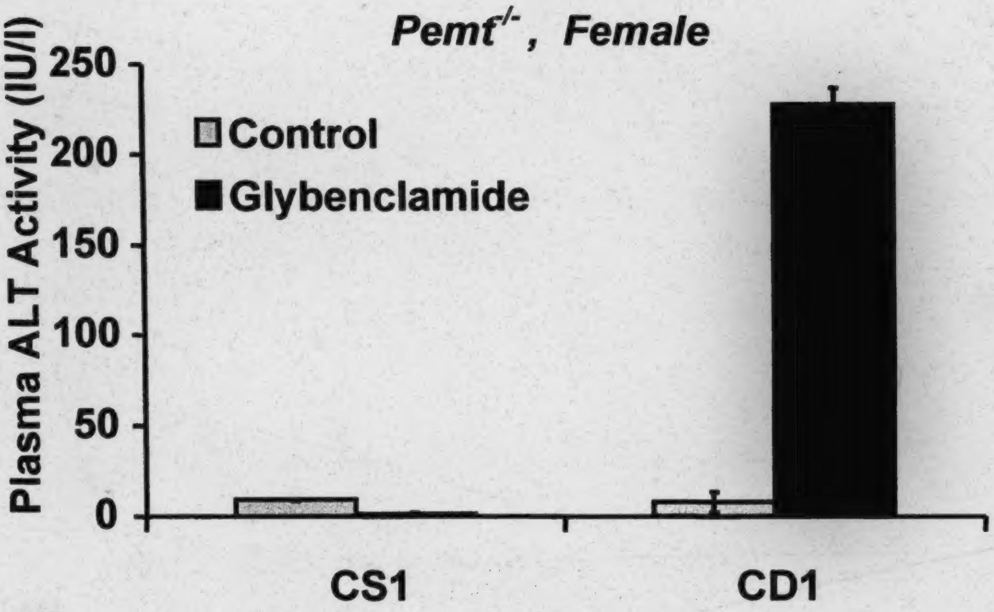

Fig. 5.9 Liver damage assays after glybenclamide treatment

Female *Pemt*$^{-/-}$ mice were fed a choline-supplemented (CS) diet containing glybenclamide of 163 μg/g diet for one day (CS1) and then changed to a choline-deficient (CD) diet containing glybenclamide of 163 μg/g diet for one day (CD1). Female *Pemt*$^{-/-}$ mice were fed a CS or CD diet without glybenclamide as controls. Plasma alanine aminotransferase (ALT) activities were measured as indicators of liver damage.

Fig. 5.10 HDL and ApoAI secretion from primary cultured hepatocytes

Male and female *Pemt*$^{-/-}$ mice were fed the CS diet for one day and then switched to the CD diet for one day. Primary hepatocytes isolated from mice as decribed in **2.2.4** were cultured in a CS or CD medium. After plating for 2 h, hepatocytes were changed to fresh medium without serum for 1 h. After that, hepatocytes were chased in a fresh medium for 2 h. Medium was collected for analysis of high density lipoprotein (HDL) particles. Medium was concentrated through a centrifugation filter with pore size of 5,000 kD. **(A)** HDL and preβ HDL particles in the medium were separated by 6% non-denatured PAGE for Western blotting with an anti-ApoAI antibody (*Chemicon*); **(B)** Total ApoAI in the medium was separated by a 12% SDS-PAGE and identified by Western blotting.

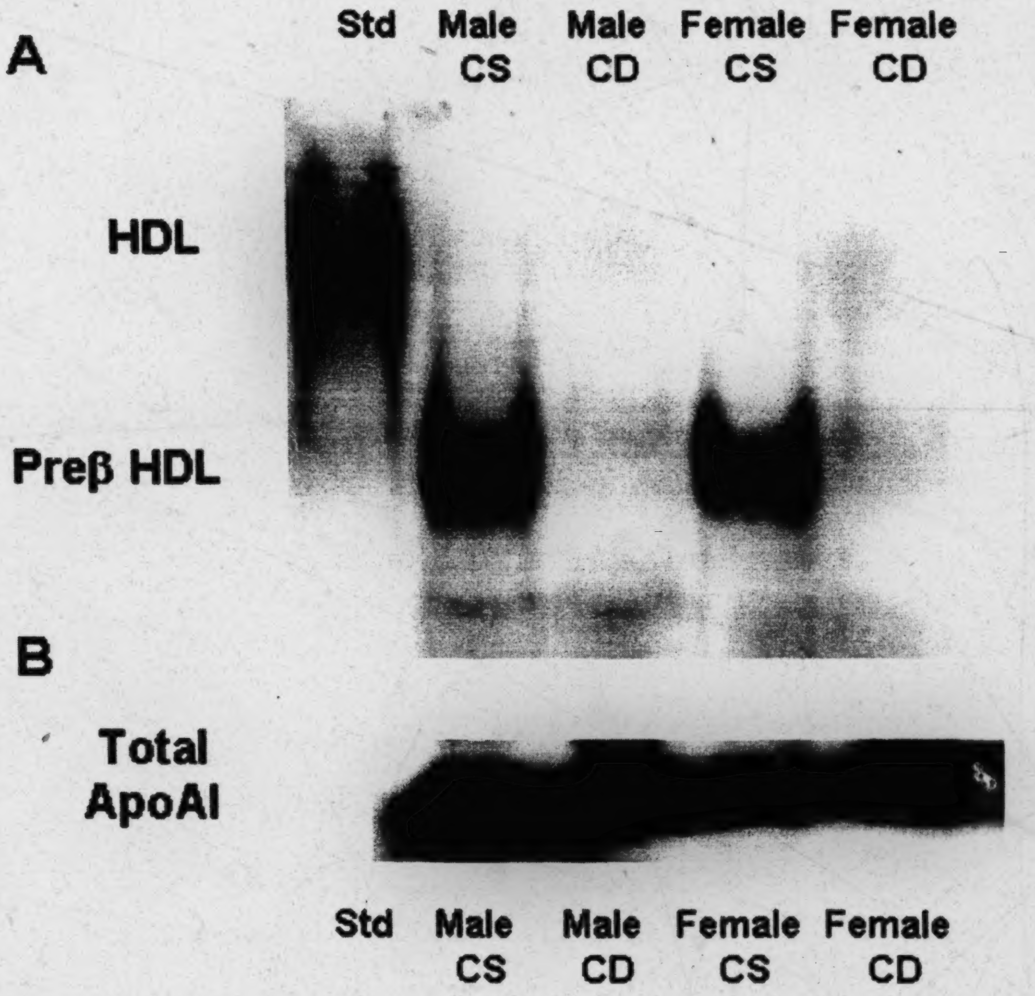
A
Std
Male CS
Male CD
Female CS
Female CD
HDL
Preβ HDL
B
Total ApoAI
Std
Male CS
Male CD
Female CS
Female CD

Fig. 5.11 The amount of PC associated with ApoAI

Male and female *Pemt*$^{-/-}$ mice were fed the CS diet for one day and then switched to the CD diet for one day. Primary hepatocytes isolated from mice as described in 2.2.4 were cultured in a CS or CD medium. After plating for 2 h, hepatocytes were changed to fresh medium without serum for 1 h. After that, hepatocytes were chased in a fresh medium for 2 h. Medium was concentrated through a centrifugation filter with pore size of 5,000 kD. Sandwich ELISA was used for analyzing the amount of PC associated with ApoAI proteins. A 96-well plate was pre-incubated with anti-ApoAI antibody for 24 h at 4°C as a catching antibody. After incubation with concentrated medium, anti-PC antibody was used for measuring the amount of PC associated with ApoAI in conjunction with a secondary antibody-conjugated with FITC. Fluorescent intensity was measured with a fluorimeter. *, $p<0.05$; **, $p<0.01$.

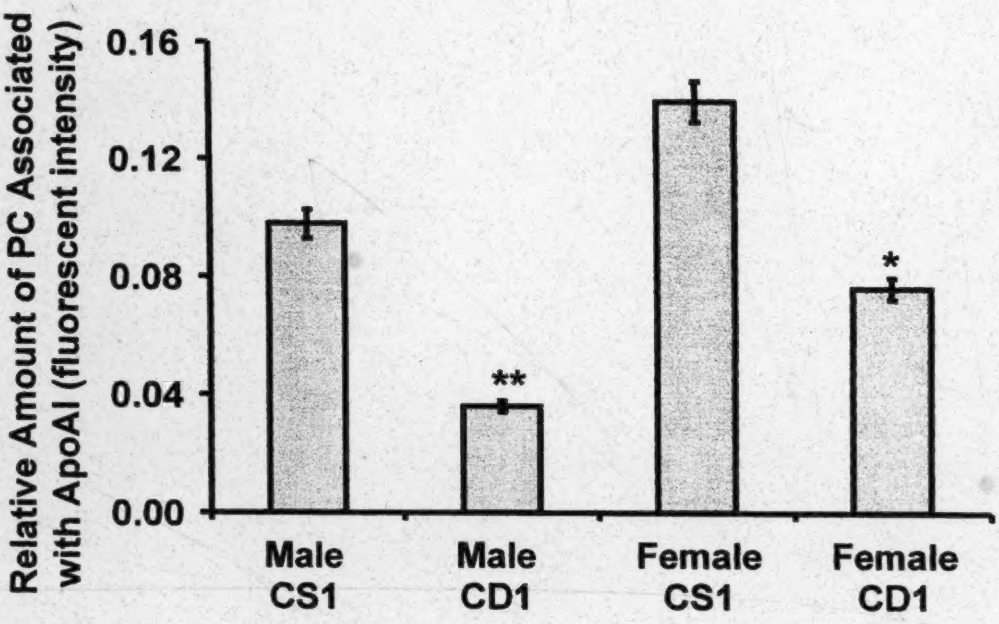
Relative Amount of PC Associated with ApoAI (fluorescent intensity)
0.16
0.12
0.08
0.04
0.00
**
*
Male CS1
Male CD1
Female CS1
Female CD1

14. Liang, H. Q., Rye, K. A., and Barter, P. J. Cycling of apolipoprotein A-I between lipid-associated and lipid-free pools. (1995) *Biochim Biophys Acta* **1257**, 31-37

15. Rye, K. A., and Barter, P. J. Formation and metabolism of prebeta-migrating, lipid-poor apolipoprotein A-I. (2004) *Arterioscler Thromb Vasc Biol* **24**, 421-428

16. Oram, J. F. HDL apolipoproteins and ABCA1: partners in the removal of excess cellular cholesterol. (2003) *Arterioscler Thromb Vasc Biol* **23**, 720-727

17. Wellington, C. L., Walker, E. K., Suarez, A., Kwok, A., Bissada, N., Singaraja, R., Yang, Y. Z., Zhang, L. H., James, E., Wilson, J. E., Francone, O., McManus, B. M., and Hayden, M. R. ABCA1 mRNA and protein distribution patterns predict multiple different roles and levels of regulation. (2002) *Lab Invest* **82**, 273-283

18. Noga, A. A., and Vance, D. E. Insights into the requirement of phosphatidylcholine synthesis for liver function in mice. (2003) *J Lipid Res* **44**, 1998-2005

Chapter 6

Choline Balance Theory

--- Summary

6.1 Choline balance and imbalance

Every metabolite has its own balance. However, the balance for each metabolite has not been elucidated. At first, we must define metabolite balance. The simplest defination is that input equals output. This is a quantitative formula, which means both input and output should have the same value. When a value for balance is zero, this indicates no input and no output. Our preliminary work initiated from this special condition, no input and no output of choline.

Choline concentration in the body is balanced by two choline acquisition pathways: dietary choline intake and the PEMT pathway, and by two choline depletion pathways: choline oxidation and biliary PC excretion (Fig. 1.2). Choline balance can be interrupted in two ways, choline deprivation or choline excess, together called choline imbalance.

6.2 Classical adaptations to choline imbalance

To maintain choline balance and adapt to choline imbalance, the metabolic regulation should be existed on the choline acquisition pathways (dietary choline intake and the PEMT pathway) and depletion pathways (biliary excretion of PC and choline oxidation). Activation of processes regulating choline balance may also be dependent on different situations.

6.2.1 Dietary choline intake

The absorption of dietary choline is mediated by choline transporters and also via uptake of lysophosphatidylcholine (lysoPC) in the intestine (1). Choline uptake was not dependent on a choline transporter during choline deprivation, since the expression of choline transporter did not increase significantly in either liver or brain during choline deprivation (Fig. 4.3). Since biliary PC accounts for > 90% of total choline uptake (biliary PC + dietary choline) (2), *Abcb4*$^{-/-}$ mice might have increased uptake of dietary choline. But, PLA_2 activity was down-regulated in *Abcb4*$^{-/-}$ background suggesting that the consumption of PC might also be down-regulated (Fig. 2.6). Therefore, the uptake of dietary choline may not change in *Abcb4*$^{-/-}$ mice. CS-*Pemt*$^{-/-}$ mice survived normally with increased PC biosynthesis through the CDP-choline pathway and maintaining the same hepatic PC levels as compared to wild-type mice (3). CS-*Pemt*$^{-/-}$ mice might have increased uptake of dietary choline since endogenous choline biosynthesis is deficient.

6.2.2 The PEMT pathway

As the only endogenous pathway of choline biosynthesis, the PEMT pathway was up-regulated during choline deprivation in several models of choline deprivation, including animals fed a CD diet and *CT*$^{-/-}$ mice (4-7). In addition, regarding PC biosynthesis, choline deprivation also up-regulated the CDP-choline pathway in a feedback way (Fig. 2.9, 2.10) (4,5,8,9). However, due to lack of initial substrate, choline, up-regulation of CT was not able to increase hepatic PC levels (Fig. 2.4) (10). Our studies suggest that the reason CT has this "idle" up-regulation might be related to increased PC turnover during choline deprivation (Chapter 2).

6.2.3 Biliary PC excretion

Biliary PC secretion leads to ~ 5% of biliary PC lost from excretion in each enterohepatic circulation. Decreased biliary PC secretion in mice fed the CD diet indicated that the choline depletion pathway via bile secretion was down-regulated during choline deprivation (Fig. 2.5) (11). Although biliary PC secretion was down-regulated (Fig. 2.5, Fig. 5.3), there was still a considerable amount of choline lost from excretion. When female *Pemt*$^{-/-}$ mice were fed a CD diet for one day, although hepatic PC levels did not decline significantly, biliary PC secretion was maintained at the same level as that in CS-*Pemt*$^{-/-}$ mice (Chapter 5). Thus, regulation of biliary PC secretion seemed not to be successful during choline deprivation. That is why CD-*Pemt*$^{-/-}$ mice died so rapidly (Chapter 2).

6.2.4 Choline oxidation

Choline oxidation in the liver was almost completely shutdown during choline deprivation in both CD-*Abcb4*$^{-/-}$/*Pemt*$^{-/-}$ mice and CD- *Pemt*$^{-/-}$ mice (Fig.

2.7). Down-regulation of choline oxidation also occurred in wild-type rats fed a CD diet (12). Thus, organisms adapt to choline deprivation by blocking the choline depletion pathway from choline oxidation to prevent the loss of choline.

6.3 New findings of adaptation to choline deprivation

However, adaptation to choline deprivation is not only restricted to the modulation of a single choline acquisition or depletion pathway. Coordinative modulation of all choline acquisition and depletion pathways and/or other metabolic pathway such as PE metabolism was hypothesized to play a critical role in adaptation to choline deprivation. By comparing two mouse models, CD-*Abcb4*$^{-/-}$/*Pemt*$^{-/-}$ mice and CD- *Pemt*$^{-/-}$ mice, we found that adaptation to choline deprivation also included choline recycling, maintenance of membrane integrity via maintenance of PC/PE ratio, choline redistribution and choline storage (Chapter 2, 3, 4 and 5).

6.3.1 Choline recycling

Chapter 2 clearly demonstrates that the maintenance of total choline level is critical for life. To achieve this, mice have to recycle choline in adaptation to choline deprivation. The adaptations facilitate the survival of CD-*Abcb4*$^{-/-}$/*Pemt*$^{-/-}$ mice. By eliminating the loss of PC into bile, these mice are able to implement significant changes in PC and choline metabolism. Notably, the oxidation of choline to betaine is markedly curtailed and choline kinase and CT activities are increased to ensure re-utilization of choline for PC biosynthesis, so called choline recycling. To guarantee choline recycling, PLA$_2$ activity and PC catabolism are increased to ensure an ample supply of choline channeled for PC biosynthesis. The conversion of choline into PC via choline recycling generates a large reserve pool of newly synthesized PC that is readily accessible at times of high demand. Meanwhile, enhanced choline recycling, therefore, allows more efficient utilization of choline when PC levels drop to 50% during choline deprivation (Chapter 2).

6.3.2 Maintenance of membrane integrity via maintenance of PC/PE ratio

Chapter 3 illustrates that adaptation to choline deprivation is also involved in modulating other metabolic pathways besides choline metabolism, such as PE metabolism. Although hepatic PC levels decreased to a similar degree in both CD3-*Pemt*$^{-/-}$ mice and CD21-*Abcb4*$^{-/-}$/*Pemt*$^{-/-}$ mice, gradual loss of hepatic PC in CD21-*Abcb4*$^{-/-}$/*Pemt*$^{-/-}$ mice compared to acute loss in CD3-*Pemt*$^{-/-}$ mice allowed mice to modulate PE metabolism. In fact, differential PC removal pathways determined different PE metabolism in two mouse models, since acute loss of hepatic PC in CD-*Pemt*$^{-/-}$ mice was mainly from biliary secretion whereas gradual loss of hepatic PC in CD-*Abcb4*$^{-/-}$/*Pemt*$^{-/-}$ mice from PC catabolism. By comparing two models of liver failure-resistant (CD-*Abcb4*$^{-/-}$/*Pemt*$^{-/-}$ mice) and -un-resistant mice (CD-*Pemt*$^{-/-}$ mice), and manipulating PC/PE ratios either *in vitro* or *in vivo*, hepatic PC/PE ratio was identified as a key regulator of membrane integrity. Thus, another adaptation to choline deprivation in CD-*Abcb4*$^{-/-}$/*Pemt*$^{-/-}$ mice is the maintenance of membrane integrity via the maintenance of a normal PC/PE ratio to escape liver failure. This adaptation was also displayed in wild-type mice fed the CD diet (Chapter 3). In addition, when the hepatic PC/PE ratio decreases, steatosis can be converted into steatohepatitis (Chapter 3).

6.3.3 Choline redistribution

In CD-*Abcb4*$^{-/-}$/*Pemt*$^{-/-}$ mice, there are two ways of maintaining brain and hepatic levels of total choline-containing metabolites for at least 3 months: choline recycling choline redistribution. Both brain and liver still maintained some activities of choline oxidase (Fig. 2.7, 4.2) but did not show significant change in the level of total choline-containing metabolites after 21 days in CD-*Abcb4*$^{-/-}$/*Pemt*$^{-/-}$ mice (Fig. 2.4, Fig. 4.1). These data indicated that brain and liver must have acquired an external supply of choline from other tissues. By injection of [^{3}H]choline into mice, choline redistribution in different tissues during choline deprivation was found not only in CD-*Abcb4*$^{-/-}$/*Pemt*$^{-/-}$ mice, but also in CD-*Pemt*$^{-/-}$ mice. Thus, when animals face the stress of choline deprivation, a fine regulatory mechanism is triggered to protect some important organs (such as brain and liver) from choline deprivation and other organs (such as muscle and/or intestine) may sacrifice their choline levels to maintain the choline level in the brain and liver, so called choline redistribution (Chapter 4). This may exist in all animals during choline deprivation.

6.3.4 Choline storage

Choline is stored as a component of phosphatidylcholine (PC) in the membrane since PC accounts for > 95% of total choline-containing metabolites. Both male and female *Pemt*$^{-/-}$ mice showed adaptive response to choline deprivation through mobilization of choline stored in extrahepatic tissues, which was achieved by enhancing the efflux of high density lipoprotein-PC (HDL-PC). However, gender-specific requirement of HDL-PC by liver might determine gender-different adaptations to choline deprivation in CD-*Pemt*$^{-/-}$ mice. This acute adaptation to choline deprivation is named as choline storage. I shall refer to this adaptation as choline storage. Choline storage was dependent on the capability of HDL-PC efflux. And choline stored in extrahepatic tissues was minimal and only able to compensate for the loss of hepatic choline for one day during choline deprivation. Although failed to adapt to choline deprivation, CD-*Pemt*$^{-/-}$ mice also showed adaptive response to mobilize extrahepatic PC to liver (Chapter 5).

6.4 Choline is an essential nutrient

Choline is an important nutrient in the diet of animals (13-18). Nevertheless, choline deprivation is not lethal in rodents and humans so it has never been clear that choline is essential for mammalian life despite claims that choline is an essential nutrient (15,18). Development of the CD-*Abcb4*$^{-/-}$/*Pemt*$^{-/-}$ mouse model enabled us to demonstrate that choline is an essential nutrient. A minimum threshold of total choline-containing metabolites in the liver required for survival appears to be ~110 nmol/mg protein (Fig. 2.4A). The level of total choline-containing compounds in *Pemt*$^{-/-}$ mice fed a CD diet for 3 days fell below this baseline. Thus, the CD-*Pemt*$^{-/-}$ mice faced a severe choline deficiency whereas the CD-*Abcb4*$^{-/-}$/*Pemt*$^{-/-}$ mice were able to establish a new choline homeostasis, thereby conserving sufficient amounts of choline metabolites for viability (Fig. 2.12A, B). After 3 days of the CD diet a turning point between life and death was reached in both mouse models. This threshold was critically dependent on the phosphocholine levels but not other choline-containing metabolites (Fig. 2.12A, B). Increased phosphocholine levels guaranteed PC biosynthesis and thereby survival of CD-*Abcb4*$^{-/-}$/*Pemt*$^{-/-}$ mice whereas decreased phosphocholine levels led to the death of CD-*Pemt*$^{-/-}$ mice. The data from these experiments provide unambiguous evidence that choline is an essential nutrient in animals.

6.5 Choline balance theory

The outcome of this thesis is the conception of the "choline balance theory" for explaining the importance of choline metabolism and illustrating the physiological significance of adaptation to choline deprivation.

The "choline balance theory" states that: There is a balance between gain and loss of choline that determines the survival of choline-containing organisms. Life of these organisms is critically dependent on the maintenance of total choline level. The ratio of PC to PE, choline recycling, choline redistribution and storage, as well as choline acquisition and depletion pathways might be adjusted in adaptations to choline imbalance (Fig. 6.1).

Mice could only survive under the conditions of either existence of both input and output of choline (wild-type mice, CS-*Pemt*$^{-/-}$ mice) or of no input and no output of choline (CD-*Pemt*$^{-/-}$/*Abcb4*$^{-/-}$ mice), but not under the conditions of either only input and no output of choline (*Abcb4*$^{-/-}$ mice) or no input and only output of choline (CD-*Pemt*$^{-/-}$ mice). Once choline balance is altered, either liver failure will be induced or cholestasis will develop, which will be lethal sooner or later (Table 6.1).

When choline balance is altered, mice attempted to reach a new balance. For example, when both *Pemt*$^{-/-}$/*Abcb4*$^{-/-}$ mice and *Pemt*$^{-/-}$ mice were fed a CD diet, there was no choline input at all. At this time, both of them minimized their output of choline via decreasing choline oxidation. When PC was still being secreted in bile, a lethal imbalance occurred in CD-*Pemt*$^{-/-}$ mice. However, when biliary PC secretion was eliminated (*Abcb4*$^{-/-}$), a new balance was reached in CD-*Pemt*$^{-/-}$/*Abcb4*$^{-/-}$ mice. When a new choline balance was achieved, mice survived.

In CD-*Pemt*$^{-/-}$/*Abcb4*$^{-/-}$ mice, this new choline balance was very special, since there was neither choline input nor choline output. Choline recycling played a critical role in this case. Therefore, balance does not only mean n = n (n ≠ 0), but also means 0 = 0, which may be critical for life.

Different means of adaptations to choline imbalance can restore choline homeostasis in different ways. However, from our results, we found that the selection of different adaptations for mice during choline deprivation is strain-dependent and gender-dependent and might be controlled by some unknown regulators. As well, mice displayed different degrees of adaptation to choline deprivation probably due to different situations of choline imbalance. So, the adaptations are not always able to overcome choline imbalance. However, the adaptation could delay the pathogenesis as it took ~ 35 weeks for *Abcb4*$^{-/-}$ mice to develop cholestasis (19,20). Therefore, choline balance is vital but not unique in determining survival status of organisms.

The establishment of the "choline balance theory" not only illustrates the basic mechanism of choline metabolism and provide new principles for underlying physiological significance of adaptation to choline deficiency, but will also provide significant guides for clinical applications in liver pathology and in choline nutrition.

6.6 Future studies

6.6.1 Adaptation to choline excess

Unlike choline deprivation, choline excess is rarely reported (http://www.fda.gov or http://www.nutrition.org/nutinfo/content/choline.shtml). Even though biliary PC secretion was blocked (*Abcb4*$^{-/-}$), hepatic PC levels did not show a significant increase (21). However, we are not able to exclude the possibility that choline excess affects PC turnover rather than the static PC levels in liver. *Abcb4*$^{-/-}$ mice showed an increase in VLDL secretion and less hepatic TG when PC was no longer secreted into bile compared with wild-type mice which might account for no change of hepatic PC level (21). In addition, elimination of biliary PC secretion caused a secondary effect, cholestasis, in humans called progressive familial intrahepatic cholestasis type 3 (PFIC3) (19,20). Interestingly, we found that both exogenous and endogenous choline deprivation attenuated liver damage in *Abcb4*$^{-/-}$ mice. *Abcb4*$^{-/-}$/*Pemt*$^{-/-}$ mice (without endogenous biosynthesis of choline) developed less liver damage as compared with severe liver damage from *Abcb4*$^{-/-}$ mice at age of 7 months (time required for developing a definite cholestasis) (Fig. 6.2). In addition, the CD diet also attenuated liver damage in *Abcb4*$^{-/-}$ mice with cholestasis (Fig. 6.2). Advantages of choline deprivation in this particular situation suggest that choline deprivation is not only detrimental but can also be beneficial under certain circumstances. The mechanism of choline deprivation attenuating cholestasis would be interesting to explore in the future studies. Choline oxidation was down-regulated during choline deprivation, but did not change during choline excess based on a comparison between CS-*Pemt*$^{-/-}$/*Abcb4*$^{-/-}$ mice and CS-*Pemt*$^{-/-}$ mice (Fig. 2.7). Thus, down-regulation of choline uptake rather than up-regulation of choline oxidation may account for slow pathogenesis in CS-*Abcb4*$^{-/-}$ mice.

Excess choline intake is toxic for human (http://www.fda.gov or http://www.nutrition.org/nutinfo/content/choline.shtml). The tolerable upper intake level for choline from dietary sources and supplements combined is 3.5 grams per day. Symptoms of choline toxicity include: fishy body odor, vomiting, increased salivation, increased sweating and hypotensive effect (low blood pressure). However, it would still be intriguing to explore whether or not choline excess is involved in pathogenesis under physiological conditions.

6.6.2 Choline replacement

Whether or not choline can be replaced by other compounds has always been an intriguing question in the field of choline research. Recently, it was reported that in yeast the functions of PC and *N*-methylated lipids in membranes could be replaced by phosphatidylpropanolamine (22). However, we found that in *Pemt*$^{-/-}$ mice choline could not be replaced by either methionine or a series of propanolamine derivatives including 1,2-, 2,1- and 1,3-propanolamine. The experiments were performed with CD-*Pemt*$^{-/-}$ mice (the unique model of complete choline deprivation). No CD-*Pemt*$^{-/-}$ mice could survive for more than 5 days when their diets were supplemented with 0.4% methionine or 0.4%

propanolamine derivatives. At the third day of dietary treatment, hepatic PC levels were decreased as found in CD-*Pemt*$^{-/-}$ mice (Fig. 6.3A). Severe liver damage and fatty liver were also found in these mice (Fig. 6.3B, C). Thus, choline is essential for animals. Since propanolamine is not found normally, perhaps choline is essential in yeast also. In the future studies, broad exploring of the substitute compound of choline might be beneficial in choline nutrition and therapeutics.

6.6.3 Generality of newly found adaptations to choline deprivation

Choline recycling, maintenance of membrane integrity via maintenance of PC/PE ratio, choline redistribution and storage were found to be adaptations to choline deprivation from the unique model, CD-*Abcb4*$^{-/-}$/*Pemt*$^{-/-}$ mice. Whether or not these adaptations exist in other situations, or what degree is the adaptation if it exists, would be worthwhile to explore in the future studies. Choline recycling probably exists in other situations of choline deprivation, since the only catabolic pathway of choline, choline oxidation was also down-regulated in rats fed the CD diet (12). The maintenance of PC/PE ratio was not only adapted in CD-*Abcb4*$^{-/-}$/*Pemt*$^{-/-}$ mice but also in CD-wild type mice. Beyond adaptations to choline derpivation, analysis of PC and PE compositions in other cell types besides hepatocytes would lead to answer whether or not the PC/PE ratio determines membrane integrity in general. Since both CD-*Abcb4*$^{-/-}$/*Pemt*$^{-/-}$ mice and CD-*Pemt*$^{-/-}$ mice showed choline redistribution during choline deprivation, I would believe that choline redistribution may exist in all animals during choline deprivation.

6.6.4 Regulation of adaptation to choline deprivation

Adaptation to choline deprivation was achieved by choline recycling, maintenance of membrane integrity via maintenance of PC/PE ratio, choline redistribution and choline storage in addition to those classical adaptations. However, regulatory mechanisms behind these adaptations are still unclear. A promising candidate is c-Jun-involved cell signaling (Chapter 2). In addition, phosphocholine and/or glycerophosphocholine (GPC) may also be key regulators during adaptation to choline deprivation, since certain studies suggest that phosphocholine and/or GPC might be involved in regulatory mechanisms via initiating cell signaling (23). Moreover, the maintenance of the relative phosphocholine level is probably an important issue to be further addressed in the future. Phospholipid-related signaling could also be candidates to be further explored in our models, such as phospholipase D (24), lysoPC (25), protein kinase C (26), phosphoinositol-3-phosphate kinase related signaling (27) and phospholipid-involved nuclear events (28).

Table 6.1 Choline Balance Theory

Choline Input	Choline Output	Mouse Models	Phenotype
++	++	WT + CS/CD	Survival
++	++	*Pemt*$^{-/-}$ + CS	Survival
++	±	*Abcb4*$^{-/-}$ + CS	Cholestasis
+	±	*Abcb4*$^{-/-}$/*Pemt*$^{-/-}$ + CS	Cholestasis*
-	+	*Pemt*$^{-/-}$ + CD	Lethal
-	-	*Abcb4*$^{-/-}$/*Pemt*$^{-/-}$ + CD	Survival

*, CS-*Abcb4*$^{-/-}$/*Pemt*$^{-/-}$ mice develop cholestasis at age of ~ 7 months.

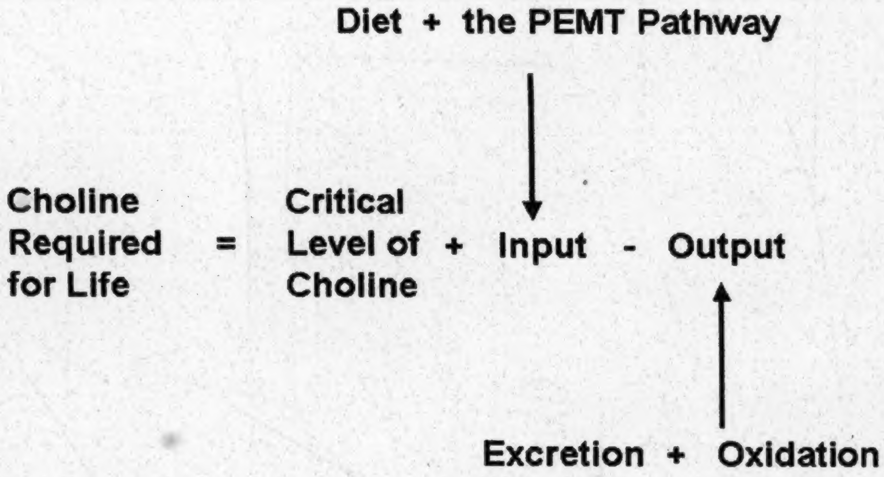
Diet + the PEMT Pathway
Choline Required for Life
=
Critical Level of Choline
+
Input
-
Output
Excretion + Oxidation

Fig. 6.1 Scheme of choline balance theory

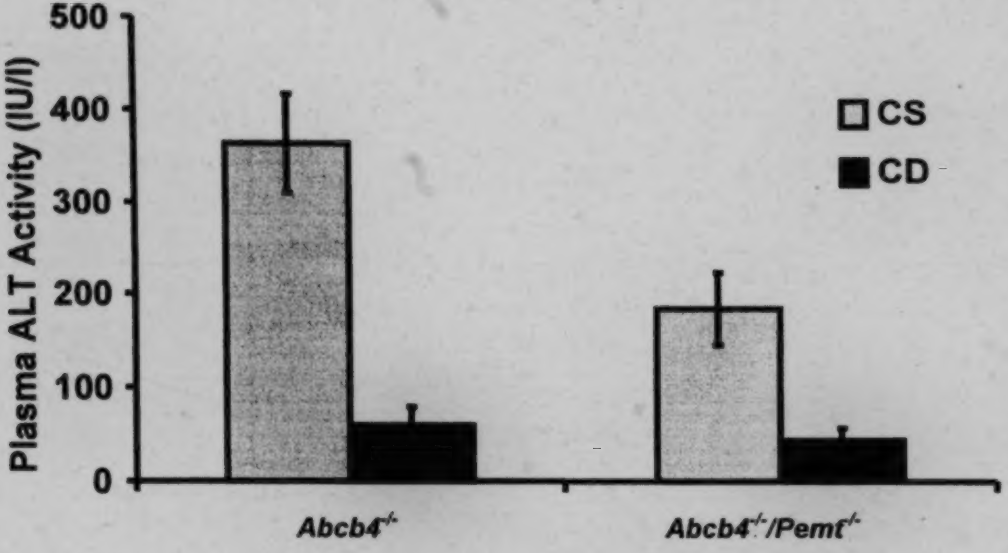

Fig. 6.2 Choline deprivation attenuated liver damage in *Abcb4*$^{-/-}$ mice

Plasma samples were collected from *Abcb4*$^{-/-}$ mice and *Abcb4*$^{-/-}$/*Pemt*$^{-/-}$ mice fed normal chow diet for 7 months or fed normal chow diet for 7 months and then switched to the CD diet for 1 week. Plasma alanine aminotransferase (ALT) activities were measured as indicators of liver damage following the method in **2.2.5**.

Fig. 6.3 Choline can not be replaced by methionine or propanolamaine

Pemt$^{-/-}$ mice were fed the CS (CS) or CD (CD) diet for 3 days as controls. In experimental groups, *Pemt*$^{-/-}$ mice were fed the CD diet with 4% methionine (CD + Met) or 4% 1,2-, 2,1- or 1,3-propanolamine (CD + 1,2-Prn, CD + 2,1-prn and CD + 1,3-Prn) for 3 days. Plasma alanine aminotransferase (ALT) activities were measured as indicators of liver damage following the method in **2.2.5**. Hepatic lipids were measured as the method in **2.2.6**. **(A)** Hepatic PC levels. **(B)** Liver damage assays. Plasma ALT activity was not detectable in CS groups. **(C)** Hepatic TG.

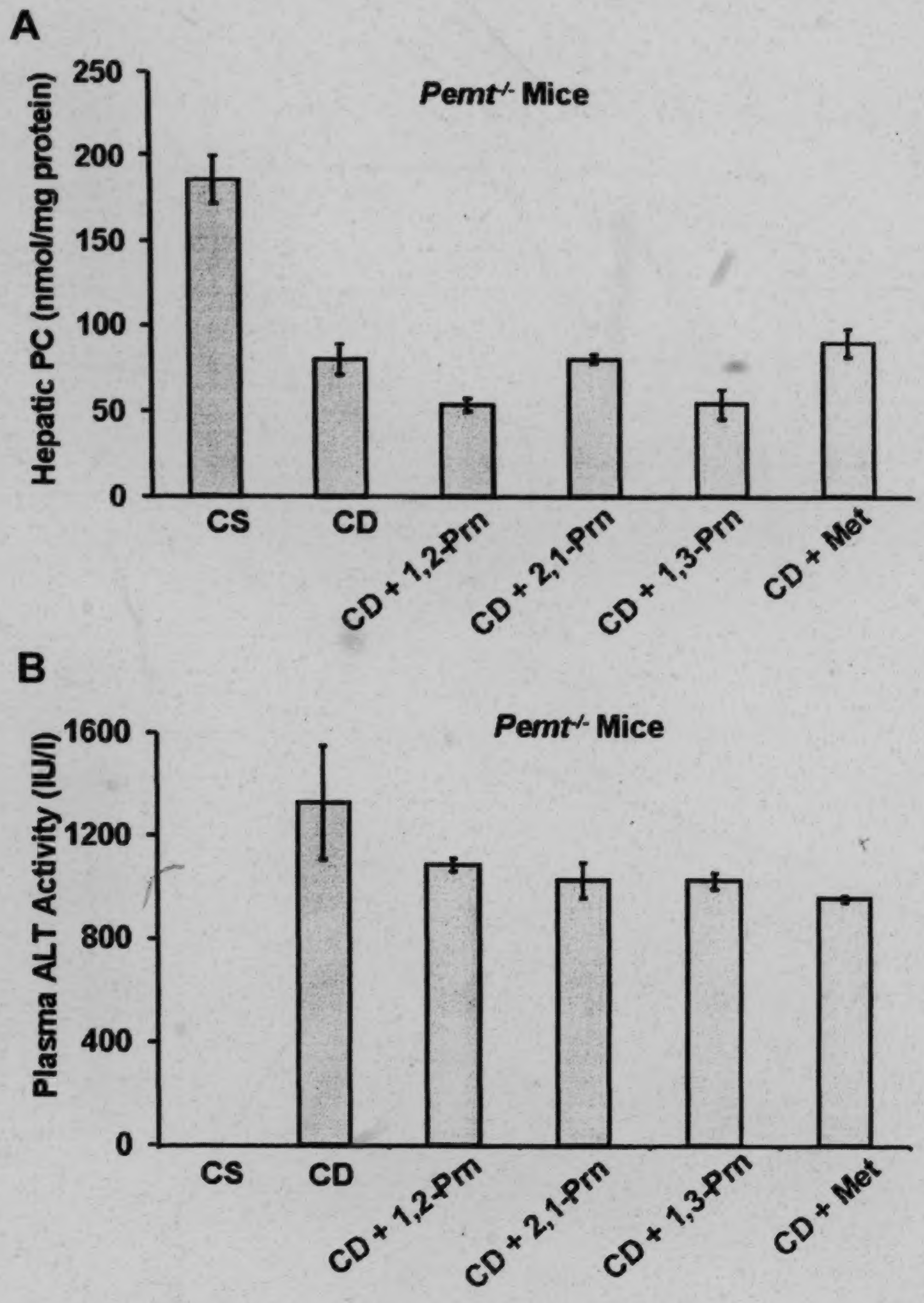
A
Pemt-/- Mice
Hepatic PC (nmol/mg protein)
250
200
150
100
50
0
CS
CD
CD + 1,2-Prn
CD + 2,1-Prn
CD + 1,3-Prn
CD + Met
B
Pemt-/- Mice
Plasma ALT Activity (IU/l)
1600
1200
800
400
0
CS
CD
CD + 1,2-Prn
CD + 2,1-Prn
CD + 1,3-Prn
CD + Met

C

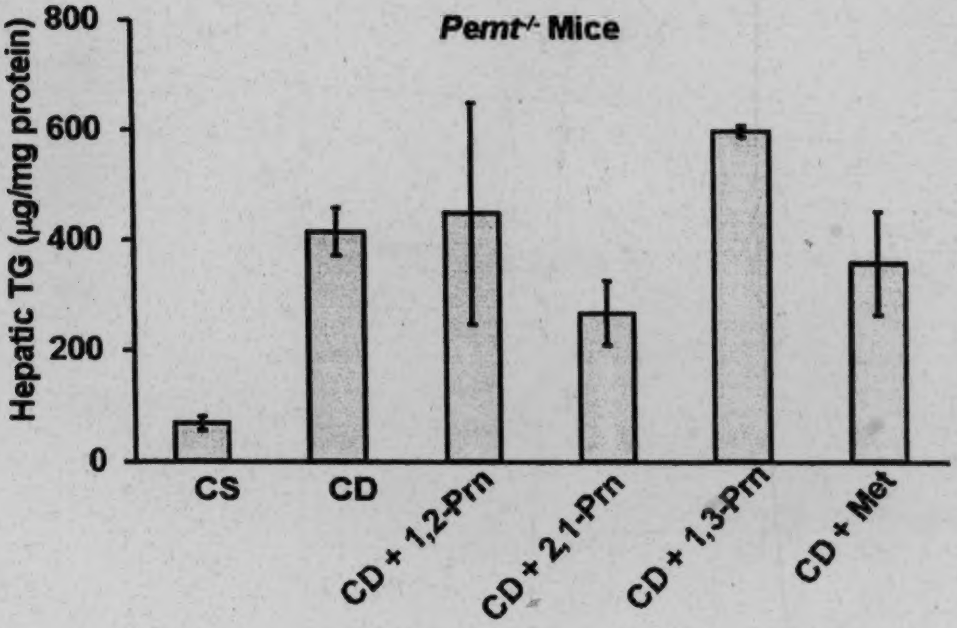

Pemt-/- Mice
Hepatic TG (µg/mg protein)
800
600
400
200
0
CS
CD
CD + 1,2-Prn
CD + 2,1-Prn
CD + 1,3-Prn
CD + Met

References

1. Tso, P., and Fujimoto, K. The absorption and transport of lipids by the small intestine. (1991) *Brain Res Bull* **27**, 477-482
2. Borgstrom, B. (1976) *Phospholipid absorption*. Lipid absorption (Rommel, K., H. Goebell, R. Bohmer, Ed.), MTP Press Ltd., London
3. Walkey, C. J., Donohue, L. R., Bronson, R., Agellon, L. B., and Vance, D. E. Disruption of the murine gene encoding phosphatidylethanolamine N-methyltransferase. (1997) *Proc Natl Acad Sci U S A* **94**, 12880-12885
4. Cui, Z., and Vance, D. E. Expression of phosphatidylethanolamine N-methyltransferase-2 is markedly enhanced in long term choline-deficient rats. (1996) *J Biol Chem* **271**, 2839-2843
5. Yao, Z. M., Jamil, H., and Vance, D. E. Choline deficiency causes translocation of CTP:phosphocholine cytidylyltransferase from cytosol to endoplasmic reticulum in rat liver. (1990) *J Biol Chem* **265**, 4326-4331
6. Jacobs, R. L., Devlin, C., Tabas, I., and Vance, D. E. Targeted deletion of hepatic CTP:phosphocholine cytidylyltransferase alpha in mice decreases plasma high density and very low density lipoproteins. (2004) *J Biol Chem* **279**, 47402-47410
7. Wang, L., Magdaleno, S., Tabas, I., and Jackowski, S. Early embryonic lethality in mice with targeted deletion of the CTP:phosphocholine cytidylyltransferase alpha gene (Pcyt1a). (2005) *Mol Cell Biol* **25**, 3357-3363

8. Vance, D. E. *Phospholipid biosynthesis in eukaryotes.* (2002) in *Biochemistry of lipids, lipoproteins and membranes* (Vance, D. E., J. E. Vance, ed), pp. 205-232, Elsevier, New York

9. Vance, D. E. *Biochemistry of lipids, lipoproteins and membranes* (2002) in *Biochemistry of Lipids, Lipoprotein and Membranes, 4th edition.* (Vance, D. E., J. E. Vance, ed), pp. 205-232, Elsevier, New York

10. Kulinski, A., Vance, D. E., and Vance, J. E. A choline-deficient diet in mice inhibits neither the CDP-choline pathway for phosphatidylcholine synthesis in hepatocytes nor apolipoprotein B secretion. (2004) *J Biol Chem* **279**, 23916-23924

11. Agellon, L. B., Walkey, C. J., Vance, D. E., Kuipers, F., and Verkade, H. J. The unique acyl chain specificity of biliary phosphatidylcholines in mice is independent of their biosynthetic origin in the liver. (1999) *Hepatology* **30**, 725-729

12. Schneider, W. J., and Vance, D. E. Effect of choline deficiency on the enzymes that synthesize phosphatidylcholine and phosphatidylethanolamine in rat liver. (1978) *Eur J Biochem* **85**, 181-187

13. Best, C. H., and Huntsman, M. E. The effects of the components of lecithine upon deposition of fat in the liver. (1932) *Journal of Physiology-London* **75**, 405-412

14. Best, C. H., Lucas, C. C., and Ridout, J. H. The lipotropic factors. (1954) *Ann N Y Acad Sci* **57**, 646-653

15. Zeisel, S. H., Da Costa, K. A., Franklin, P. D., Alexander, E. A., Lamont, J. T., Sheard, N. F., and Beiser, A. Choline, an essential nutrient for humans. (1991) *Faseb J* **5**, 2093-2098

16. Zeisel, S. H., and Blusztajn, J. K. Choline and human nutrition. (1994) *Annu Rev Nutr* **14**, 269-296

17. Blusztajn, J. K. Choline, a vital amine. (1998) *Science* **281**, 794-795

18. Zeisel, S. H. Choline: an essential nutrient for humans. (2000) *Nutrition* **16**, 669-671

19. Smit, J. J., Schinkel, A. H., Oude Elferink, R. P., Groen, A. K., Wagenaar, E., van Deemter, L., Mol, C. A., Ottenhoff, R., van der Lugt, N. M., van Roon, M. A., and et al. Homozygous disruption of the murine mdr2 P-glycoprotein gene leads to a complete absence of phospholipid from bile and to liver disease. (1993) *Cell* **75**, 451-462

20. Jacquemin, E. Role of multidrug resistance 3 deficiency in pediatric and adult liver disease: one gene for three diseases. (2001) *Semin Liver Dis* **21**, 551-562

21. Voshol, P. J., Havinga, R., Wolters, H., Ottenhoff, R., Princen, H. M., Oude Elferink, R. P., Groen, A. K., and Kuipers, F. Reduced plasma cholesterol and increased fecal sterol loss in multidrug resistance gene 2 P-glycoprotein-deficient mice. (1998) *Gastroenterology* **114**, 1024-1034

22. Choi, J. Y., Martin, W. E., Murphy, R. C., and Voelker, D. R. Phosphatidylcholine and N-methylated phospholipids are nonessential in Saccharomyces cerevisiae. (2004) *J Biol Chem* **279**, 42321-42330

23. Kiss, Z. Regulation of mitogenesis by water-soluble phospholipid intermediates. (1999) *Cell Signal* **11**, 149-157

24. Foster, D. A., and Xu, L. Phospholipase d in cell proliferation and cancer. (2003) *Mol Cancer Res* **1**, 789-800

25. Prokazova, N. V., Zvezdina, N. D., and Korotaeva, A. A. Effect of lysophosphatidylcholine on transmembrane signal transduction. (1998) *Biochemistry (Mosc)* **63**, 31-37

26. Ventura, C., and Maioli, M. Protein kinase C control of gene expression. (2001) *Crit Rev Eukaryot Gene Expr* **11**, 243-267

27. Stenmark, H., and Gillooly, D. J. Intracellular trafficking and turnover of phosphatidylinositol 3-phosphate. (2001) *Semin Cell Dev Biol* **12**, 193-199

28. Alessenko, A. V., and Burlakova, E. B. Functional role of phospholipids in the nuclear events. (2002) *Bioelectrochemistry* **58**, 13-21

Appendix I

Why is Serine Sufficient for Phosphatidylethanolamine Biosynthesis during Cell Culture?

Summary

A major pathway for *de novo* phosphatidylethanolamine (PE) biosynthesis is the CDP-ethanolamine pathway (the Kennedy pathway). The rate-limiting enzyme, CDP:phosphoethanolamine cytidylyltransferase (ET) controls the flux from ethanolamine to PE. Mammalian cells are normally cultured without ethanolamine since the medium contains ample serine and that can be incorporated into phosphatidylserine (PS) and then decarboxylated into PE. However, attenuating PE biosynthesis by RNA interference targeted to ET (ETi) showed that not only the incorporation of ethanolamine into PE, but also the incorporation of serine into PE was inhibited. Since serine can also be converted into phosphoethanolamine by sphingosine-1-phosphate lyase, the results suggest that PE biosynthesis in cells cultured in ethanolamine-free medium is mainly from the sphingosine-1-phosphate lyase pathway rather than the PS decarboxylation pathway.

Introduction

Phosphatidylethanolamine (PE) is the second most abundant phospholipid in mammalian cells compared with phosphatidylcholine. The major pathway for *de novo* PE biosynthesis is the CDP-ethanolamine pathway (the Kennedy pathway) (1), in which ethanolamine is phosphorylated into phosphoethanolamine by choline/ethanolamine kinase. Phosphoethanolamine is then converted into CDP-ethanolamine by the rate-limiting enzyme, CDP:

phosphoethanolamine cytidylyltransferase (ET). Finally, CDP-ethanolamine is combined with diacylglycerol to form PE by CDP-ethanolamine: 1,2-diacylglycerol ethanolaminephosphotransferase (EPT) (Fig. 1). In addition, the headgroup of PE, phosphoethanolamine, can be obtained from the cleavage of sphingosine-1-phosphate by sphingosine-1-phosphate lyase. Moreover, PE can also be synthesized from phosphatidylserine (PS) decarboxylation (Fig. 1).

However, cells can be cultured without ethanolamine as the medium contains ample amount of serine. Thus, sufficient phosphatidylethanolamine can be obtained through the PS decarboxylation pathway. This was challenged by our recent finding that the PS decarboxylation pathway could not compensate for the loss of PE levels when the CDP-ethanolamine pathway was inhibited by RNA interference targeted to ET (ETi) (Chapter 3).

Here, we report that PE biosynthesis in cells cultured in ethanolamine-free medium is mainly from the sphingosine-1-phosphate lyase pathway rather than the PS decarboxylation pathway.

Experimental Procedures

Preparation of primary hepatocytes. *Pemt*$^{-/-}$ mice were fed a choline-supplemented diet for 24 h and then fed a choline-deficient (CD) diet (*ICN*) for 2 days (CD-*Pemt*$^{-/-}$). Hepatocytes were prepared and cultured (2) in CS medium

(Dulbecco's modified Eagle's medium + 17 % fetal bovine serum) or CD medium (Dulbecco's modified Eagle's medium without choline + 17 % delipidated/dialyized fetal bovine serum).

RNA interference (RNAi) of ET in cultured hepatocytes. RNAi sequence, 5'-AAGCACAACTGTGACTTCTCT-3', targeted to the mRNA of ET was inserted into p*Silencer* 4.1-CMV vectors (*Ambion*) to produce ETi vectors. A control sequence of ETi, 5'-AATCACAGCTATCACTGCTCT-3', was inserted into p*Silencer* 4.1-CMV vectors to produce an ETi control vector. Lipofectamine™ 2000 (*Invitrogen*) was used as carrier for transfection. Three μg of ETi or control vectors were transfected into 4 h-plated hepatocytes (1 X 10^6 cells) isolated from CD-*Pemt*$^{-/-}$ mice for 24 h. For ETi transfection into wild-type hepatocytes, 6 μg of ETi or control vectors were transfected into suspended hepatocytes (1 X 10^6 cells) freshly isolated from wild-type mice with 5% fetal bovine serum for 24 h. After transfection for 24 h, cells were incubated with 20 μCi [^{3}H]serine or [^{3}H]ethanolamine for 2 h.

Lipids Analyses. Hepatocytes were homogenized in 5 vol buffer [10 mM Tris-HCl, pH 7.2, containing 150 mM NaCl, 1 mM EDTA, 1 mM dithiothreitol, 1 mM phenylmethylsulfonyl fluoride, 1:100 protease inhibitors cocktail (*Sigma*, P8340)]. The homogenates were centrifuged for 5 min at 600 × g and supernatants were collected. Protein was quantified by the method of Bradford (3). Total lipids were extracted from liver homogenates, plasma and bile (4). Lipids were separated by thin layer chromatography (TLC). The bands of lipids were scraped from TLC plates and counted in a scintillation counter. For the dissection of headgroup and fatty acyl chains from phospholipids, the bands of lipids scraped from TLC plates were incubated with 6 mM sulfuric acid and 1 mM methanol for 2 h at 80°C. After this, lipid extraction and TLC separation were performed. The bands of headgroups and fatty acyl chains were scraped from TLC plates and counted in a scintillation counter.

Results

ETi inhibited incorporation of serine into PE in CD-*Pemt*$^{-/-}$ hepatocytes.

Previously we found that ETi effectively reduced PE levels through inhibition of the CDP-ethanolamine pathway in CD-*Pemt*$^{-/-}$ hepatocytes *in vitro* and *in vivo* (Chapter 3). When CD-*Pemt*$^{-/-}$ hepatocytes were labeled with [^{3}H]ethanolamine for 2 or 24 h, ETi caused about 36% or 46% reduction in the incorporation of ethanolamine into PE (Fig. 2A, B). Interestingly, when CD-*Pemt*$^{-/-}$ hepatocytes were labeled with [^{3}H]serine for 2 or 24 h (Fig. 2C, D), we found that ETi resulted in a similar reduction in the incorporation of serine into PE compared to [^{3}H]ethanolamine labeling. When cells were labeled with [^{3}H]ethanolamine, radioactivity in [^{3}H]phosphoethanolamine were much higher than that in [^{3}H]PE further confirmed that the conversion of phosphoethanolamine into CDP-ethanolamine is the rate-limiting step of PE biosynthesis (Fig. 2A, E) (1). However, the higher radioactivity of

[^{3}H]phosphoethanolamine resulted in difficulty in distinguishing differences in phosphoethanolamine levels between control and ETi hepatocytes (Fig. 2E, upper panel). Only when the radioactivity of [^{3}H]phosphoethanolamine in control hepatocytes was subtracted from that in ETi hepatocytes, a significant increase in accumulation of [^{3}H]phosphoethanolamine after ETi treatment became obvious (Fig. 2E, lower panel). However, [^{3}H]phosphoethanolamine only accumulated when cells were labeled with [^{3}H]ethanolamine but not with [^{3}H]serine labeling (Fig. 2E, F). These data suggest that the conversion of serine into phosphoethanolamine could be down-regulated when the CDP-ethanolamine pathway was attenuated. Since serine has diverse metabolism *in vivo*, once serine is no longer used for phosphoethanolamine biosynthesis, it may flow to other pathways, such as triacylglycerol synthesis.

[^{3}H]serine was mainly incorporated into fatty acyl chains of triacylglycerol rather than other cellular lipids

When wild-type hepatocytes were labeled with [^{3}H]serine for 2 h, most of radioactivity was found in the triacylglycerol fractions as compared with other cellular lipids (Fig. 3A, B). This indicated that the majority of [^{3}H]serine labeling in phospholipds might be in the fatty acyl chains rather than headgroups. Thus, dissection of PE into headgroup and fatty acyl chains is necessary for illustrating *de novo* PE biosynthesis.

ETi inhibited incorporation of serine into PE in wild-type hepatocytes

When wild-type hepatocytes were labeled with [^{3}H]ethanolamine for 2 h, ETi caused about a 20% reduction in the incorporation of ethanolamine into PE ($p<0.05$) (Fig. 3C). Moreover, when wild-type hepatocytes were labeled with [^{3}H]serine for 2 h, we found that ETi resulted in similar reduction in the incorporation of serine into PE compared to [^{3}H]ethanolamine labeling (Fig. 3D) but no effect on the incorporation of serine into PS (Fig. 3E). To further confirm this reduction, we dissected PE and PS into headgroup and fatty acyl chains by acid hydrolysis. We found that ETi attenuated the incorporation of serine into PE by inhibiting the production of ethanolamine headgroup ($p<0.05$) rather than fatty acyl chains, and the incorporation of serine into PS was not decreased by ETi from either headgroup or fatty acyl chains (Fig. 3E, F).

Discussion

We found that serine-derived PE could not compensate for the loss of PE from the inhibition of PE biosynthesis by ETi (Chapter 3). CD-*Pemt*$^{-/-}$ hepatocytes showed leaky cell membranes (Chapter 3) that allowed higher transfection efficiency of ETi compared with wild-type hepatocytes. Higher transfection efficiency consequently caused increased inhibition of the incorporation of ethanolamine into PE by ETi in CD-*Pemt*$^{-/-}$ hepatocytes as compared with wild-type hepatocytes (Fig. 2A, 3C). However, the interesting finding was that following the increased inhibition of the incorporation of ethanolamine into PE by

ETi, the inhibition of the incorporation of serine into PE was also increased by ETi. In either CD-*Pemt*$^{-/-}$ hepatocytes or wild-type hepatocytes, the reduction in the incorporation of serine into PE by ETi suggested that serine-derived PE was mainly from the CDP-ethanolamine pathway rather than the PS decarboxylation pathway. Meanwhile, ETi did not affect incorporation of serine into PS. In other words, serine-derived PE was mainly from the sphingosine-1-phosphate lyase pathway rather than the PS decarboxylation pathway.

The sphingosine-1-phosphate lyase pathway has been found to be the pathway for breakdown of sphingolipid signaling (5). The reason researchers in the field of PE metabolism did not pay too much attention to this pathway might be due to its involvement in cell signalingthat led to the thought that it was a quantitatively minor pathway. Phosphoethanolamine from the cleavage of sphingosine-1-phosphate is an end product of this signaling pathway. Ceramide and sphingosine-1-phosphate are two major molecules regulating cell signaling pathway in opposite ways (6). People found that only trace amount of these compounds could be detectable in cells. However, the reason why signaling molecules are maintained at trace levels is that the turnover of these molecules is very rapid. Based on the literature, Van Veldhoven and Mannaerts found that the turnover of sphingosine-1-phosphate was 14.7 nmol/min/g liver (7). This indicated that the end product of this signaling pathway, liver could produce ~5.7 mg phosphoethanolamine every day for a 20 g mouse with a 2 g liver (7,8). In addition to liver, sphingosine-1-phosphate lyase is ubiquitously distributed in most tissues, especially abundant in the small intestine and thymus (8). Since the ethanolamine content in the diet is ~8 g/kg diet (9), it is estimated that the dietary ethanolamine uptake for a 20 g mouse is ~24 mg per day. Thus, besides of ethanolamine recycling PE catabolism (10), the sphingosine-1-phosphate lyase pathway contributes a considerable pool of ethanolamine metabolites *in vivo*.

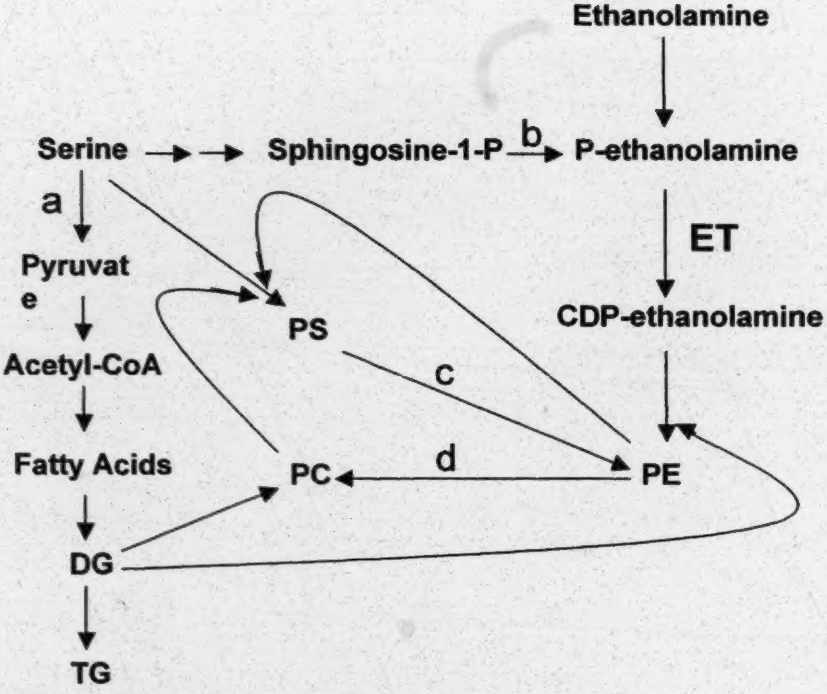
Ethanolamine
Serine
Sphingosine-1-P
b
P-ethanolamine
a
Pyruvat e
ET
PS
CDP-ethanolamine
Acetyl-CoA
c
Fatty Acids
d
PC
PE
DG
TG

Fig. 1 Pathways of PE biosynthesis in the liver

P-ethanolamine, phosphoethanolamine; DG, diacylglycerol; TG, triacylglycerol; Sphingosine-1-P, sphingosine-1-phosphate; PE, phosphatidylethanolamine. **a**, serine dehydratase; **b**, sphingosine-1-phosphate lyase; **c**, phosphatidylserine decarboxylase; **d**, PE *N*-methyltransferase.

Fig. 2 ETi inhibited incorporation of serine into PE in CD-*Pemt*$^{-/-}$ hepatocytes

Primary hepatocytes isolated from *Pemt*$^{-/-}$ mice fed a choline-deficient (CD) diet for 2 days (CD-*Pemt*$^{-/-}$ hepatocytes) were plated for 4 h. After transfection of 3 μg of ETi or control vectors into hepatocytes (1 X 10^{-6} cells) for 24 h, cells were incubated with 20 μCi [^{3}H]serine or [^{3}H]ethanolamine for 2 h or 24 h. **A**, Incorporation of [^{3}H]ethanolamine into [^{3}H]PE for 2 h; **B**, Incorporation of [^{3}H]ethanolamine into [^{3}H]PE for 24 h; **C**, Incorporation of [^{3}H]serine into [^{3}H]PE for 2 h; **D**, Incorporation of [^{3}H]serine into [^{3}H]PE for 24 h; **E**, Incorporation of [^{3}H]ethanolamine into [^{3}H]phosphoethanolamine for 2 h; **F**, Incorporation of [^{3}H]serine into [^{3}H]phosphoethanolamine for 2 h.

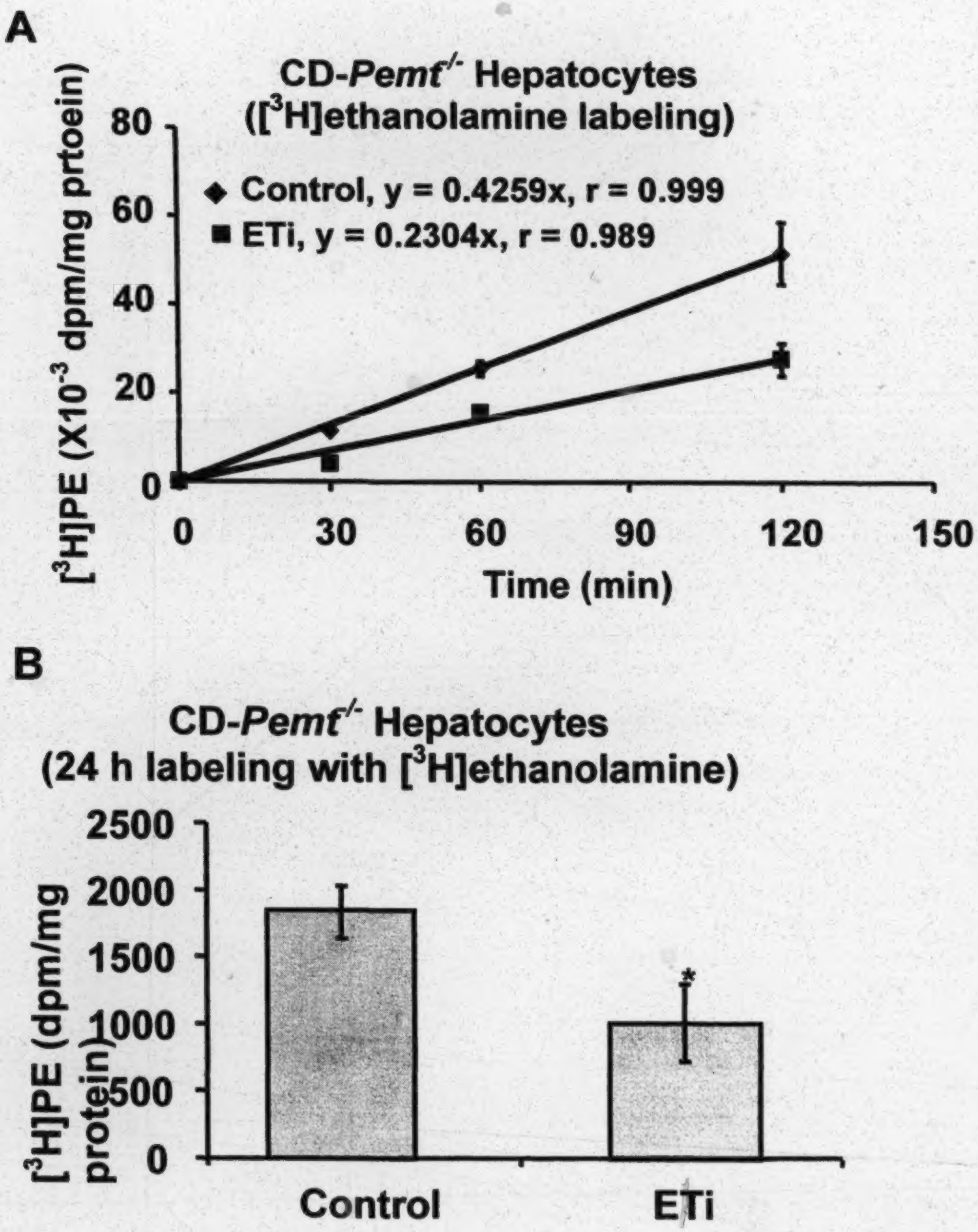
A
CD-*Pemt*$^{-/-}$ Hepatocytes
([^{3}H]ethanolamine labeling)
◆ Control, y = 0.4259x, r = 0.999
■ ETi, y = 0.2304x, r = 0.989
[^{3}H]PE (X10^{-3} dpm/mg prtoein)
80
60
40
20
0
0
30
60
90
120
150
Time (min)
B
CD-*Pemt*$^{-/-}$ Hepatocytes
(24 h labeling with [^{3}H]ethanolamine)
[^{3}H]PE (dpm/mg protein)
2500
2000
1500
1000
500
0
*
Control
ETi

C

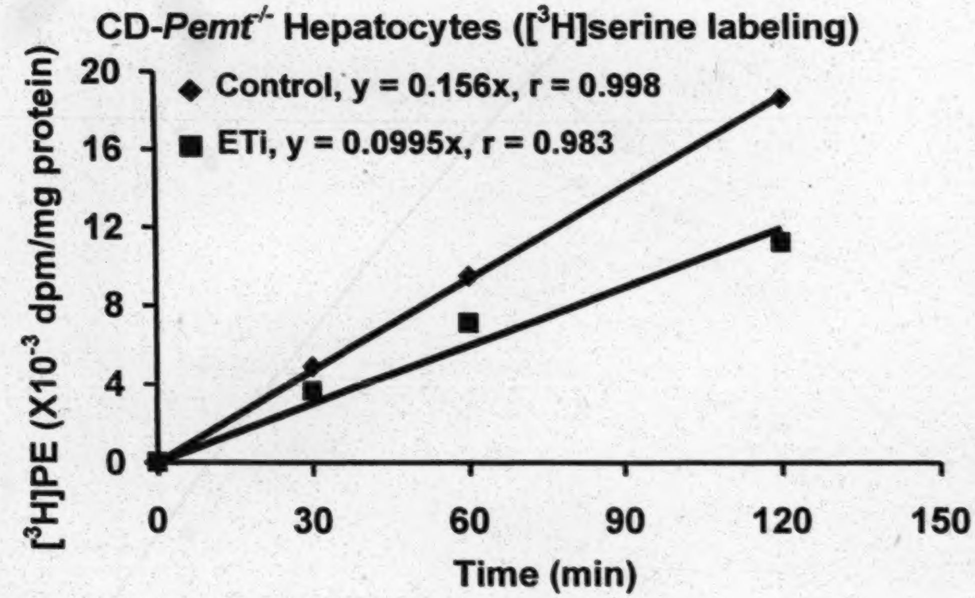
CD-Pemt-/- Hepatocytes ([3H]serine labeling)
[3H]PE (X10-3 dpm/mg protein)
20
16
12
8
4
0
◆ Control, y = 0.156x, r = 0.998
■ ETi, y = 0.0995x, r = 0.983
0
30
60
90
120
150
Time (min)

D

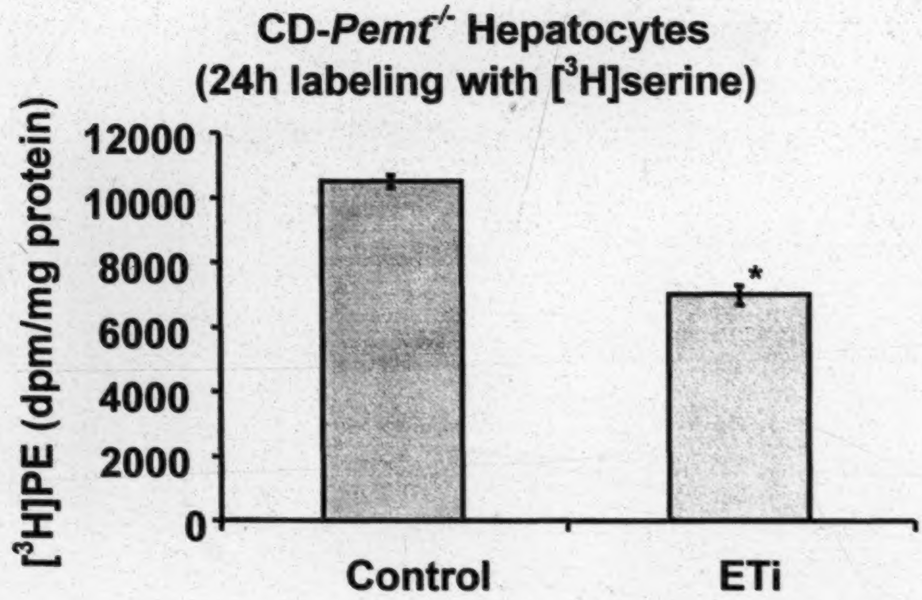
CD-Pemt-/- Hepatocytes
(24h labeling with [3H]serine)
[3H]PE (dpm/mg protein)
12000
10000
8000
6000
4000
2000
0
*
Control
ETi

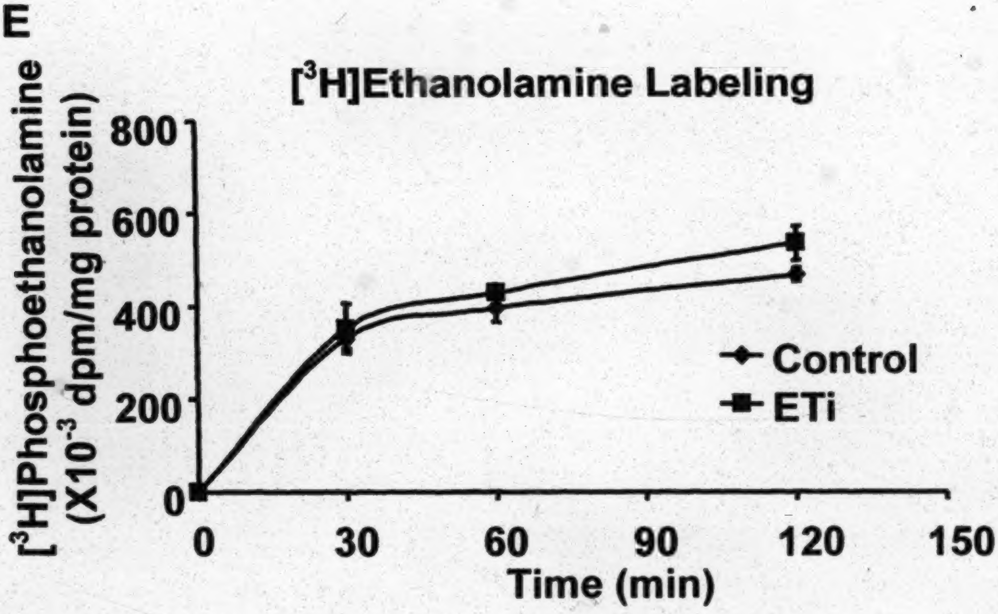
E
[^{3}H]Ethanolamine Labeling
[^{3}H]Phosphoethanolamine (X10^{-3} dpm/mg protein)
800
600
400
200
0
0
30
60
90
120
150
Time (min)
Control
ETi

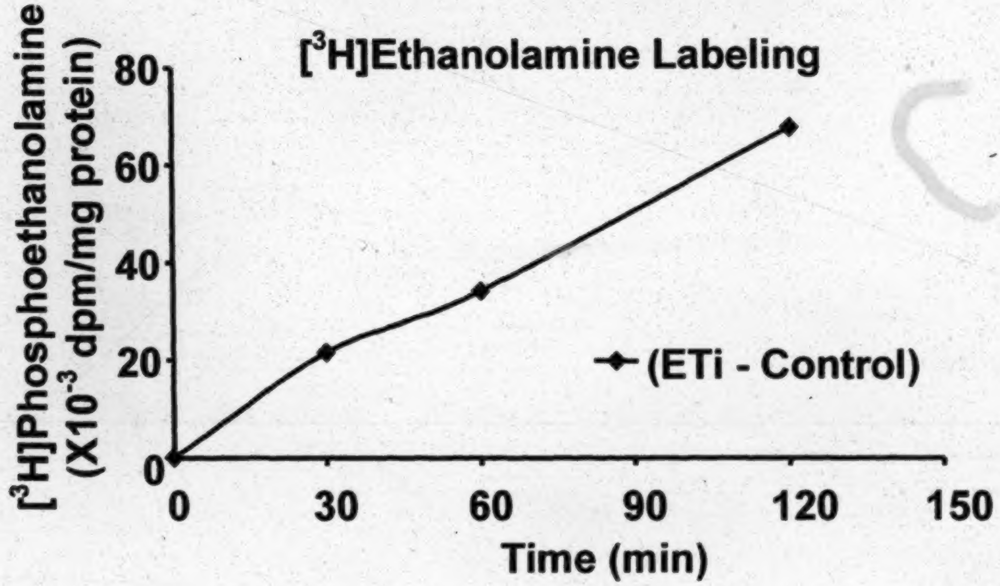
[^{3}H]Ethanolamine Labeling
[^{3}H]Phosphoethanolamine (X10^{-3} dpm/mg protein)
80
60
40
20
0
0
30
60
90
120
150
Time (min)
(ETi - Control)

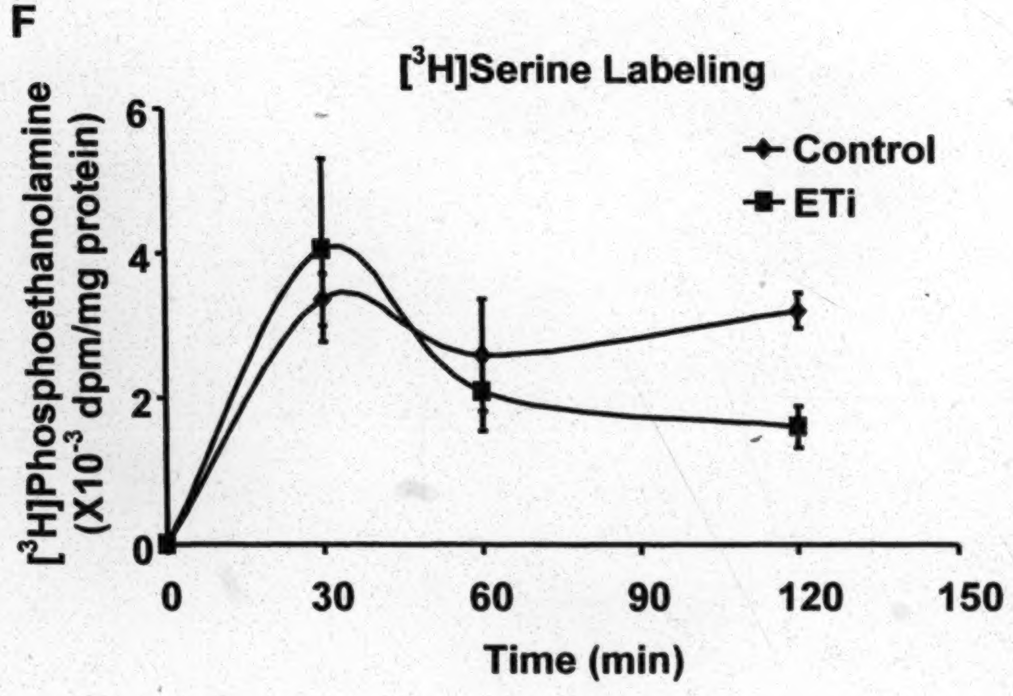
F
[3H]Serine Labeling
[3H]Phosphoethanolamine (X10-3 dpm/mg protein)
6
4
2
0
Control
ETi
0
30
60
90
120
150
Time (min)

Fig. 3 ETi inhibited incorporation of serine into PE in wild-type hepatocytes

Primary hepatocytes isolated from wild-type mice (wild-type hepatocytes) were plated for 4 h. After transfection of 3 μg of ETi or control vectors into hepatocytes (1 X 10^{-6} cells) for 24 h, cells were incubated with 20 μCi [^{3}H]serine or [^{3}H]ethanolamine for 2 h. **A, B**, Incorporation of [^{3}H]serine into cellular lipids; FA, fatty acids; DG, diacylglycerol; PC, phosphatidylcholine; PE, phosphatidylethanolamine; PS, phosphatidylserine; TG, triacylglycerol. **C**, Incorporation of [^{3}H]ethanolamine into [^{3}H]PE; **D**, Incorporation of [^{3}H]serine into [^{3}H]PE. **E**, Incorporation of [^{3}H]serine into [^{3}H]PS.

A

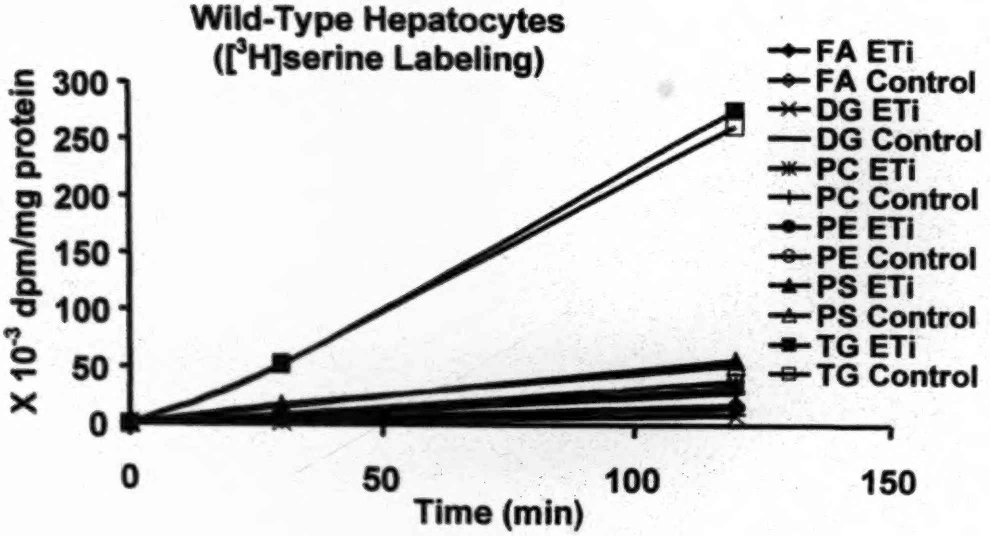

Wild-Type Hepatocytes
([³H]serine Labeling)
X 10⁻³ dpm/mg protein
300
250
200
150
100
50
0
0
50
100
150
Time (min)
FA ETi
FA Control
DG ETi
DG Control
PC ETi
PC Control
PE ETi
PE Control
PS ETi
PS Control
TG ETi
TG Control

B

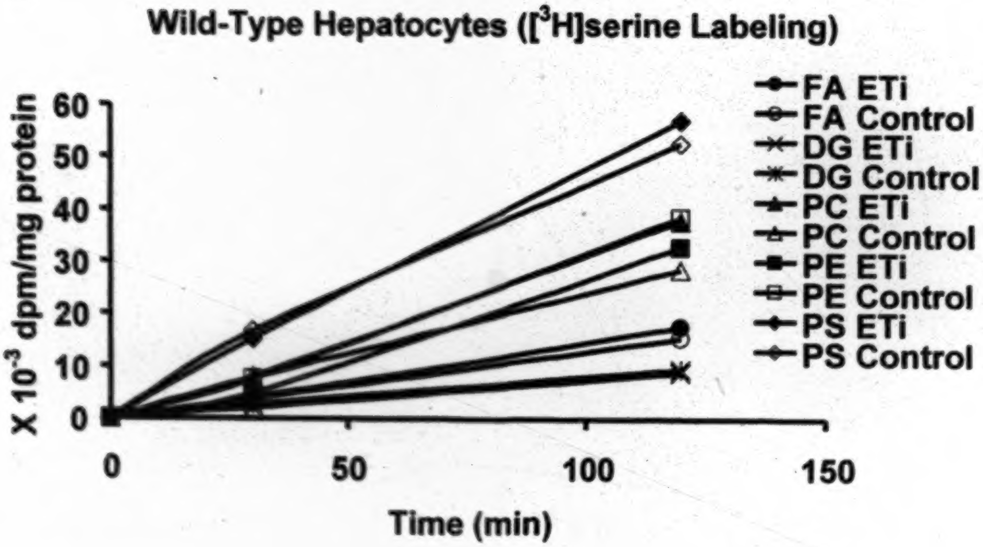

Wild-Type Hepatocytes ([³H]serine Labeling)
X 10⁻³ dpm/mg protein
60
50
40
30
20
10
0
0
50
100
150
Time (min)
FA ETi
FA Control
DG ETi
DG Control
PC ETi
PC Control
PE ETi
PE Control
PS ETi
PS Control

C

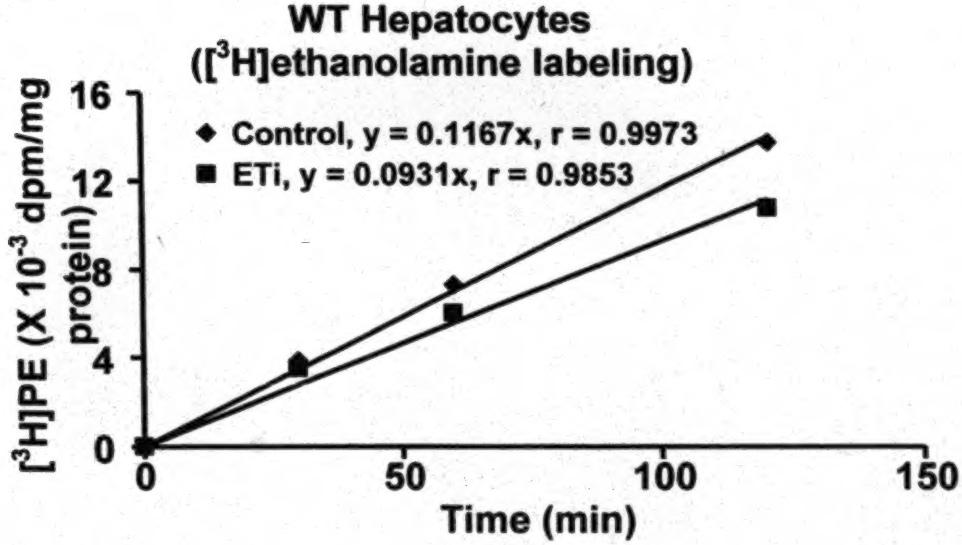
WT Hepatocytes ([^{3}H]ethanolamine labeling)

D

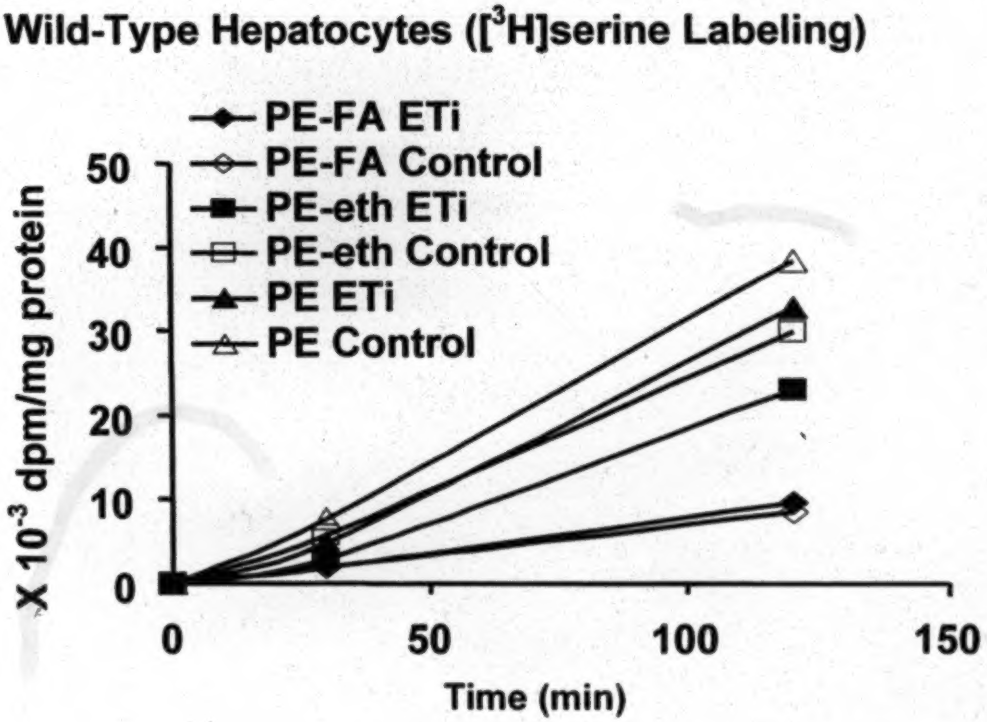
Wild-Type Hepatocytes ([^{3}H]serine Labeling)

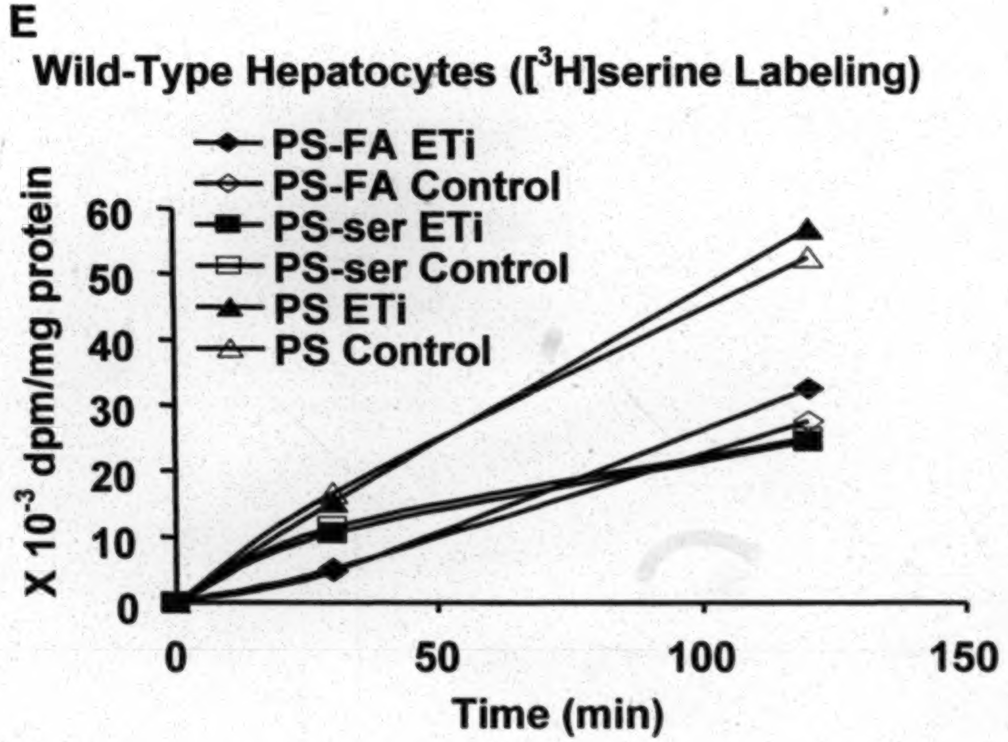
E
Wild-Type Hepatocytes ([3H]serine Labeling)
PS-FA ETi
PS-FA Control
PS-ser ETi
PS-ser Control
PS ETi
PS Control
X 10-3 dpm/mg protein
0
10
20
30
40
50
60
0
50
100
150
Time (min)

References

1. Bladergroen, B. A., and van Golde, L. M. CTP:phosphoethanolamine cytidylyltransferase. (1997) *Biochim Biophys Acta* **1348**, 91-99
2. Klaunig, J. E., Goldblatt, P. J., Hinton, D. E., Lipsky, M. M., Chacko, J., and Trump, B. F. Mouse liver cell culture. I. Hepatocyte isolation. (1981) *In Vitro* **17**, 913-925
3. Bradford, M. M. A rapid and sensitive method for the quantitation of microgram quantities of protein utilizing the principle of protein-dye binding. (1976) *Anal Biochem* **72**, 248-254
4. Bligh, E. G., and Dyer, W. J. A rapid method of total lipid extraction and purification. (1959) *Can. J. Biochem. Physiol.* **37**, 911-917
5. Van Veldhoven, P. P. Sphingosine-1-phosphate lyase. (2000) *Methods Enzymol* **311**, 244-254
6. Cuvillier, O., Pirianov, G., Kleuser, B., Vanek, P. G., Coso, O. A., Gutkind, S., and Spiegel, S. Suppression of ceramide-mediated programmed cell death by sphingosine-1-phosphate. (1996) *Nature* **381**, 800-803
7. Van Veldhoven, P. P., and Mannaerts, G. P. Subcellular localization and membrane topology of sphingosine-1-phosphate lyase in rat liver. (1991) *J Biol Chem* **266**, 12502-12507
8. Ikeda, M., Kihara, A., and Igarashi, Y. Sphingosine-1-phosphate lyase SPL is an endoplasmic reticulum-resident, integral membrane protein with

the pyridoxal 5'-phosphate binding domain exposed to the cytosol. (2004) *Biochem Biophys Res Commun* **325**, 338-343

9. Shimada, Y., Morita, T., and Sugiyama, K. Dietary eritadenine and ethanolamine depress fatty acid desaturase activities by increasing liver microsomal phosphatidylethanolamine in rats. (2003) *J Nutr* **133**, 758-765

10. Shiao, Y. J., and Vance, J. E. Evidence for an ethanolamine cycle: differential recycling of the ethanolamine moiety of phosphatidylethanolamine derived from phosphatidylserine and ethanolamine. (1995) *Biochem J* **310 (Pt 2)**, 673-679

Appendix II

Does PEMT protect against liver cancer?

Introduction

Abnormally enhanced cell division leads to tumors. When hepatocytes divide out of control, liver cancer or hepatoma develops. In eukaryotic cells, cell division is not only involved in the replications of DNA and proteins, but also lipids. The latter is critical for the formation of membrane systems for newly formed cells. PC is the major phospholipid in the membrane of animal cells. Thus, PC biosynthesis is up-regulated during cell division (1). In eukaryotic cells, the CDP-choline pathway is the major pathway for PC biosynthesis, in which the rate-limiting enzyme, CTP:phosphocholine cytidylyltransferase (CT) is finely regulated at both transcriptional levels and post-translational levels to meet the requirements for *de novo* PC biosynthesis (1). In liver, the CDP-choline pathway accounts for ~70% of PC biosynthesis, and the PEMT pathway for the rest of ~ 30% (1). However, there was no PEMT activity detectable in fetal liver and hepatoma cells (2-4). PEMT activity and expression were also diminished in carcinogen-induced liver tumors and human liver cancers (5,6). PEMT only occurred one day before birth and stabilized in adults (2). Partial hepatectomy was accompanied by a marked reduction of PEMT expression and activity with activated hepatocyte division (7). PEMT over-expression in hepatoma cells inhibited cell proliferation, induced apoptosis and partially reversed the neoplastic phenotype. (8,9). Thus, fast-dividing cells do not contain PEMT, but have a higher level of CT. Thus, a reasonable hypothesis is that PEMT might attenuate cell division.

The inverse relationship between PEMT activity and hepatocyte division suggests this enzyme, its product, or its substrate may be involved in the control of hepatocyte proliferation. Therefore, the hypothesis proposed is PEMT protects against liver cancer.

However, the first *in vivo* evidence was against this hypothesis, since *Pemt*$^{-/-}$ mice grew normally, and there was no liver phenotype and no liver cancer occurred even during long-term breeding under a normal diet. This was surprised us since PEMT may guard against the development of liver cancer induced by exogenous stress.

Therefore, an alternative hypothesis was proposed that *Pemt*$^{-/-}$ mice might more readily develop liver cancer than wild-type (*Pemt*$^{+/+}$) mice during hepatocarcinogenesis.

Experimental procedures

Hepatocarcinogenesis

Two-step strategy was used for hepatocarcinogenesis including initiation and promotion. First, mice of one week before weaning (at age of 2 weeks) were injected intraperitoneally (i.p.) with diethylnitrosamine (DENA), 50 mg/g body weight. And at age of 4 weeks, DENA-treated mice were fed drinking water with 5g/l trichloroacetic acid (TCA) routinely until being sacrificed after 6, 9 and 12 months.

Histological and pathological Analysis

Livers were collected from mice after carcinogenesis and photographed. Hepatocarcinogenesis was evaluated by a pathologist, Dr. Mark Lee from the University of Alberta Hospital.

Results

Tumor-like nodules occurred more frequently in the livers of *Pemt*$^{-/-}$ mice than that in wild-type mice

At 6 months, no tumor-like nodules were found in the liver of either *Pemt*$^{-/-}$ mice or wild-type mice. At 9 months, there was no significance occurrence of nodules in *Pemt*$^{-/-}$ mice and wild-type mice. After 12 months, tumor-like nodules dramatically increased in the liver of *Pemt*$^{-/-}$ mice but not in the liver of wild-type mice (Fig. 1). This was consistent with the visional observations of livers (Fig. 2). However, these nodules were suggested to be fat accumulation by a pathologist (name the person), even though fat accumulation is a preliminary step of cancer development during carcinogenesis.

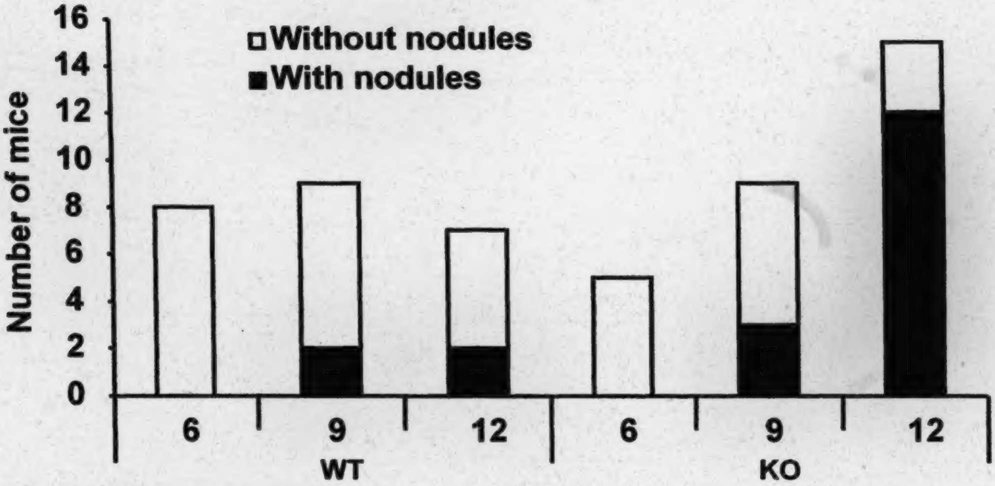

Fig. 1 Occurrence of nodules in mice livers

Pemt$^{+/+}$ mice (WT) and *Pemt*$^{-/-}$ mice (KO) were sacrificed after carcinogenesis for 6, 9 and 12 months. Nodules were visualized by a pathologist.

Fig. 2 Carcinogenesis in mice livers (photos)

Pemt$^{+/+}$ mice (WT) and *Pemt*$^{-/-}$ mice (KO) were sacrificed after carcinogenesis for 6, 9 and 12 months.

6 months

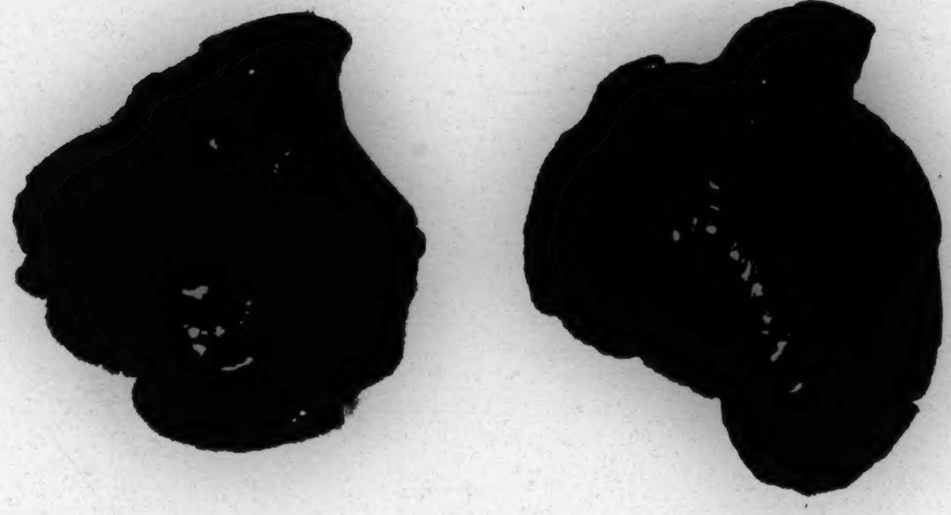

KO **WT**

9 months

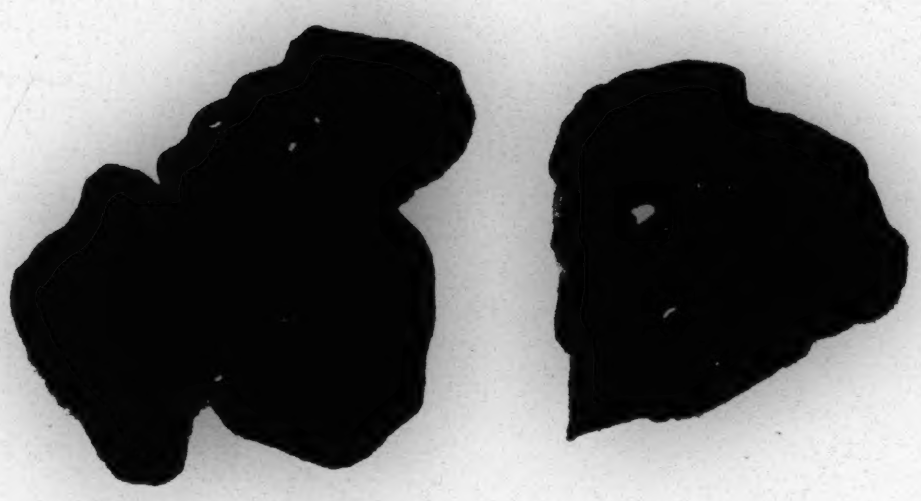

KO **WT**

12 months

References

1. Vance, D. E. (2002) *Phospholipid biosynthesis in eukaryotes.* in *Biochemistry of lipids, lipoproteins and membranes* (Vance, D. E., J. E. Vance, ed), pp. 205-232, Elsevier, New York
2. Cui, Z., Shen, Y. J., and Vance, D. E. (1997) *Biochim Biophys Acta* 1346, 10-16
3. Zou, W., Li, Z., and Cui, Z. (2000) *Zhonghua Gan Zang Bing Za Zhi* 8, 230-232
4. Tessitore, L., Sesca, E., Bosco, M., and Vance, D. E. (1999) *Carcinogenesis* 20, 561-567
5. Tessitore, L., Dianzani, I., Cui, Z., and Vance, D. E. (1999) *Biochem J* 337 (Pt 1), 23-27
6. Tessitore, L., Marengo, B., Vance, D. E., Papotti, M., Mussa, A., Daidone, M. G., and Costa, A. (2003) *Oncology* 65, 152-158
7. Houweling, M., Cui, Z., Tessitore, L., and Vance, D. E. (1997) *Biochim Biophys Acta* 1346, 1-9
8. Cui, Z., Houweling, M., and Vance, D. E. (1995) *Biochem J* 312 (Pt 3), 939-945
9. Zou, W., Li, Z. Y., Li, Y. L., Ma, K. L., and Tsui, Z. C. (2002) *Biochim Biophys Acta* 1581, 49-56

Appendix III

Where is Anti-PEMT1 Antibody?

sufficient protein from PEMT purification for producing antibody. Secondly, the anti-PEMT2 antibody was raised from a chemically synthesized carboxyl-terminal sequence (F5) of rat PEMT protein, thus, potential modifications of natural PEMT proteins might affect the binding.

However, the production of anti-PEMT1 antibody will not only identify the subcellular localizations of this protein, but will also help to elucidate the differences between PEMT1 and PEMT2, including protein compositions, modifications and functions, etc.

Experimental Summaries

The first trial of producing anti-PEMT1 antibody

A previously synthesized F2-BSA conjugate (F2 is the second hydrophilic fragments of PEMT from amino-terminus, see Fig. 1) in D. Vance's lab was used to raise antibody in rabbits following a standard procedure (7). Serum obtained from immunized rabbits bind to both F2 fragment and BSA (Fig. 2A). After removing anti-BSA antibody through a BSA-conjugated column, the purified antibody only binds to F2 fragment but not BSA (Fig. 2B). However, this antibody did not bind to any PEMT in ER or MAM. Interestingly, this antibody binds to a small peptide (~10 kD) in the liver as well as the anti-PEMT2 serum did (Fig. 3, 4). By comparing F2 and F5 (carboxyl-terminal), I found both of them had a conserved motif of RKXS/TR, which was a cAMP- and cGMP-dependent protein kinase phosphorylation site (Fig. 5). In addition, F2 fragment had another protein kinase C phosphorylation site, [ST]-x-[RK], overlapping with the cAMP- and cGMP-dependent protein kinase phosphorylation site (Fig. 6). Thus, these data suggested that there might be phosphorylation modifications in the F2 fragment of PEMT in both ER and MAM (Fig. 7).

The second trial of producing anti-PEMT1 antibody

Meanwhile, since the anti-PEMT2 antibody was raised from the carboxyl-terminal fragment (F5) of PEMT protein, I constructed a recombinant protein containing two amino-terminal fragments (F1 and F2) fusing them with a 6XHis tag and a GST tag (His, histine; GST, glutathione-*S*-transferase), F1-6XHis-F2-GST recombinant protein (FGST) (Fig. 2). First, I cloned F1 and F2 sequences from mouse PEMT cDNA and changed the genetic code with preference to *E. coli*, and then inserted F1 and F2 sequences into GST fusion expression vector pET41b(+) (*Invitrogen*) with a 6XHis•Tag between two fragments (Fig. 8). Finally, the constructed vector was transformed into *E. coli* cells BL21 (DE3) and protein expression was induced by IPTG (isopropyl-beta-D-thiogalactopyranoside) (Fig. 9). Since FGST proteins formed inclusion bodies, Ni-column purification for His•Tag was performed under denatured conditions with 6 M urea. After purification through an affinity-chromatography column for His•Tag and then for GST•Tag, purified FGST (Fig. 10) was injected into rabbits to raise antibody following a standard procedure (7). Immunized serum was further purified through a FGST-conjugated column. Unfortunately, this antibody only bound to GST but not F1 and F2 fragments (Fig. 11).

The third trial of producing anti-PEMT1 antibody

In this case, we attempted to use full-length PEMT to raise antibody. I cloned mouse PEMT cDNA and changed the genetic code to the preference of *E. coli*, and then inserted PEMT sequence into GST fusion expression vector pET41b(+) with a cleavage site of enterokinase between PEMT and Tag sequences. The construct also contained a His•Tag and a S•Tag (S•Tag is an epitope tag composed of a 15 residue peptide, KETAAAKFERQHMDS, derived from the pancreatic ribonuclease A) (Fig. 12). Finally, the constructed vector was transformed into *E. coli* cells BL21 (DE3) and protein expression was induced by IPTG. Although this full-length transmembrane protein, PEMT was expressed in *E. coli* (Fig. 13), protein expression levels were very low. Thus, I attempted to promote protein expression by increasing serine concentrations in the medium (Fig. 14). Eventually, the expression of this recombinant protein was improved in *E. coli* strains C41 (DE3) (Fig. 15), which is preferentially used for membrane protein expression. After purification through affinity-chromatography columns for His•Tag and S•Tag respectively (Fig. 16), purified GST-PEMT was cleaved by enterokinase (Fig. 17). PEMT proteins were further purified through a GST•Tag column. However, Purified PEMT was not ample to be injected into rabbits to raise antibody following a standard procedure.

The fourth trial of producing anti-PEMT1 antibody

Since it was hard to express membrane proteins especially transmembrane proteins in *E. coli*, I attempted to express a recombinant protein containing all hydrophilic fragments of PEMT with a His•Tag (rPEMT-F: F1-6XHis-F2-F3-F4) or with a His•Tag and two 6Xglycine linkers (rPEMT-FG: F1-6XHis-F2- 6XGly-F3- 6XGly-F4) in *E. coli* (Fig. 18). The latter rPEMT-FG was to mimic the transmembrane structure of PEMT. I cloned F3 and F4 sequences from mouse PEMT cDNA and combined with previous F1-6XHis-F2 sequence with or without 6XGly linkers, and then inserted rPEMT-F or rPEMT-FG sequences into expression vector pET41b(+). Finally, the constructed vector was transformed into *E. coli* cells C41 (DE3) and induced for protein expression by IPTG. Since both rPEMT-F and rPEMT-FG proteins formed inclusion bodies, Ni-column purification for His•Tag was performed under denatured conditions with 6 M urea. After purification through affinity-chromatography columns for His•Tag, another purification through electronic transfer was performed for further purifying proteins. Purified rPEMT-F and rPEMT-FG proteins (Fig. 19) were injected into rabbits respectively to raise antibodies following a standard procedure (7). Immunized serum was further purified through a rPEMT-F or rPEMT-FG protein-conjugated column respectively. However, neither anti-rPEMT-F nor anti-rPEMT-

FG antibody was able to bind to hepatic PEMT, even though they bind to antigens nicely (Fig. 20, 21). This also suggests that the hydrophilic fragments of hepatic PEMT might be highly modified, since both rPEMT-F and rPEMT-FG proteins from *E. coli* cells were not supposed to be modified.

The last trial of producing anti-PEMT1 antibody

DNA Vaccination (vector immunoization) is a newly developed method to produce antibody, which is based on mammalian promoter-driven expression of exogenous proteins in animal muscles to stimulate the immunization more vigorously (8-10).

Strategy:

1. Construct the vector containing the target gene with a mammalian promoter;
2. Transfer the vector into animal tissues via electroporation.

Procedures:

1. Construct mouse *Pemt* into pCI vector (*Promega*);
2. Identify the vector via transient expression in mammalian cells (McAd7777);
3. Prepare plasmid via the Giga preparation method to produce vectors in mg yield;
4. Electroporate vectors into rabbits muscles;
5. Collect polyclonal and monoclonal antibodies.

Unfortunately, antibodies obtained from this experiment were still not able to bind to hepatic PEMT.

Exploring the reasons --- phosphorylation modifications of PEMT

An interesting finding was that after liver homogenates and crude microsome fractions were incubated with alkaline phosphatase, one-fold increase in PEMT protein was visualized from Western blotting with anti-PEMT2 antibody, and this was not found in MAM fractions (Fig. 22). This indicated that the reason why anti-PEMT2 antibody could only bind to PEMT2 but not PEMT1 could be that PEMT1 was phosphorylated at the carboxyl-terminal but not PEMT2. In addition, this also suggested that hepatocytes might have the same amount of PEMT1 as PEMT2 (Fig. 22, 23A). Cui reported that PEMT activity in ER (PEMT1) was 2 ~ 3-fold higher than that in MAM (PEMT2) (Fig. 23B) (2). Combined with our findings that alkaline phosphatase-treated liver homogenates showed obvious reduction of PEMT activity (Fig. 24), I conclude that phosphorylation of PEMT at the carboxyl-terminal up-regulated PEMT activity. In addition, long-term storage of liver homogenates in a -70°C freezer causing the loss of PEMT activity might result from spontaneous dephosphorylation (Fig. 24).

As mentioned before, the chemically synthesized carboxyl-terminal sequence of PEMT used for raising anti-PEMT2 antibody contained a putative cAMP-dependent protein kinase (PKA) phosphorylation site. When liver homogenates and MAM fractions were incubated with PKA catalytic subunits

(Sigma), we found that anti-PEMT2 antibody was no longer binding to PEMT2 in liver homogenates and showed decreased binding to PEMT2 in MAM fractions (Fig. 25). The latter might result from incomplete reactions with PKA. These results indicated that the carboxyl-terminal sequence of hepatic PEMT2 was not phosphorylated. This finding was further supported by the observations that chemically synthesized carboxyl-terminal sequence of PEMT (F5) conjugated with BSA (BSA-F5) showed decreased binding to anti-PEMT2 antibody after incubation with PKA catalytic subunits (Fig. 26).

Therefore, in mice and rats, the carboxyl-terminus of PEMT1 but not PEMT2 may be phosphorylated by PKA. However, in humans, the carboxyl-terminus of both PEMT1 and PEMT2 may not be phosphorylated.

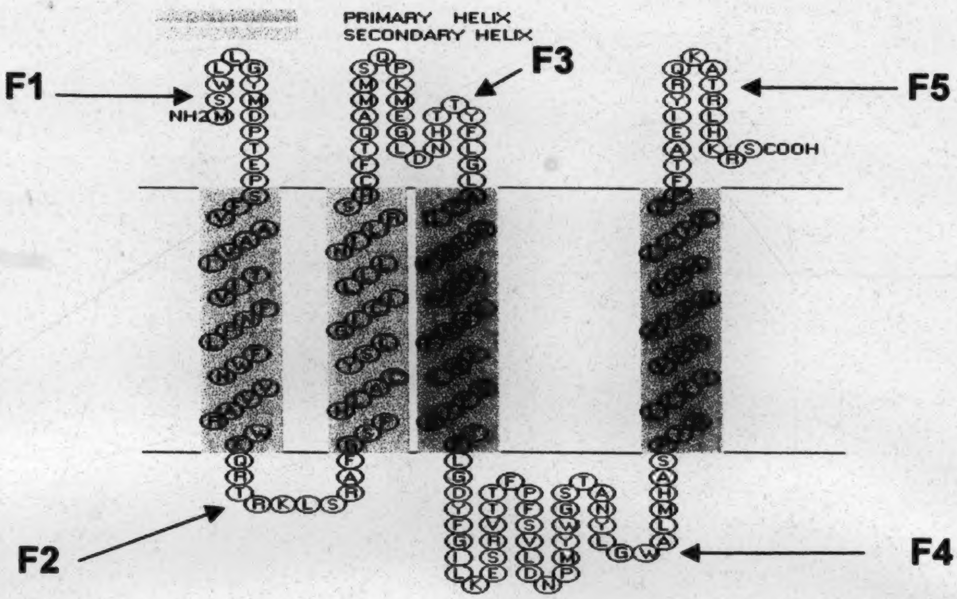
PRIMARY HELIX
SECONDARY HELIX
F1
F2
F3
F4
F5
NH2
COOH

Fig. 1 Topological Structure of mouse PEMT (mPEMT)

A putative structure of mPEMT protein was produced from www.topo.com. PEMT contains 4 transmembrane domains and 5 hydrophilic fragments (F1 ~ F5).

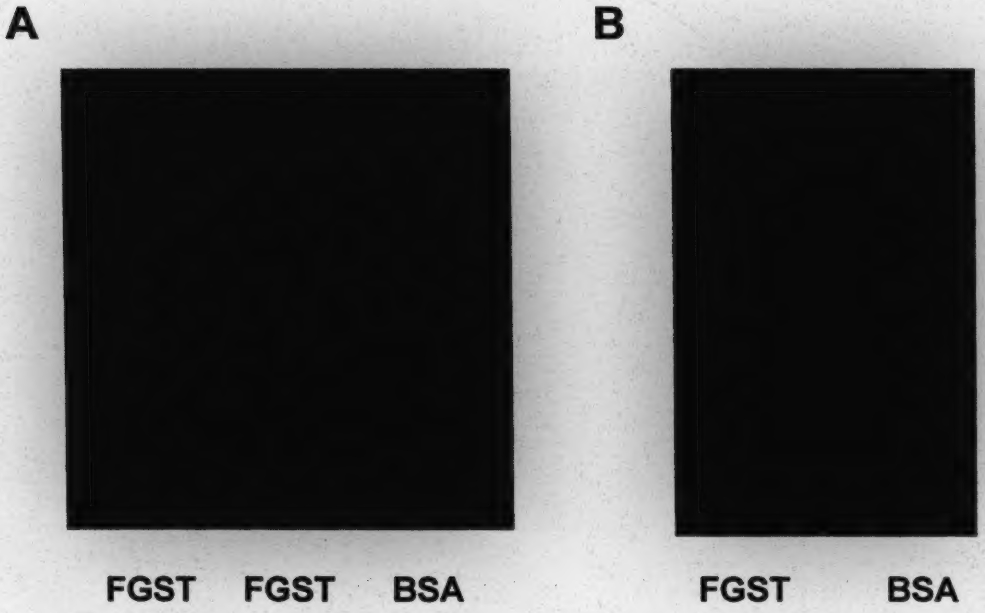

Fig. 2 Anti-F2 antibody bind to F2 fragments

F2-BSA was used for immunization to produce antibody. Western blotting was performed to identify antibodies. **(A)** Anti-F2-BSA serum was not only able to bind to F2-containing protein (FGST) but also to BSA. **(B)** Purified anti-F2 antibody was only able to bind to -containing protein (FGST) but not BSA. FGST, F1-6XHis-F2-GST recombinant protein expressed in *E. coli*; BSA, Bovine Serum Albumin; F2, Fragment 2 of mouse PEMT.

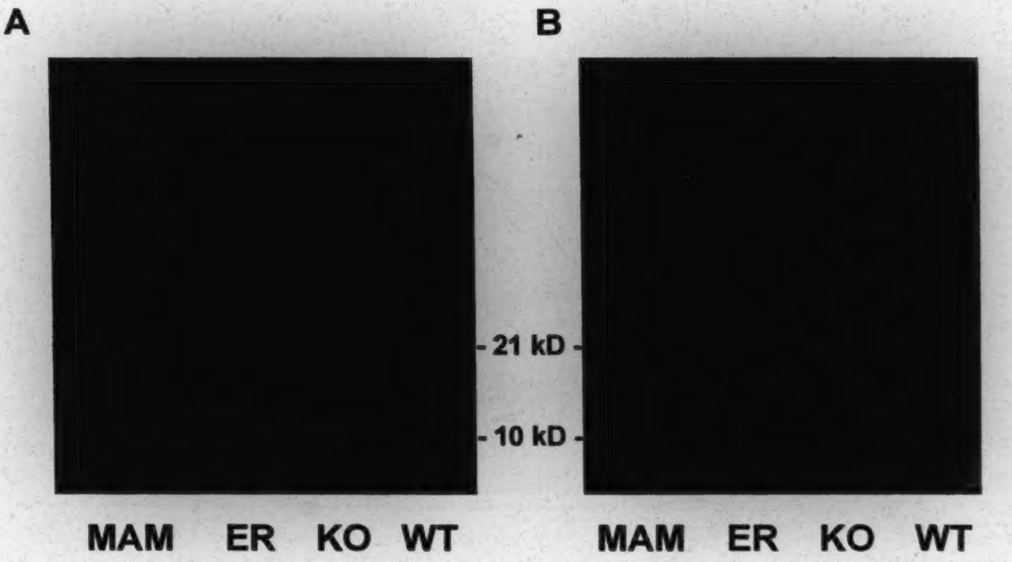

Fig. 3 Purified anti-F2 antibody was not able to bind natural mouse PEMT

Western blotting analysis with purified anti-PEMT2 antibody **(A)** and anti-F2 antibody **(B)** was performed with liver homogenates and subcellular fractions. MAM, mitochondria associated membrane; ER, endoplasmic reticulum; KO, liver homogenates from *Pemt*$^{-/-}$ mice; WT, liver homogenates from *Pemt*$^{+/+}$ mice.

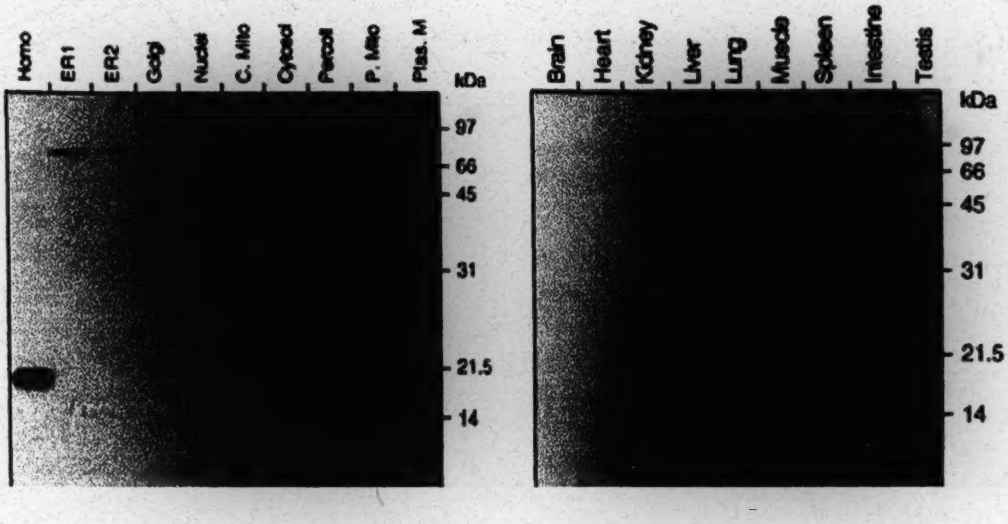
Homo
ER1
ER2
Golgi
Nuclei
C. Mito
Cytosol
Percoll
P. Mito
Plas. M
kDa
97
66
45
31
21.5
14
Brain
Heart
Kidney
Liver
Lung
Muscle
Spleen
Intestine
Testis
kDa
97
66
45
31
21.5
14

Fig. 4 Original western blotting analysis with anti-PEMT2 antibody from Zheng Cui (*JBC,* 268: 16655)

Percoll fractions, MAM.

```
         F2:  rweqrtRKLS R-----
C-terminal:   yr----RKAT Rlhkrs
       (F5)

                    **** *
                    R K X S/T R
```

Fig. 5 Alignment between F2 and F5 fragments of mPEMT

A homolog was found between F2 and F5 (C-terminal) fragments.

F2: RWEQRTRKLSR

---

cAMP- and cGMP-dependent protein kinase phosphorylation site.
[RK](2)-x-[ST].
Site : 7 to 10 RKLS

---

Protein kinase C phosphorylation site.
[ST]-x-[RK].
Site : 6 to 8 TRK

C-terminal (F5): YRRKATRLHKRS

---

cAMP- and cGMP-dependent protein kinase phosphorylation site.
[RK](2)-x-[ST].
Site : 3 to 6 RKAT

Fig. 6 Putative Phosphorylation Sites of PEMT Fragments

Putative Phosphorylation Sites of PEMT Fragments (F2 and F5) were analyzed with software from www. Expsy.com.

	MAM	ER	Cytosol
Anti-C-terminal Abs:	PEMT2	no	~10 kD protein
Anti-F2 Abs:	no	no	~10 kD protein

Possible modification sites:	C-terminal (F5)	F2
cAMP- and cGMP-dependent protein kinase phosphorylation site	RKAT	RKLS
Protein kinase C phosphorylation site	no	TRK

Fig. 7 Relations between anti-PEMT2 antibody and anti-F2 antibody

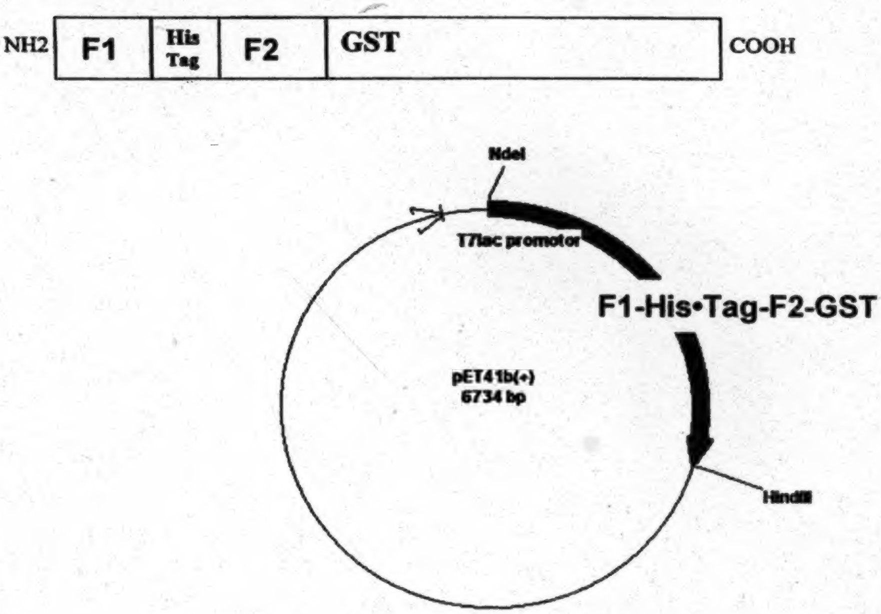
NH2
F1
His Tag
F2
GST
COOH
NdeI
T7lac promotor
F1-His•Tag-F2-GST
pET41b(+)
6734 bp
HindIII

Fig. 8 Construct scheme of F1-His•Tag-F2-GST (FGST) recombinant protein

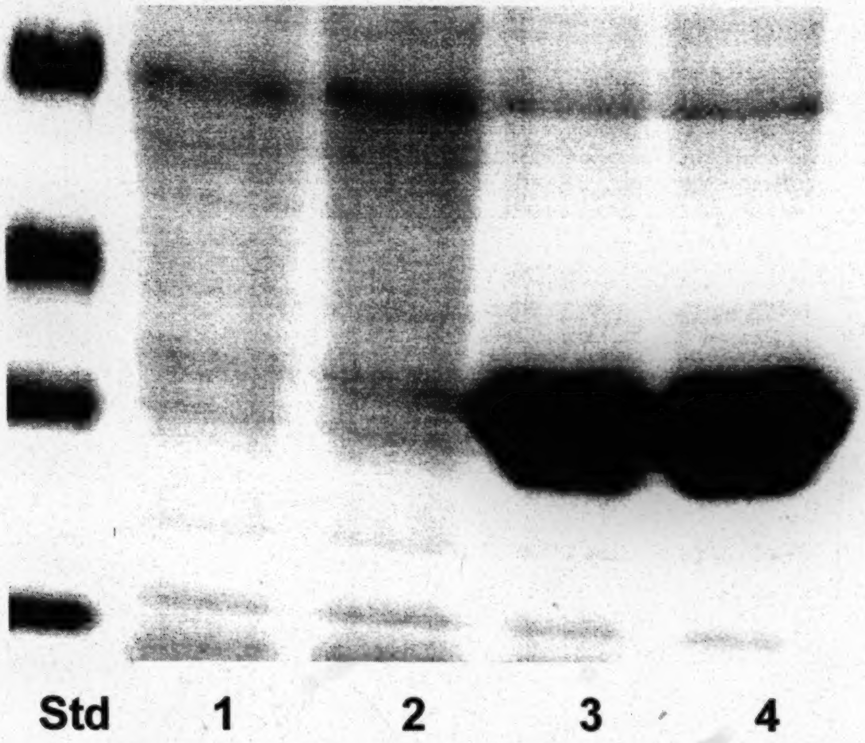

Fig. 9 Induction of F1-His•Tag-F2-GST (FGST) protein expression by IPTG

Comassie Blue staining of a 12% SDS-PAGE gel loaded with cell homogenates from *E.coli* was used to identify FGST expression. 1, 2, Before IPTG induction; 3, 4, After IPTG induction; Std, protein standards.

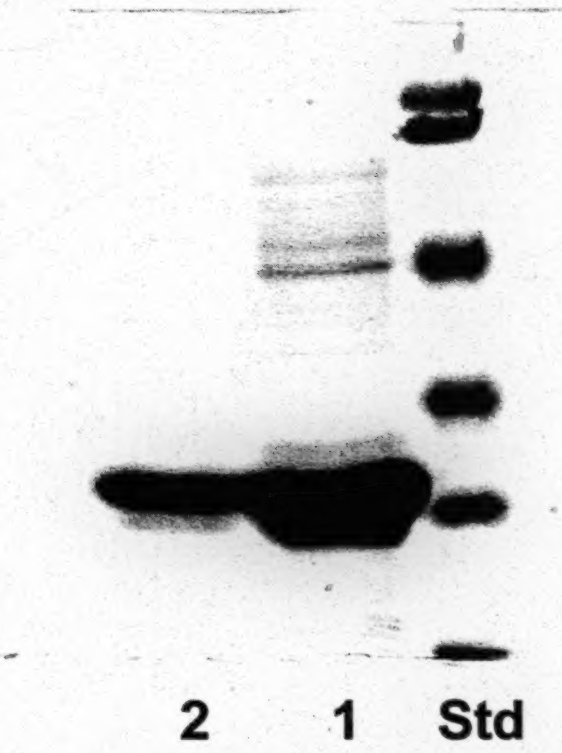

Fig. 10 Purification of F1-His•Tag-F2-GST (FGST) Fusion Proteins

Comassie Blue staining of a 12% SDS-PAGE gel was used to identify the purity of FGST protein. His•Tag involved affinity purification was performed with a Ni-exchange column and showed in lane 2. 1, Purified inclusion bodies; 2, Purified proteins; Std, protein standards.

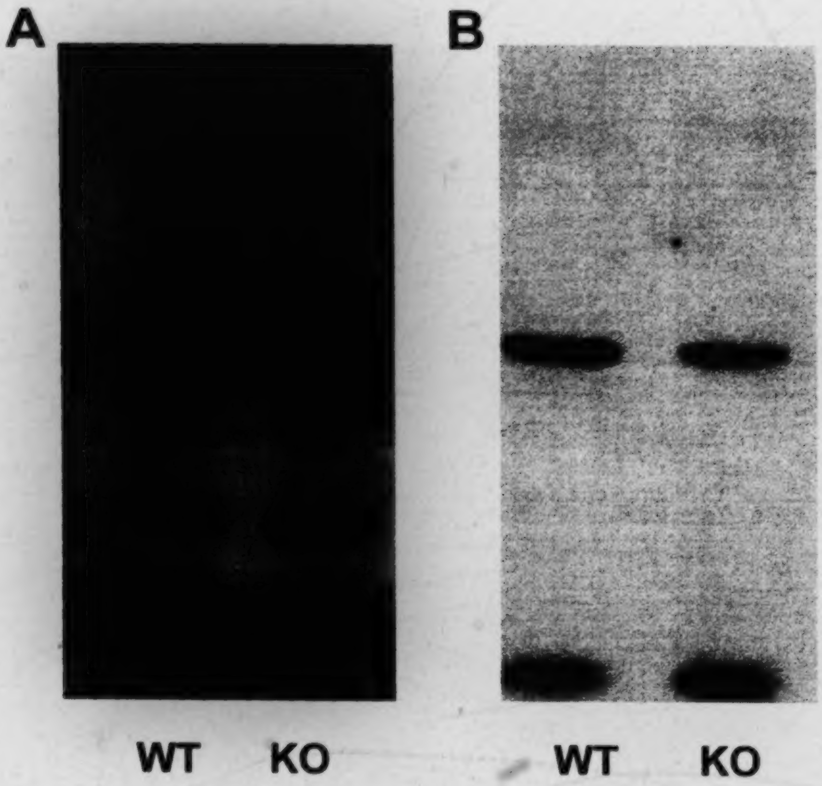

Fig. 11 Anti-FGST antibody only binds to GST but not PEMT

Western blotting analysis with purified anti-GST antibody **(A)** and anti-FGST antibody **(B)** was performed with liver homogenates. KO, liver homogenates from *Pemt*$^{-/-}$ mice; WT, liver homogenates from *Pemt*$^{+/+}$ mice. Can you put MW markers on the figure??

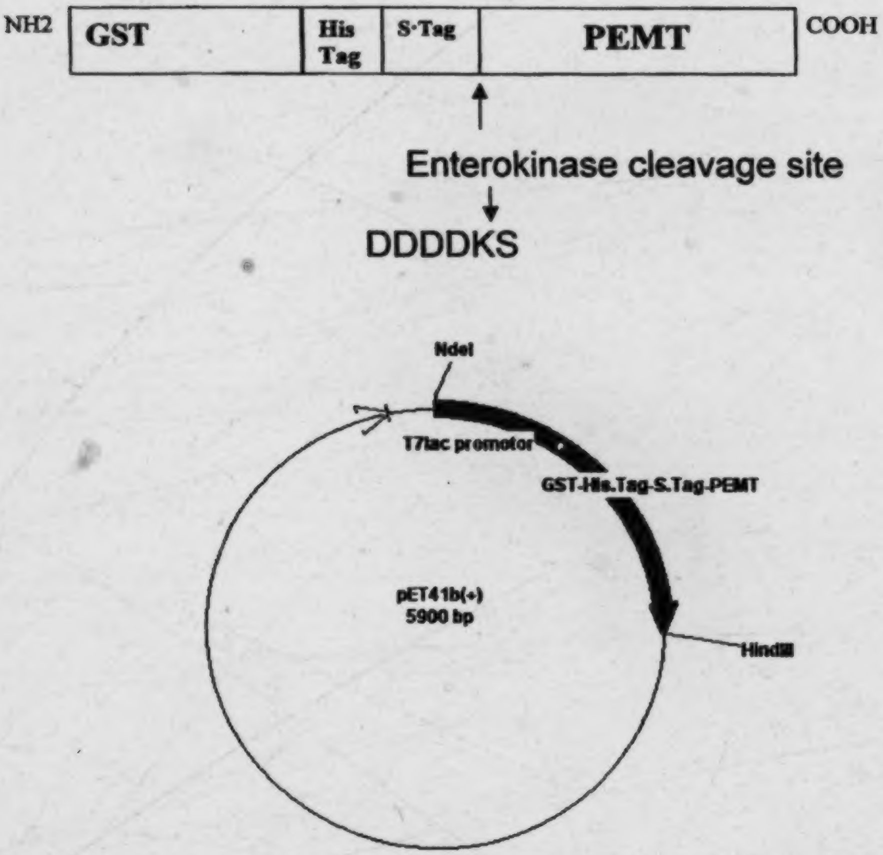
NH2
GST
His Tag
S·Tag
PEMT
COOH
Enterokinase cleavage site
DDDDKS
NdeI
T7lac promotor
GST-His.Tag-S.Tag-PEMT
pET41b(+)
5900 bp
HindIII

Fig. 12 Construct scheme of GST-His•Tag-S•Tag-PEMT (GST-PEMT) recombinant protein

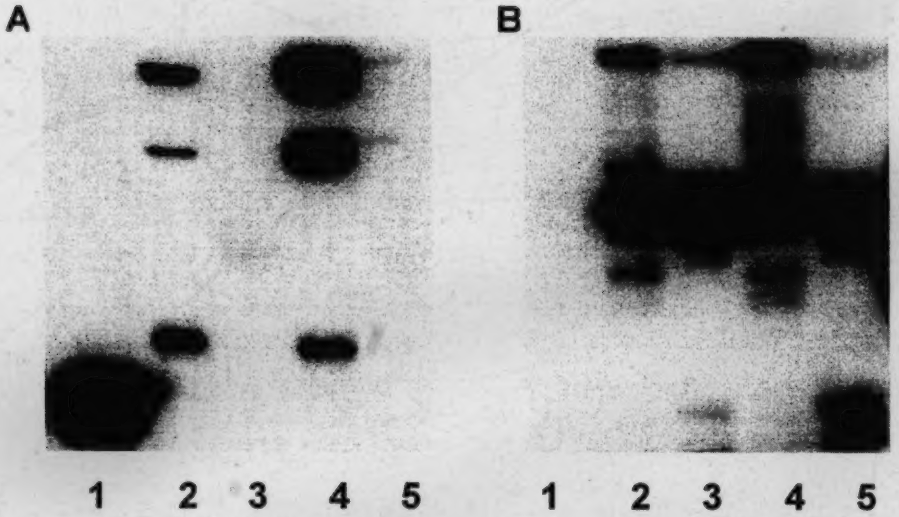

1: MAM; 2,4: after induction; 3,5: before induction

Fig. 13 Induction of GST-PEMT Expression in *E. coli* BL21 (DE3) by IPTG

Western blotting analysis with purified anti-PEMT2 antibody **(A)** and anti-GST antibody **(B)** was performed with cell homogenates from *E. coli* and MAM. MAM, mitochondria associated membrane. 1, MAM; 2 & 4, after induction; 3 & 5, before induction. MW markers would be good

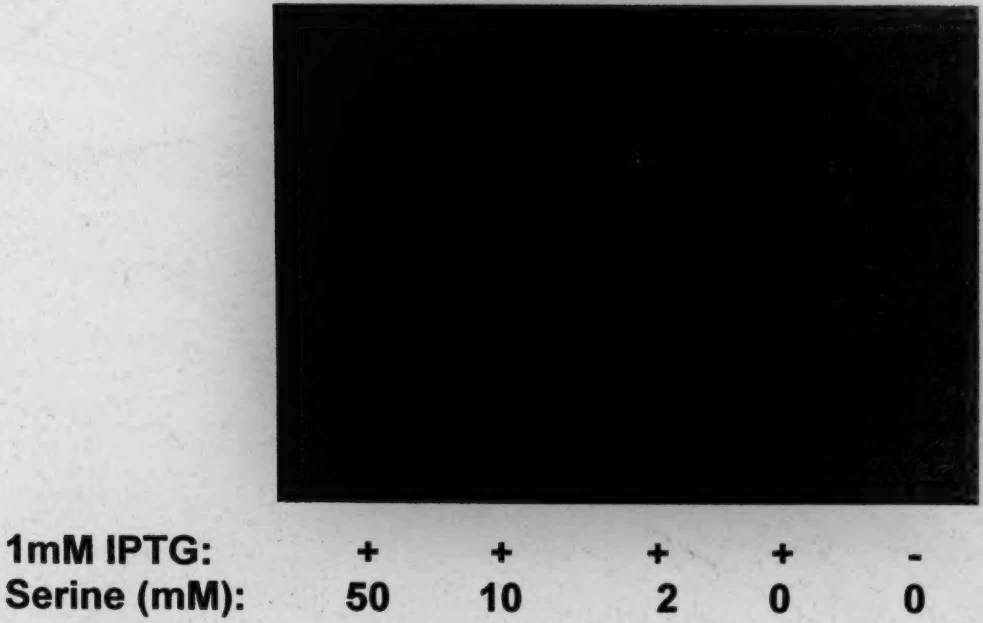

Fig. 14 Serine promotes GST-PEMT expression in *E. coli* BL21 (DE3)

Western blotting analysis with purified anti-PEMT2 antibody was performed with cell homogenates from *E. coli*. Up to 50 mM serine was added to culture medium with IPTG. MW markers.

Fig. 15 GST-PEMT expressions in *E. coli* strain C41 (DE3)

Western blotting analysis with purified anti-PEMT2 antibody was performed with cell homogenates from *E. coli.* 1, GST-PEMT expression in *E. coli* strain BL21 (DE3); 2, 3, 4 and 5, GST-PEMT expressions in different colonies of *E. coli* strain C41 (DE3). MW markers or at least put an arrow pointing to the PEMT band or where the PEMT bands should be.

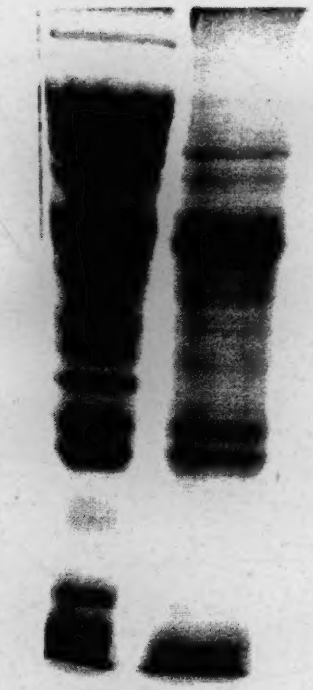

Fig. 16 Purification of GST-His•Tag-S•Tag-PEMT (GST-PEMT) fusion proteins

Comassie Blue staining of a 12% SDS-PAGE gel was used to identify the purity of FGST protein. His•Tag involved affinity purification was performed with a Ni-exchange column and showed in lane 3. 1, cell homogenates; 2, insoluble fractions; 3, purified proteins.

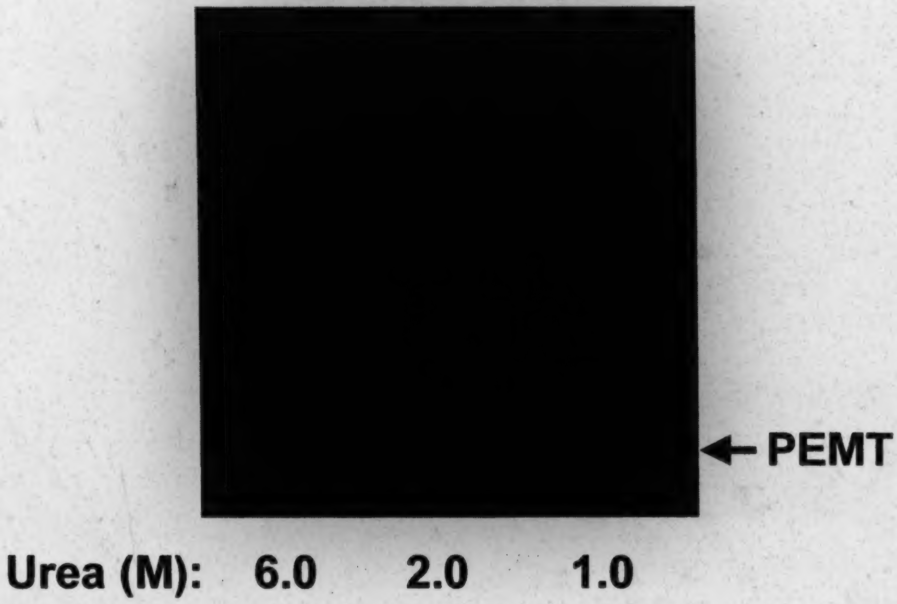

Fig. 17 Cleavage of PEMT from GST-PEMT fusion proteins.

Western blotting analysis with purified anti-PEMT2 antibody was performed to identify the cleavage of purified GST-PEMT fusion proteins. Purified fusion proteins (in 6.0 M urea) were dialyzed to low concentrations of urea buffer (2.0 M, 1.0 M) and then digested by enterokinase.

Antigen: rPEMT-F

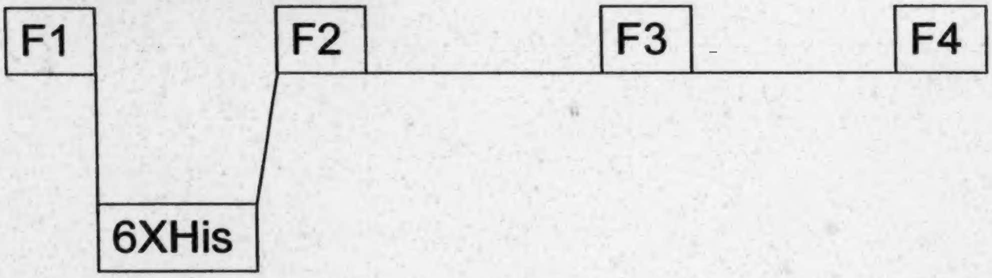

Antigen: rPEMT-FG

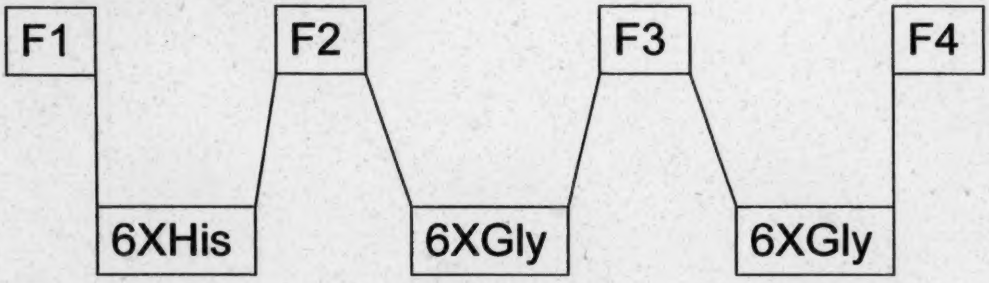

Fig.18 Construct scheme of rPEMT-F and rPEMT-FG recombinant proteins

F1 ~ F4 fragments were linked together with a 6XHis•Tag insertion between F1 and F2 fragments to construct a recombinant protein, rPEMT-F. F1 ~ F4 fragments were linked together with a 6XHis•Tag insertion between F1 and F2 fragments and two 6XGly (glycine) linkers between F3 to F5 fragments to construct a recombinant protein, rPEMT-FG.

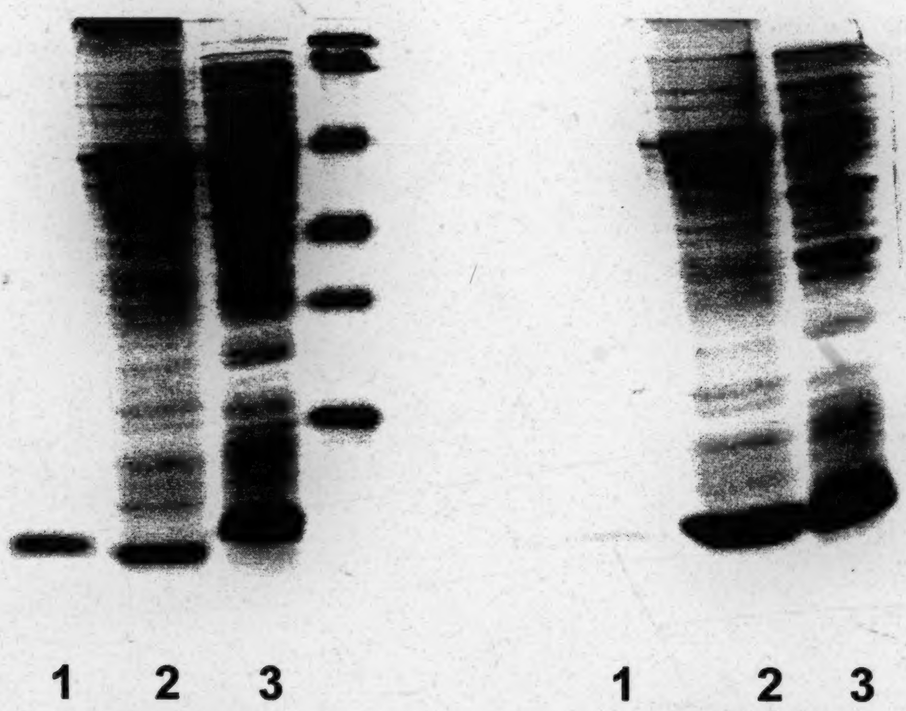

rPEMT-F

rPEMT-FG

Fig. 19 Purification of rPEMT-F and rPEMT-FG recombinant proteins

Comassie Blue staining of a 12% SDS-PAGE gel was used to identify the purity of rPEMT-F and rPEMT-FG recombinant proteins. His•Tag involved affinity purification was performed with a Ni-exchange column and shown in lane 1. 1, purified proteins; 2, purified inclusion bodies; 3, cell homogenates.

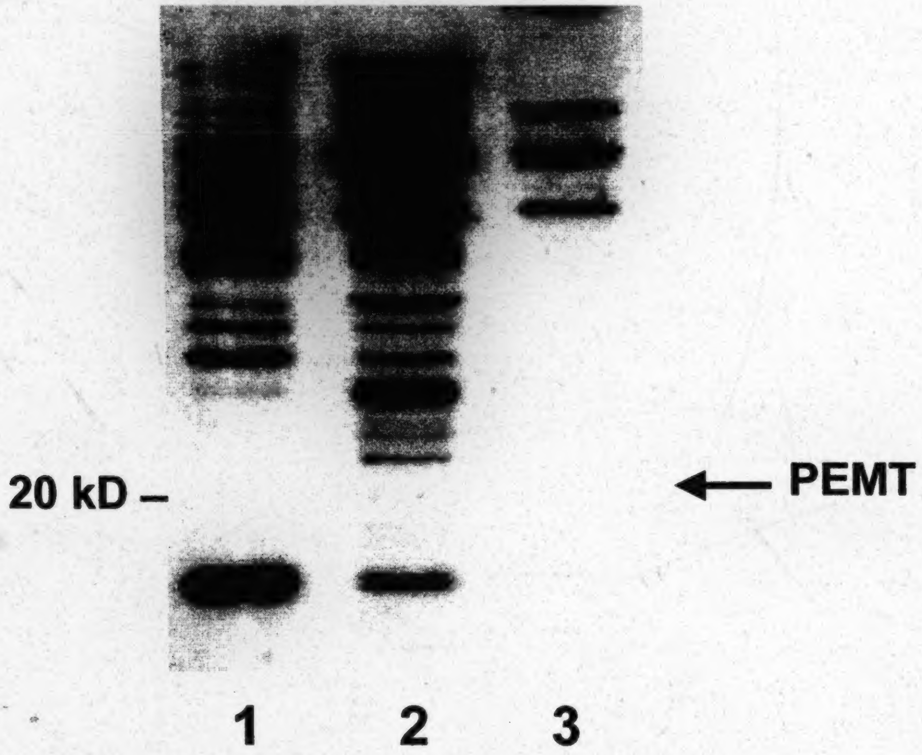

Fig. 20 Anti-rPEMT-F Antibody did not bind to natural PEMT

Western blotting analysis with anti-rPEMT-F serum was performed with liver homogenates and subcellular fractions. 1, WT, liver homogenates from *Pemt*$^{+/+}$ mice; 2, microsome fractions from livers of *Pemt*$^{+/+}$ mice; 3, MAM, mitochondria associated membrane.

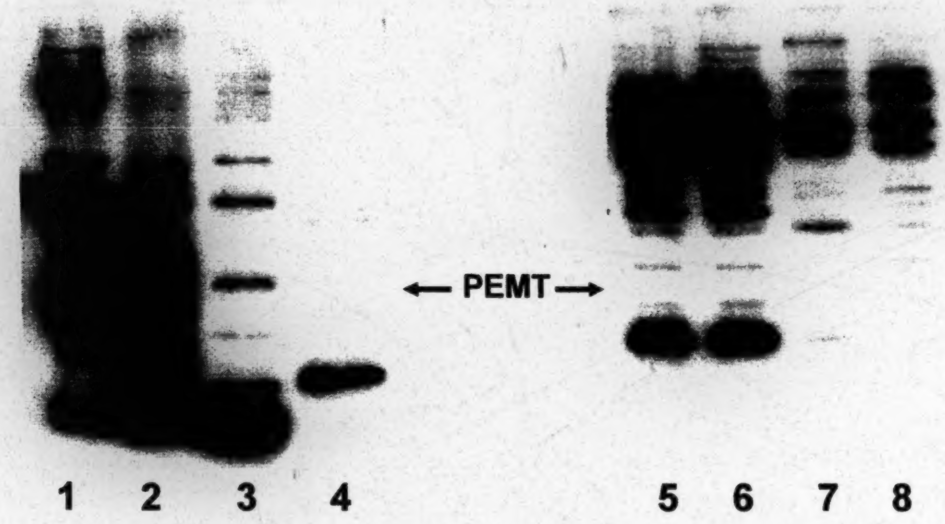

Fig. 21 Anti-rPEMT-FG Antibody did not bind to natural PEMT

Western blotting analysis with anti-rPEMT-FG serum was performed with cell homogenates and subcellular fractions. 1, *E. coli* cell homogenates with GST-PEMT expression; 2 & 3, *E. coli* cell homogenates with PEMT expression; 4, *E. coli* cell homogenates with rPEMT-FGWT; 5, liver homogenates from *Pemt*$^{-/-}$ mice; 6, liver homogenates from *Pemt*$^{+/+}$ mice; 7, MAM, mitochondria associated membrane; 8, microsome fractions from livers of *Pemt*$^{+/+}$ mice.

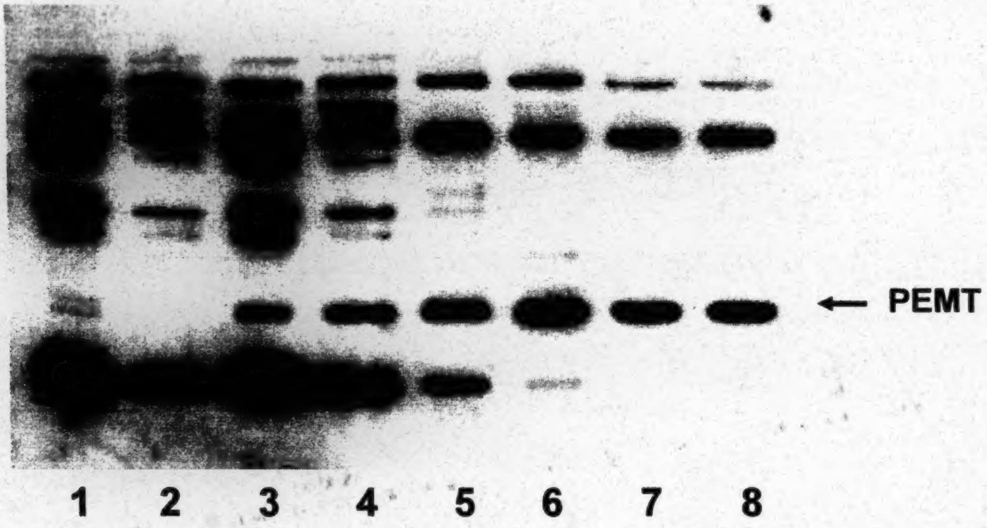

Fig. 22 Dephosphorylation increased binding of anti-PEMT2 antibody to PEMT

Dephosphorylation was performed by incubating samples with alkaline phosphatase. Western blotting analysis with anti-PEMT2 serum was performed with liver homogenates and subcellular fractions. 1, 3, 5 & 7, without dephosphorylation; 2, 4, 6 & 8, with dephosphorylation. 1 & 2, liver homogenates from *Pemt*$^{-/-}$ mice; 3 & 4, liver homogenates from *Pemt*$^{+/+}$ mice; 5 & 6, microsome fractions from livers of *Pemt*$^{+/+}$ mice; 7 & 8, MAM, mitochondria associated membrane.

Fig. 23 PEMT expressions and activities in ER and MAM

(A) Levels of PEMT expression were quantified by densitometry of western blotting analysis in Fig. 22. **(B)** PEMT activities were assayed in ER and MAM fractions (adopted from Z. Cui's *JBC* paper give reference not what you have here).

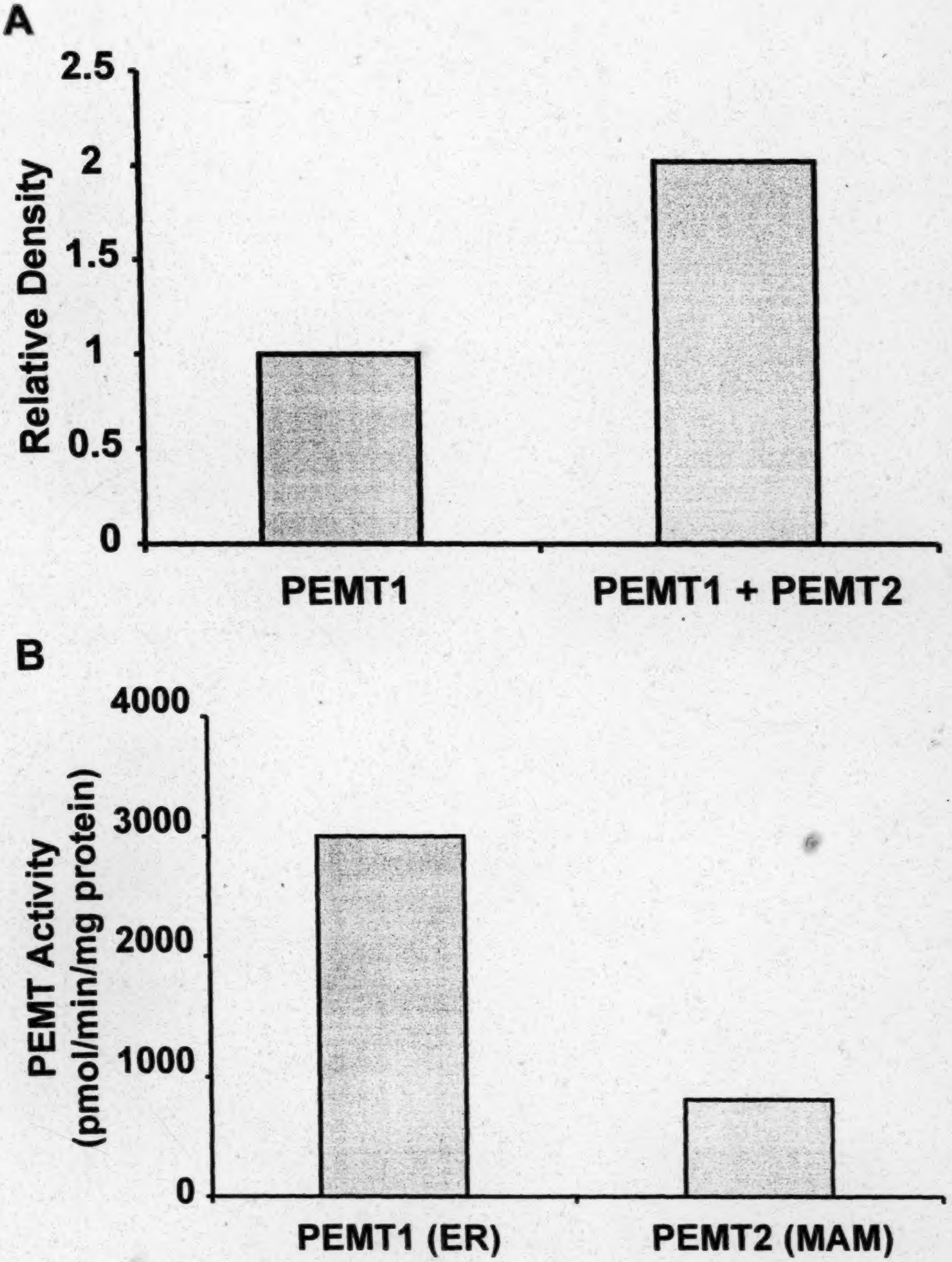
A
Relative Density
2.5
2
1.5
1
0.5
0
PEMT1
PEMT1 + PEMT2
B
PEMT Activity (pmol/min/mg protein)
4000
3000
2000
1000
0
PEMT1 (ER)
PEMT2 (MAM)

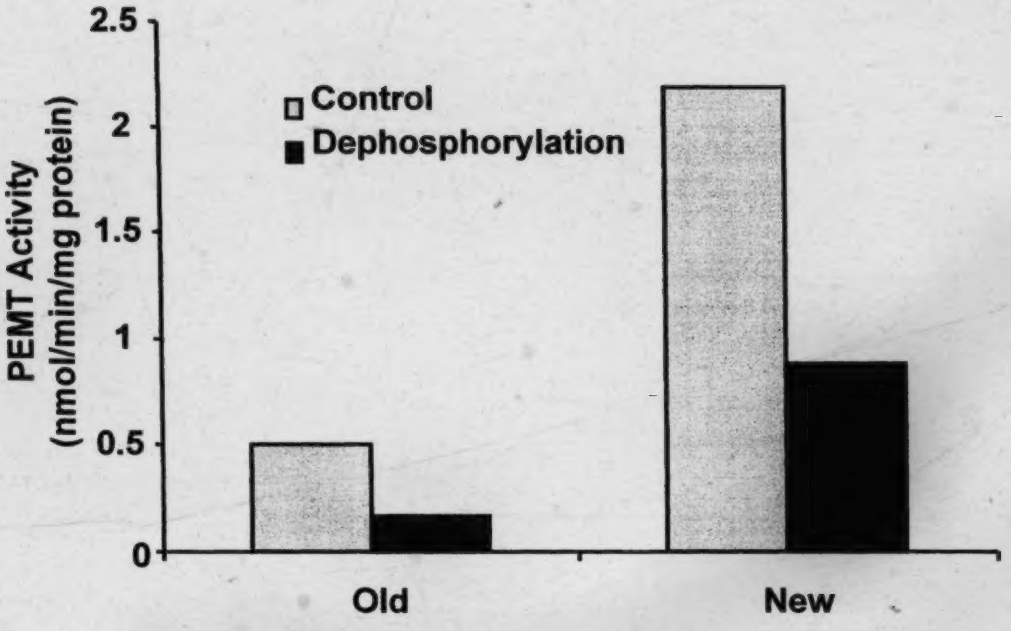

Fig. 24 Dephosphorylation reduced PEMT activities.

Assays of PEMT activities in liver homogenates were performed with (Dephosphorylation) or without the treatment with alkaline phosphatase (Control). Old, liver homogenates stored in -70°C freezer for 6 months; New, freshly made liver homogenates.

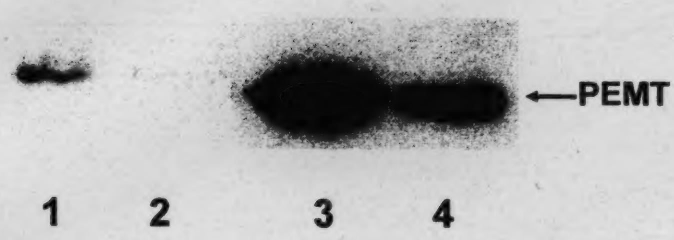

Fig. 25 Phosphorylation inhibited the binding of anti-PEMT2 antibody to PEMT

PKA catalytic subunits were used for phosphorylation. Western blotting analysis with anti-PEMT2 serum was performed with liver homogenates and subcellular fractions. 1 & 3, without phosphorylation; 2 & 4, with phosphorylation. 1 & 2, liver homogenates from *Pemt*$^{+/+}$ mice; 3 & 4, MAM, mitochondria associated membrane.

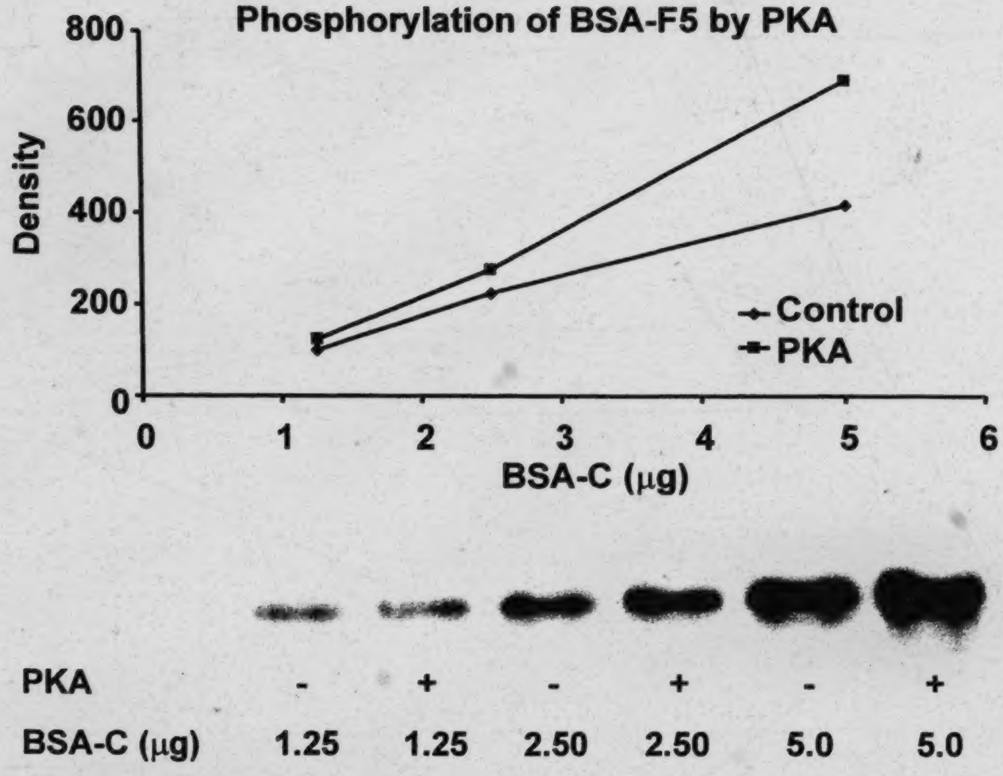

Fig. 26 Phosphorylation inhibited the binding of anti-PEMT2 antibody to F5-BSA conjugates.

PKA catalytic subunits were used for phosphorylation. Western blotting analysis with anti-PEMT2 serum was performed with F5-BSA conjugates, the antigen used for raising anti-PEMT2 antibody. Levels of PEMT expression were quantified by densitometry of Western blotting analysis. 1.25, 2.5 and 5.0 g F5-BSA conjugates were incubated with (PKA) or without PKA catalytic subunits (control).

References

1. Vance, D. E. *Phospholipid biosynthesis in eukaryotes.* (2002) in *Biochemistry of lipids, lipoproteins and membranes* (Vance, D. E., J. E. Vance, ed), pp. 205-232, Elsevier, New York
2. Cui, Z., Vance, J. E., Chen, M. H., Voelker, D. R., and Vance, D. E. Cloning and expression of a novel phosphatidylethanolamine N-methyltransferase. A specific biochemical and cytological marker for a unique membrane fraction in rat liver. (1993) *J Biol Chem* **268**, 16655-16663
3. Shields, D. J., Agellon, L. B., and Vance, D. E. Structure, expression profile and alternative processing of the human phosphatidylethanolamine N-methyltransferase (PEMT) gene. (2001) *Biochim Biophys Acta* **1532**, 105-114
4. Walkey, C. J., Cui, Z., Agellon, L. B., and Vance, D. E. Characterization of the murine phosphatidylethanolamine N-methyltransferase-2 gene. (1996) *J Lipid Res* **37**, 2341-2350
5. Ridgway, N. D., and Vance, D. E. Phosphatidylethanolamine N-methyltransferase from rat liver. (1992) *Methods Enzymol* **209**, 366-374
6. Shields, D. J., Lehner, R., Agellon, L. B., and Vance, D. E. Membrane topography of human phosphatidylethanolamine N-methyltransferase. (2003) *J Biol Chem* **278**, 2956-2962

7. Ausubel, F. M., Brent, R., Kingston, R. E., Moore, D. D., Seidman, J. G., Smith, J. A., and Struhl, K. (1999) *Short Protocols in Molecular Biology*, Wiley

8. Aihara, H., and Miyazaki, J. Gene transfer into muscle by electroporation in vivo. (1998) *Nat Biotechnol* **16**, 867-870

9. Widera, G., Austin, M., Rabussay, D., Goldbeck, C., Barnett, S. W., Chen, M., Leung, L., Otten, G. R., Thudium, K., Selby, M. J., and Ulmer, J. B. Increased DNA vaccine delivery and immunogenicity by electroporation in vivo. (2000) *J Immunol* **164**, 4635-4640

10. Selby, M., Goldbeck, C., Pertile, T., Walsh, R., and Ulmer, J. Enhancement of DNA vaccine potency by electroporation in vivo. (2000) *J Biotechnol* **83**, 147-152